WPPSS-FTS--129

BWR TRANSIENT ANALYSIS MODEL

Washington Public Power Supply System
3000 George Washington Way
P. O. Box 968
Richland, Washington 99352

June 1990

BWR TRANSIENT ANALYSIS MODEL

WPPSS-FTS-129

June 1990

Principal Engineers

Y. Y. YUNG
S. H. BIAN
D. E. BUSH

Contributing Engineer

B. M. Moore

Approved: Robert O. Vosburgh Date: June 8, 1990
R. O. Vosburgh
Manager, Safety & Reliability Analysis

D L Larkin Date: 6/8/90
D. L. Larkin
Manager, Engineering Analysis & Nuclear Fuel

DISCLAIMER

This report was prepared by the Washington Public Power Supply System ("Supply System") for submittal to the Nuclear Regulatory Commission, NRC. The information contained herein is accurate to the best of the Supply System's knowledge. The use of information contained in this document by anyone other than the Supply System, or the NRC is not authorized and with respect to any unauthorized use, neither the Supply System nor its officers, directors, agents, or employees assume any obligation, responsibility, or liability or makes any warranty or representation concerning the contents of this document or its accuracy or completeness.

ACKNOWLEDGEMENTS

The Supply System acknowledges the efforts of Mr. J. C. Chandler, Consultant, and Mr. J. T. Cronin, Yankee Atomic Electric Company for their reviews and comments on this report. The Supply System also acknowledges the consulting reviews and recommendations provided by Energy Incorporated and Yankee Atomic Electric Company during the course of development of this model. The information provided by Philadelphia Electric Company and Pennsylvania Power & Light Company is greatly appreciated.

ABSTRACT

A system transient model for the WNP-2 Nuclear Plant based on the RETRAN-02 computer code is described. The model is applicable to a wide range of transients but is primarily intended for analysis of the limiting pressurization transients considered for reload core licensing. The model is qualified by comparisons to a range of power ascension test transients and to the Peach Bottom Unit 2 Turbine Trip Tests. A representative application of the model for licensing basis calculations of the limiting pressurization transients (based on WNP-2 end of cycle 4 conditions) is also presented.

The benchmark comparisons show good agreement between calculated and measured data, thereby demonstrating the Supply System's capability to perform transient analyses for licensing applications.

TABLE OF CONTENTS

TABLE OF CONTENTS (Continued)

TABLE OF CONTENTS (Continued)

LIST OF FIGURES

LIST OF FIGURES (Continued)

LIST OF FIGURES (Continued)

LIST OF TABLES

1.0 INTRODUCTION

This report describes and presents qualification results of a transient analysis model for WNP-2. WNP-2 is a boiling water reactor using a BWR/5 Nuclear Steam Supply System (NSSS) provided by General Electric (GE). This model, which was developed by the Washington Public Power Supply System ("Supply System"), uses the RETRAN-02 MOD04 ("RETRAN-02" or "RETRAN") computer code[1]. Supply System intends to use this model for core reload analysis and plant operational support.

RETRAN-02 is a one-dimensional, thermal-hydraulic, transient analysis computer code developed by the Electric Power Research Institute (EPRI). It is a variable nodalization code requiring the user to input a system model consisting of control volumes, heat slabs, and a flow path network.

The development of the input for the model presented in this report, representing the WNP-2 plant, was based on as-built drawings and vendor specifications. The WNP-2 nodalization network was developed through comparison of model predictions to experimental data.

The RETRAN-02 computer code is the result of a code development effort sponsored by EPRI. The code developers and several utility users have provided model qualification studies in

earlier work. Reports and conclusions based on code predictions of various separate effects tests, system effects experiments, and power reactor startup tests can be found in the RETRAN-02 documentation, which also contains the NRC Staff's Safety Evaluation Report (SER) for RETRAN-02. RETRAN-02 has been widely utilized by utilities and their agents on a variety of transient problems. This report provides further qualification of RETRAN-02 and the Supply System's ability to analyze WNP-2 transient behavior through the application of RETRAN-02 to the analysis of

1. WNP-2 Power Ascension Tests;

2. Peach Bottom 2 Cycle 2 Turbine Trip Tests; and

3. WNP-2 Licensing Basis Analysis.

The results of these evaluations are presented in Chapters 3.0 and 4.0 of this report.

The WNP-2 RETRAN-02 model described in Chapter 2 is a best-estimate model. It is designed to serve as a best-estimate, general purpose, systems analysis tool. It can be used for a wide range of purposes, including design changes, operational transient evaluations, and simulation qualification. The WNP-2 RETRAN-02 model is qualified by comparison of best-estimate data predictions with plant data collected during testing. To analyze

limiting transients for core reload design in support of technical specification action, a Licensing Basis Model is developed by modifying the Best Estimate Model with conservative assumptions. The Licensing Basis Model is described in Chapter 4, which also contains example calculations with the conservative model.

The Supply System's reload transient analysis methods are based on the EPRI code package as depicted in Figure 1.1. The steady state core physics codes and models used to provide input to the transient analysis models are described and qualified in elsewhere[2]. The SIMTRAN-E MOD3A ("SIMTRAN-E") code[3] collapses the three-dimensional neutronics data generated by the steady state core physics codes to the one-dimensional neutronics input required by RETRAN-02 and calculates the moderator density and fuel temperature dependencies. The one-dimensional kinetics parameter dependencies generated by SIMTRAN-E are modified as described in Appendix A to account for differences between the RETRAN-02 one-dimensional and SIMULATE-E three-dimensional moderator density calculations. RETRAN-02 is used to model the NSSS and the VIPRE-01 MOD02 ("VIPRE-01") code[4] is used to model a single fuel assembly for thermal margin evaluations. Thermal margin evaluation for WNP-2 is described and qualified in a separate Licensing Topical Report (to be submitted later).

FIGURE 1.1

Supply System Reload Transient Analysis Methods
Computer Code Flow Chart

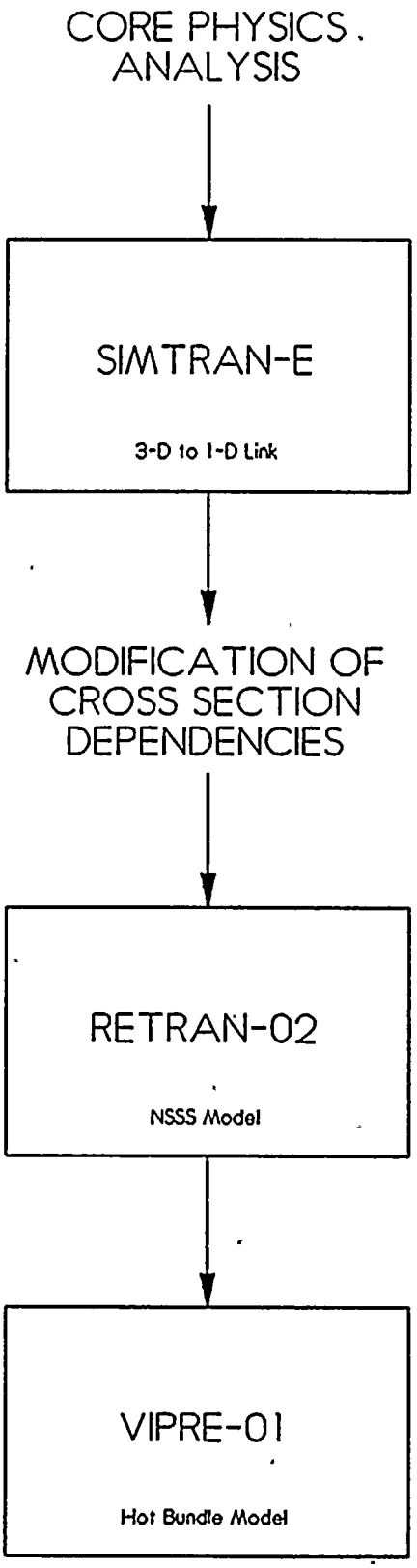

2.0 MODEL DESCRIPTION

This chapter describes the WNP-2 RETRAN-02 Best Estimate Model developed to analyze a wide range of transients. This development was based on many years of on-going experience with the code and includes several revisions of the model based on that experience.

A diagram of the nodalization selected for the WNP-2 RETRAN-02 model is illustrated in Figures 2.1 to 2.4, including control volumes, junctions and heat conductors. A description of the primary inputs to the code is given in the subsequent sections.

FIGURE 2.1

WNP-2 RETRAN MODEL (Vessel)

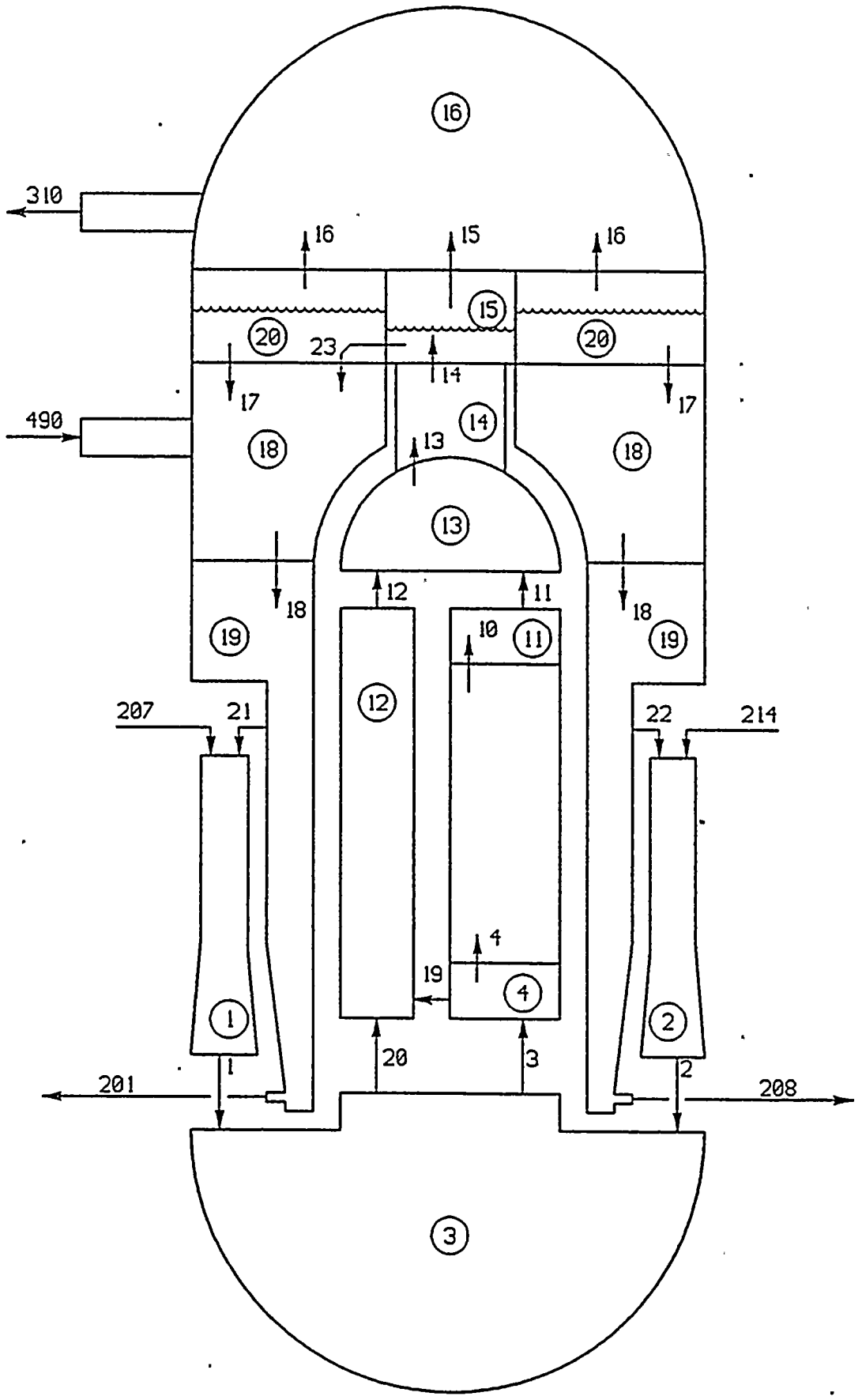

FIGURE 2.2

WNP-2 RETRAN MODEL (Active Core Region)

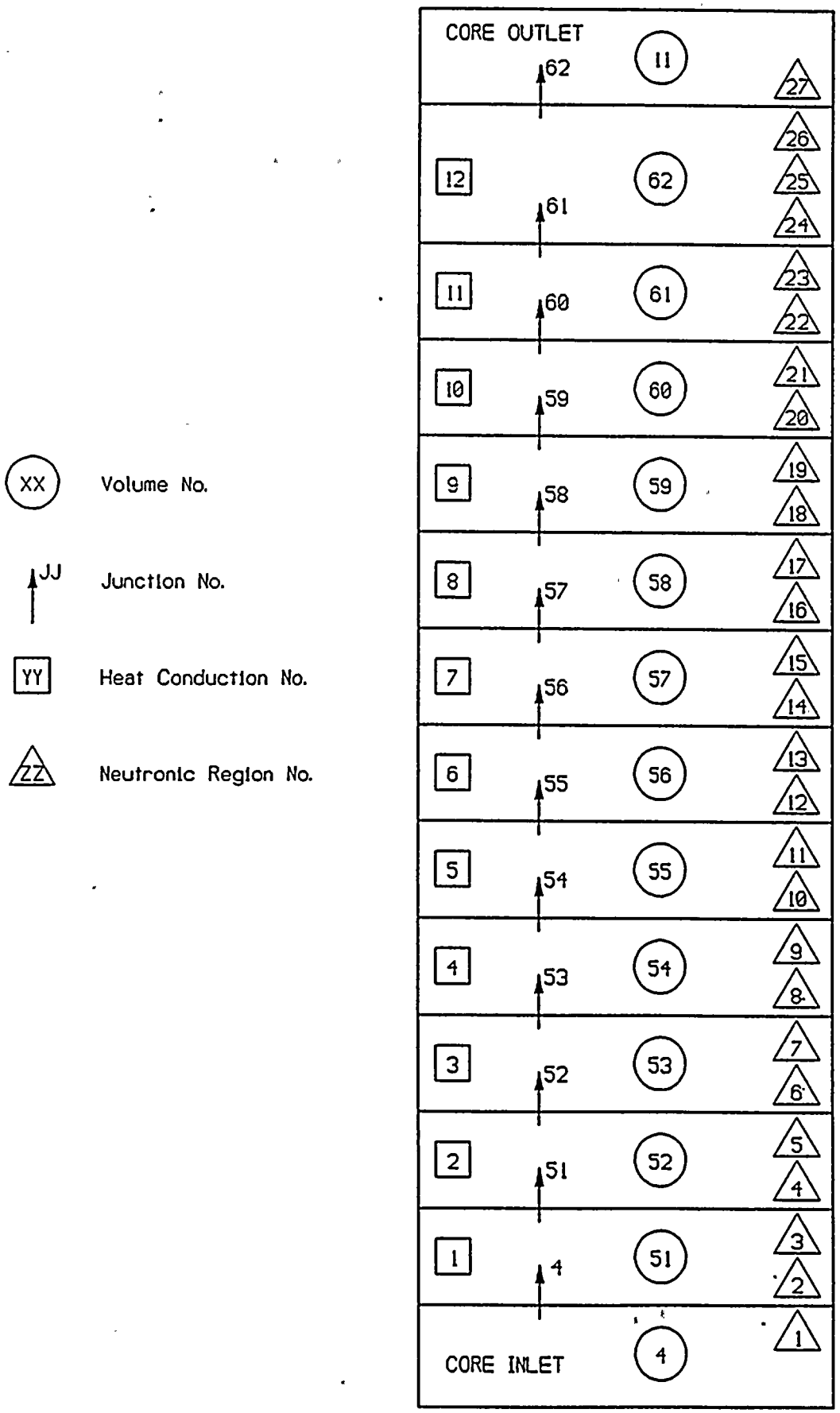

FIGURE 2.3

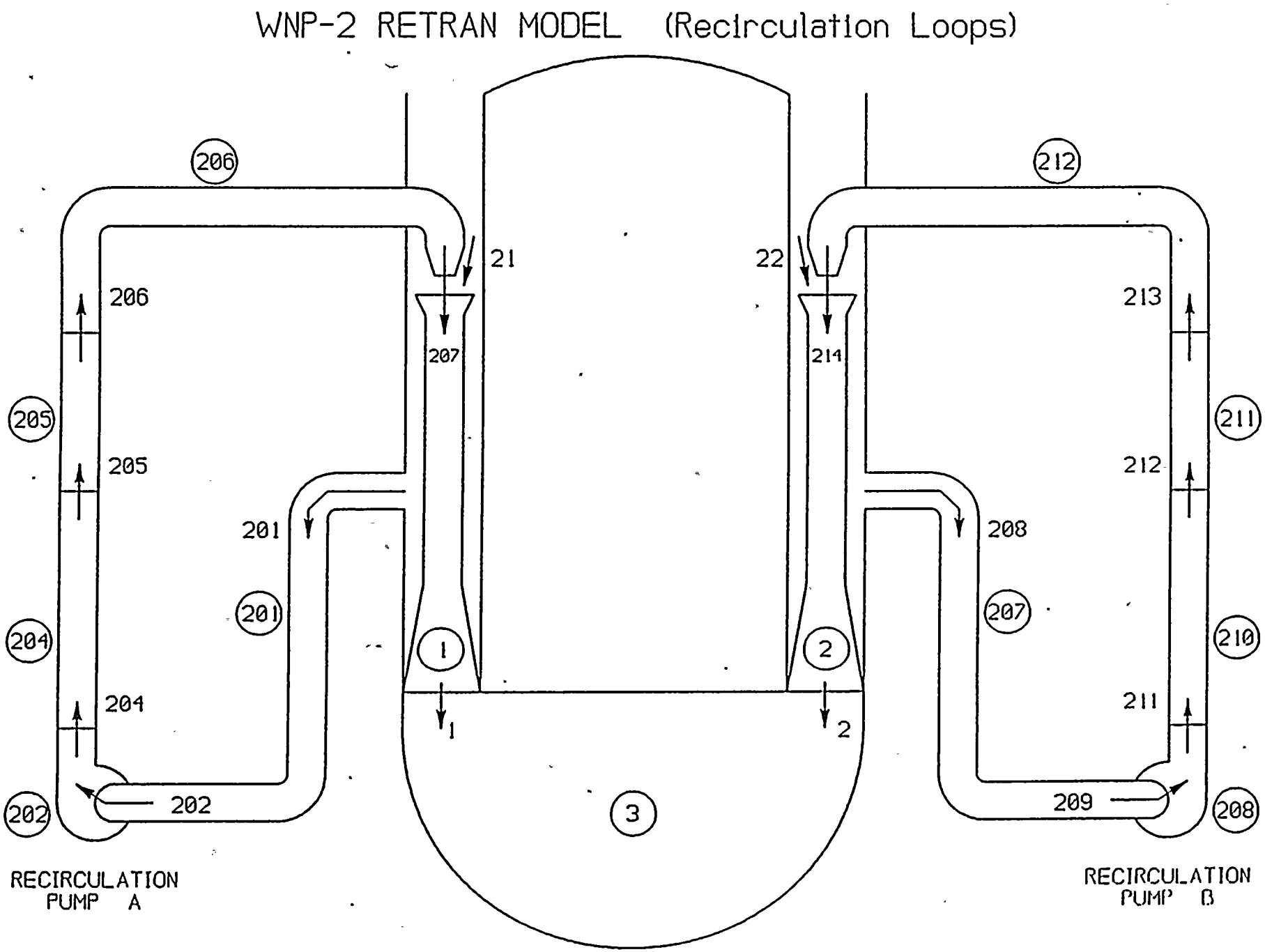
WNP-2 RETRAN MODEL (Recirculation Loops)
206
212
21
22
206
213
207
214
205
211
205
212
201
208
201
207
204
210
1
2
204
211
1
2
202
202
209
208
3
RECIRCULATION PUMP A
RECIRCULATION PUMP B

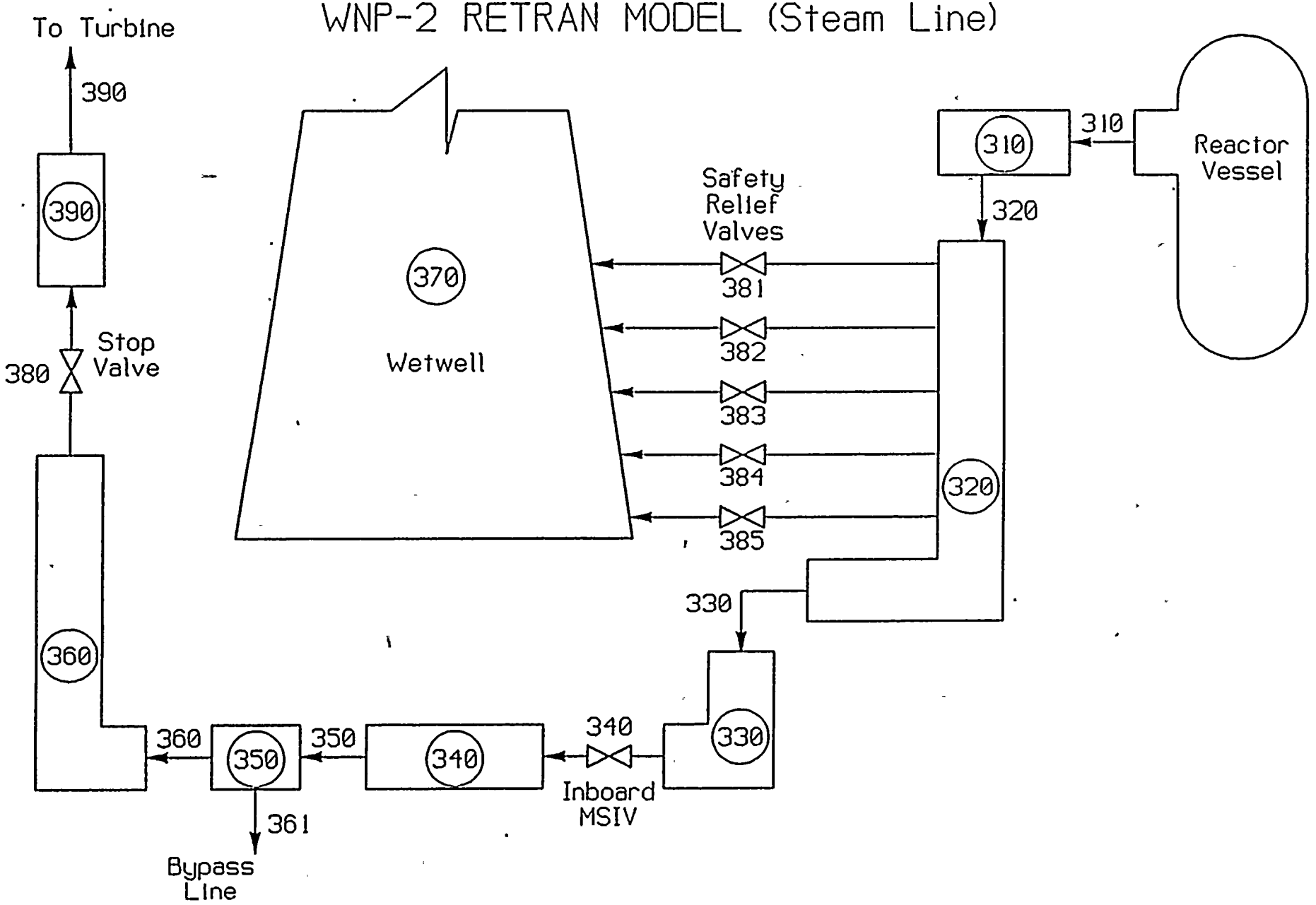
WNP-2 RETRAN MODEL (Steam Line)
To Turbine
390
390
Stop Valve
380
360
370
Wetwell
Safety Relief Valves
381
382
383
384
385
310
310
Reactor Vessel
320
320
330
330
340
340
Inboard MSIV
350
350
360
361
Bypass Line

2.1 Model Geometry

2.1.1 Control volumes, Junctions, and Heat Conductors

The geometric data used in calculating the control volumes, junctions, and heat conductors was obtained from as-built plant drawings.

The control volume nodes are defined as distinct regions within the primary system, such as the steam dome or downcomer. Where further nodalization is required due to limits in code assumptions, these regions are divided into subregions (e.g., upper, middle, lower downcomers). System components such as jet pumps, steam separators, and recirculation pumps are also typically described as single control volumes.

A list of the key input parameters for the control volumes, junctions, and heat conductors is presented in Tables 2.1.1 through 2.1.3. A brief description of the nodalization is presented in Sections 2.1.2 through 2.1.5.

2.1.2 Steam and Feedwater Lines

The four main steam lines are lumped into one composite line, which is divided into seven control volumes (see Figure 2.4). Three of the volumes model the steam lines inboard of the Main

Steam Isolation Valves (MSIVs). The second inboard volume (Vol. 320) is connected to the junctions representing the safety/relief valves. The next three volumes model the steam lines from MSIVs to the turbine stop valves. The third outboard volume (Vol. 360) provides the pressure feedback signal to the Pressure Control System. The last steam line volume (Vol. 390) models the piping which connects the turbine stop valve and the turbine control valves.

The flows from steam line to the turbine (through Jct. 390) and to the condenser (through Jct. 361) are modeled as negative fill junctions with flow rates controlled by the Pressure Control System.

The feedwater lines are modeled as a positive fill junction with flow rate controlled by the Feedwater Control System. Explicit modeling of the lines and pumps is not necessary for transient simulation.

2.1.3 Vessel Internals

A single volume is used to model the steam space above the steam separators. The downcomer region is divided into three volumes. The upper downcomer volume models the region surrounding the steam separators and includes the normal steam-water interface. This volume is modeled using the RETRAN 'non-equilibrium' option

to allow superheating of the steam above the steam-water interface during pressurization events. The middle downcomer volume models the region surrounding the standpipes. This is the volume where the feedwater flow mixes with the liquid flow from the steam separators . The lower downcomer volume models the region surrounding the core shroud and jet pumps. Flows to the recirculation loops and jet pump suctions are from this volume.

A single volume is used to model the fluid region below the core support plate (lower plenum). The upper plenum region above the upper guide plate and the standpipes are both modeled as single volumes. A single volume is used to model the internal region of the 225 steam separators.

2.1.4 Recirculation Loops

The two recirculation loops are modeled separately. In each recirculation loop, five control volumes are used to represent the recirculation pump and loop piping. A single volume is used to model ten jet pumps driven by the recirculation loop. A special two-stream momentum mixing option is used by RETRAN to describe the interaction of the recirculation loop drive flow with the suction flow from the downcomer. A more detailed description of the recirculation pump and jet pump is provided in Section 2.2.

2.1.5 Core Region

Twelve control volumes are used to model the active region of the core. Additionally, single volumes are used to model the unheated core inlet region and core outlet region. The entire core bypass region is modeled with one control volume.

Twelve heat conductors are used to represent the reactor fuel, one per active volume. A standard, cylindrical, three-region representation of the fuel rods is used with six nodes in the fuel, one node in the gap and four nodes in the cladding. The material conductivity and heat capacity for the UO2 fuel and the Zircaloy cladding are taken from MATPRO[5] and WREM[6] data. A constant value provided by vendor[7] is used for the gap conductance in the average core region.

The calculated water density of each active core and reflector volume and fuel temperature from each heat conductor are used to provide feedback to the associated neutronic regions (see Figure 2.2). A total of twenty-seven neutronic regions are used in the one-dimensional kinetics calculation (Twenty-five in the active core and one per reflector volume).

A RETRAN non-conducting heat exchanger model is used to model the addition of direct heating to the core bypass volume. A constant fraction of the core power is used for the core bypass heating.

The direct moderator heating model is included to account for direct energy deposition into the active core volumes due to gamma and neutron heating.

TABLE 2.1.1

VOLUME GEOMETRIC DATA

VOLUME NUMBER	VOLUME (FT3)	HEIGHT (FT)	FLOW LENGTH (FT)	FLOW AREA (FT2)	HYDRAULIC DIAMETER (FT)	ELEV. (FT)	DESCRIPTION
1	136.942	16.517	16.517	19.897	1.592	9.917	JET PUMP
2	136.942	16.517	16.517	19.897	1.592	9.917	JET PUMP
3	2240.000	17.281	21.450	114.280	0.781	0.000	LOWER PLENUM
4	66.640	0.745	0.745	89.474	0.045	17.281	CORE INLET
11	111.280	1.198	1.198	83.955	0.045	30.526	CORE EXIT
12	950.708	14.443	14.443	65.825	0.182	17.281	CORE BYPASS
13	943.000	3.816	3.816	247.120	17.738	31.724	UPPER PLENUM
14	400.000	8.918	8.918	44.853	0.505	35.540	STANDPIPE
15	442.834	6.167	7.092	71.807	0.641	44.458	SEPARATOR
16	6285.300	18.544	21.100	270.000	20.768	50.615	DOME
18	2196.700	10.221	8.531	257.496	2.256	34.302	MID DOWNCOMER
19	2498.700	24.177	9.960	103.350	2.162	10.125	LOWER DOWNCOMER
20	1901.700	7.812	7.812	149.621	0.732	42.823	UPPER DOWNCOMER
51	83.955	1.000	1.000	83.955	0.045	18.026	ACS #1
52	83.955	1.000	1.000	83.955	0.045	19.026	ACS #2
53	83.955	1.000	1.000	83.955	0.045	20.026	ACS #3
54	83.955	1.000	1.000	83.955	0.045	21.026	ACS #4
55	83.955	1.000	1.000	83.955	0.045	22.026	ACS #5
56	83.955	1.000	1.000	83.955	0.045	23.026	ACS #6
57	83.955	1.000	1.000	83.955	0.045	24.026	ACS #7
58	83.955	1.000	1.000	83.955	0.045	25.026	ACS #8
59	83.955	1.000	1.000	83.955	0.045	26.026	ACS #9
60	83.955	1.000	1.000	83.955	0.045	27.026	ACS #10
61	83.955	1.000	1.000	83.955	0.045	28.026	ACS #11
62	125.933	1.500	1.500	83.955	0.045	29.026	ACS #12
201	148.000	34.682	58.360	2.536	1.797	-19.409	RRC #1 SUCTION
202	30.500	3.375	12.027	2.536	1.797	-16.510	RRC #1 PUMP
204	115.000	21.979	45.347	2.536	1.797	-15.492	RRC #1 HEADER INLET
205	43.500	1.193	9.727	2.236	1.193	6.487	RRC #1 HEADER
206	91.710	20.116	25.980	3.530	0.948	7.680	RRC #1 RISER
207	148.000	34.682	58.360	2.536	1.797	-19.409	RRC #2 SUCTION
208	30.500	3.375	12.027	2.536	1.797	-16.510	RRC #2 PUMP
210	115.000	21.979	45.347	2.536	1.797	-15.492	RRC #2 HEADER INLET
211	43.500	1.193	9.727	2.236	1.193	6.487	RRC #2 HEADER
212	91.710	20.116	25.980	3.530	0.948	7.680	RRC #2 RISER
310	446.430	33.509	37.490	11.908	1.947	21.464	STEAM OUTLET
320	275.370	2.200	23.125	11.908	1.947	21.206	STEAM LINE
330	555.400	39.090	46.641	11.908	1.947	-15.930	STEAM LINE
340	504.280	7.146	42.348	11.908	1.947	-21.792	STEAM LINE
350	2747.160	6.861	170.589	16.104	2.264	-28.650	STEAM LINE
360	1654.540	25.882	102.741	16.104	2.264	-40.903	STEAM LINE
370	2.56E+5	42.610	42.610	4520.000	75.862	21.460	CONTAINMENT
390	86.750	2.350	10.001	8.674	2.350	-16.196	STEAM LINE

TABLE 2.1.2

JUNCTION GEOMETRIC DATA

JCT. NO.	CONNECTS VOLUME FROM	TO	FLOW AREA (FT2)	ELEV. (FT)	INERTIA (1/FT)	LOSS COEF.	HYDRAULIC DIAMETER (FT)	DESCRIPTION
1	1	3	19.8970	9.9170	0.5089	1.8300	1.5920	JET PUMP #1 DISCH
2	2	3	19.8970	9.9170	0.5089	1.8300	1.5920	JET PUMP #2 DISCH
3	3	4	22.6680	17.2813	0.0980	-1.0000	0.1960	CORE INLET
4	4	51	54.1390	18.0261	0.0101	3.2690	0.0270	CORE #1 INLET
10	62	11	63.0464	30.5261	0.0161	0.4117	0.0319	ACS #12 EXIT
11	11	13	83.9550	31.7240	0.0149	0.7300	0.0446	CORE OUTLET
12	12	13	55.9920	31.7240	0.1174	0.6800	0.3022	BYPASS OUTLET
13	13	14	45.1400	35.5400	0.1071	0.4100	0.5054	STANDPIPE INLET
14	14	15	33.7960	44.4580	0.4390	-1.0000	0.1569	SEPARATOR INLET
15	15	16	30.6800	50.6250	0.0885	-1.0000	0.4167	SEPARATOR OUTLET
16	20	16	239.3200	50.6250	0.0652	23.5000	0.0518	LOWER DOME INLET
17	20	18	149.6210	42.8330	0.0427	0.1800	0.7320	MID DOWNCOMER INLET
18	18	19	85.1340	34.3020	0.0648	0.2700	2.7500	LOWER DOWNCOMER IN
19	4	12	1.5000	17.2813	0.1139	-1.0000	0.0028	CORE BYPASS INLET #2
20	3	12	0.8420	17.2813	0.2036	6.9851	0.0019	CORE BYPASS INLET #1
21	19	1	1.7730	26.4340	4.7330	0.0542	0.2100	JET PUMP #1 SUCTION
22	19	2	1.7730	26.4340	4.7330	0.0542	0.2100	JET PUMP #2 SUCTION
23	15	18	51.8250	44.5030	0.0659	4.0100	0.0895	UPPER DOWNCOMER IN
51	51	52	83.9550	19.0261	0.0119	0.0000	0.0446	ACS #1 EXIT
52	52	53	83.9550	20.0261	0.0119	1.2400	0.0446	ACS #2 EXIT
53	53	54	83.9550	21.0261	0.0119	1.2400	0.0446	RCS #3 EXIT
54	54	55	83.9550	22.0261	0.0119	0.0000	0.0446	ACS #4 EXIT
55	55	56	83.9550	23.0261	0.0119	1.2400	0.0446	ACS #5 EXIT
56	56	57	83.9550	24.0261	0.0119	0.0000	0.0446	ACS #6 EXIT
57	57	58	83.9550	25.0261	0.0119	1.2400	0.0446	ACS #7 EXIT
58	58	59	83.9550	26.0261	0.0119	1.2400	0.0446	ACS #8 EXIT
59	59	60	83.9550	27.0261	0.0119	0.0000	0.0446	ACS #9 EXIT
60	60	61	83.9550	28.0261	0.0119	1.2400	0.0446	ACS #10 EXIT
61	61	62	83.9550	29.0261	0.0149	1.2400	0.0446	ACS #11 EXIT
201	19	201	2.5360	14.3750	11.5544	0.2450	1.7969	RRC LOOP #1
202	201	202	2.5360	-16.5100	13.8775	0.6300	1.7969	RRC LOOP #1
204	202	204	1.7924	-15.4920	11.3119	-1.0000	1.7969	RRC LOOP #1
205	204	205	2.5360	6.4870	11.1157	0.5460	1.7969	RRC LOOP #1
206	205	206	3.5300	7.6800	5.8550	1.2860	0.9480	RRC LOOP #1
207	206	1	0.4609	26.4340	3.8530	0.2122	0.1083	RRC LOOP #1
208	19	207	2.5360	14.3750	11.5544	0.2450	1.7969	RRC LOOP #2
209	207	208	2.5360	-16.5100	13.8775	0.6300	1.7969	RRC LOOP #2
211	208	210	1.7924	-15.4920	11.3119	-1.0000	1.7969	RRC LOOP #2
212	210	211	2.5360	6.4870	11.1157	0.5460	1.7969	RRC LOOP #2
213	211	212	3.5300	7.6800	5.8550	1.2860	0.9480	RRC LOOP #2
214	212	2	0.4609	26.4340	3.8530	0.2122	0.1083	RRC LOOP #2
310	16	310	11.9080	54.0000	1.6132	0.2721	1.9470	STEAM LINE
320	310	320	11.9080	22.4300	2.5451	0.3391	1.9470	STEAM LINE

TABLE 2.1.2 (CONT.)

JUNCTION GEOMETRIC DATA

JCT. NO.	CONNECTS VOLUME FROM	TO	FLOW AREA (FT2)	ELEV. (FT)	INERTIA (1/FT)	LOSS COEF.	HYDRAULIC DIAMETER (FT)	DESCRIPTION
330	320	330	3.6370	22.1800	2.9294	0.1852	1.0760	STEAM LINE
340	330	340	4.1250	-15.1300	3.7365	0.1541	1.1460	STEAM LINE
350	340	350	16.1040	-21.7920	7.0746	0.4203	1.9470	STEAM LINE
360	350	360	16.1040	-27.5200	8.4864	1.1780	2.2640	STEAM LINE
380	360	390	14.1860	-15.0210	3.7664	2.5762	2.1250	STEAM LINE
381	320	370	0.2238	21.4600	0.9757	0.2630	0.3775	SRV INLET
382	320	370	0.4477	21.4600	0.9757	0.2630	0.3775	SRV INLET
383	320	370	0.4477	21.4600	0.9757	0.2630	0.3775	SRV INLET
384	320	370	0.4477	21.4600	0.9757	0.2630	0.3775	SRV INLET
385	320	370	0.4477	21.4600	0.9757	0.2630	0.3775	SRV INLET
602	0	13	1.0000	31.7240	0.0077	0.0000	1.1284	HPCS
601	0	16	1.0000	69.1580	0.0391	0.0000	1.1284	RCIC LINE
490	0	18	5.0000	41.1000	0.0166	0.0000	0.1333	FEEDWATER LINE
390	0	390	1.0000	-16.1960	0.5765	-1.0000	1.1280	TURBINE NEG FILL
361	0	350	1.0000	-28.6500	5.2965	-1.0000	1.3440	STEAM BYP NEG FILL

TABLE 2.1.3

HEAT CONDUCTOR GEOMETRIC DATA

HEAT COND. NO.	VOLUME ON: LEFT (INSIDE)	RIGHT (OUTSIDE)	GEOMETRY TYPE	NO.	CONDUCTOR VOLUME (FT3)	SURFACE AREA LEFT (FT2)	RIGHT (FT2)	DESCRIPTION
1	0	51	CYL.	1	60.27	0.	5990.	FUEL RODS CORE 1
2	0	52	CYL	1	60.27	0.	5990.	FUEL RODS CORE 2
3	0	53	CYL.	1	60.27	0.	5990.	FUEL RODS CORE 3
4	0	54	CYL.	1	60.27	0.	5990.	FUEL RODS CORE 4
5	0	55	CYL.	1	60.27	0.	5990.	FUEL RODS CORE 5
6	0	56	CYL	1	60.27	0.	5990.	FUEL RODS CORE 6
7	0	57	CYL.	1	60.27	0.	5990.	FUEL RODS CORE 7
8	0	58	CYL.	1	60.27	0.	5990.	FUEL RODS CORE 8
9	0	59	CYL.	1	60.27	0.	5990.	FUEL RODS CORE 9
10	0	60	CYL	1	60.27	0.	5990.	FUEL RODS CORE 10
11	0	61	CYL.	1	60.27	0.	5990.	FUEL RODS CORE 11
12	0	62	CYL.	1	60.27	0.	5990.	FUEL RODS CORE 12

2.2 Component models

The transient behavior of a BWR is influenced by the characteristics of its various components (i.e., pumps, separators, etc.). A description of the major component models in the WNP-2 RETRAN model is given in this section.

2.2.1 Safety/Relief Valves

WNP-2 has 18 relief valves arranged in groups of 2 to 4 valves at a common setpoint. Each of the groups of valves at a common setpoint is represented by a junction connecting the steam line to a sink volume in the RETRAN model. The area of the junctions is taken as the flow area of the valve times the number of valves being modeled. When the valve is opened with the steam line pressurized, the junction flow becomes choked and the Moody critical flow option is chosen in RETRAN to calculate the choked flow rate. Contraction coefficients are used on valve junctions to get the specified flow at the reference pressure.

The opening and closing of the relief valve junctions is controlled by the RETRAN trips based on the pressure in the steam line volume (Vol. 320) containing the relief valves. When the volume 320 pressure reaches the specified setpoint pressure, the valve is opened linearly after a specified delay. When the

pressure drops below the reclosure pressure, the valve is completely closed in a stepwise manner.

2.2.2 Steam Separators

The steam separators couple the reactor core and the steam dome. The appropriate emphasis in modeling the separators is on achieving the proper coupling between these regions.

The 225 steam separators are modeled as a single component. An equilibrium volume is used with the standard RETRAN phase separation model (i.e., Bubble Rise model). Referring to Figure 2.1, the interior of the separators is represented by volume 15. The entering two-phase fluid flow is represented by junction 14. Separation takes place within volume 15. Junctions 15 and 23 represent the steam and separated liquid flow paths.

The separator input parameters which have the most significant affect on system response are the separator inlet inertia and the pressure drop across the separators. The separator inertia is determined from vendor's data[8]. It is calculated as a function of the separator inlet quality at the transient initial condition. The separator inlet and exit loss coefficients are determined by RETRAN using the steady state initialization option. The pressure drop distribution at the rated operating condition has been checked to be in agreement with vendor's calculation[7].

2.2.3 Recirculation Pumps

The centrifugal pump model in RETRAN is used to represent the WNP-2 recirculation pumps. The pump unique characteristics (i.e., moment of inertia, rated values for pump flow, head and torque) and the pump homologous curves supplied to the RETRAN pump model are based on pump manufacturer's data[9]. Since the recirculation flow control is achieved by varying the position of the flow control valve, not by varying the pump speed, the recirculation pump motor is modeled with a constant speed.

2.2.4 Jet Pumps

Each recirculation loop in the WNP-2 RETRAN model drives ten jet pumps lumped as one. The RETRAN jet pump model option (momentum mixing) is used to simulate the momentum exchange between the jet pump drive flow and suction flow in the jet pump throat section. A single control volume is used to model each lumped jet pump.

Jet pump behavior is characterized through the M-ratio and N-ratio (M-N) dependency. The M-ratio is the ratio of suction flow to the drive flow. The N-ratio is the ratio of specific energy increase of the suction flow to the specific energy decrease in the drive flow. The M-N characteristic is a curve of N-ratio as

a function of M-ratio. To determine the WNP-2 jet pump M-N characteristic, a RETRAN sub-model of the recirculation loop and jet pumps was set up. Pressure distribution data from the vendor[10] was used to determine the suction and drive nozzle loss coefficients. All other junction and volume geometry data were calculated using design drawings. The M-N curve generated with this model is compared to vendor's data in Figure 2.2.1. The comparison shows that this modeling technique provides an acceptable representation of the performance characteristic of the WNP-2 jet pumps.

2.2.5 Core Hydraulic Performance

Core flow performance is determined by hydraulic form loss coefficients. Appropriate values for these coefficients are determined through sensitivity studies linking core flow to core inlet enthalpy, reactor pressure, core power level, and power distribution. The form loss coefficients are set to match values calculated with a steady-state thermal-hydraulic model which was developed with the FIBWR code[11] and has been benchmarked against plant data. Initial values of core bypass flow and core support plate pressure drop are determined by steady-state thermal-hydraulic calculation and input to RETRAN. The RETRAN algebraic slip option is used to account for differences in in-core phase velocities. The subcooled void model is included for neutronic feedback calculation.

FIGURE 2.2.1

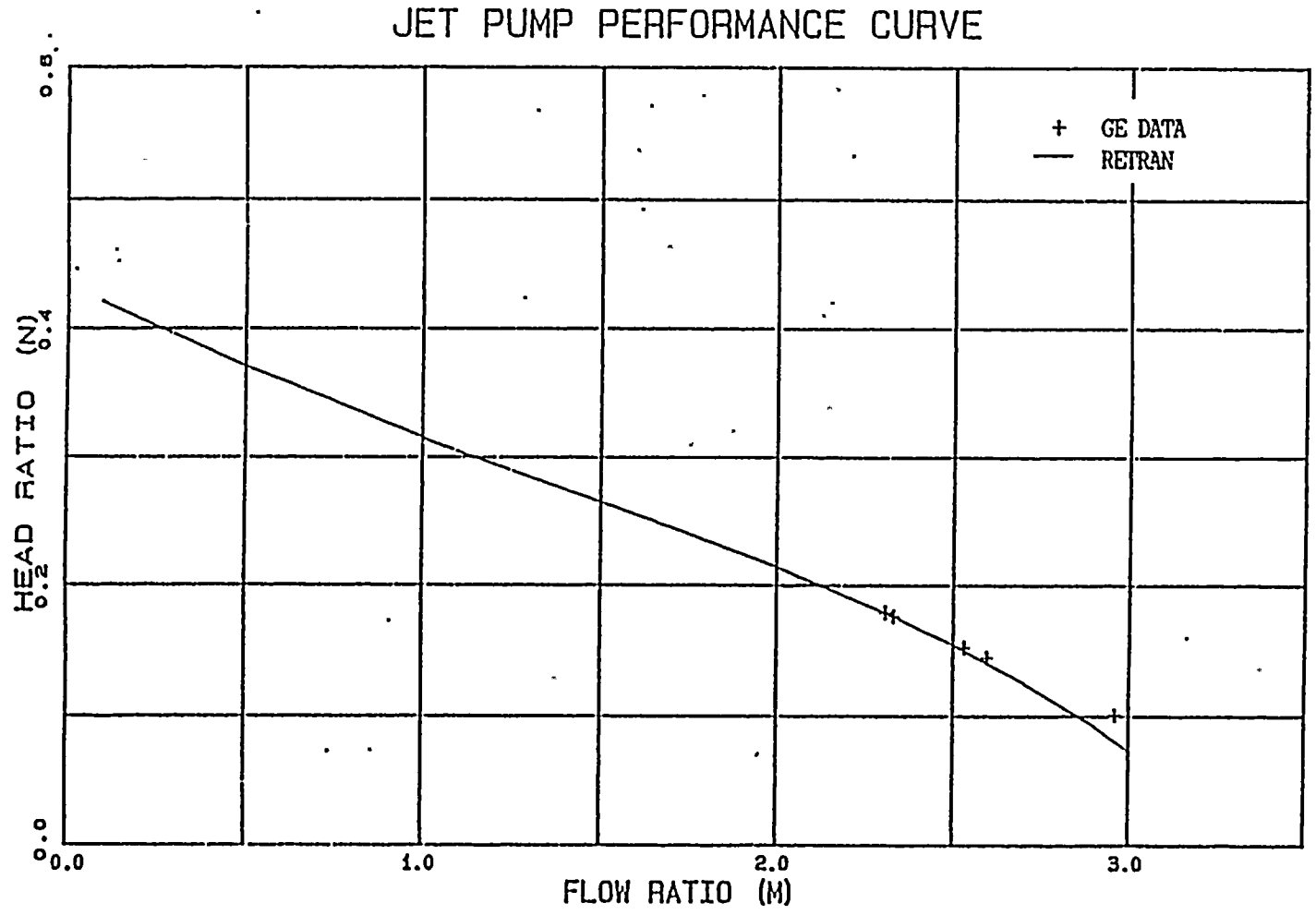
JET PUMP PERFORMANCE CURVE
+ GE DATA
RETRAN
HEAD RATIO (N)
0.0
0.2
0.4
0.6
0.0
1.0
2.0
3.0
FLOW RATIO (M)

2.3 Trip Logic

RETRAN provides switching type control elements (i.e., trips) which allow for the actuation of various process events such as the activation of a pump or the closure of a valve. These actuations may be accomplished either directly, by specifying the process variable trip setpoint or indirectly, by specifying the time at which a particular trip is to occur. This trip logic is used in the WNP-2 RETRAN model to simulate the Reactor Protection System (RPS) and to initiate various transients and equipment actuations or failures. Table 2.3.1 provides a listing of the trip logic in the WNP-2 RETRAN model. This trip logic can be expanded to incorporate additional trips if they are needed.

TABLE 2.3.1

DESCRIPTION OF TRIP LOGIC

TRIP ID	ACTION TAKEN	CAUSES OF TRIP ACTIVATION
01	End calculation	Simulate transient time > setpoint
02	Turbine Trip (initiate stop valve closure)	Control block -8 (water level) > setpoint (L8)
03	Initiate MSIV closure	Control block -8 (water level) < setpoint (L2) Volume 360 (turbine inlet) pressure < setpoint
05	Initiate Scram	Normalized power > setpoint Volume 16 (steam dome) pressure > setpoint Control block -8 (water level) < setpoint (L3) Trip #02 activated Trip #03 activated
06	Open S/R valve group 1	Volume 320 (steam line) pressure > setpoint
-06	reclose S/R valve group 1	Volume 320 (steam line) Pressure < setpoint
	Trips +07 through +10 are used for other four S/R valve groups	
11	Trip recirculation pumps	Simulated transient time > setpoint Trip #02 activated Volume 16 (steam dome) pressure > setpoint Control block -8 (water level) < setpoint (L2)
12	Trip FW turbine	Control block -8 (water level) > setpoint (L8)
13	RCIC initiation	Control block -8 (water level) < setpoint (L2)
-13	Trip RCIC	Control block -8 (water level) > setpoint (L8)
14	Initiate HPCS	Control block -8 (water level) < setpoint (L2)
-14	Trip HPCS	Control block -8 (water level) > setpoint (L8)

2.4 Control Logic

The RETRAN trip controls discussed in Section 2.3 provide discrete (on/off) control. RETRAN also provides control system elements (such as summers, lags, etc.) that can be used to model various plant systems and their controllers. All RETRAN variables available for editing can be used as control element inputs. The control inputs used in the WNP-2 RETRAN model are listed in Table 2.4.1.

2.4.1 Feedwater Control System

The Feedwater Control System comprises a level control system and a feedwater flow delivery system. The level control system allows for either one-element or three-element control. In one-element control, the controller output is only a function of the difference in setpoint and sensed level. In three-element control which is normally used, an additional steam-feed mismatch is added to the level error. All controller settings and gains are based on actual plant settings and vendor's Control System Design Report[12]. The feedwater delivery system is represented by the simulation of the pump flow actuator based on vendor provided plant specific information.

Figure 2.4.1 illustrates the WNP-2 Feedwater Control System model. Upon reactor scram, the Feedwater Control System switches

to one-element control and the water level setpoint is lowered 18 inches.

2.4.2 Pressure Control System

The Pressure Control System is composed of a reactor pressure regulation system, a turbine control valve system, and a steam bypass valve system. The signals from the pressure regulation system to turbine control valve and steam bypass system can be regulated either by the difference in turbine inlet pressure and its setpoint or by the load-speed error signal. The primary settings which affect the pressure regulation system output are the regulation gain and lag-lead time constants. They are based on vendor provided data[12,13]. The turbine-generator is not modeled and the turbine speed is specified as a function of time.

Figure 2.4.2 illustrates the WNP-2 Pressure Control System model. Upon a turbine trip, the turbine control valve demand signal is grounded, thus the turbine bypass valve demand is set equal to the pressure regulator demand. This will cause the bypass valves to open immediately, rather than waiting through the pressure regulator lag time constant.

2.4.3 Recirculation Flow Control System

WNP-2 is operated with the recirculation flow control system set in manual control mode. No control element is required and the flow control valve position is modeled with a function generator.

2.4.4 Direct Bypass Heating

The nonconducting heat exchanger model is used to account for direct bypass heating. The heat removal rate for this heat exchanger is determined by a control system. It is assumed to be a constant fraction of the transient core power as shown in Figure 2.4.3.

TABLE 2.4.1

CONTROL INPUT DEFINITION

ID NO.	VARIABLE SYMBOL	DESCRIPTION
01	WP**	Steam (Jct. 330) flow (% NBR)
02	WP**	FW (Jct. 490) flow (% NBR)
03	LIQV	Middle downcomer (Vol. 18) liquid volume (ft**3)
04	LIQV	Lower downcomer (Vol. 19) liquid volume (ft**3)
05	LIQV	Upper downcomer (Vol. 20) liquid volume (ft**3)
06	CONS	Fraction of total core power deposited directly in core bypass region
07	CONS	Constant of 1.0
08	POWR	active core (less core bypass) power (MW)
09	PRES	Turbine inlet (Vol. 390) pressure (psia)
10	TRIP	Scram (trip ID=5) activation indicator
11	CONS	Constant of 0.0
12	WP**	Steam (Jct. 16) flow (% NBR)
13	PRES	Turbine stop valve inlet (Vol. 360) pressure (psia)
18	TIMX	Simulation time (sec)
19	PRES	Turbine bypass inlet (Vol. 350) pressure (psia)
21	WQCR	Heat transferred from clad to coolant for core section 1 (Btu/lbm)
		ID No. 22 through 32 are used for heat to coolant for other core sections
50	CONS	Constant of 1.0
51	TRIP	Turbine trip (ID=2) activation indicator
52	CONS	Turbine speed reference (100%)
53	CONS	Load bias (10%)

FIGURE 2.4.1

Feedwater Control System

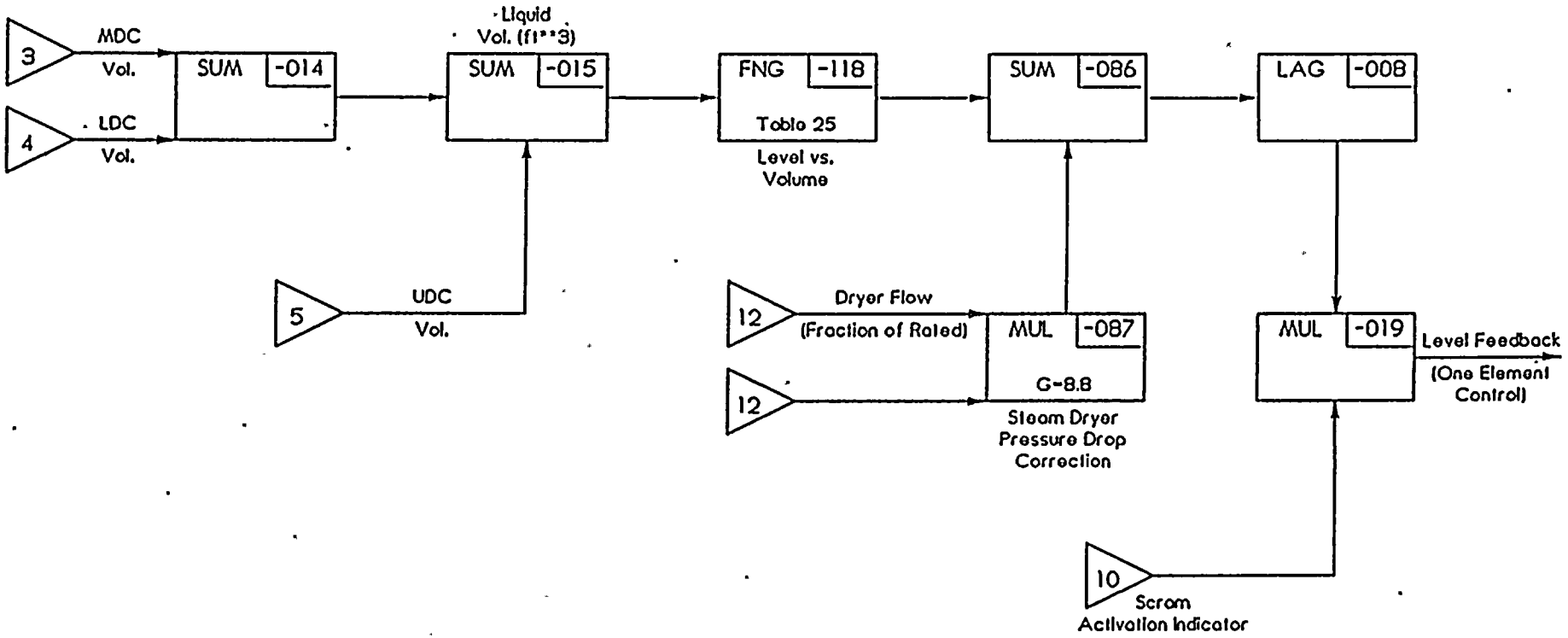

FIGURE 2.4.1 (CONT.)

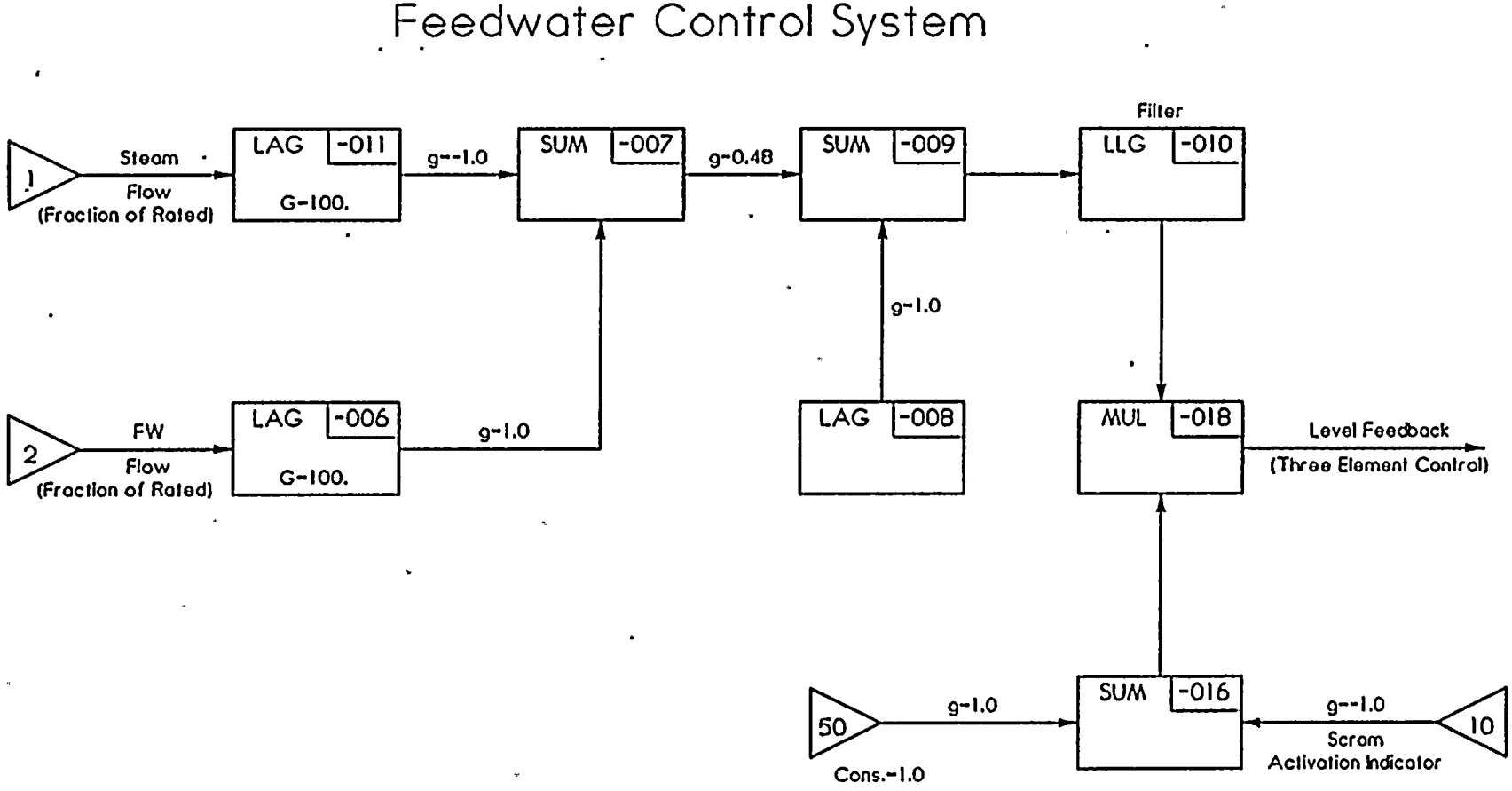

FIGURE 2.4.1 (CONT.)

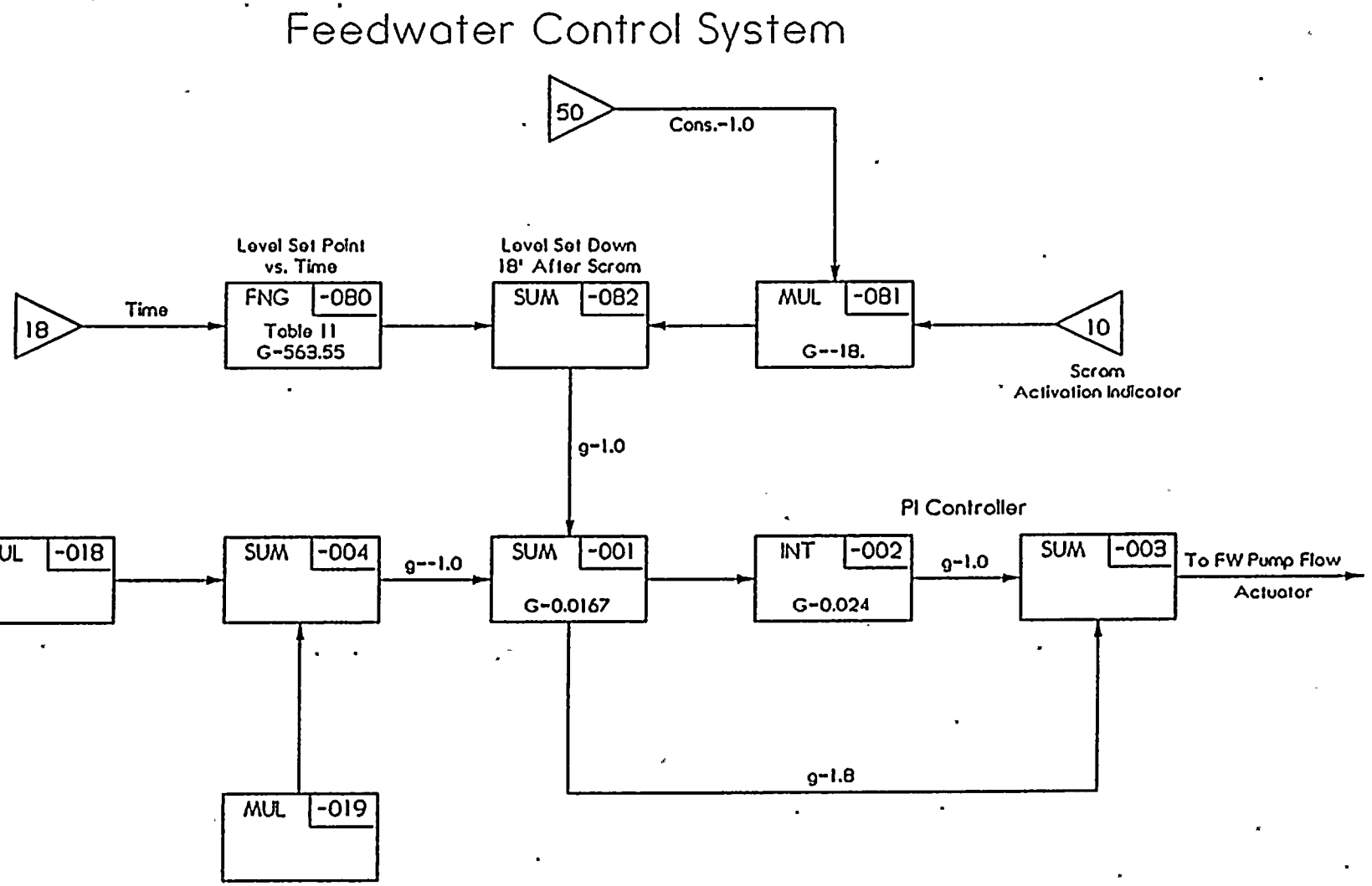

FIGURE 2.4.1 (CONT.)

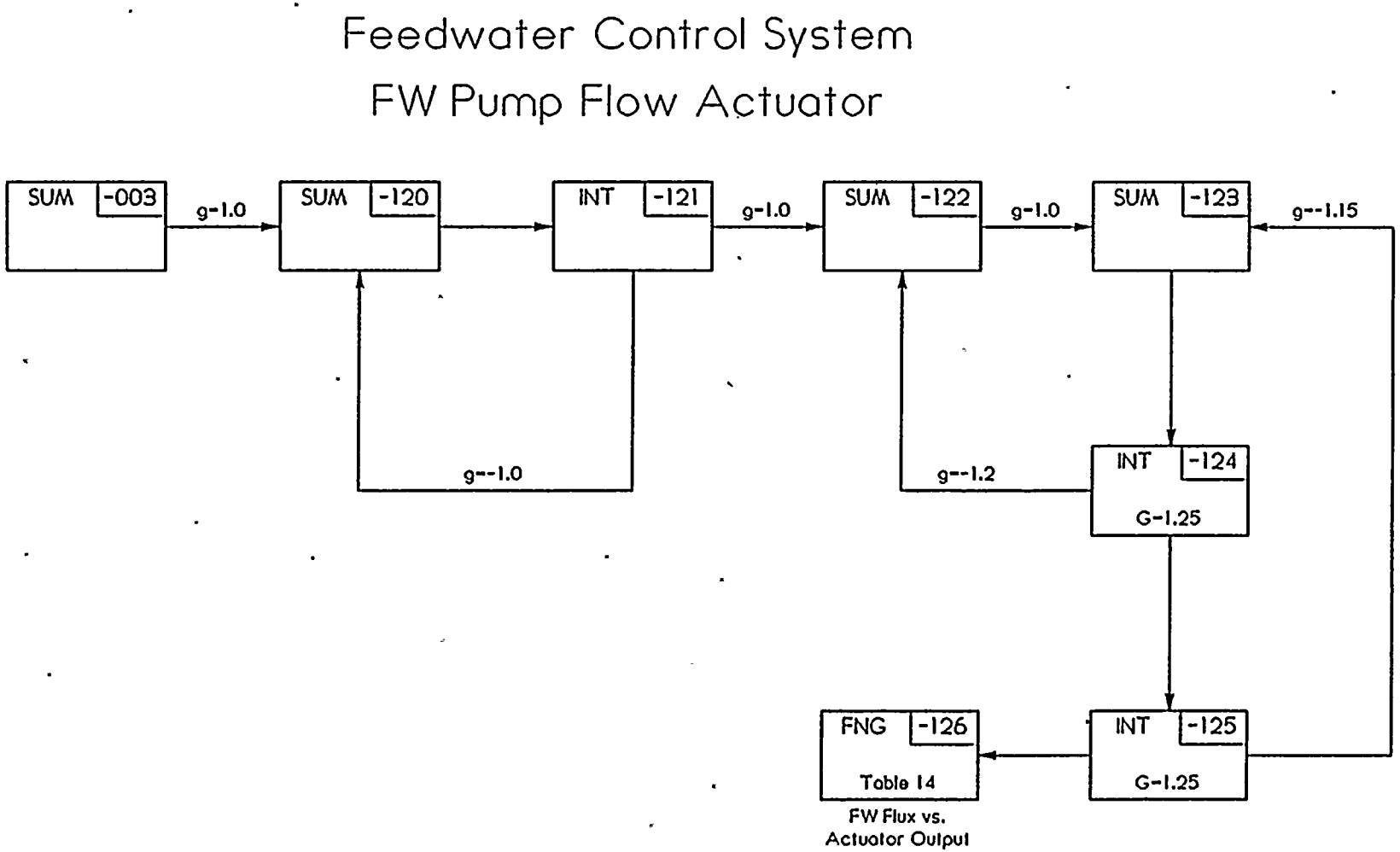

FIGURE 2.4.2

Pressure Control System

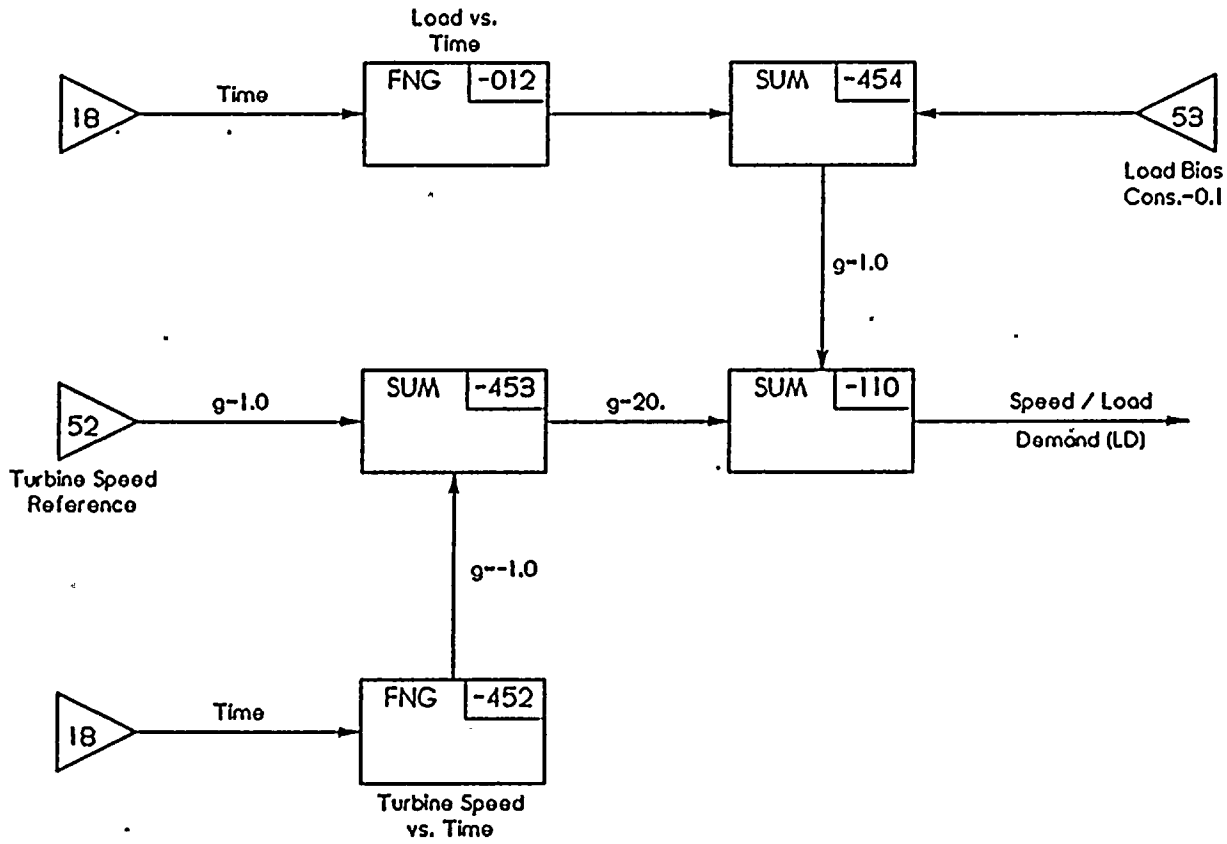

FIGURE 2.4.2 (CONT.)

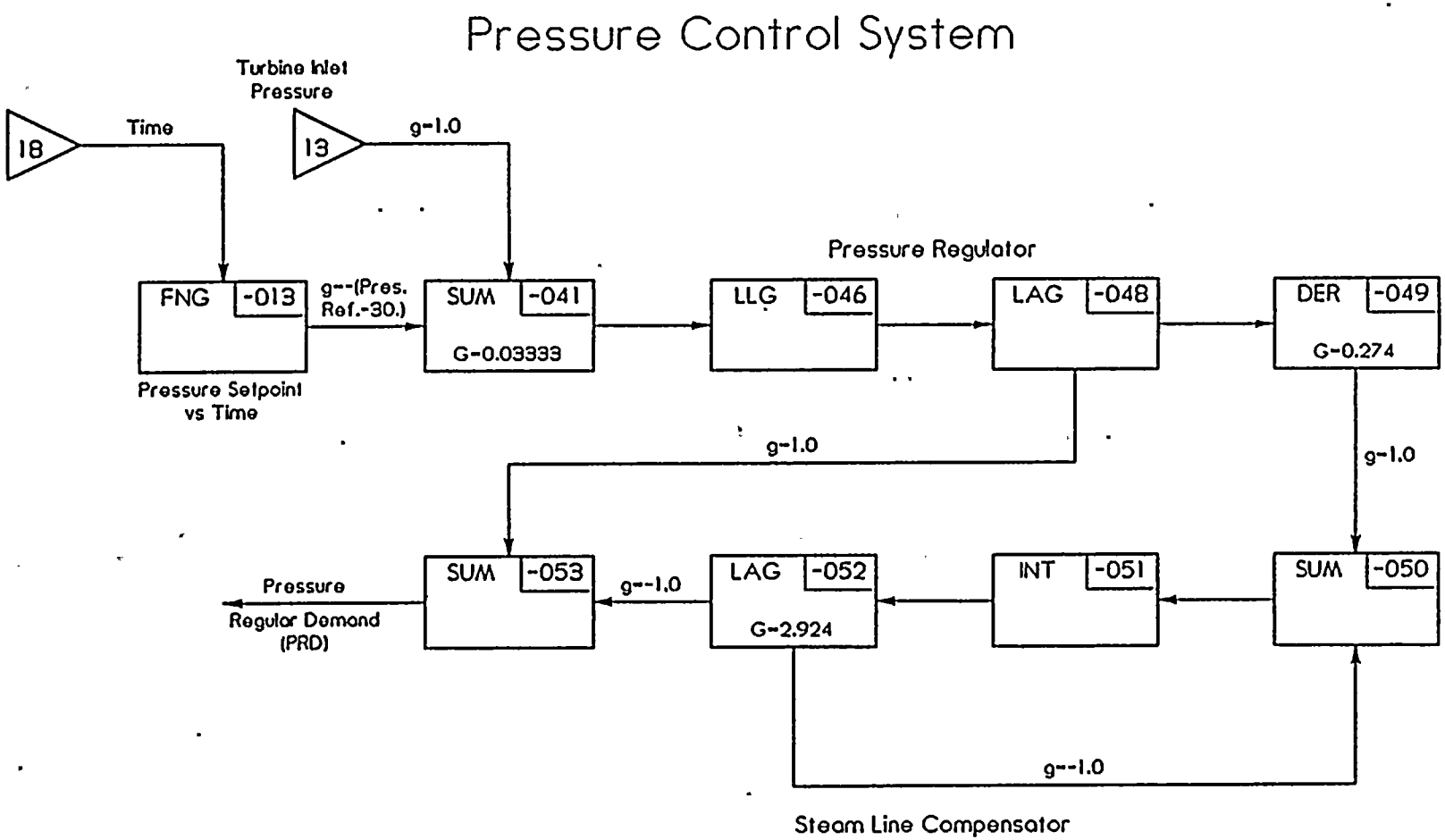

FIGURE 2.4.2 (CONT.)

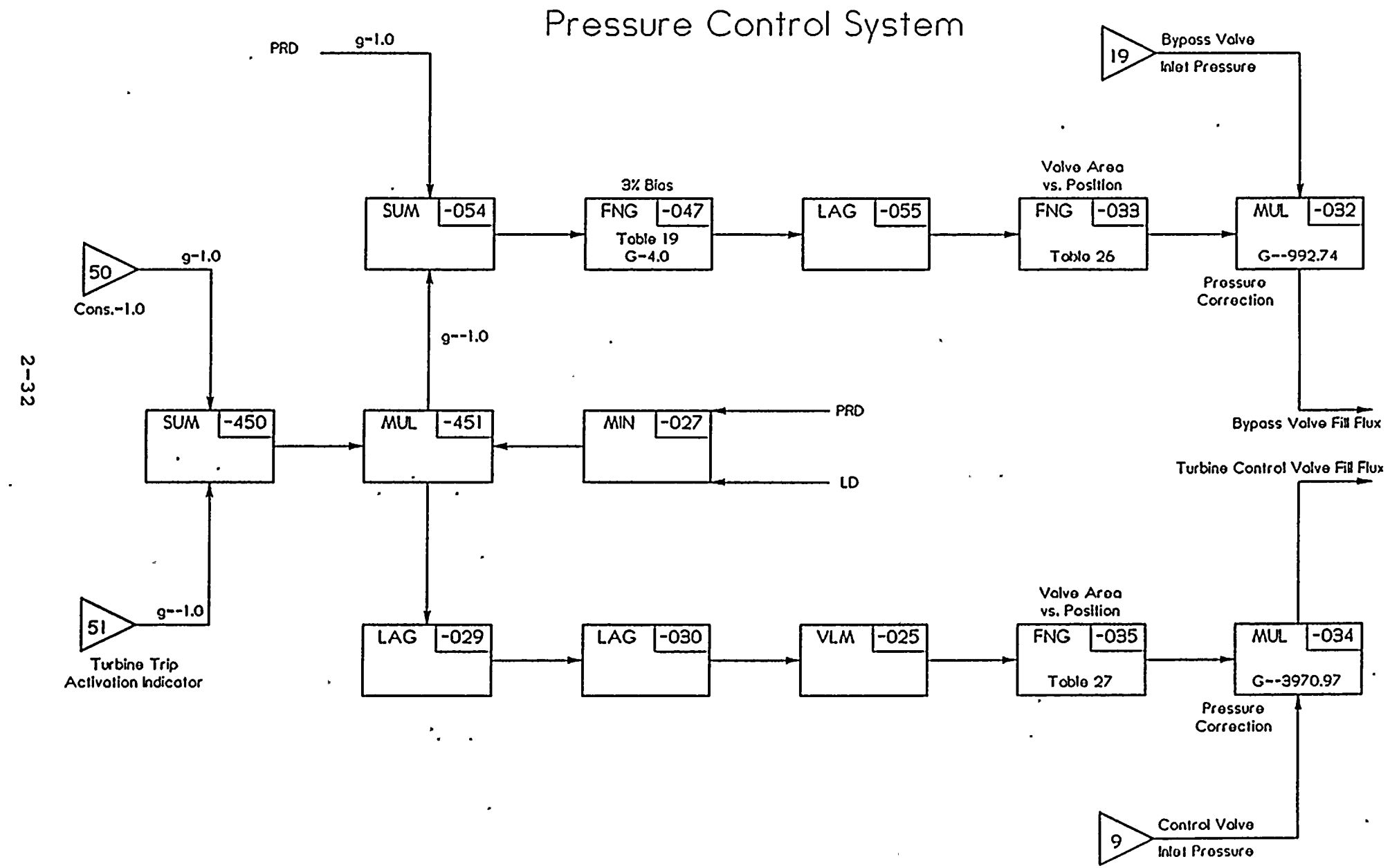

FIGURE 2.4.3

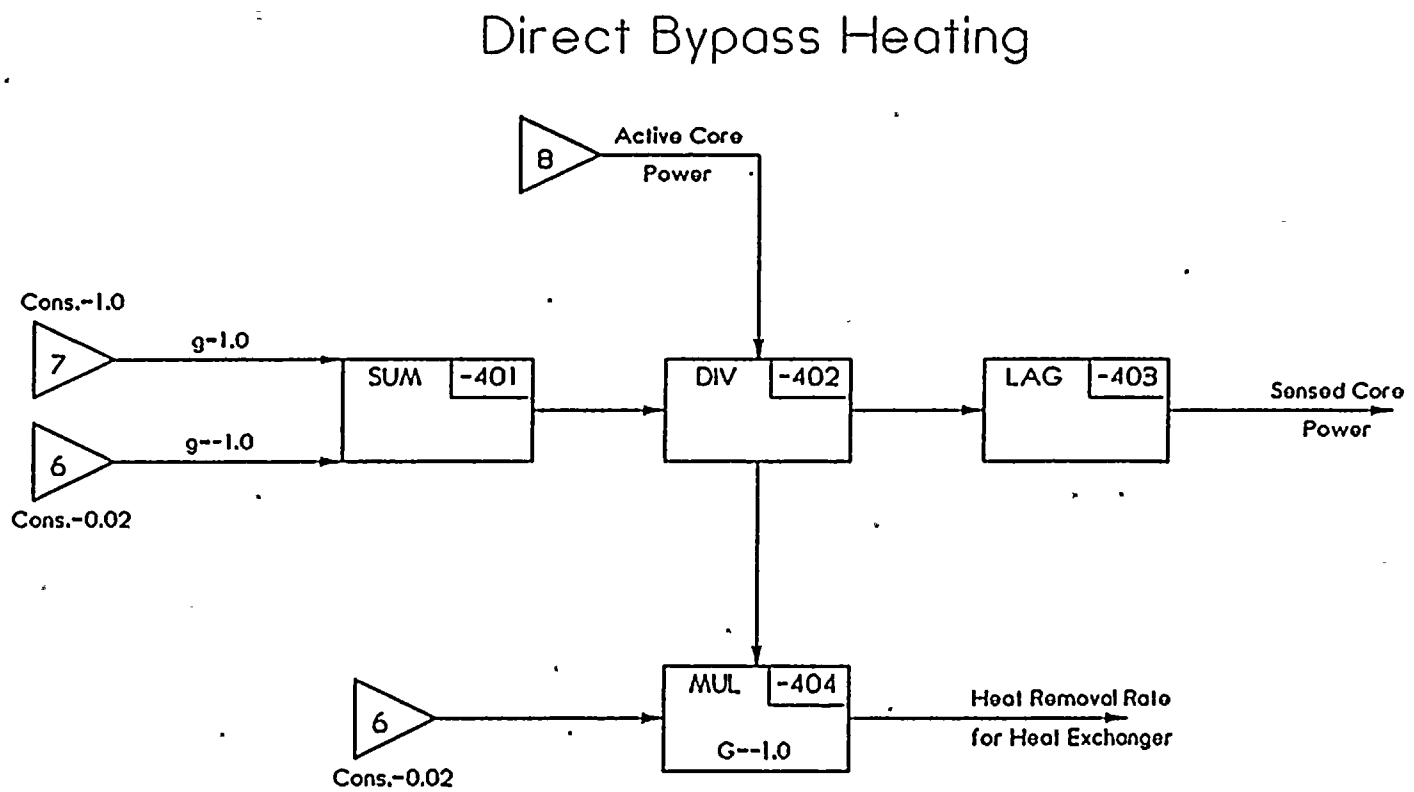
Direct Bypass Heating
8
Active Core
Power
Cons.-1.0
7
g-1.0
SUM
-401
DIV
-402
LAG
-403
Sensed Core
Power
6
g--1.0
Cons.-0.02
MUL
-404
6
G--1.0
Heat Removal Rate
for Heat Exchanger
Cons.-0.02

2.5 Steady-state Initialization

The RETRAN steady-state initialization option is used to initialize the model. The parameters specified for the initialization of WNP-2 model are dome pressure, core inlet enthalpy, core flows (flow through core active region and flow from lower plenum to core inlet region), recirculation flow, jet pump suction flow, feedwater and steam flows.

In addition to the inputs for the thermal-hydraulic initialization, the values of the various controller setpoints are specified and the output of certain active controlled elements (e.g., integrators, lags, etc.) are specified. The consistency of the thermal-hydraulic and control system initialization can be confirmed by running a null transient and observing that the values of important process variables do not deviate significantly from their initial values.

2.6 RETRAN Kinetics

The RETRAN-02 MOD04 code has both point kinetics and one-dimensional kinetics capabilities. Selection of point or one-dimensional kinetics for a given transient depends on the accuracy requirements of the simulation. Point kinetic is used in simulation where the axial power shape is relatively constant during the period of interest. Pressurization transients are

typically analyzed with one-dimensional kinetics because the reactivity effects of void collapse and control rod movement play an important role in determining the overall results of the calculation. The one-dimensional kinetics model provides a more accurate calculation of these effects (particularly control) than the point kinetics model.

All system model analyses presented in this report use nuclear cross section information prepared by the core analysis methodology described elsewhere. Computer data files containing kinetics parameter dependencies are produced by CASMO-2, and three-dimensional nodal characteristics of the core are determined in SIMULATE-E. SIMTRAN-E collapses corewide cross section from three-dimensional form to one-dimensional or point kinetics form required by RETRAN. SIMULATE-E and RETRAN calculate moderator density differently; the SIMTRAN-E cross sections are adjusted manually to account for the difference. Appendix A provides additional detail on the calculation of nuclear data for RETRAN.

3.0 QUALIFICATION

The objective of this chapter is to compare the Supply System's RETRAN simulation with WNP-2 power ascension tests (PAT) and Peach Bottom turbine trip tests. The Supply System performed these benchmark analyses to qualify the WNP-2 RETRAN model and to demonstrate user qualifications. The benchmarks comprise four WNP-2 PAT tests and three Peach Bottom turbine trip tests.

These benchmark analyses, which were performed in the best-estimate mode, qualify the WNP-2 RETRAN model for the licensing basis analysis presented in the next chapter.

3.1 WNP-2 Power Ascension Tests

During the period of October -December 1984, a series of power ascension tests (PAT) at near full power were performed at WNP-2[14]. The data from these tests is available for verifying the WNP-2 RETRAN model. All of the transients analyzed in this chapter were recorded during the initial WNP-2 PAT testing.

The best-estimate model described in chapter 2 was used in the PAT analyses. The licensing basis model differs in setpoints and equipment specifications. Best-estimate analyses verify the modeling; the use of conservative input in the licensing basis model assures conservatism in the output.

The power ascension tests chosen for benchmark are as follows:

1. Water level setpoint change - This transient is used mainly to benchmark the feedwater control system, water level prediction and general stability of the RETRAN model.

2. Pressure regulator setpoint changes - This transient is used to benchmark the pressure regulator control system, RETRAN stability and system model accuracy.

3. One recirculation pump trip - This transient is to benchmark the pump coastdown characteristics and system response to an asymmetric recirculation flow variation.

4. Generator load rejection with bypass - This transient is used to benchmark the steam line modeling and system pressurization behavior.

Since the PAT transients are milder than the limiting transients in licensing basis analysis, the first three transients were analyzed using the point-kinetics core modeling. The one-dimensional kinetics model was also run for the recirculation pump trip case to demonstrate the validity of the point kinetics model for these relatively mild events.

The load rejection with bypass transient was analyzed using the

one-dimensional kinetics model. This treatment is consistent with the example licensing basis transient analysis (load rejection without bypass) in the next chapter.

3.1.1 Water level Setpoint Change (Test PAT 23A)

The purpose of Test PAT 23A was to demonstrate that the master level controller does not produce divergent or oscillatory behavior in level control system related variables such as water level. Test PAT 23A was performed at 95.1% power and 96.8% flow. The test procedure consisted of a six-inch step increase in vessel water level setpoint, a delay to allow the system to reach a new equilibrium condition, and a six-inch step decrease in vessel water level setpoint.

The feedwater control system master controller varies feedwater flow to maintain vessel water level at a specified setpoint. The feedwater controller uses vessel water level and the mismatch between steam flow and feedwater flow to demand variations in the feedwater pump speed, which determines feedwater flow. The controller responds to an increase in vessel water level setpoint by increasing feedwater flow, which increases downcomer water level. The downcomer water temperature decreases and causes a drop in core inlet temperature, which produces a slight core power increase. As water level increases, the feedwater controller reduces feedwater flow, which reduces power. Both core power and feedwater flow attain new steady state values at approximately their initial values, while water level stabilizes at the new setpoint.

3.1.1.1 RETRAN Modeling of Test

To model the test, a general function table used in the level setpoint control block (Control Block 80) is changed to reflect the step change of the level setpoint. Since the test condition is near the rated condition, the standard RETRAN base model at rated condition is used to start the transient simulation.

3.1.1.2 Results

The water level setpoint step change test was analyzed to demonstrate the adequacy of the feedwater controller and vessel water level models. This comparison also verifies the adequacy of the neutronics and vessel internals models. Figure 3.1.1 shows the measured and calculated feedwater flow response. Similarly, Figure 3.1.2 shows the measured and calculated narrow range water level. These plots show that the RETRAN model predicts events and timing consistent with the data.

Figure 3.1.2 indicates that RETRAN calculates a water level that approaches a value that is six inches higher than the initial water level at about 20 seconds after the setpoint change. The measured data indicates a higher asymptotic value of 7.8 inches in water level change, which may indicate an inconsistency between the level step change used in the analysis and actual test.

Other parameters (steam flow, dome pressure and core power) are not plotted because they did not show any significant changes (less than 3% variation from steady state values) throughout the test.

Figure 3.1.1

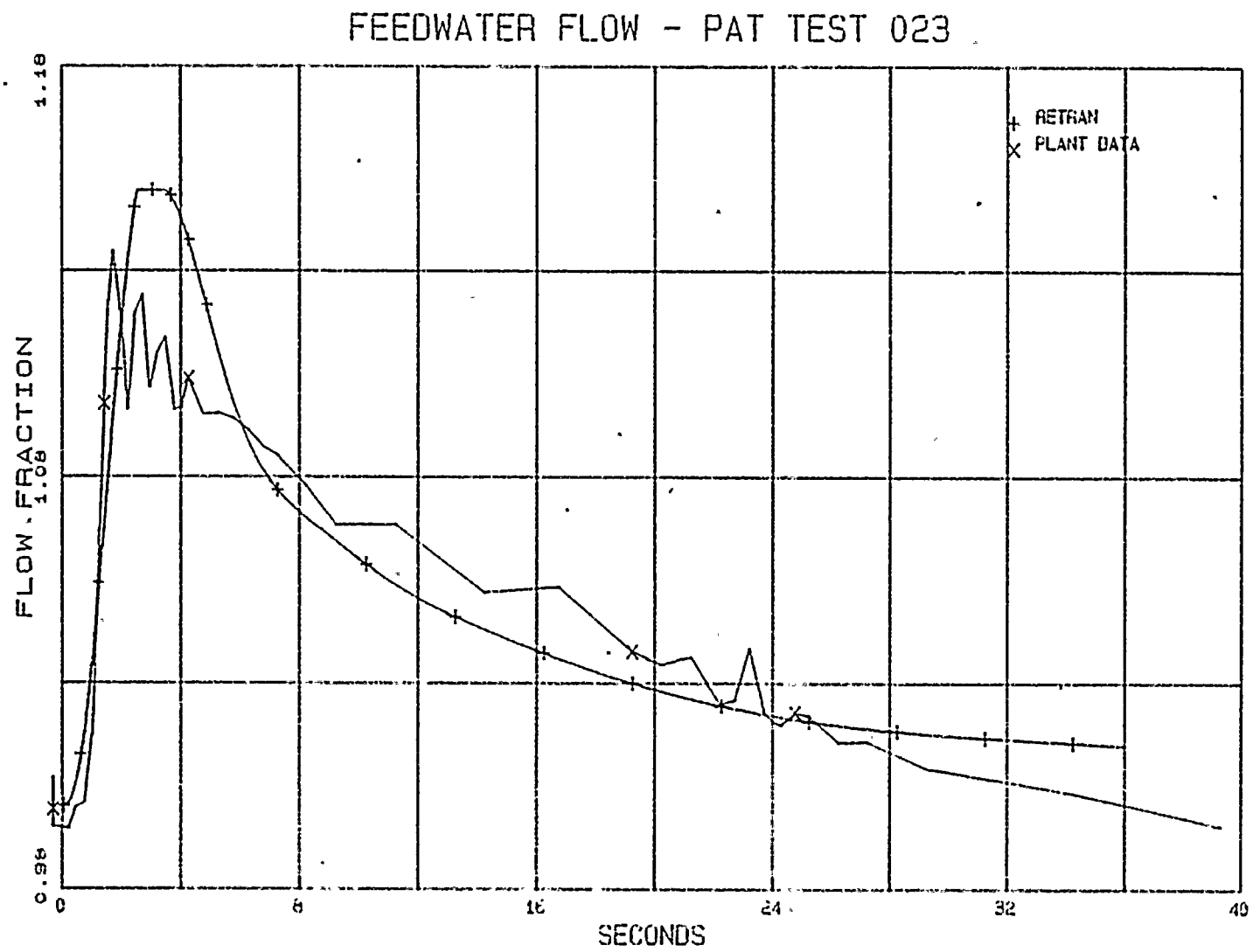
FEEDWATER FLOW - PAT TEST 023
RETRAN
PLANT DATA
FLOW.FRACTION
1.18
1.08
0.98
0
8
16
24
32
40
SECONDS

Figure 3.1.2

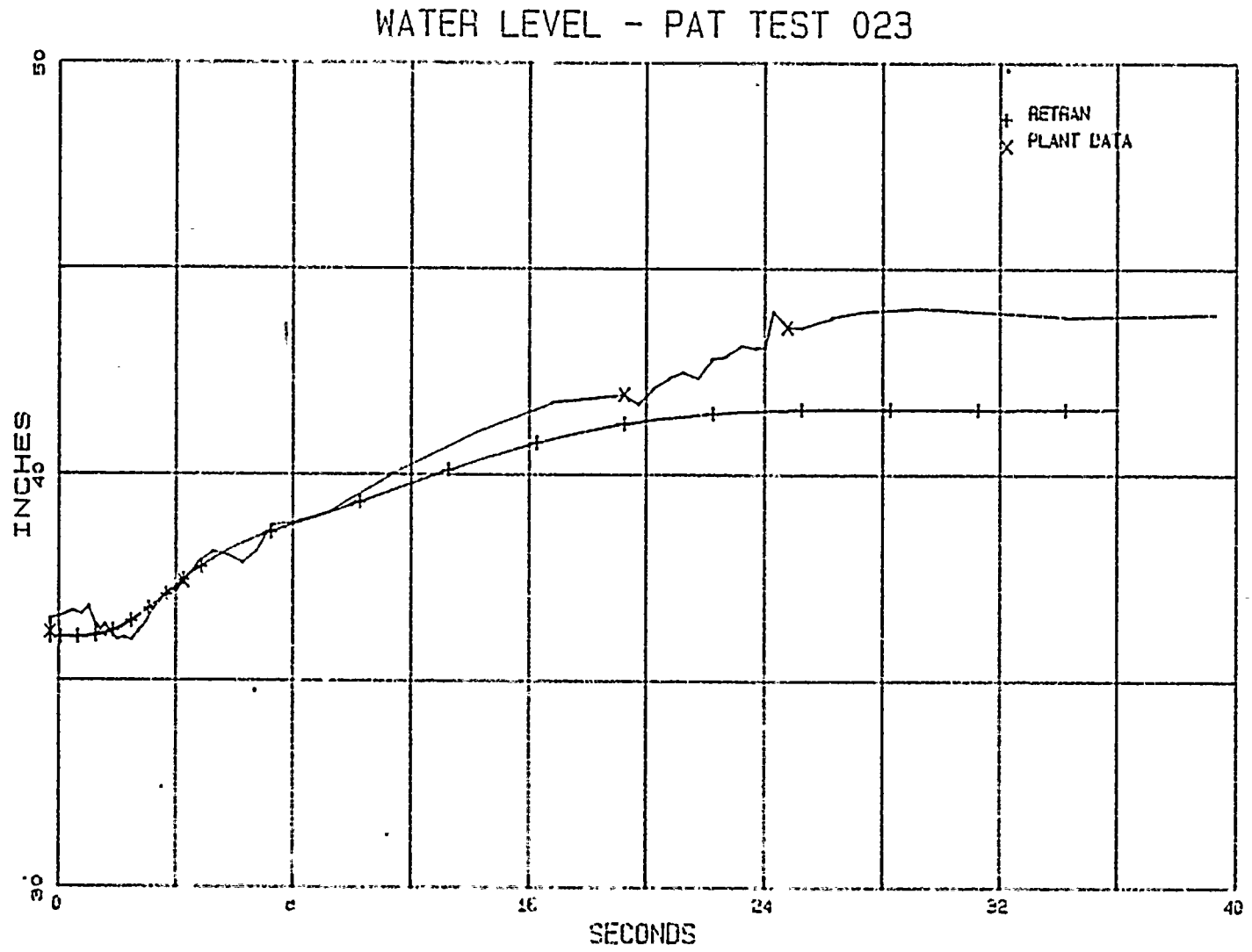
WATER LEVEL - PAT TEST 023
RETRAN
PLANT DATA
INCHES
50
40
30
0
8
16
24
32
40
SECONDS

3.1.2 Pressure Regulator Setpoint Changes (PAT 22)

The purpose of Test PAT 22 was to demonstrate that no divergent characteristics in pressure control system response exist. Test PAT 22 was performed at 97.5% power and 95.9% flow. The test procedure consisted of a 10-psi step decrease in pressure regulator setpoint, a delay to allow the system to reach a new equilibrium condition, and a 10-psi step increase in pressure regulator setpoint to the original value.

Under normal operating conditions, a decrease in pressure regulator setpoint will cause the controlling pressure regulator channel and the Digital Electro-Hydraulic Control System (DEH) to open the turbine control valves. The resulting increased steam flow will cause steam line and dome pressure to decrease. Decreased system pressure increases core voiding and produces a core power reduction. As pressure regulator pressure decreases, the pressure regulator and DEH control system begin closing the turbine control valves to maintain pressure at the new setpoint.

3.1.2.1 RETRAN Modeling of Test

Test PAT 22 was analyzed in the best-estimate mode. The initial dome pressure in the RETRAN model is 1020 psia, which differs slightly from the 990-psia test pressure. The transient is very mild and the response to the step change in pressure setpoint was

not expected to be sensitive to the small difference in initial pressure.

To model the test, a general function table used for the pressure setpoint control block (Control Block 13) is changed to reflect the step change of the pressure setpoint.

3.1.2.2 Results

The decrease in pressure regulator pressure setpoint causes a rapid increase in pressure regulator output. The turbine control valves open, decreasing system pressure and increasing core voids. The subsequent power decrease reduces steam flow again. A new system steady state condition is attained at a decreased system pressure.

Figure 3.1.3 shows the measured and calculated transient pressure response. The pressure settles out at about 10 psi below the initial pressure, indicating good alignment of the pressure system control model.

Figure 3.1.4 presents the measured and calculated power behavior. The system stabilizes back to the initial power rapidly, and the RETRAN model predicts this behavior consistently with the data.

Figure 3.1.5 Shows the measured and calculated steam flow. Figure 3.1.6 presents the measured and calculated feedwater flow. The

calculation matches the plant data closely in both of these areas.

The simulation/data comparisons indicate that the pressure regulation control system in the WNP-2 RETRAN model performs as intended.

Figure 3.1.3

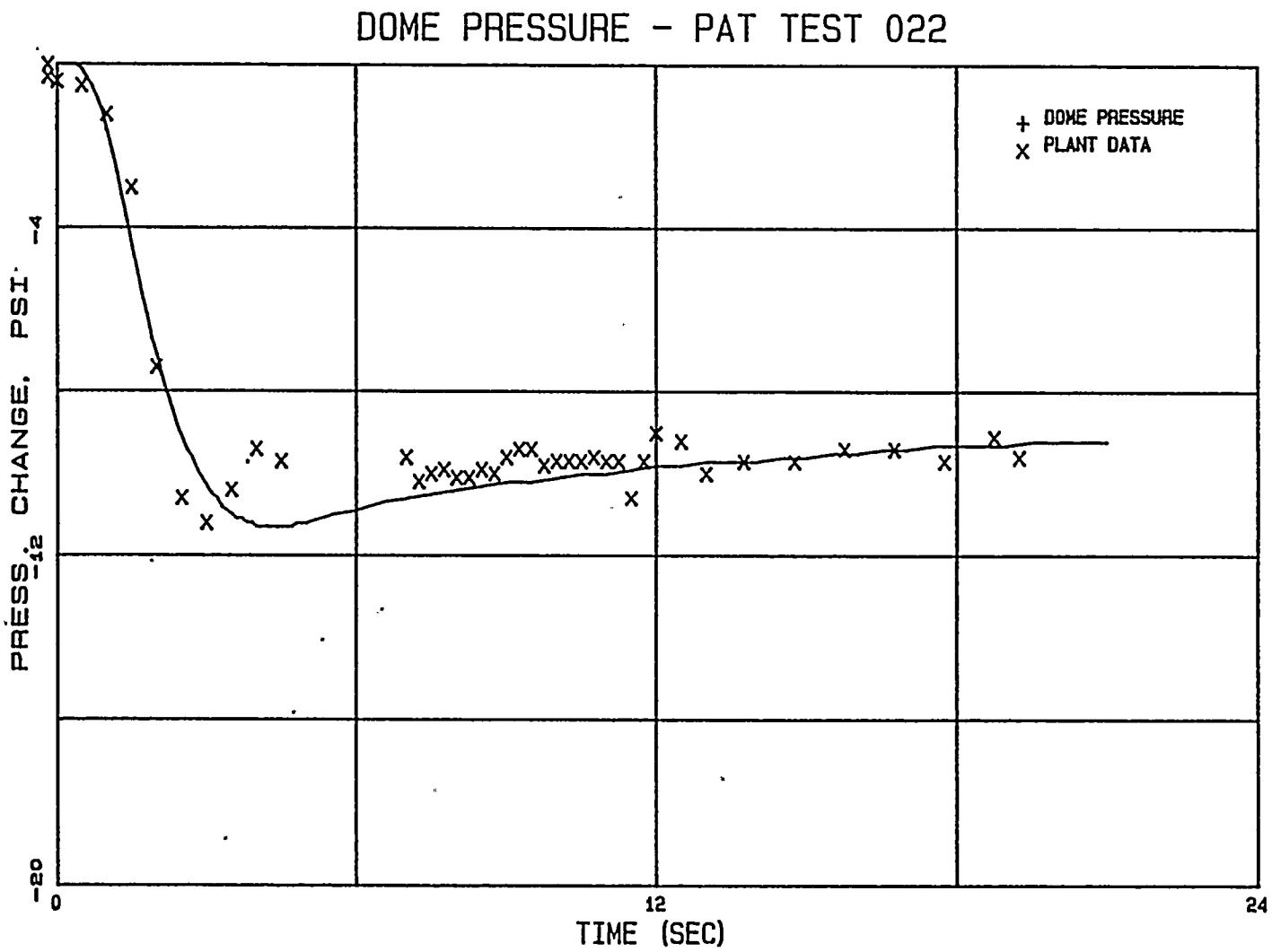
DOME PRESSURE - PAT TEST 022
+ DOME PRESSURE
X PLANT DATA
PRESS. CHANGE, PSI
-4
-12
-20
0
12
24
TIME (SEC)

Figure 3.1.4

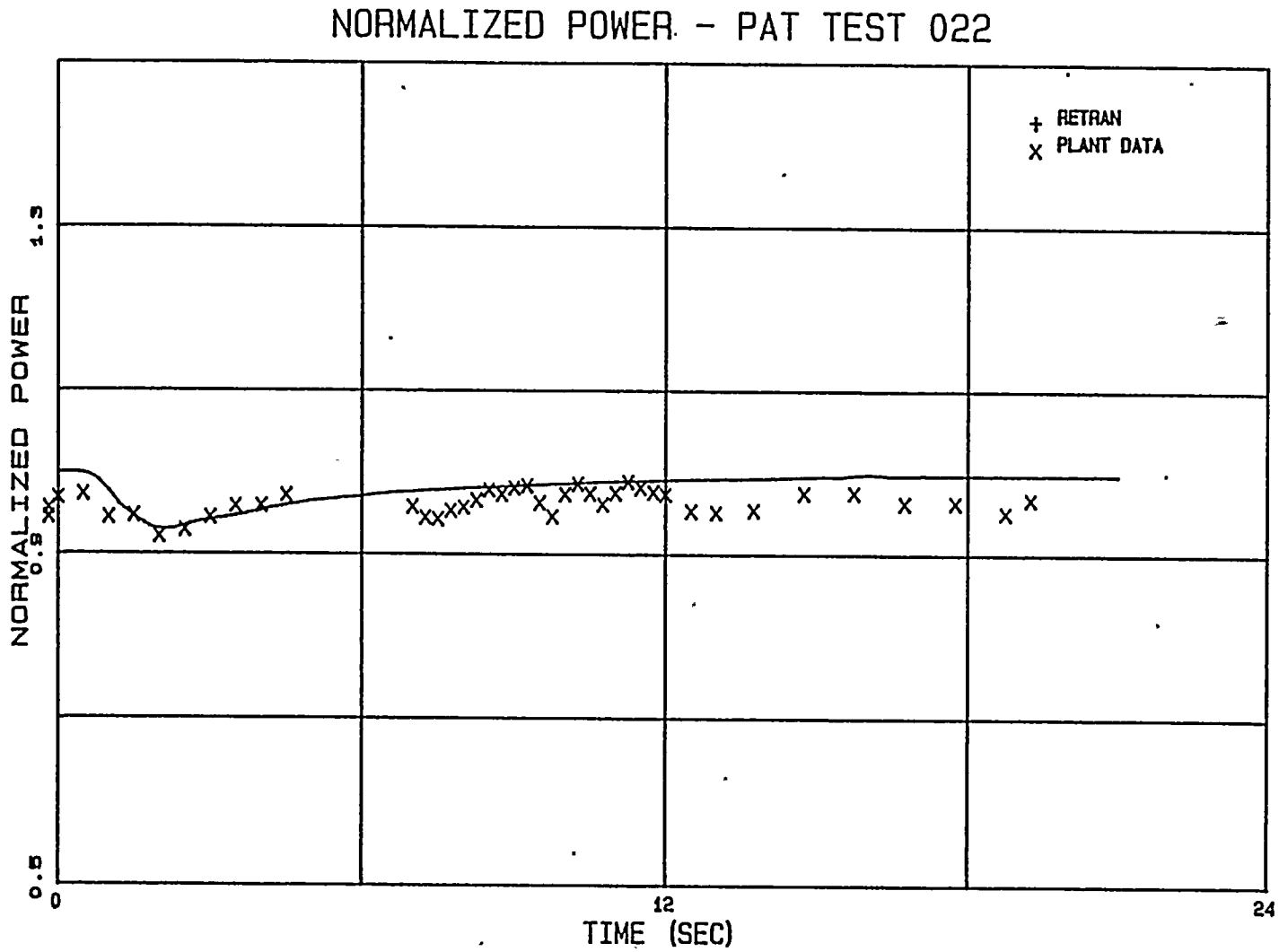
NORMALIZED POWER - PAT TEST 022
RETRAN
PLANT DATA
NORMALIZED POWER
1.5
0.5
0
12
24
TIME (SEC)

Figure 3.1.5

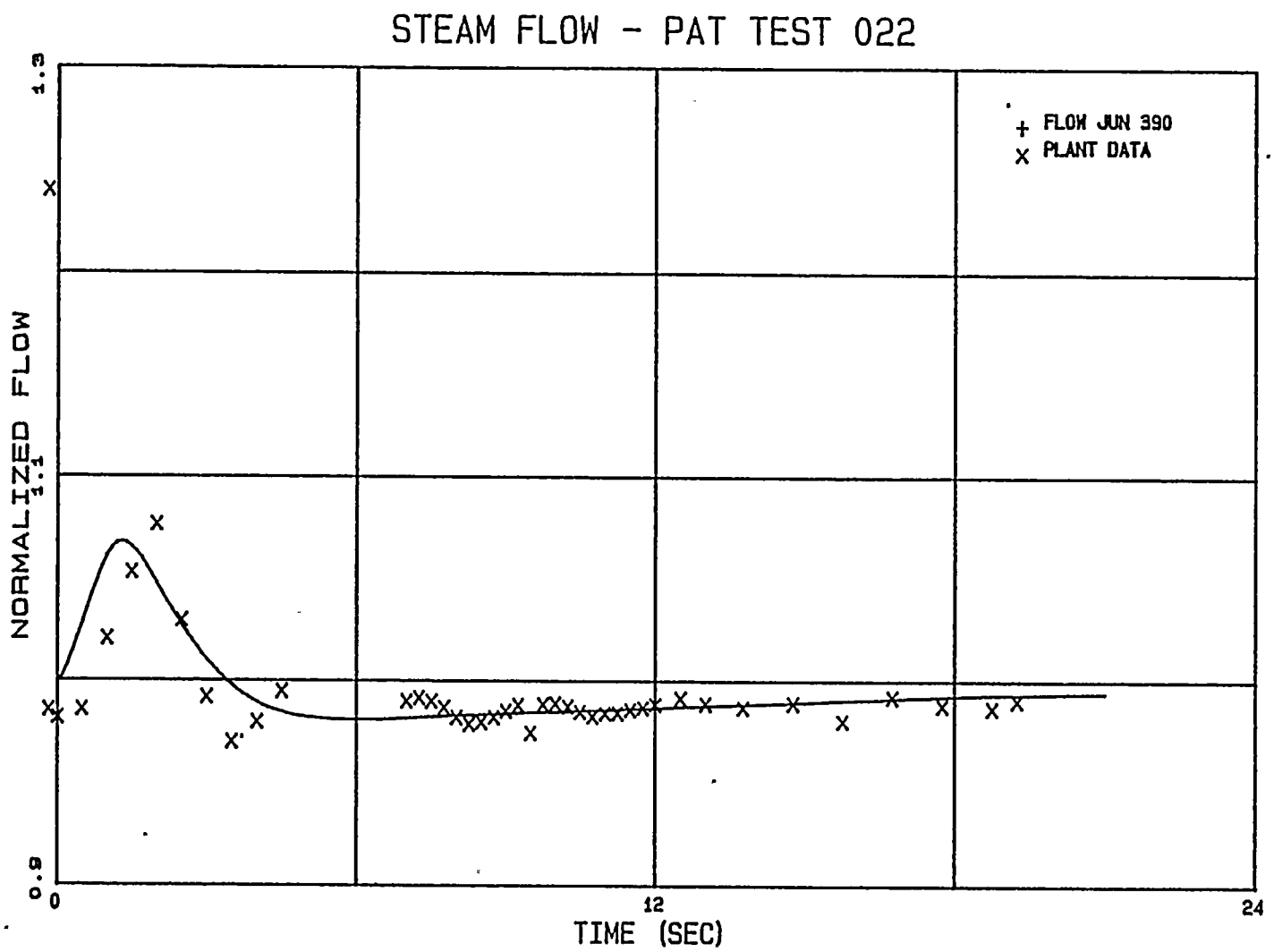
STEAM FLOW - PAT TEST 022
+ FLOW JUN 390
X PLANT DATA
NORMALIZED FLOW
1.3
1.1
0.9
0
12
24
TIME (SEC)

Figure 3.1.6

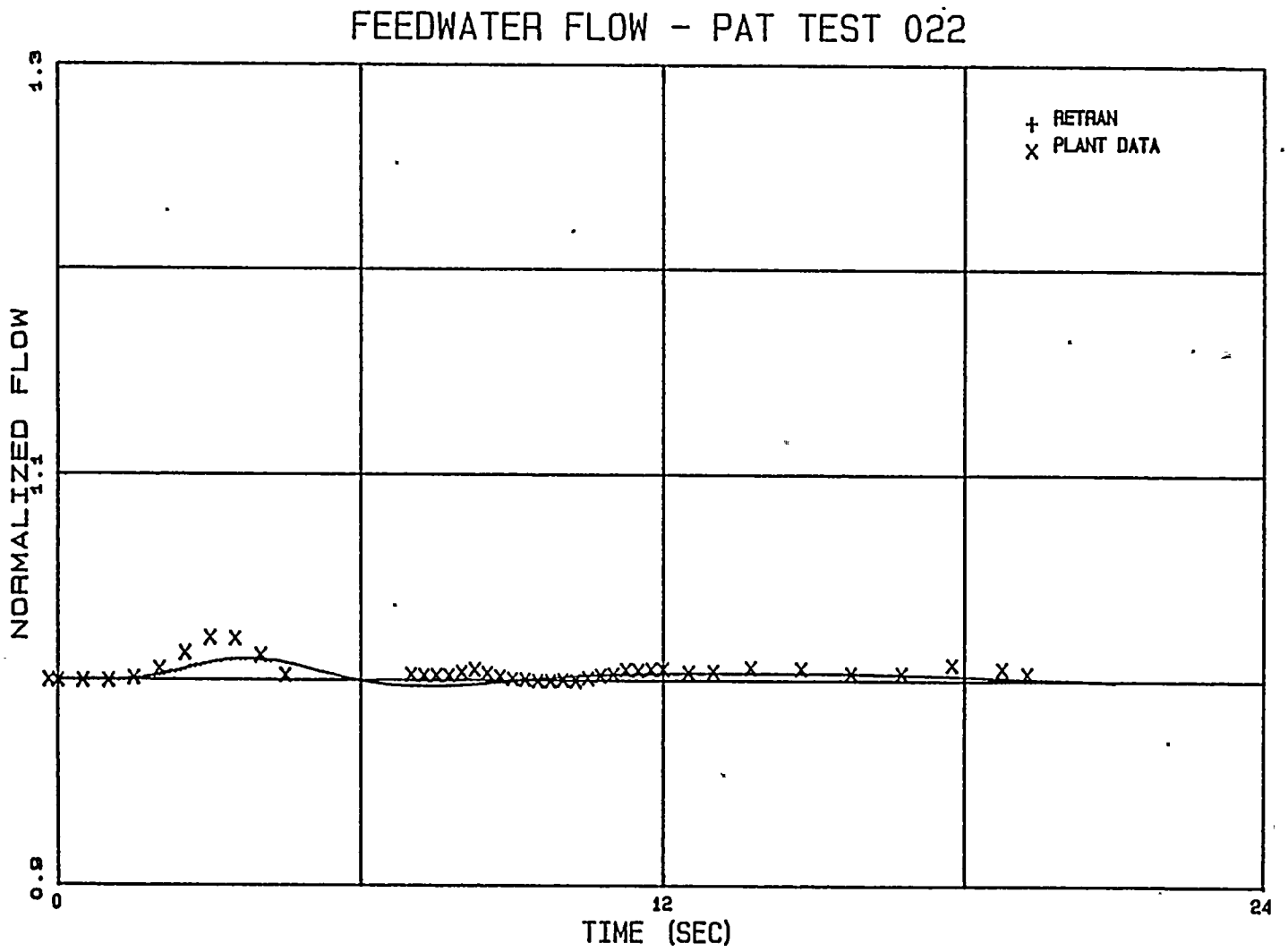
FEEDWATER FLOW - PAT TEST 022
RETRAN
PLANT DATA
NORMALIZED FLOW
1.3
1.1
0.9
0
12
24
TIME (SEC)

3.1.3 One Recirculation Pump Trip (Test PAT 30A)

The data taken during Test PAT 30A was used to verify the performance of the recirculation system. The test also demonstrated that the water level can be controlled without resulting in turbine trip and/or scram. Test PAT 30A was performed at 96.2% power and 100% flow. The test was initiated by tripping one recirculation pump using the Recirculation Pump trip (RPT) breaker.

Core flow decreases following a single pump trip. The resulting increase in void formation causes a rise in reactor water level, which in the test was not enough to cause a high level trip of the main turbine or the feedwater pumps. The higher core void level reduces core power. Core average heat flux and voids lag behind core power. As the core heat flux decreases, core voids decrease and void feedback effects cause power to rise slightly before leveling off. A new system equilibrium is reached at single pump conditions with a reduced power, core flow, and pressure.

3.1.3.1 RETRAN Modeling of Test

Test PAT 30A was analyzed with the best-estimate model at rated power and flow. The transient was initiated by introducing a recirculation pump trip in Recirculation Loop A at time zero.

A Test PAT 30A case with one-dimensional kinetics was run to

evaluate the effect of void feedback on the core power calculation at lower core flow conditions and the results compared to the point-kinetics model. Unadjusted cross sections for Beginning of Cycle 1 conditions were used in the one-dimensional core analysis. (See Appendix A for a description of cross section adjustments.) Use of the unadjusted cross sections is acceptable because the one-pump trip transient is very mild. The data comparison in the next section supports this assumption.

3.1.3.2 Results

The Test PAT 30A benchmark validates the recirculation pump coastdown characteristics and the system model response to asymmetric recirculation flow disturbances. Neutronics, core hydraulics, pressure regulator control system, and feedwater models were validated in the analysis. Figure 3.1.7 shows measured and calculated recirculation drive flow for the tripped loop (Loop A) for the point kinetics case. Figure 3.1.8 shows measured and calculated recirculation drive flow for the unaffected loop (Loop B). The calculated flow tracks measured data in both comparisons. The Loop B flow increases slightly as the transient is initiated and stabilizes at a higher value. The unaffected loop sees a lower flow resistance after one pump is tripped. Figures 3.1.9 and 3.1.10 show the same comparisons for the case using one-dimensional kinetics. These comparisons are very similar to the cases with point-kinetics model, supporting the use of the point kinetics

model in the other PAT test benchmarks.

Figure 3.1.11 shows the normalized jet pump flow for Loop A. Figure 3.1.12 shows the jet pump flow for Loop B. Again the RETRAN results track the data. Figures 3.1.13 and 3.1.14 are the same comparisons for the case using one-dimensional kinetics. A comparison with the point-kinetics model showed no difference in the calculated jet pump flows.

The initial reduction in core flow causes an increase in core voiding, which causes core power to decrease. As the core heat flux decreases (lagging core power by the fuel rod thermal time constant), core voids decrease from their maximum and core power increases slightly. A new, lower equilibrium power level is attained. Figure 3.1.15 shows that the RETRAN core hydraulic and neutronic models calculate transient core power consistently with the data. Figure 3.1.16 is the corresponding plot for the one-dimensional RETRAN model. The one-dimensional model gives a slightly better match with the plant data than the point kinetics model later in the transient because the one-dimensional model tracks the void feedback in the core more accurately than the point kinetics model. The fluctuations observed at about 4 seconds and 16 seconds in the one-dimensional case are also the results of detailed axial void feedback.

Figures 3.1.17 and 3.1.18 show the core heat flux behavior

calculated by the point-kinetics model and the one-dimensional model respectively. Both track the plant data with the one-dimensional model yielding slightly better results.

Figure 3.1.7

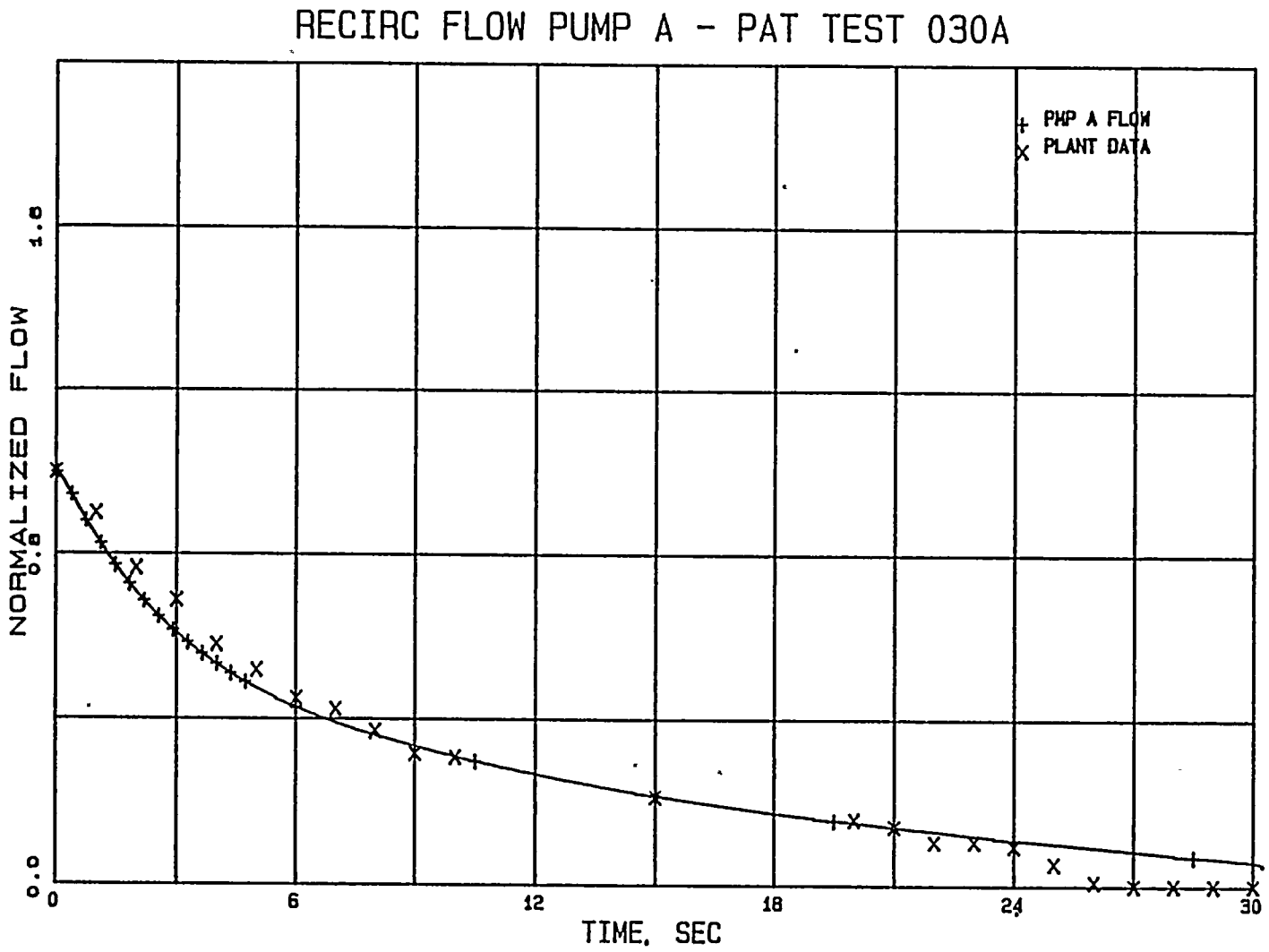
RECIRC FLOW PUMP A - PAT TEST 030A
PHP A FLOW
PLANT DATA
NORMALIZED FLOW
1.6
0.8
0.0
0
6
12
18
24
30
TIME, SEC

Figure 3.1.8

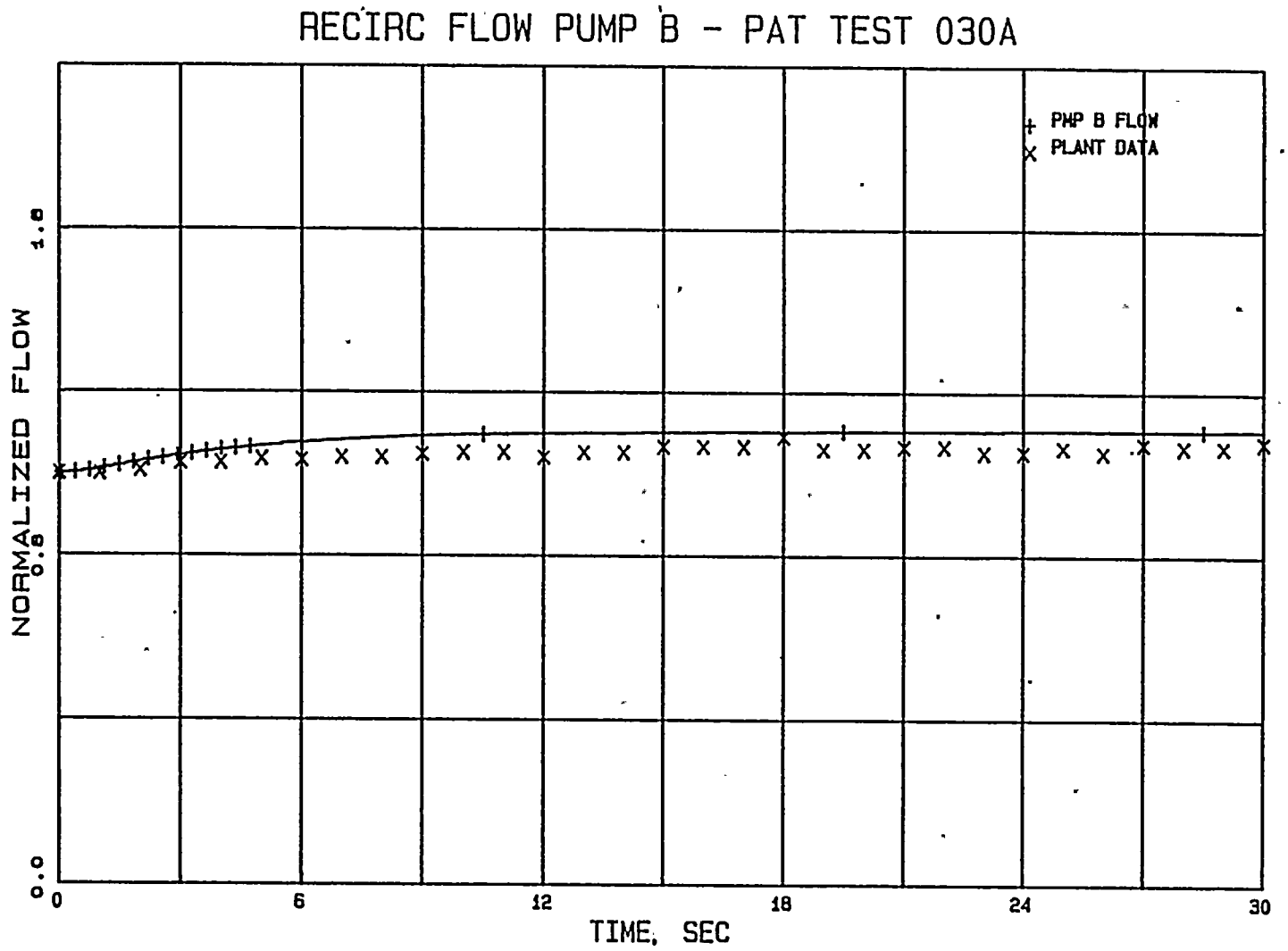
RECIRC FLOW PUMP B - PAT TEST 030A
PMP B FLOW
PLANT DATA
NORMALIZED FLOW
1.6
0.8
0.0
0
6
12
18
24
30
TIME, SEC

Figure 3.1.9

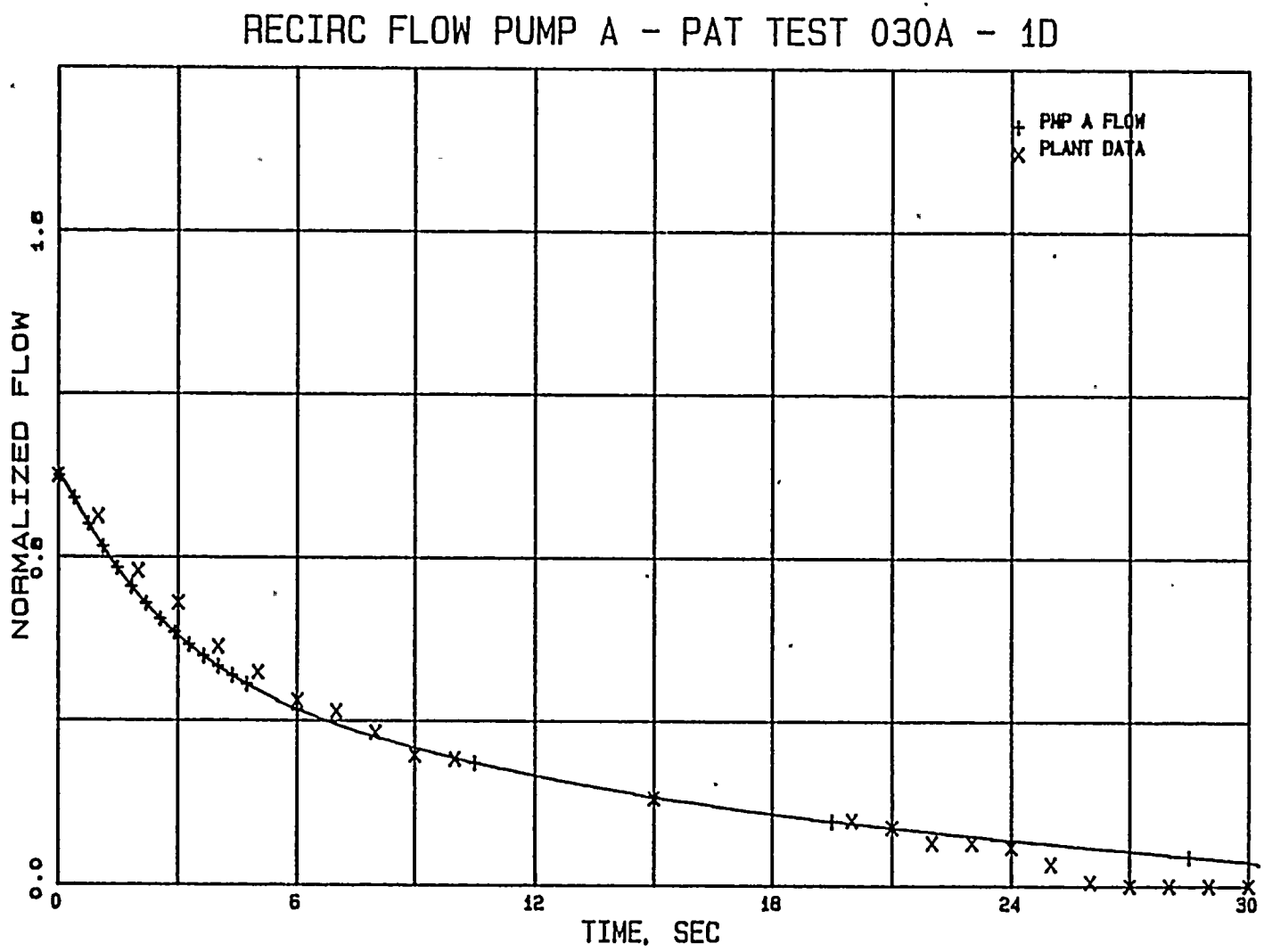
RECIRC FLOW PUMP A - PAT TEST 030A - 1D
PMP A FLOW
PLANT DATA
NORMALIZED FLOW
1.6
0.8
0.0
0
6
12
18
24
30
TIME, SEC

Figure 3.1.10

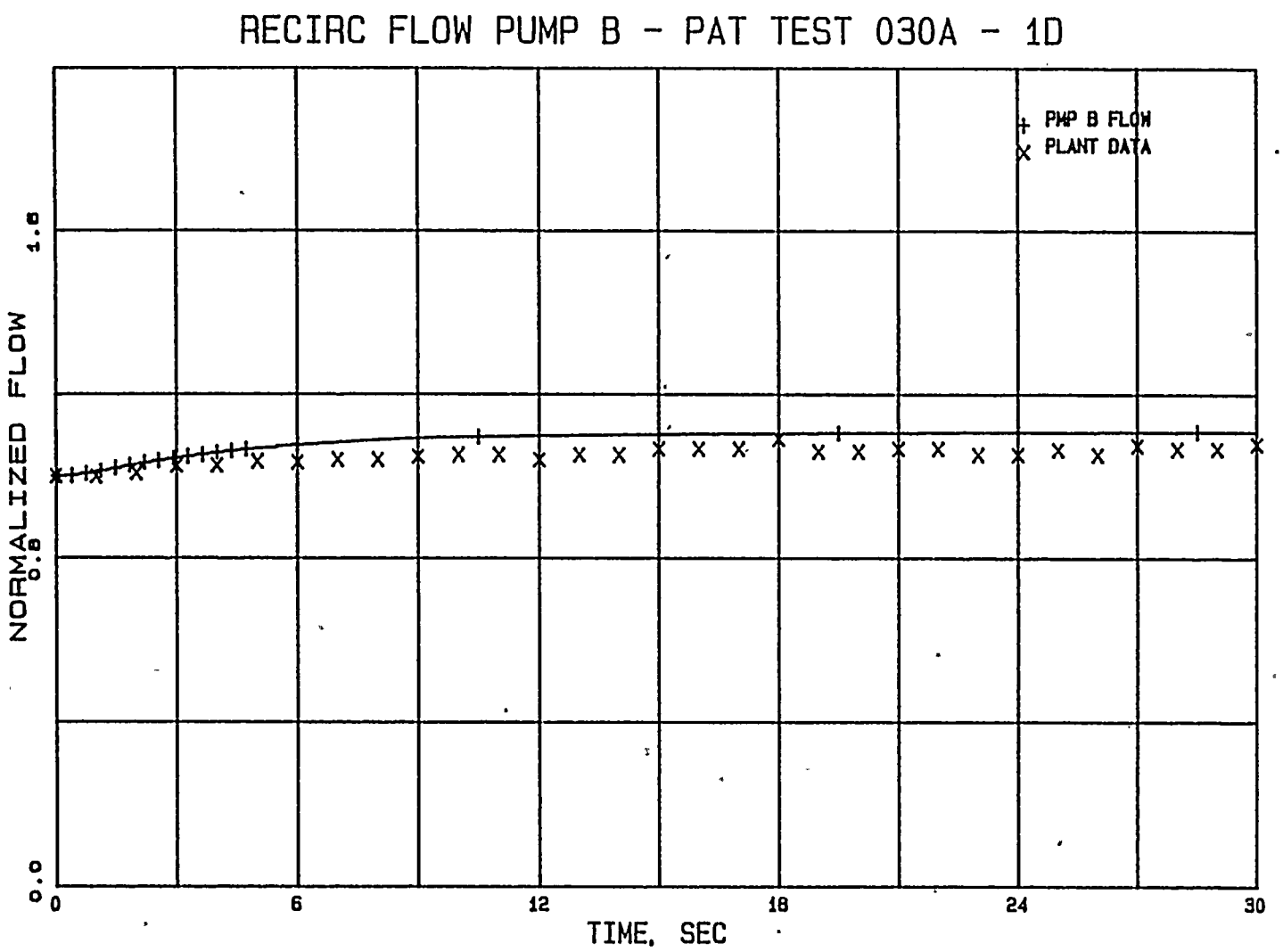
RECIRC FLOW PUMP B - PAT TEST 030A - 1D
PMP B FLOW
PLANT DATA
NORMALIZED FLOW
1.6
0.8
0.0
0
6
12
18
24
30
TIME, SEC

Figure 3.1.11

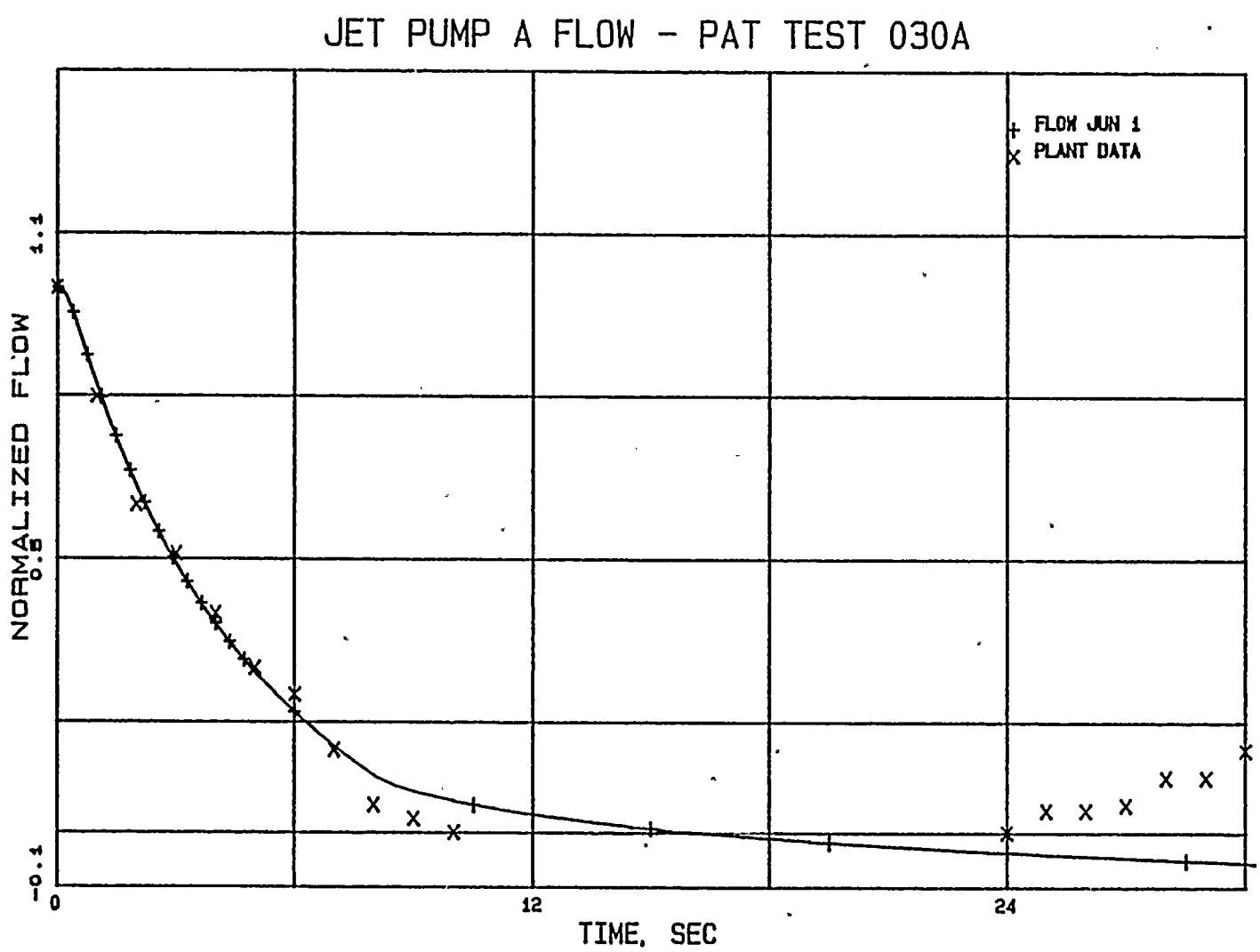
JET PUMP A FLOW - PAT TEST 030A
FLOW JUN 1
PLANT DATA
NORMALIZED FLOW
1.1
0.5
-0.1
0
12
24
TIME, SEC

Figure 3.1.12

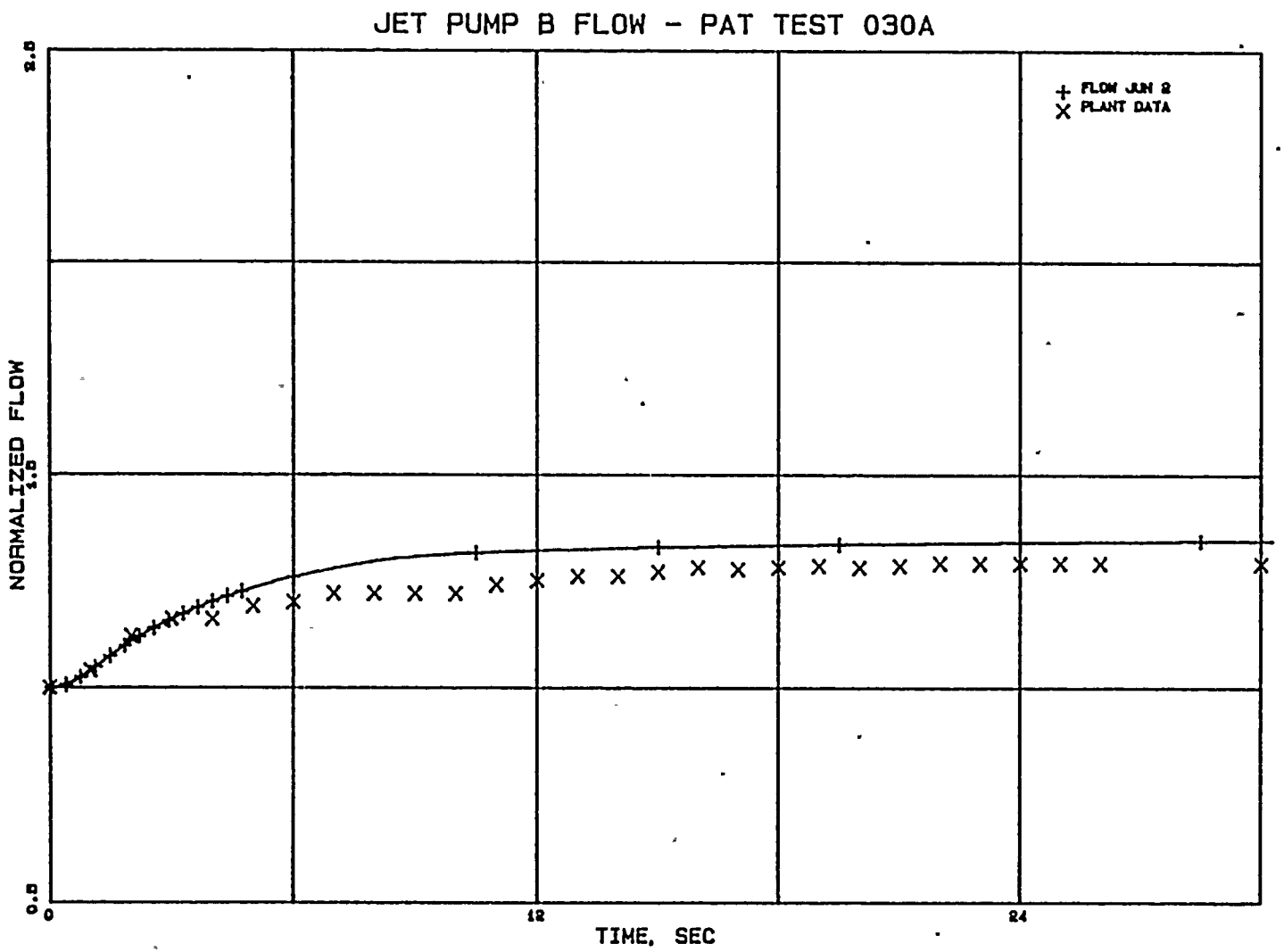
JET PUMP B FLOW - PAT TEST 030A
FLOW JUN 2
PLANT DATA
NORMALIZED FLOW
2.0
1.0
0.0
0
12
24
TIME, SEC

Figure 3.1.13

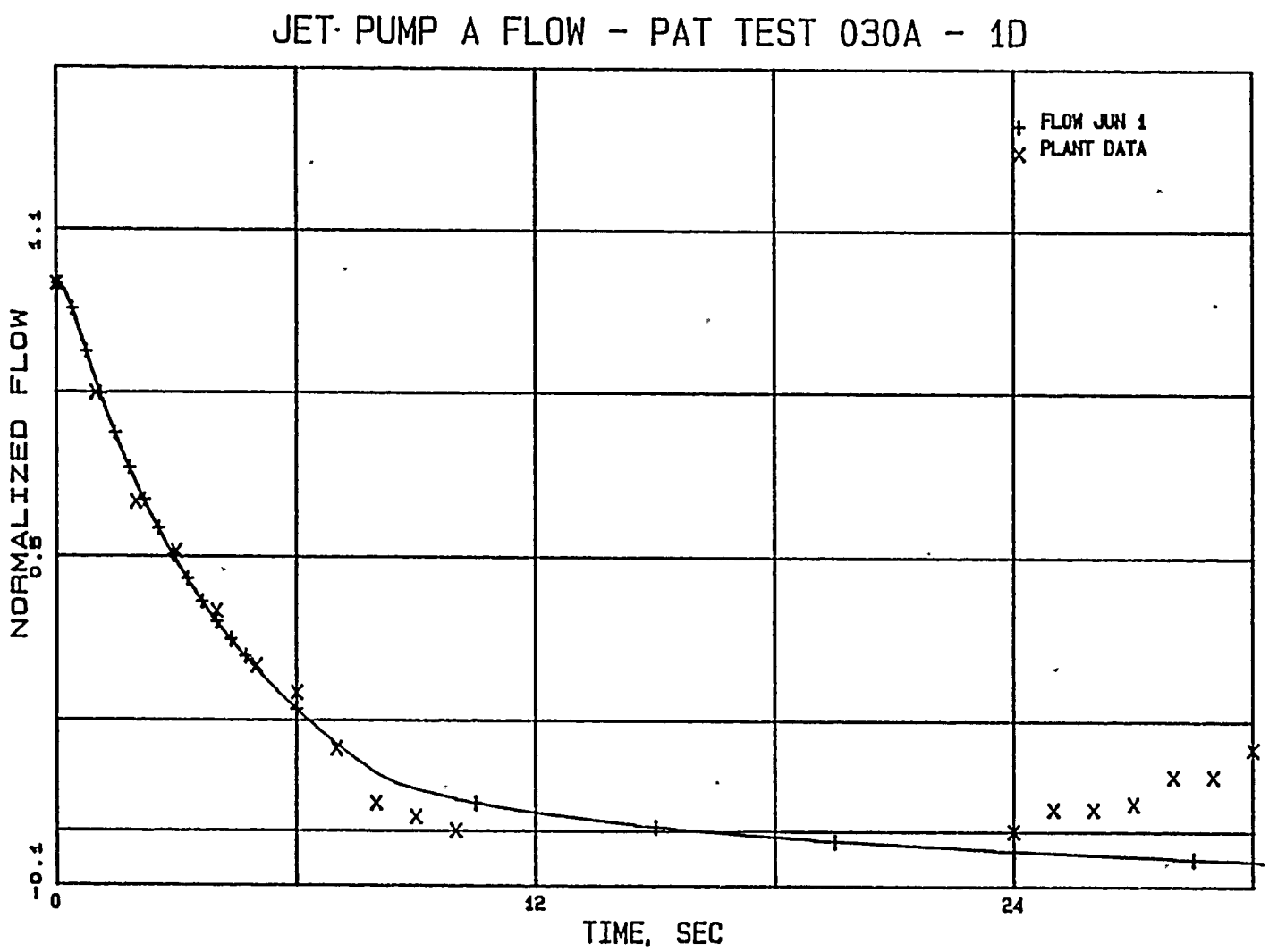
JET PUMP A FLOW - PAT TEST 030A - 1D
FLOW JUN 1
PLANT DATA
NORMALIZED FLOW
1.1
0.5
-0.1
0
12
24
TIME, SEC

Figure 3.1.14

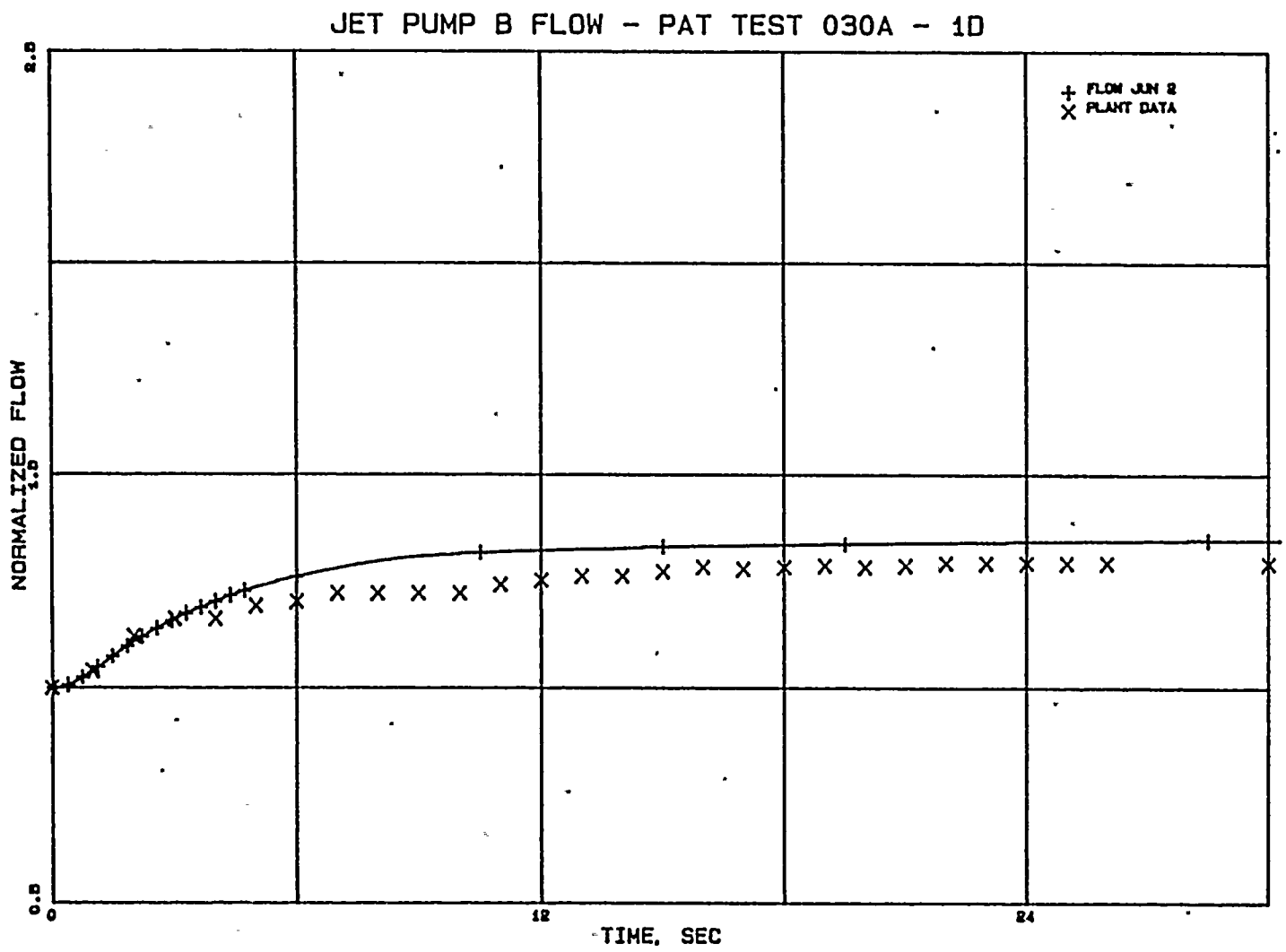
JET PUMP B FLOW - PAT TEST 030A - 1D
FLOW JUN 2
PLANT DATA
NORMALIZED FLOW
2.0
1.0
0.0
0
12
24
TIME, SEC

Figure 3.1.15

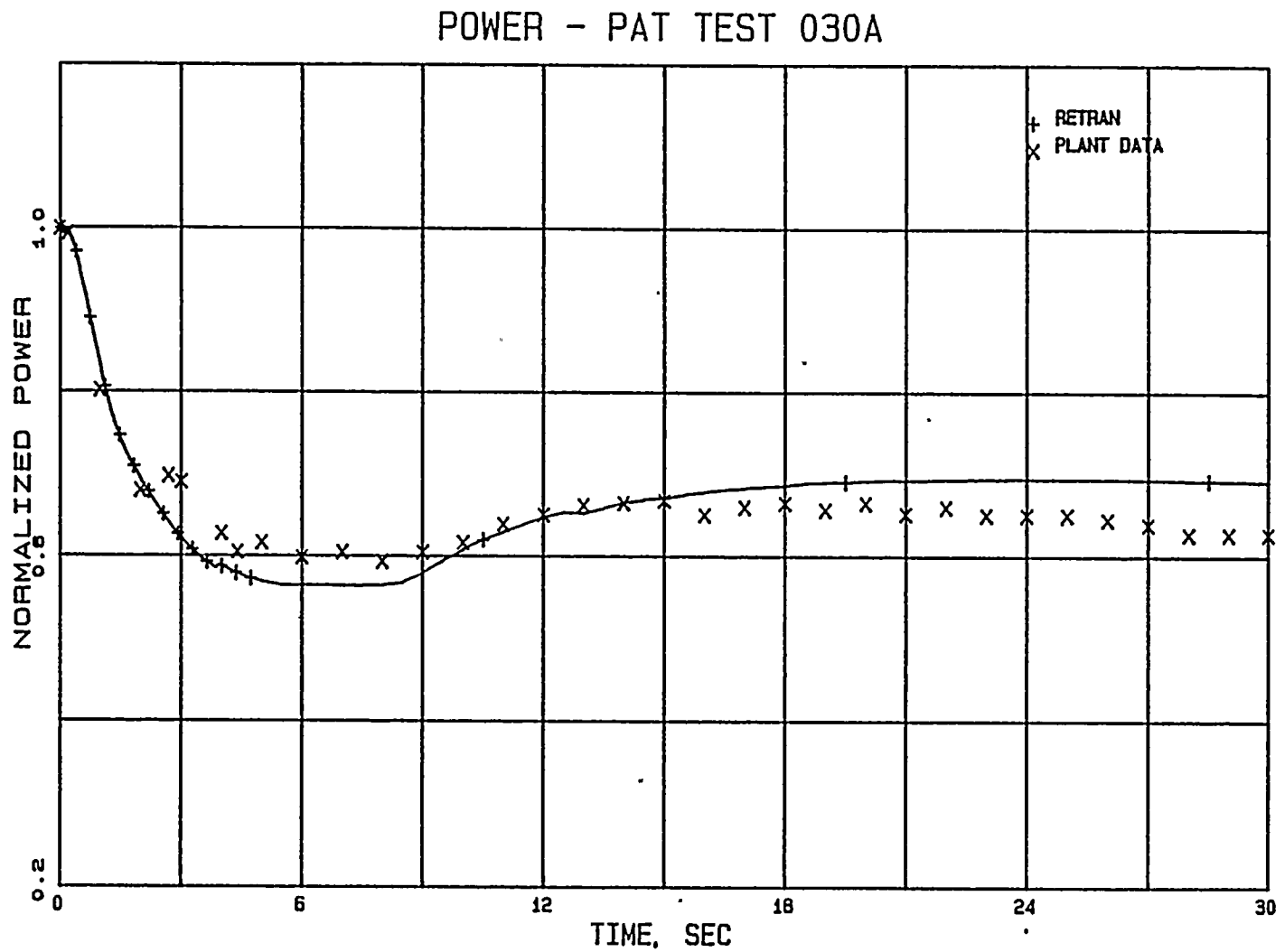
POWER - PAT TEST 030A
RETRAN
PLANT DATA
NORMALIZED POWER
1.0
0.8
0.2
0
6
12
18
24
30
TIME, SEC

Figure 3.1.16

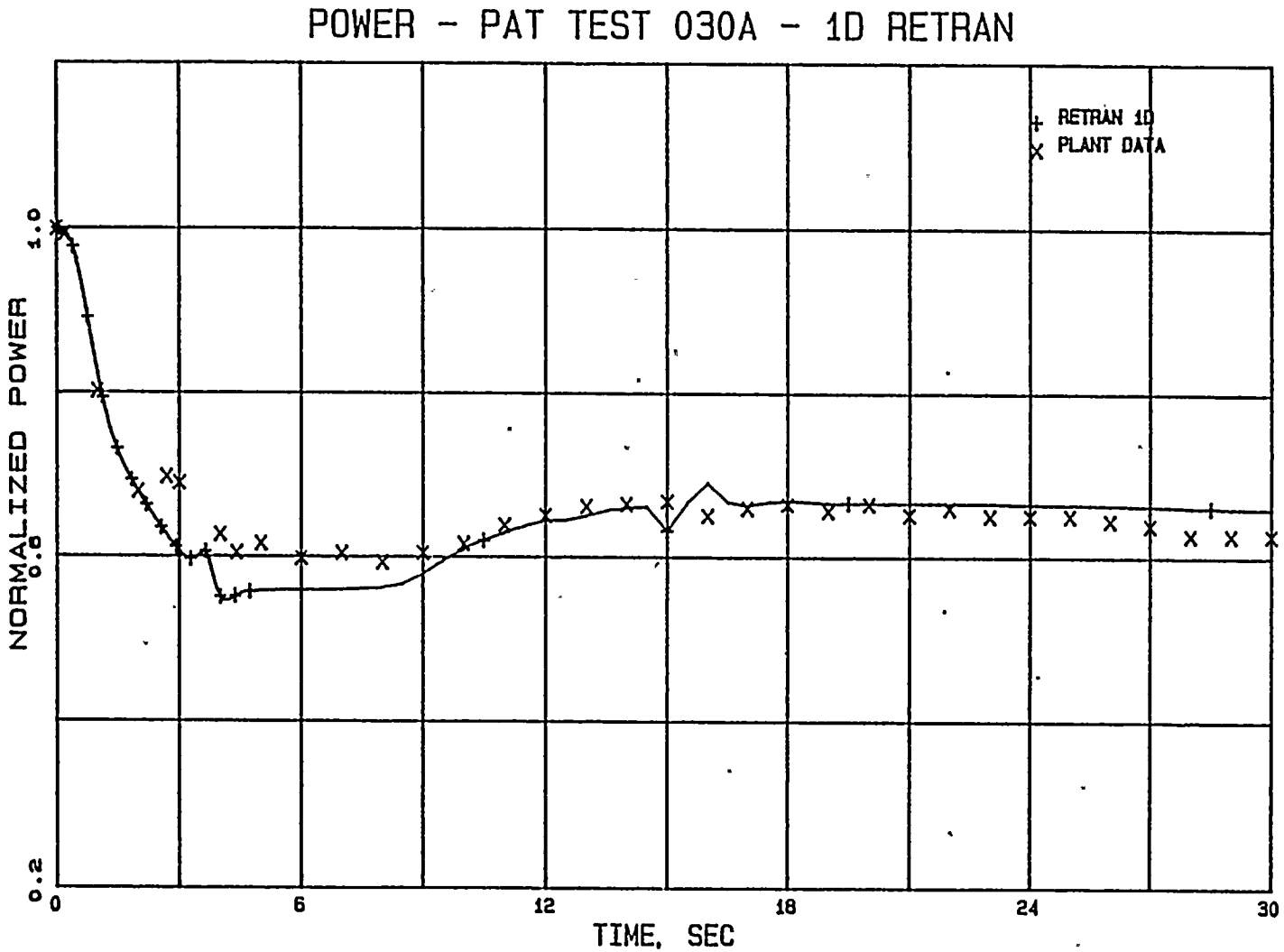
POWER - PAT TEST 030A - 1D RETRAN
RETRAN 1D
PLANT DATA
NORMALIZED POWER
1.0
0.8
0.2
0
6
12
18
24
30
TIME, SEC

Figure 3.1.17

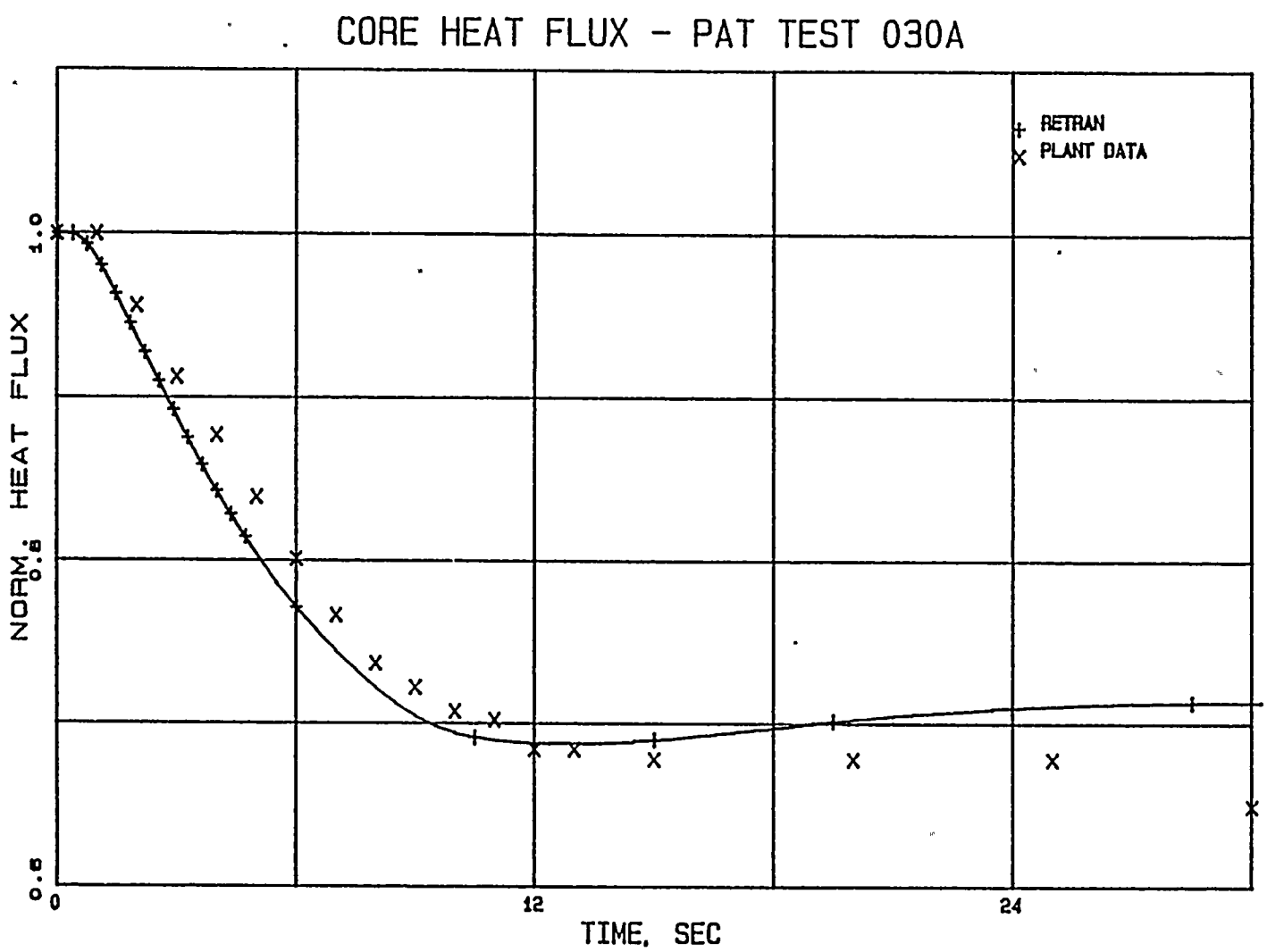
CORE HEAT FLUX - PAT TEST 030A
RETRAN
PLANT DATA
NORM. HEAT FLUX
1.0
0.8
0.6
0
12
24
TIME, SEC

Figure 3.1.18

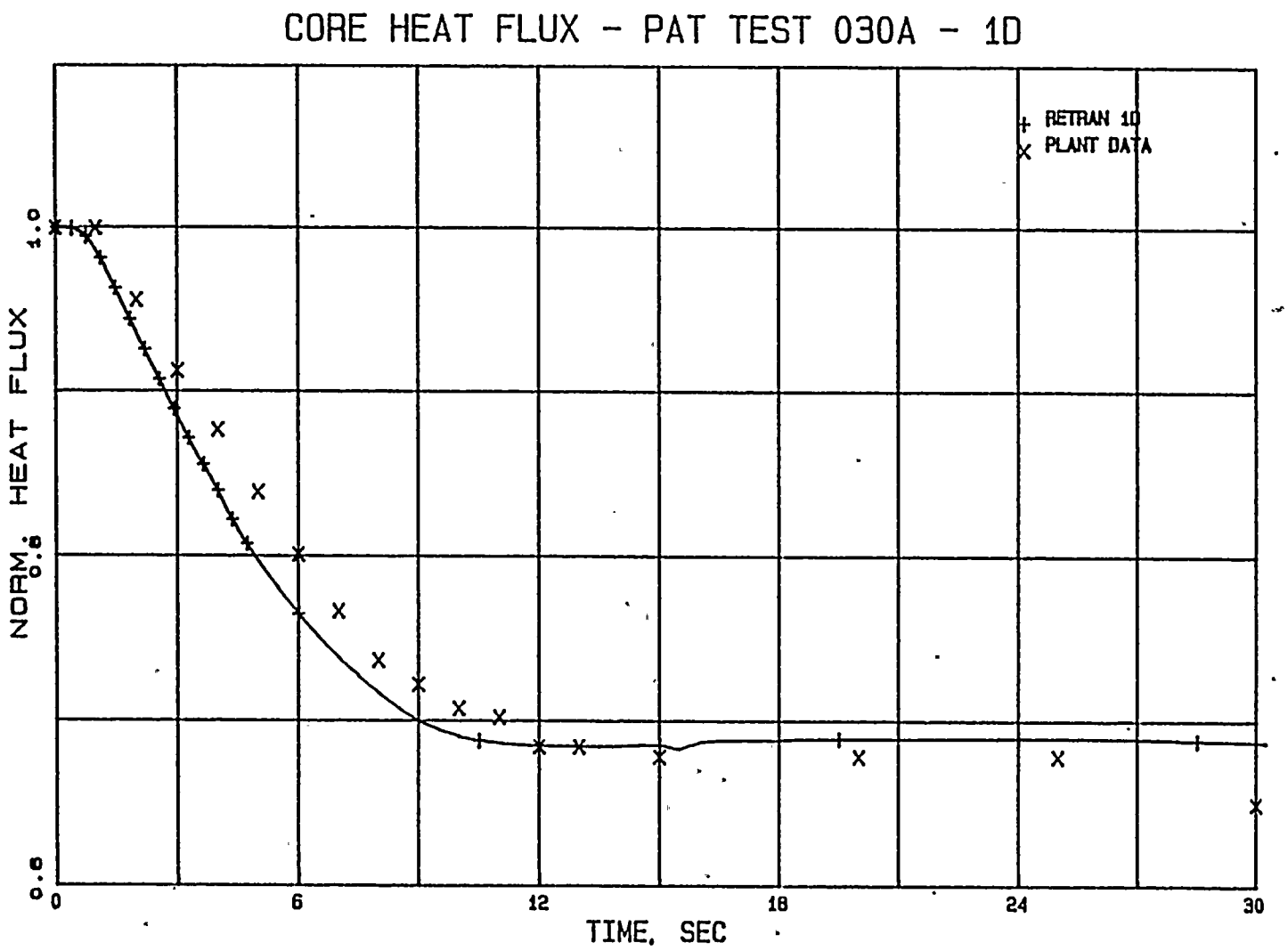
CORE HEAT FLUX - PAT TEST 030A - 1D
RETRAN 1D
PLANT DATA
NORM. HEAT FLUX
1.0
0.8
0.6
0
6
12
18
24
30
TIME, SEC

3.1.4 Generator Load Rejection With Bypass (PAT 27)

Test PAT 27 was performed at 97.5% power and 95.4% flow. The procedure was initiated by the activation of the main generator trip pushbutton.

The rapid closure of the turbine control valves pressurizes the steam lines. As the pressure wave reaches the core, positive void reactivity is induced. Scram is initiated by the turbine control valve fast closure pressure switch. The early scram results in negative overall reactivity throughout the test. The net effect is a power decrease shortly after the initiation of the transient.

The pressure wave traveling through the downcomer to the lower plenum creates a core inlet flow spike. The turbine control valve closure also initiates the recirculation pump trip (RPT). Substantial reduction in core flow does not begin, however, until after the flow spike (at approximately one second).

The generator load rejection activates the fast opening of the turbine bypass valves to relieve vessel pressure. Since the capacity of the bypass is less than the test power level, dome pressure increases until the SRVs lift to limit the pressure rise. For this event Group 1 SRVs opened.

3.1.4.1 RETRAN Modeling of Test

The manual generator load rejection trip was set to occur at 0.0 seconds. The turbine control valve performance was taken from the test data. In the WNP-2 RETRAN model a single valve (Junction 380) at the end of steam line simulates both turbine control and stop valves. When the control valve fast closure is activated, its corresponding delay time and closure time are input so that Junction 380 simulates a control valve. Observed control rod performance data was used as the RETRAN scram time.

The maximum bypass flow for the base deck is set at the design value of 25% of rated steam flow. Plant data supports a value of 37% maximum bypass flow, which was used for this simulation.

The one-dimensional kinetics model was used in this simulation. As mentioned in Section 3.1.3, for a mild transient as in this case, uncorrected one-dimensional cross sections are sufficient.

3.1.4.2 Results

Figure 3.1.19 shows the calculated and measured variation in the Average Power Range Monitor (APRM) signal during the Test PAT 27. The APRM signal is proportional to the neutron flux. The output from RETRAN is adjusted so that the decay power is subtracted from the total power before it is compared to the measured data.

Test PAT 27 is the only benchmarked power ascension test which resulted in a reactor scram. Figure 3.1.19 shows that the RETRAN prediction tracks the initiation and progress of the scram closely, indicating acceptable scram modeling.

Recirculation Pump Trip (RPT) causes a rapid decrease in recirculation drive flows and loop flows. The WNP-2 RETRAN model contains two separate recirculation loops. Figure 3.1.20 and 3.1.21 show that RETRAN follows the rates of decrease for both loops. The lower flow predicted for Loop B is due to uncertainty of delay time for RPT initiation and a RETRAN deficiency which results in calculating slightly asymmetrical loop flows in a symmetric system with symmetric transient conditions. However, the differences in flows are small. They are not expected to affect the overall accuracy of the simulation. Figure 3.1.22 compares the calculated and measured core flow. The RETRAN model's ability to calculate drive and loop flows for a RPT is further demonstrated by the analysis of the one-pump trip test (Test PAT 30A) described in Section 3.1.3.

Turbine control and stop valve closure causes a rapid system pressurization. Figure 3.1.23 shows measured and calculated wide range dome pressure during the test. RETRAN predicts the pressure transient accurately, particularly during the first two seconds, which encompasses the core power transient. The measured pressure spike at 0.3 seconds appeared only in the wide range Division 2

signal; wide range Division 1 and narrow range signals do not show this deviation. The apparent pressure spike may have been an instrument aberration. The plant data shows that one relief valve opened while a second one opened and closed repeatedly. The WNP-2 RETRAN model treats the first two SRVs with lowest pressure setpoint as a single equivalent valve. Both SRVs opened in the RETRAN simulation and the RETRAN pressure results are lower after about 5 seconds.

Figure 3.1.24 shows the steam flow variation. The oscillation in the flow rate from 0 to 3 seconds is caused by pressurization waves after the turbine control and stop valves are closed.

Figure 3.1.19

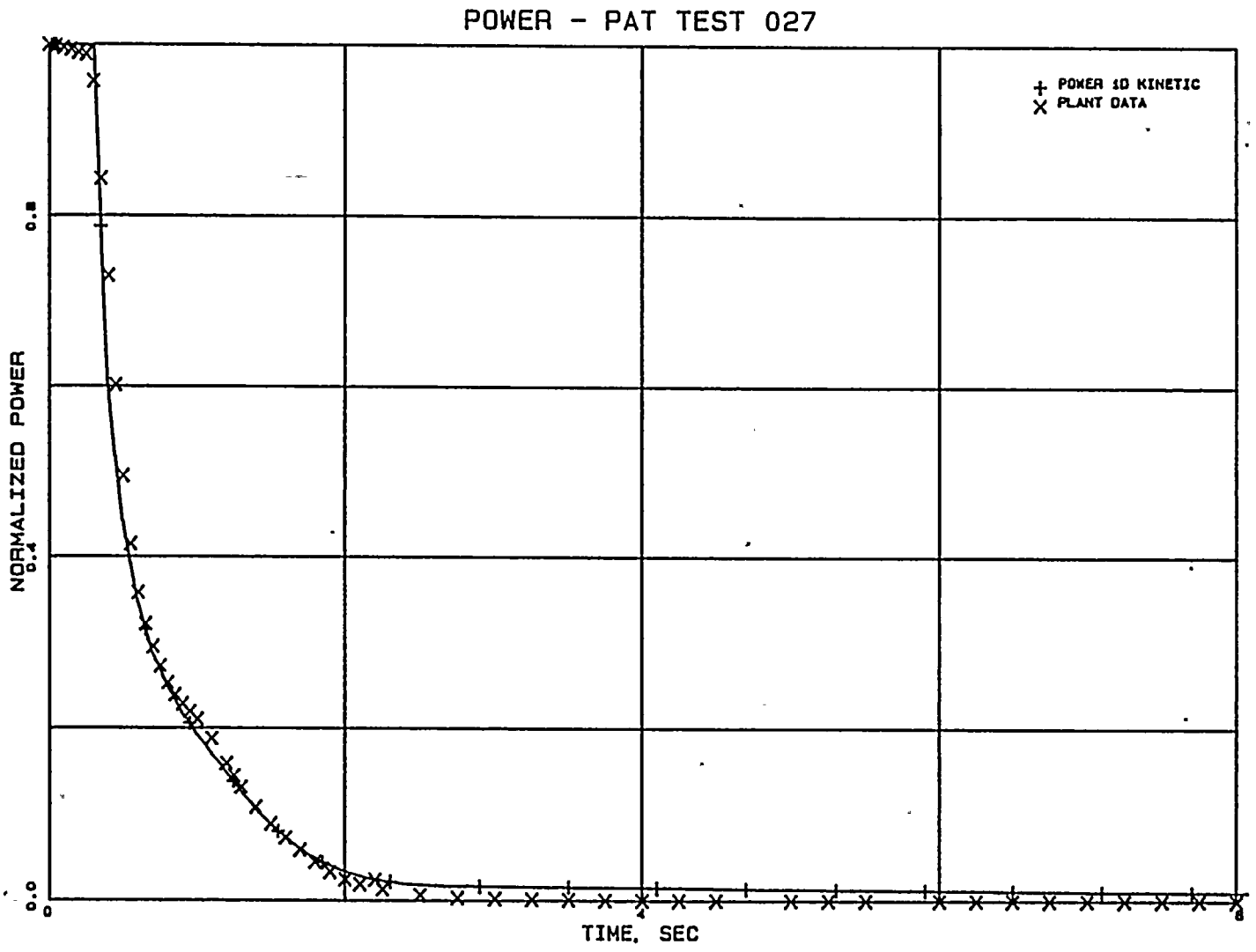
POWER - PAT TEST 027
POWER 1D KINETIC
PLANT DATA
NORMALIZED POWER
0.8
0.4
0.0
0
4
8
TIME, SEC

Figure 3.1.20

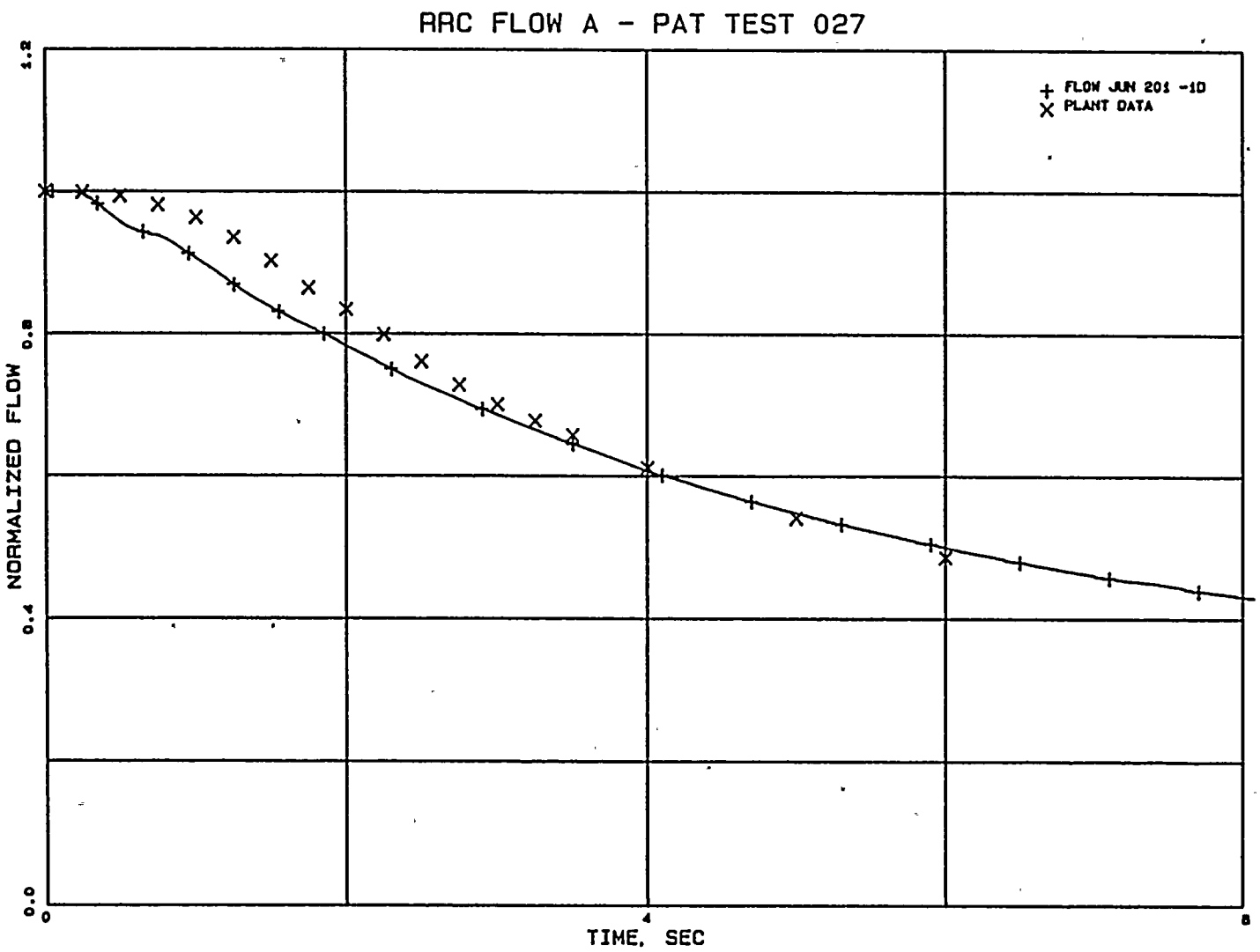
ARC FLOW A - PAT TEST 027
+ FLOW JUN 201 -10
X PLANT DATA
NORMALIZED FLOW
1.2
0.8
0.4
0.0
0
4
8
TIME, SEC

Figure 3.1.21

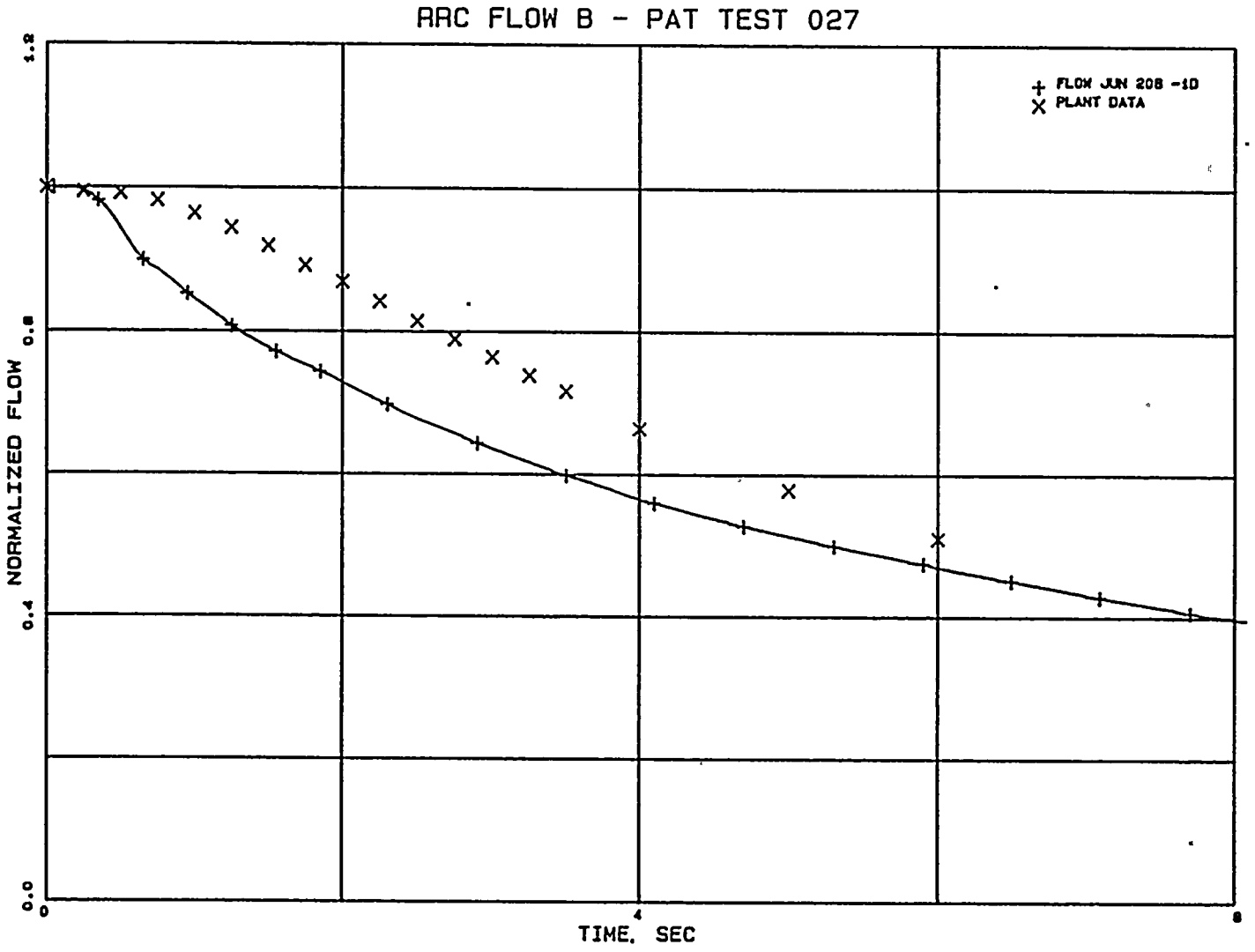
RRC FLOW B - PAT TEST 027
FLOW JUN 208 -10
PLANT DATA
NORMALIZED FLOW
1.2
0.8
0.4
0.0
0
4
8
TIME, SEC

Figure 3.1.22

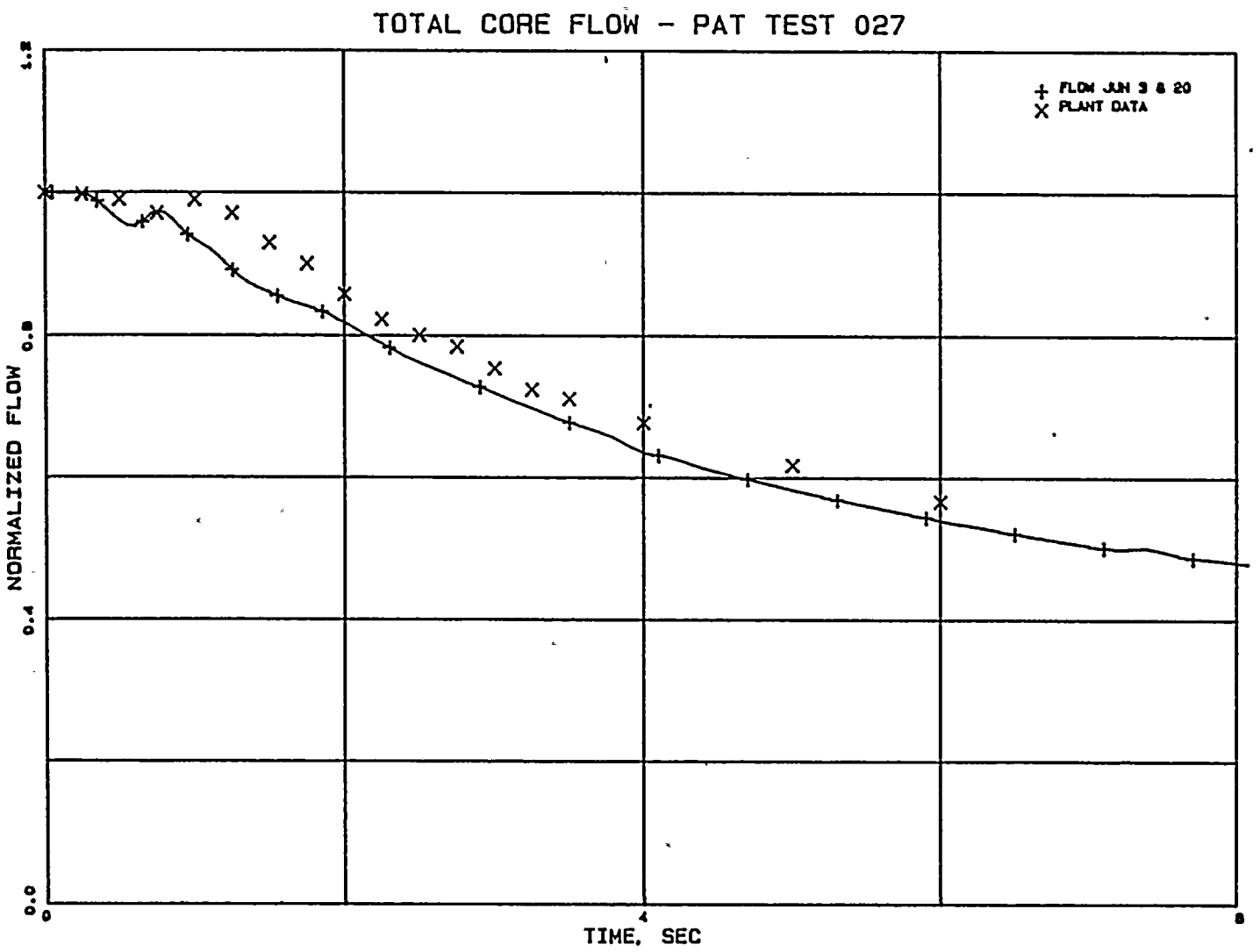
TOTAL CORE FLOW - PAT TEST 027
FLOW JUN 3 & 20
PLANT DATA
NORMALIZED FLOW
1.2
0.8
0.4
0.0
0
4
8
TIME, SEC

Figure 3.1.23

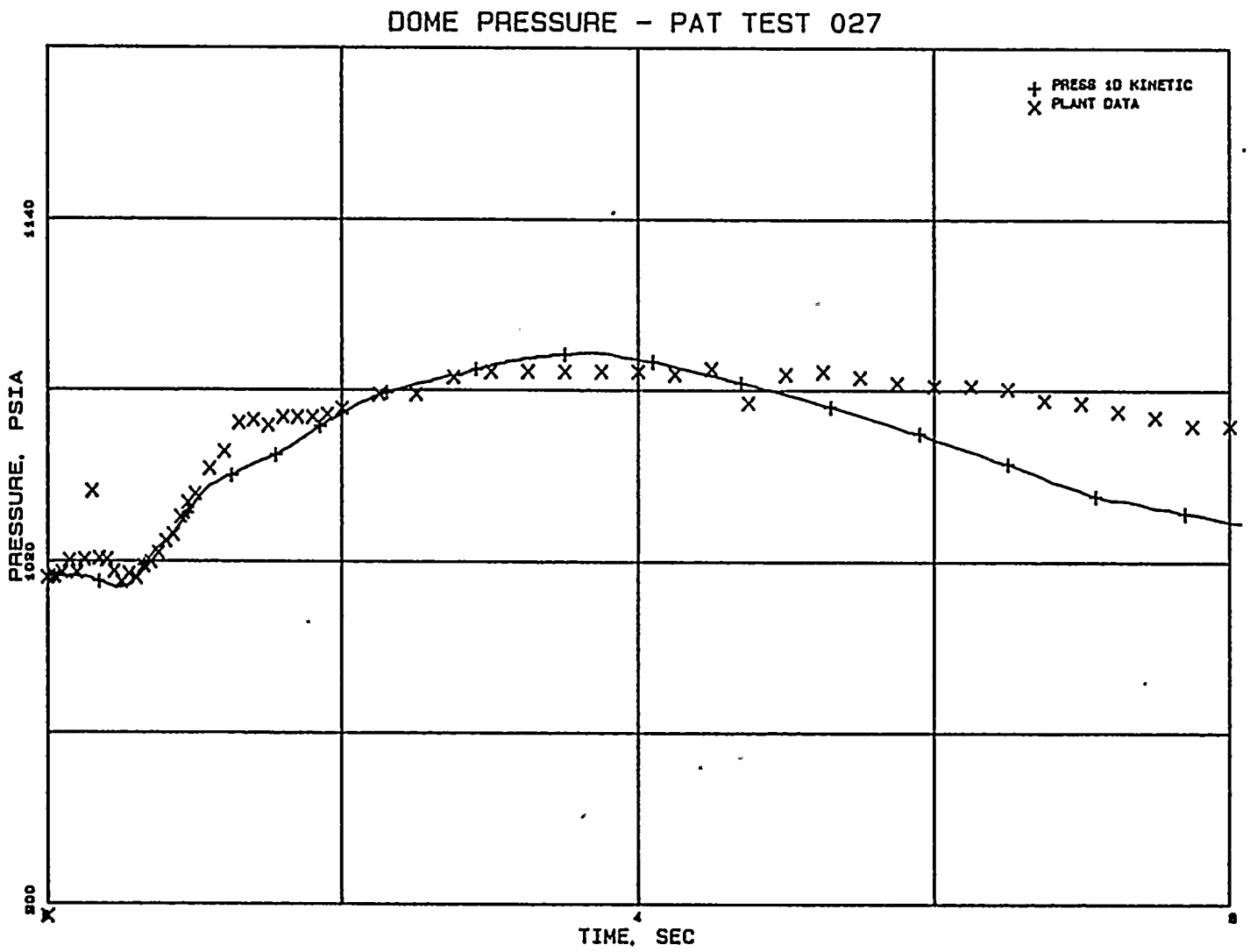
DOME PRESSURE - PAT TEST 027
+ PRESS 1D KINETIC
X PLANT DATA
PRESSURE, PSIA
1140
1020
900
4
8
TIME, SEC

Figure 3.1.24

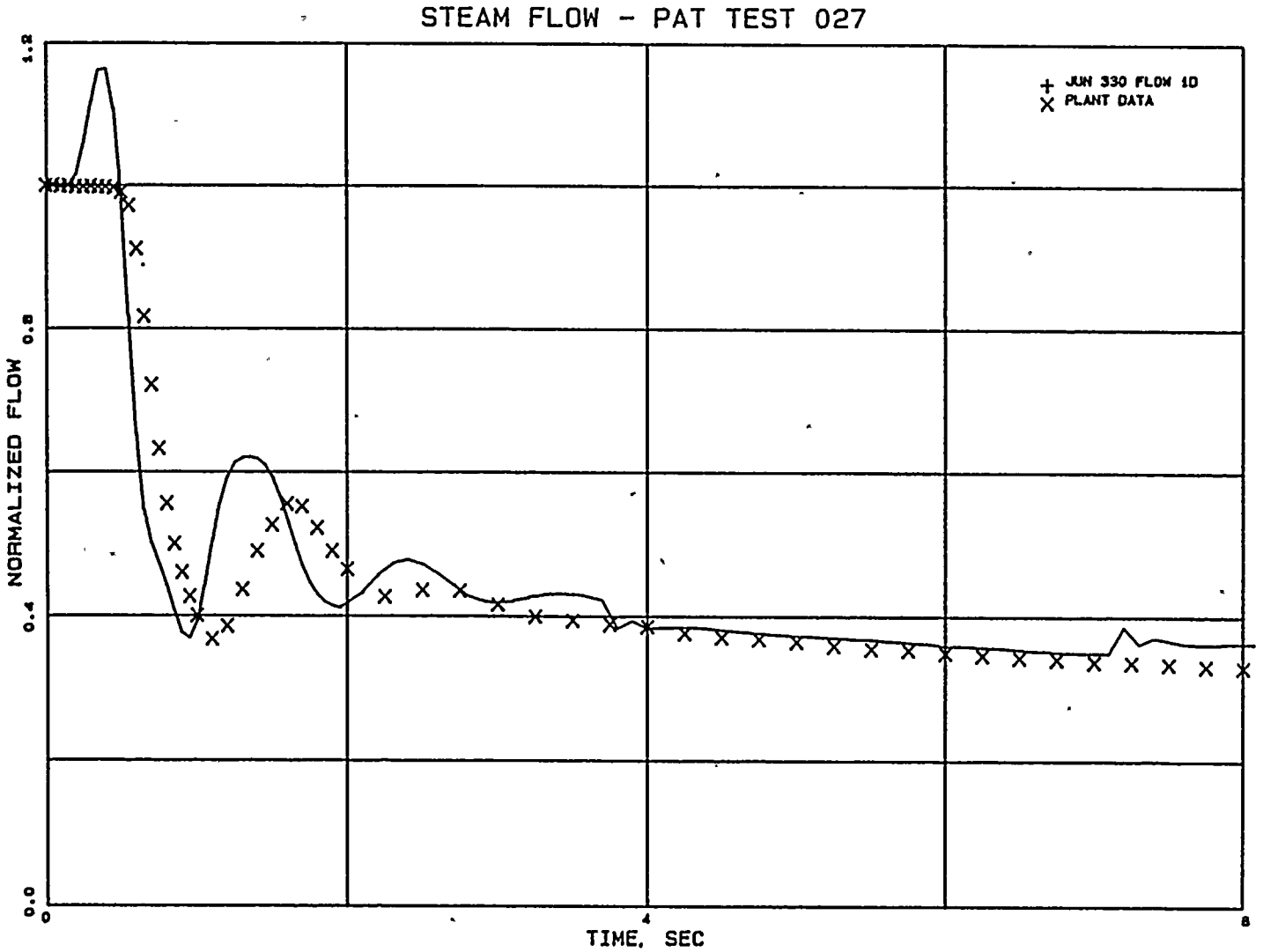
STEAM FLOW - PAT TEST 027
JUN 330 FLOW 1D
PLANT DATA
NORMALIZED FLOW
1.2
0.8
0.4
0.0
0
4
8
TIME, SEC

3.2 Peach Bottom Turbine Trip Tests

The model predictions in the power ascension tests benchmark demonstrate the accuracy and abilities of most of the elements in the WNP-2 RETRAN model. These benchmarks cover expected operation, but normal startup testing does not cover circumstances which challenge the core operating limits. To establish the overall accuracy of the RETRAN model and methods under design basis conditions, the Supply System performed an analysis of the three pressurization transient tests conducted at Peach Bottom Atomic Power Station Unit 2 (PB2) at the end of Cycle 2.

3.2.1 Test Description

In April of 1977, in conjunction with the GE and EPRI, the PB2 licensee performed three pressurization transient tests. These tests (TT1, TT2, and TT3) were performed near the end of operating Cycle 2.

In order to obtain the most accurate data possible for verification of modeling techniques, special instrumentation was installed to monitor important process parameters. In addition, the tests were conducted in such a manner (i.e., delayed scram times, etc.) as to best reproduce typical end-of-cycle licensing

conditions. A detailed description of each test can be found in the EPRI documentation[15]

Table 3.2.1 lists the initial reactor power and core flow for each test. These values were obtained from the process computer P-1 edit taken prior to each test. The test conditions were such that the pressurization resulted in a significant positive neutron flux transient. Each test was initiated by manually tripping the main turbine which resulted in rapid closure of the turbine stop valves.

TABLE 3.2.1

PEACH BOTTOM TURBINE TRIP TESTS

INITIAL CONDITIONS

	POWER		CORE FLOW	
TEST	(MW)	(% NBR)	(Mlbm/hr)	(% NBR)
TT1	1562	47.4	101.3	98.8
TT2	2030	61.6	82.9	80.9
TT3	2275	69.1	101.9	99.4

3.2.2 Peach Bottom Unit 2 Model Description

The Peach Bottom model incorporates the modeling techniques of the WNP-2 model. A schematic of the model is shown in Figure 3.2. (The WNP-2 model is shown in Figures 2.1 through 2.4.) The nodalization within the reactor vessel is identical except that the two downcomer volumes are combined into one in the Peach Bottom model. The two recirculation loops are combined into one in the Peach Bottom model. It is represented by two nodes whereas the WNP-2 model has five nodes for each recirculation loop. The Peach Bottom model includes the entire main steam bypass system whereas the WNP-2 model uses a negative fill junction. This model is the best estimate bypass system model of Hornyik and Naser[16], and was included to provide a realistic simulation of this component. Because the steam line geometry has a significant effect on pressurization transients, the geometric data for the steam line from Philadelphia Electric Company's topical report[17] was used. The Peach Bottom steam line is modeled with six nodes whereas the WNP-2 steam line is modeled with seven nodes. An additional node was used in the WNP-2 model to provide more accurate pressure for SRVs lifting. SRVs did not open during the Peach Bottom turbine trip tests. The physical dimensions and characteristics of the dominant fuel type were used. The dimensions and characteristics for the dominant 7x7 fuel type were obtained from EPRI documentation[18].

FIGURE 3.2 PB2 RETRAN MODEL

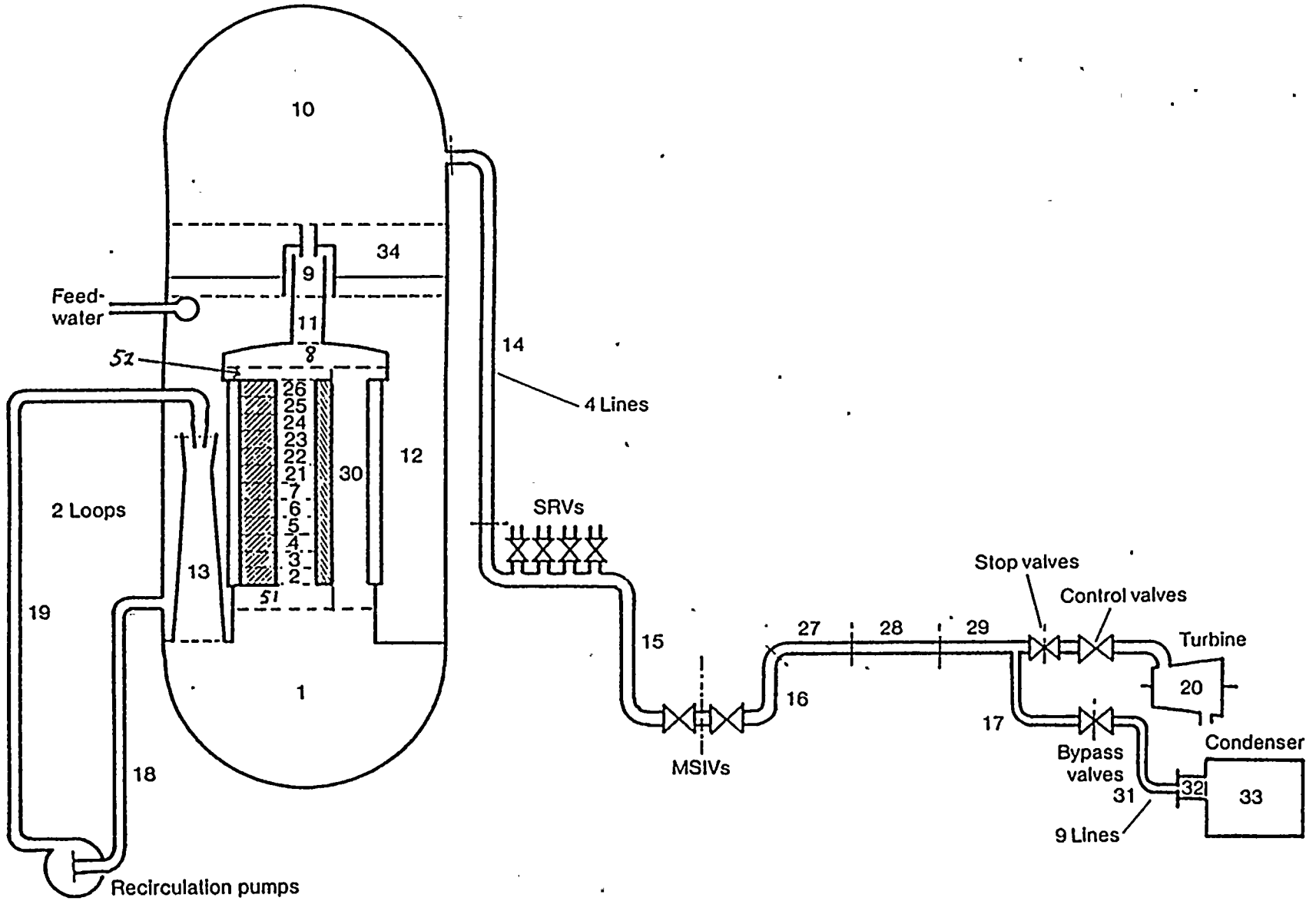

3.2.3 Initial Conditions and Model Inputs

The PB2 model described in Section 3.2.2 was used with initial conditions based on available plant data. Values for core power, core flow, core inlet enthalpy and initial steam flow were based on process computer P-1 edits taken before each transient test. The steam dome pressures were obtained from the recorded data.

The core bypass flow and pressure drop were calculated for each test with the SIMULATE-E MOD03 computer code[19]. Recirculation flows were initialized to be consistent with reactor conditions. Initial water levels were input to match the data for each test.

Additional data was used to specify other RETRAN inputs. These include the Turbine Stop Valve (TSV) position vs. time signal and the Turbine Bypass Valve (BPV) position vs. time signal. A linear TSV opening was assumed with the stroke time obtained from measured data. The BPV flow area was assumed to be proportional to the measured position. The TSV position signal for TT1 failed, so the average of the TT2 and TT3 signals was used.

The control rod scram time and speed can be estimated from the measured rod position relay outputs. The average of the measured scram speeds (31 rods during each test) is plotted in Reference 15 and was used with correction for rod acceleration for all

three tests. All of the control rods were assumed to insert at the average speed.

The feedwater flow rate was specified as a constant value for each test. The short duration of the tests minimizes the potential effects of the feedwater control system. The constant flow assumption was validated through an additional analysis using feedwater flow characteristics provided by Philadelphia Electric Company. Both analyses provided the same results for transient power and pressure responses.

Since Peach Bottom Turbine trip tests were pressurization transients, they were analyzed using the one-dimensional kinetics model. The SIMULATE-E code was used to generate the RETRAN one dimensional kinetics data at the initial conditions for each test. A stepwise depletion of cycles 1 and 2 based on the EPRI documentation[18] was used to determine the fuel exposure, void history and control history at the time of the tests. The basic procedures described in Section 2.6 and Appendix A were used to develop each of the three sets of kinetic data.

The values of the primary parameters needed to specify the initial conditions for each test are summarized in Table 3.2.2.

TABLE 3.2.2

PEACH BOTTOM TURBINE TRIP TESTS

SUMMARY OF INITIAL INPUT PARAMETERS

	TTI	TT2	TT3
Core Thermal Power (MW)	1562.0	2030.0	275.0
Total Core Flow (lbm/sec)	28139.0	23028.0	28306.0
Core Bypass Flow (lbm/sec)	1636.50	1384.87	1762.75
Core Plate Pressure Drop (psid)	16.6	11.61	17.71
Steam Dome Pressure (psia)	991.6	976.1	986.6
Core Inlet Enthalpy (Btu/lbm)	528.0	518.1	521.6
Steam Flow (lbm/sec)	1628.0	2183.0	2461.0
Recirculation Flow (lbm/sec)	9386.0	7686.0	9443.0

3.2.4 Comparison to Test Data

3.2.4.1 Pressure Comparisons

The RETRAN predicted pressures at the turbine inlet, steam dome, and core upper plenum are compared to the measured data in Figures 3.2.1 through 3.2.9. The predictions have been corrected for sensor and sensing line delays based on information provided in the EPRI documentation[15]. The measured data was taken directly from the data tape and has not been filtered to remove sensing line resonances. The accurate prediction of the propagation of the pressure wave from the turbine stop valves to the reactor steam dome demonstrates that the steam line dynamic characteristics are accurately represented by the RETRAN steam line model. The initial pressure oscillation in the steam dome is slightly overpredicted for TT1 and slightly underpredicted for TT2 and TT3. The predictions track the trends in the data consistently.

A comparison of the RETRAN predicted core upper plenum/core exit pressures to the filtered (to remove sensing line resonances) measured data for the first 1.5 seconds of each test is presented in Figures 3.2.10 through 3.2.12. The predictions have been corrected for sensor and sensing line delays. Adequate prediction of the core upper plenum pressure response is essential to transient power predictions. As indicated by the

figures, there is reasonable agreement between the predicted and measured upper plenum pressure for TT2 and TT3. The RETRAN predicted pressure for TT1 is slightly higher than the measured data. The initial pressurization rates and general trends are predicted well for each test.

FIGURE 3.2.1

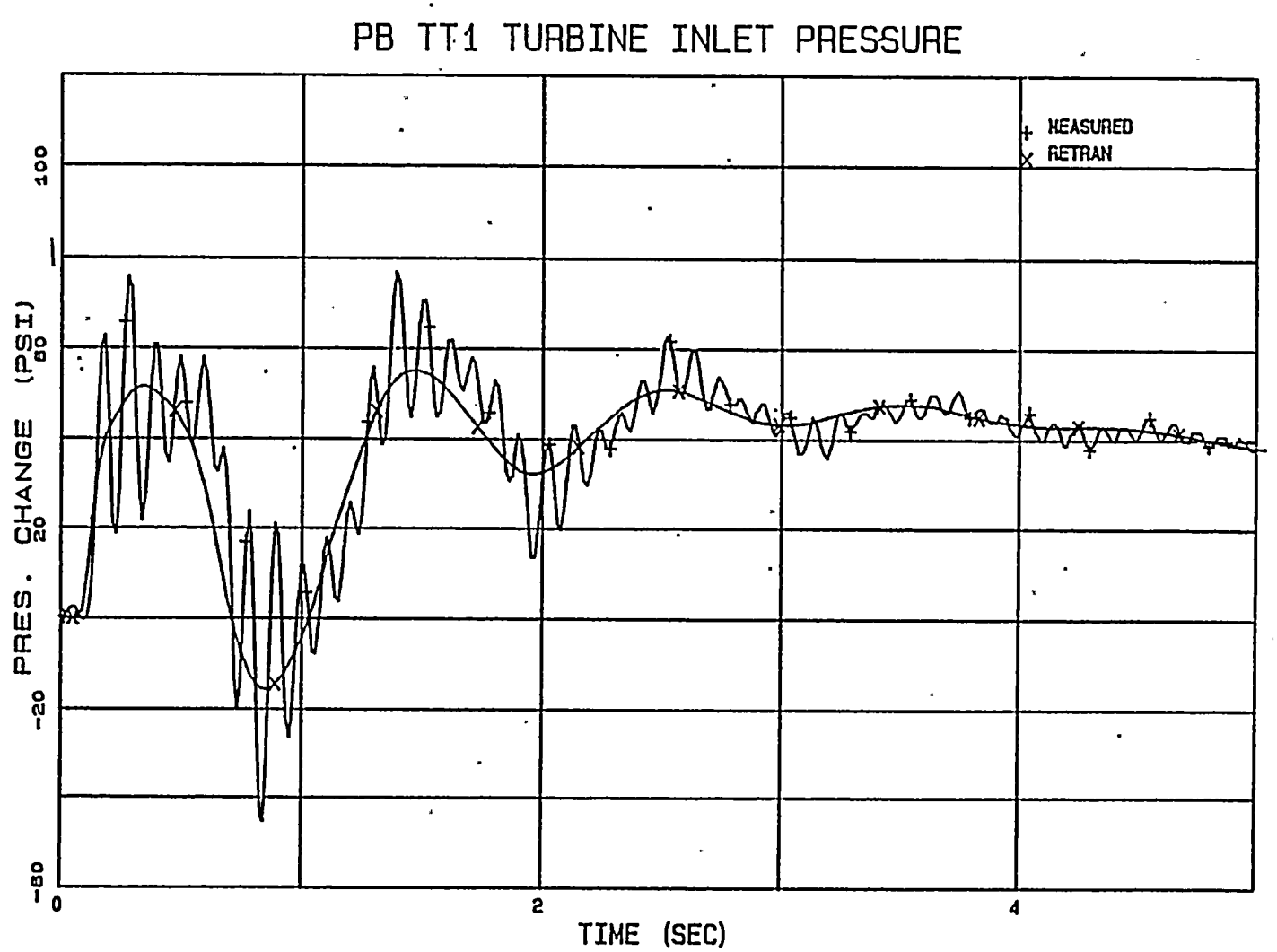
PB TT1 TURBINE INLET PRESSURE
MEASURED
RETRAN
PRES. CHANGE (PSI)
100
80
20
-20
-80
0
2
4
TIME (SEC)

FIGURE 3.2.2

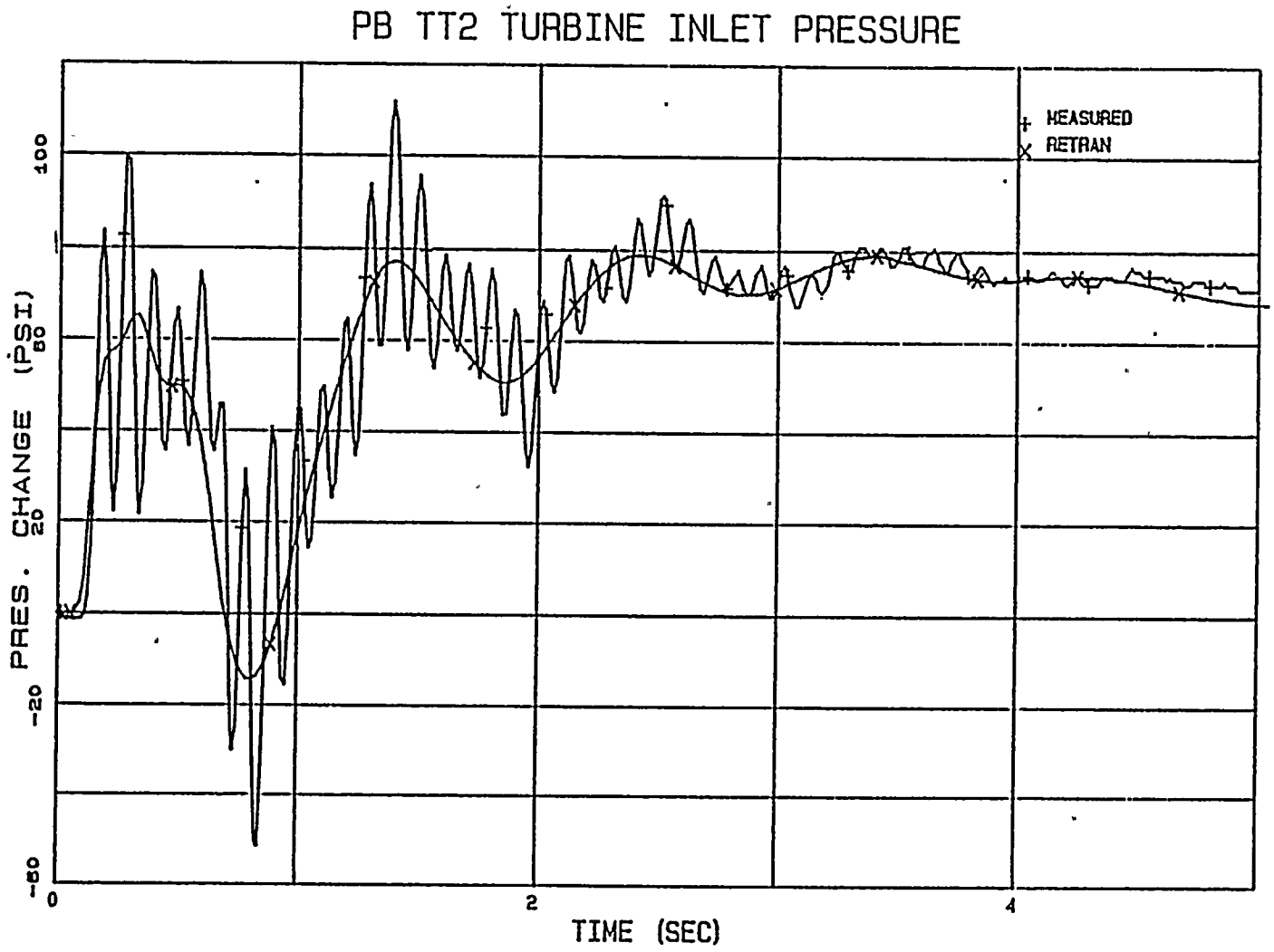
PB TT2 TURBINE INLET PRESSURE
MEASURED
RETRAN
PRES. CHANGE (PSI)
100
80
20
-20
-80
0
2
4
TIME (SEC)

FIGURE 3.2.3

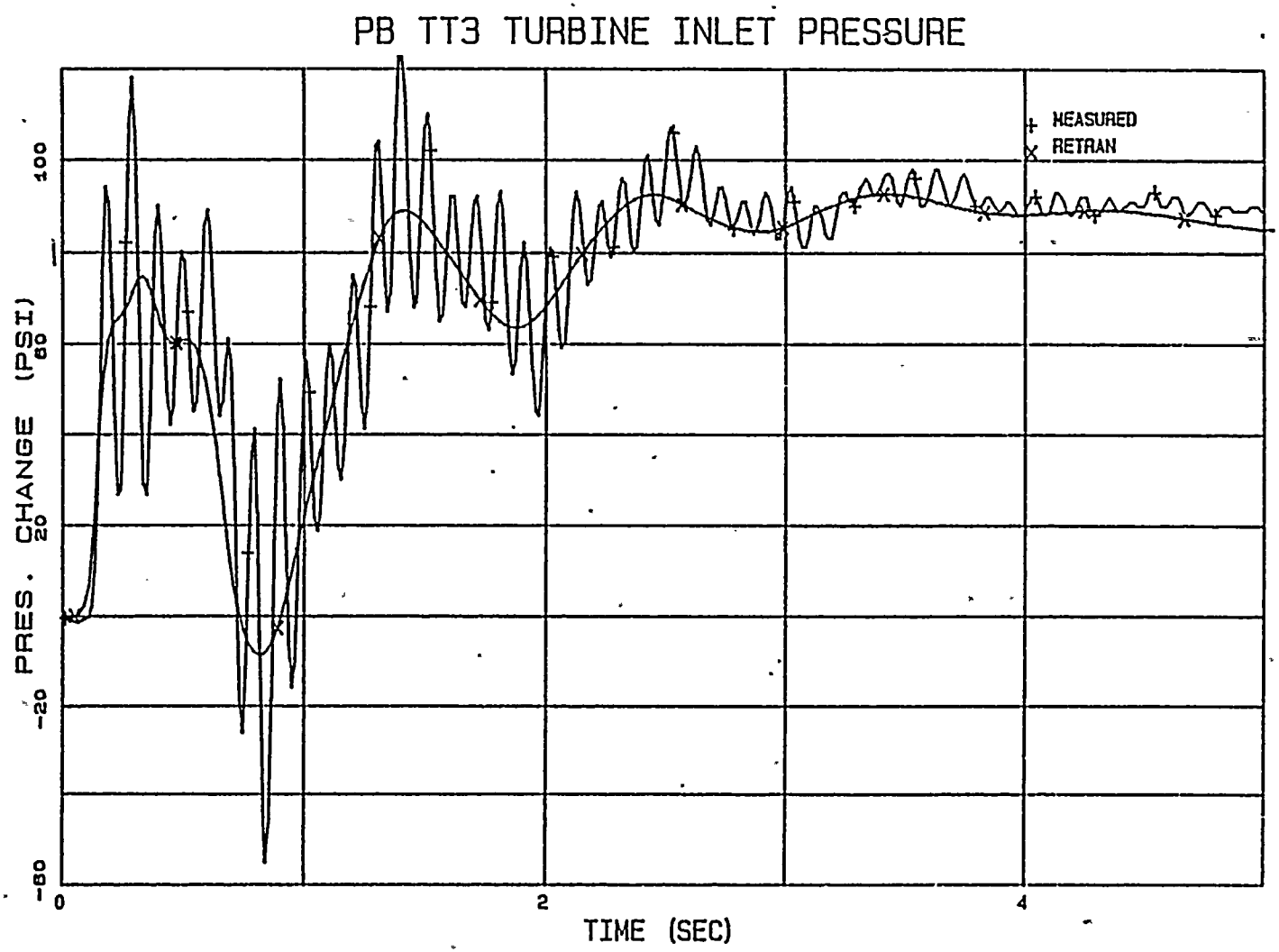
PB TT3 TURBINE INLET PRESSURE
MEASURED
RETRAN
PRES. CHANGE (PSI)
100
60
20
-20
-60
0
2
4
TIME (SEC)

FIGURE 3.2.4

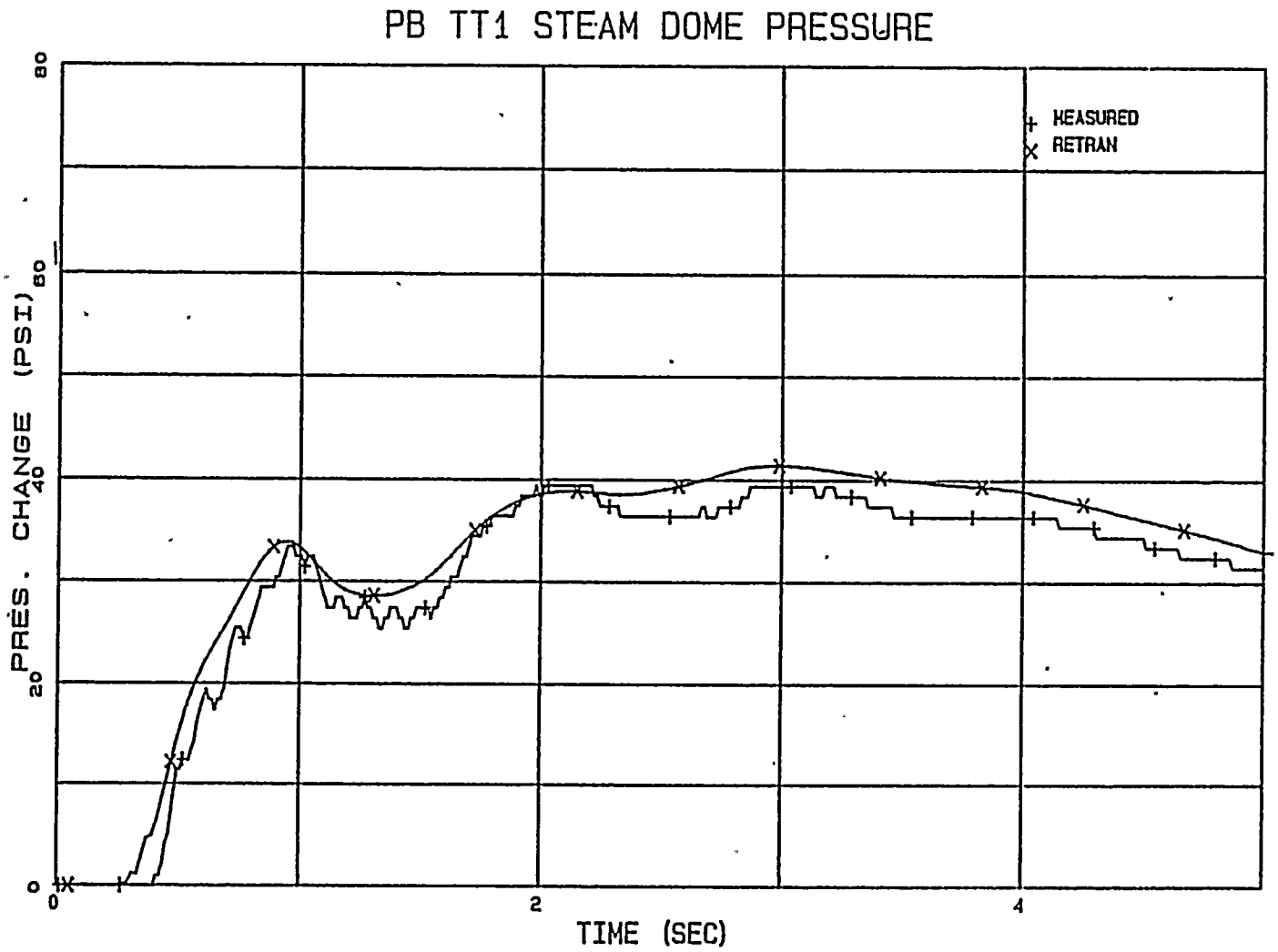
PB TT1 STEAM DOME PRESSURE
MEASURED
RETRAN
PRES. CHANGE (PSI)
0
20
40
60
80
0
2
4
TIME (SEC)

FIGURE 3.2.5

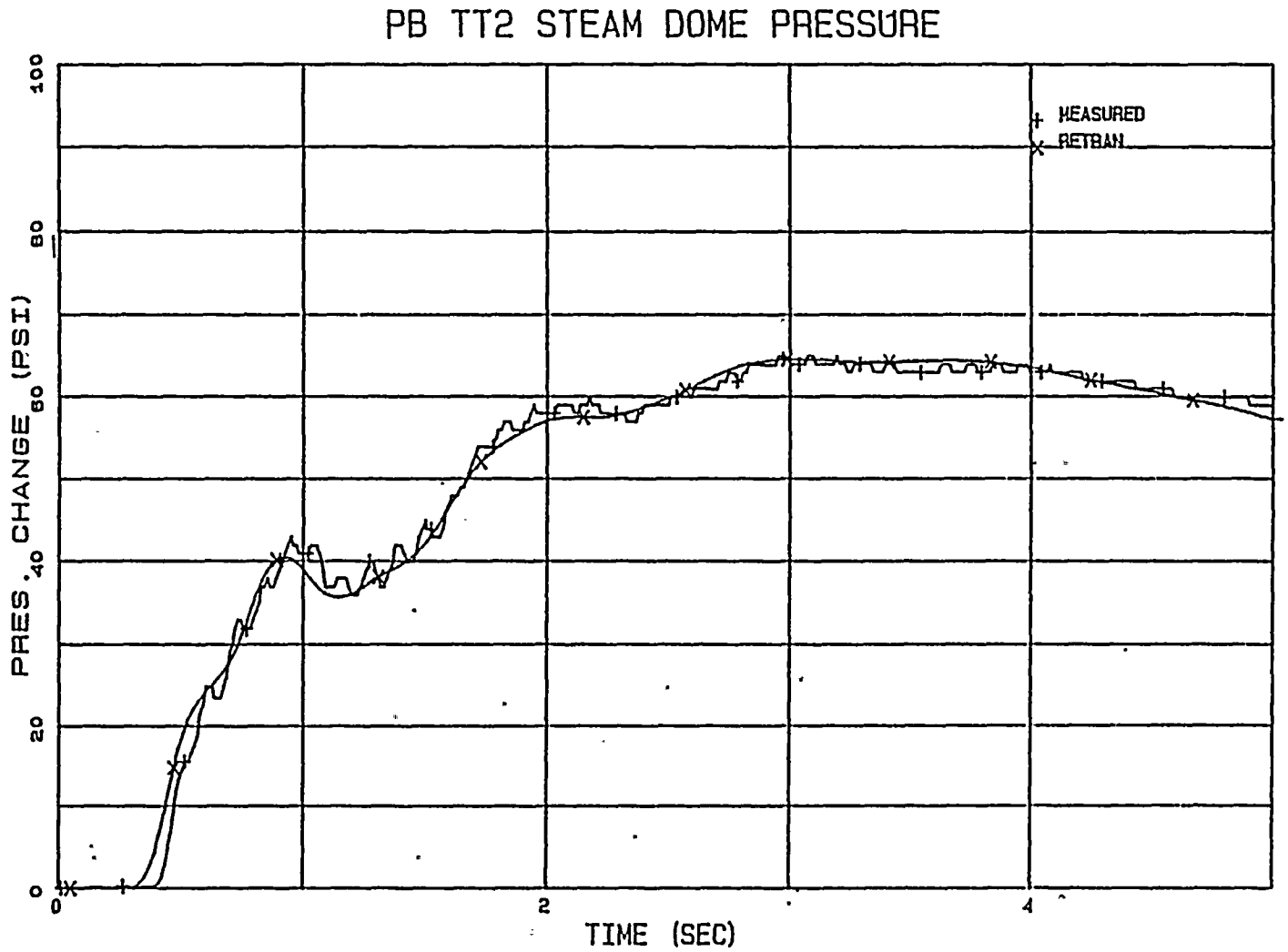
PB TT2 STEAM DOME PRESSURE
MEASURED
RETRAN
PRES. CHANGE (PSI)
0
20
40
60
80
100
0
2
4
TIME (SEC)

FIGURE 3.2.6

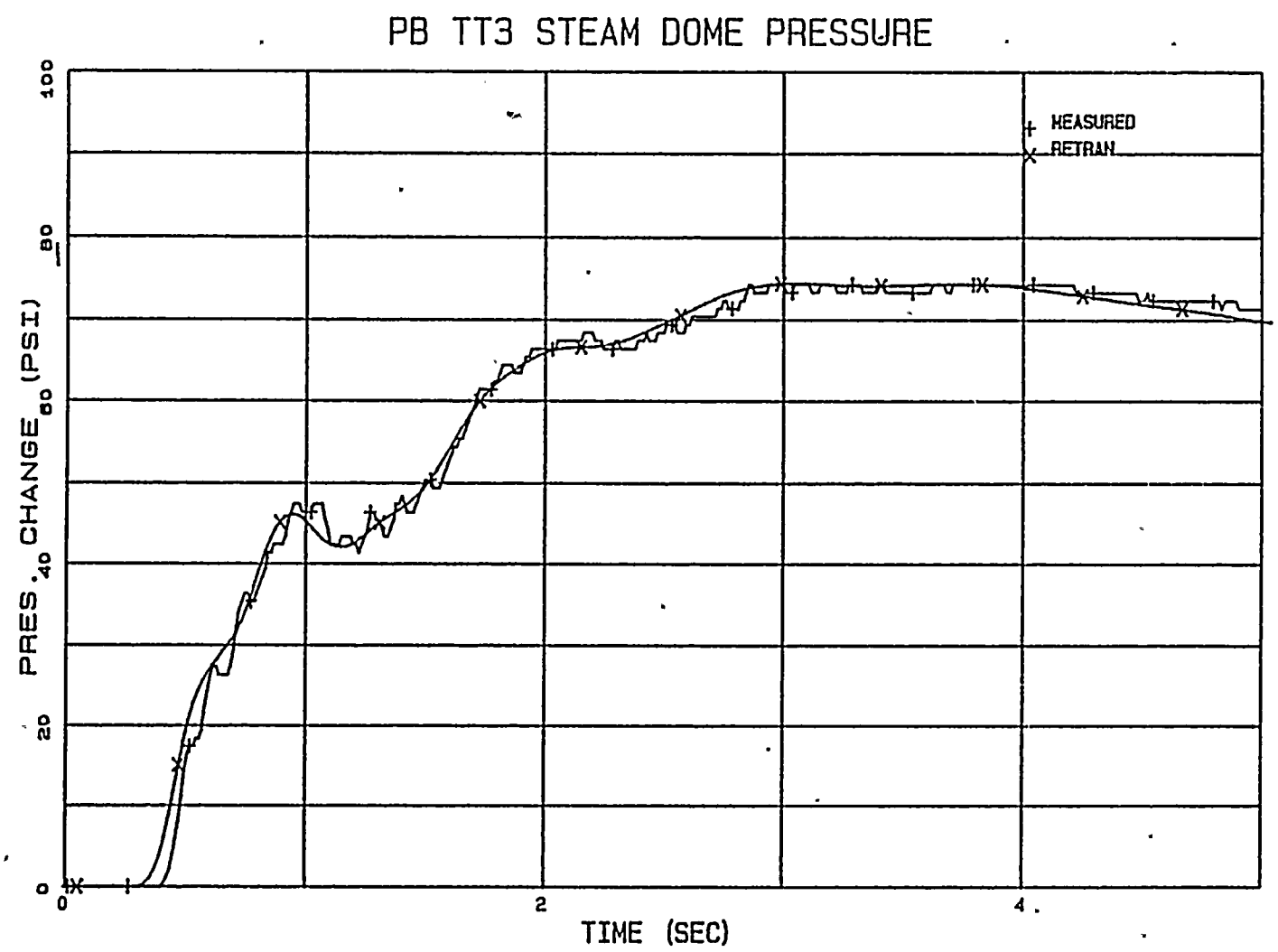
PB TT3 STEAM DOME PRESSURE
MEASURED
RETRAN
PRES. CHANGE (PSI)
100
80
60
40
20
0
0
2
4
TIME (SEC)

FIGURE 3.2.7

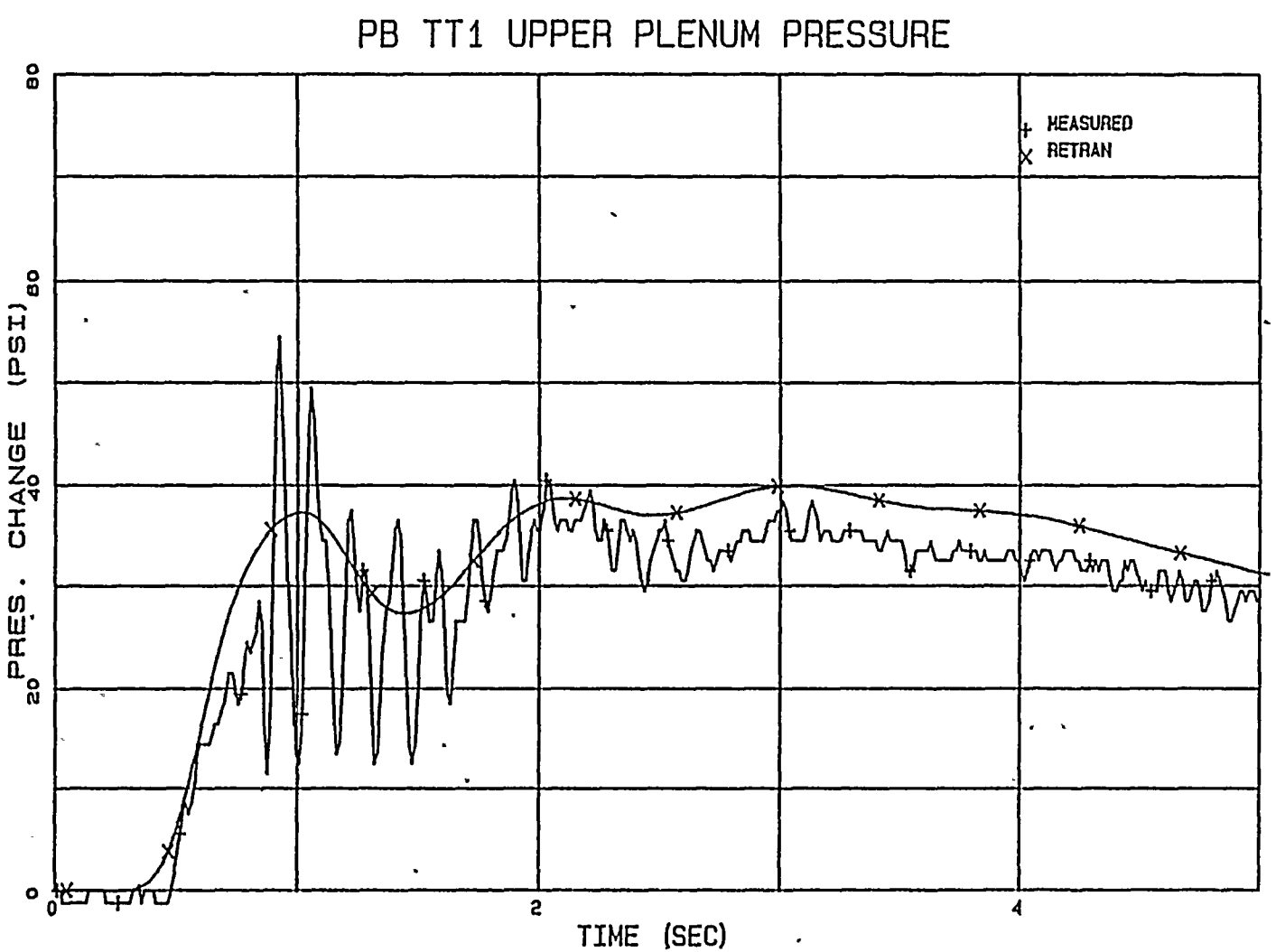
PB TT1 UPPER PLENUM PRESSURE
MEASURED
RETRAN
PRES. CHANGE (PSI)
0
20
40
80
80
0
2
4
TIME (SEC)

FIGURE 3.2.8

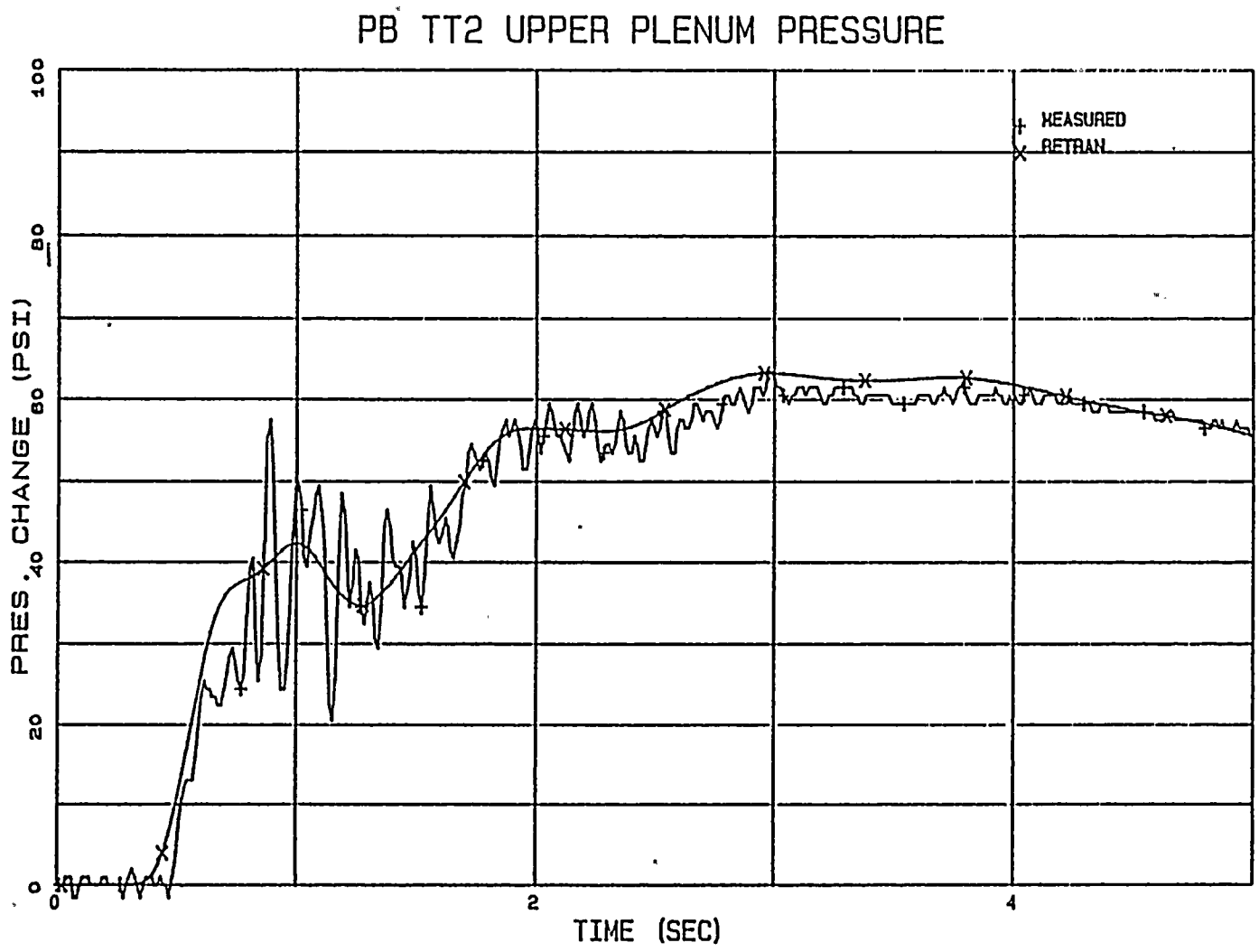
PB TT2 UPPER PLENUM PRESSURE
MEASURED
RETRAN
PRES. CHANGE (PSI)
0
20
40
60
80
100
0
2
4
TIME (SEC)

FIGURE 3.2.9

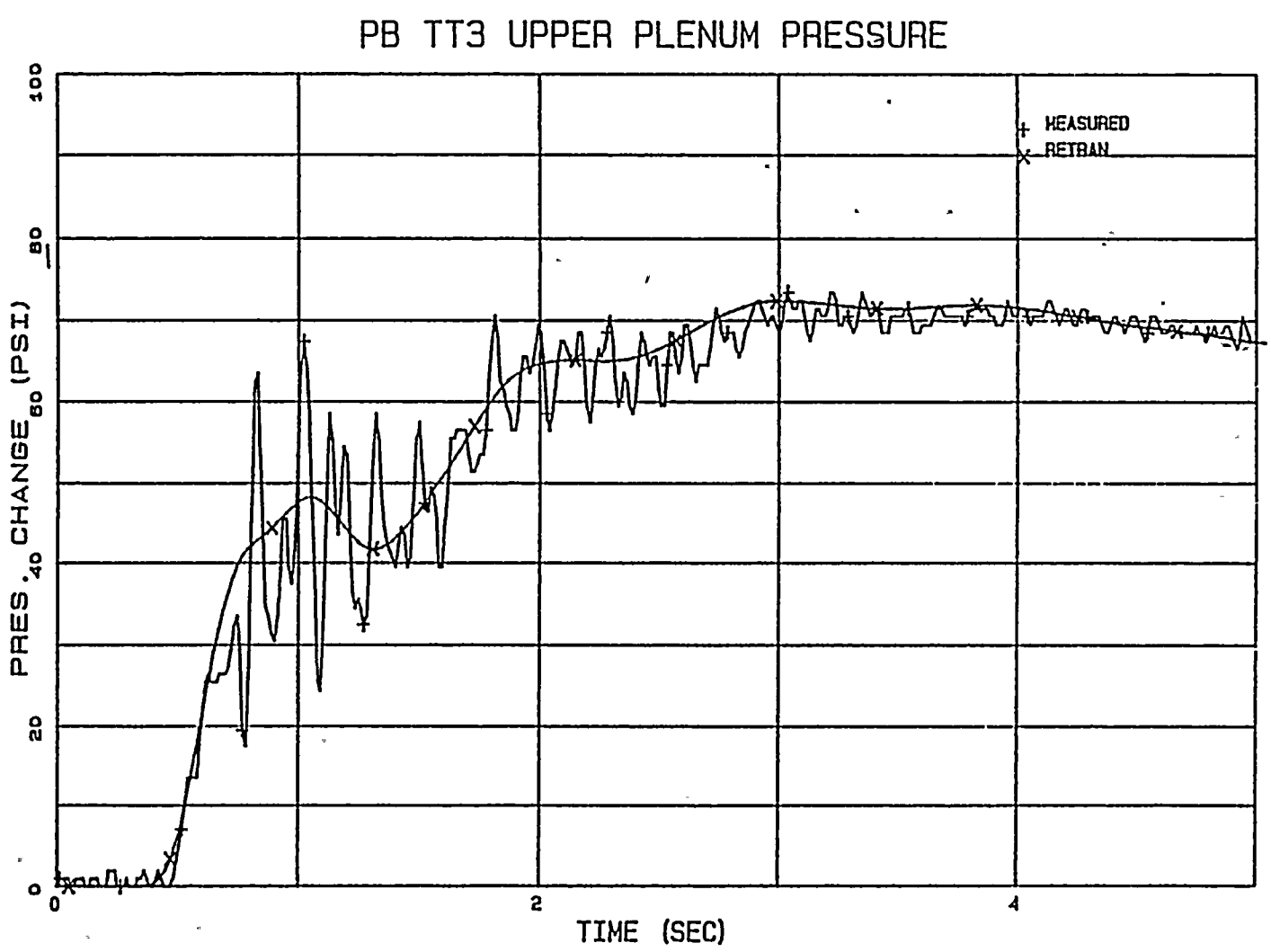
PB TT3 UPPER PLENUM PRESSURE
MEASURED
RETRAN
PRES. CHANGE (PSI)
0
20
40
60
80
100
0
2
4
TIME (SEC)

FIGURE 3.2.10

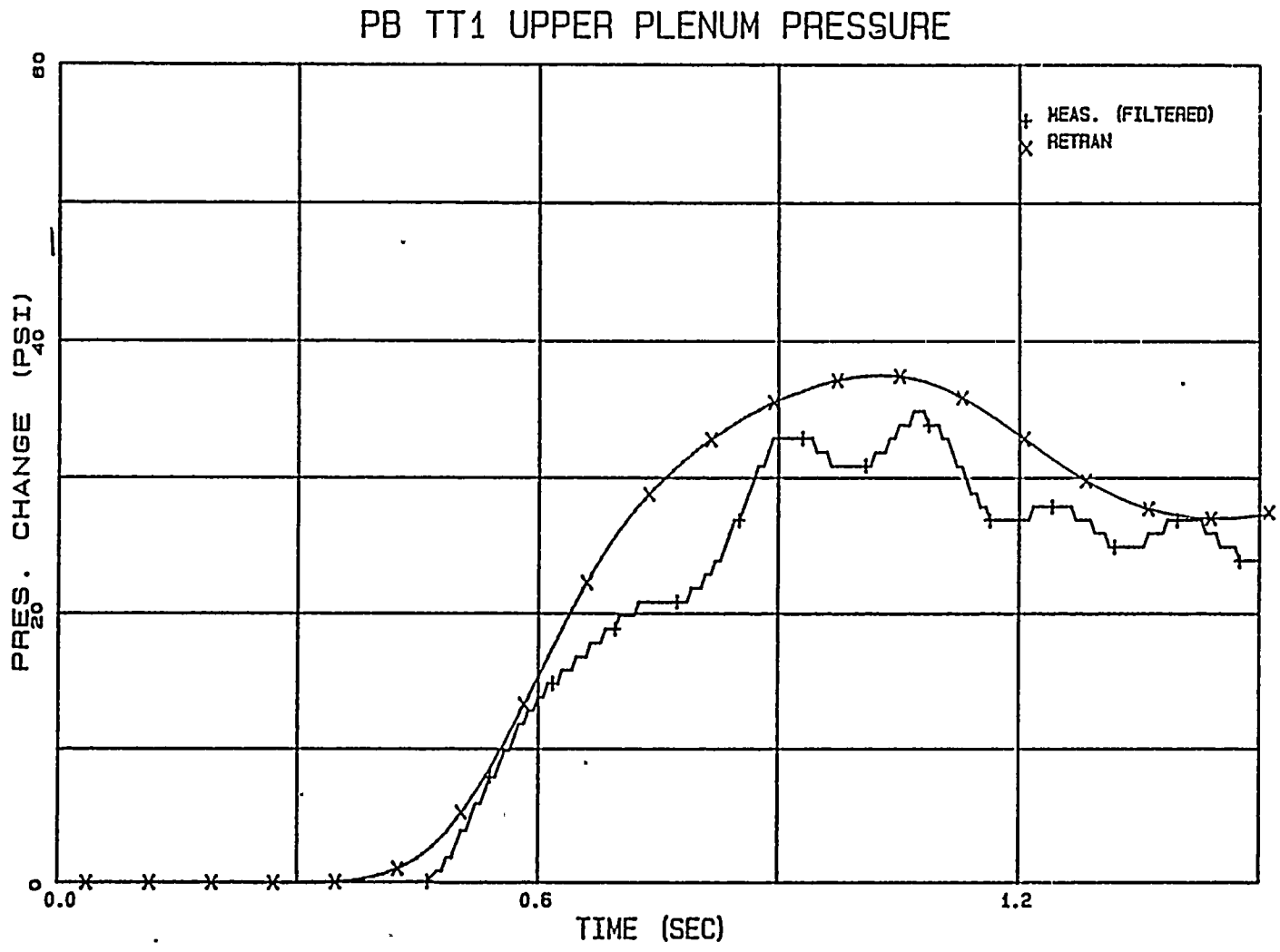
PB TT1 UPPER PLENUM PRESSURE
MEAS. (FILTERED)
RETRAN
PRES. CHANGE (PSI)
0
20
40
60
0.0
0.6
1.2
TIME (SEC)

FIGURE 3.2.11

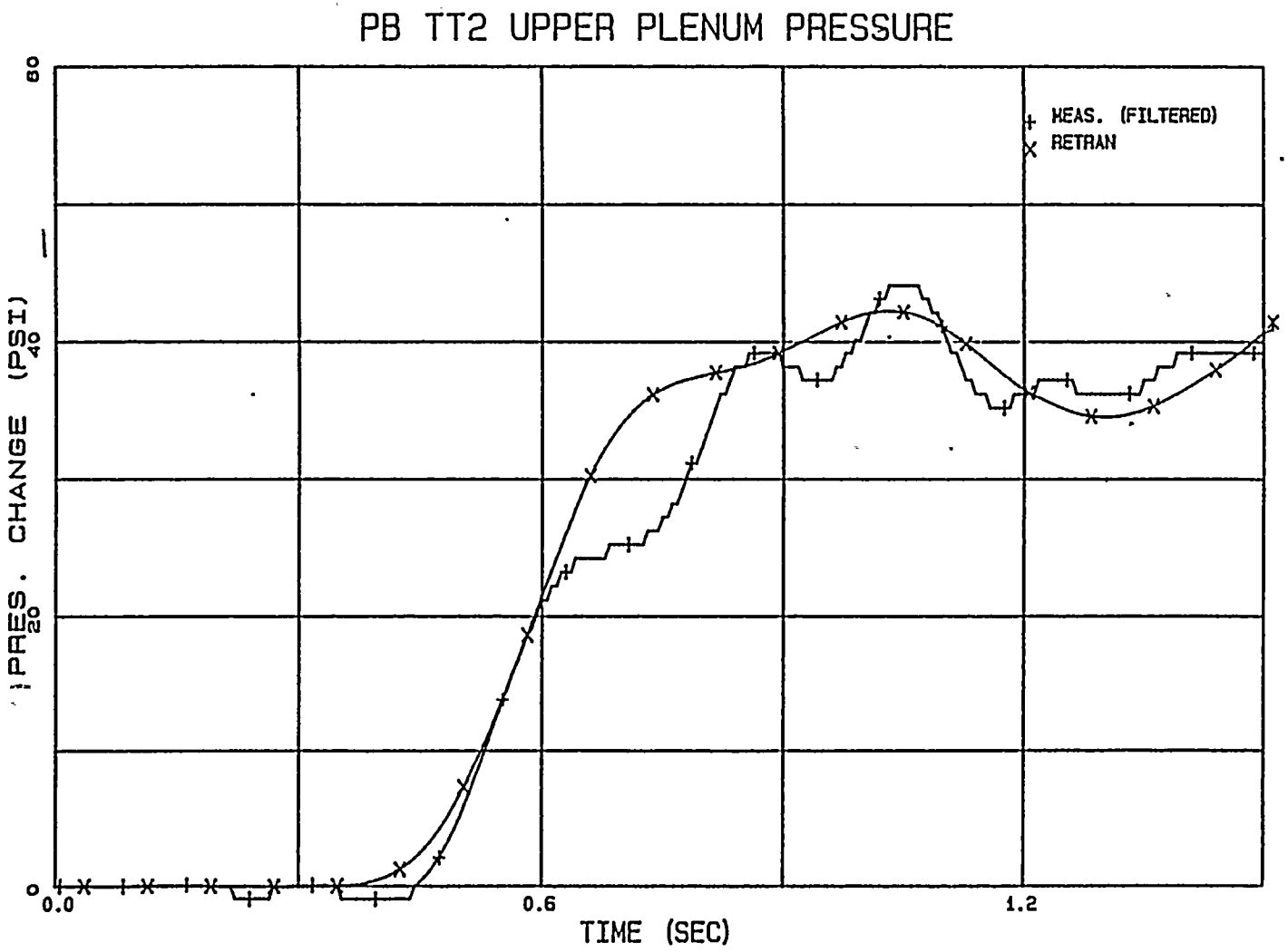
PB TT2 UPPER PLENUM PRESSURE
MEAS. (FILTERED)
RETRAN
PRES. CHANGE (PSI)
0
20
40
60
0.0
0.6
1.2
TIME (SEC)

FIGURE 3.2.12

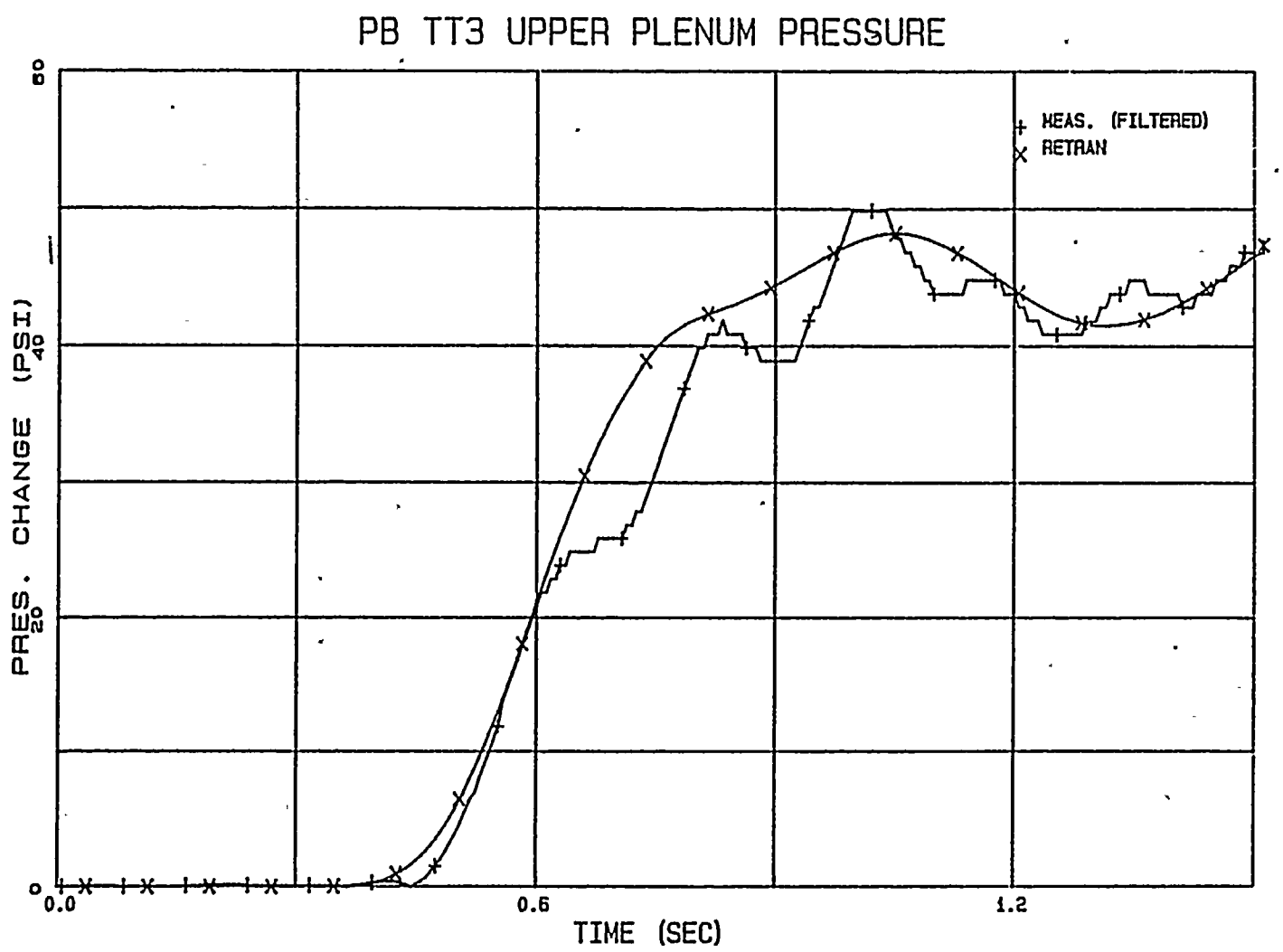
PB TT3 UPPER PLENUM PRESSURE
MEAS. (FILTERED)
RETRAN
PRES. CHANGE (PSI)
60
40
20
0
0.0
0.6
1.2
TIME (SEC)

3.2.4.2 Power and Reactivity Comparisons

Figures 3.2.13 through 3.2.27 compare the predicted core average neutron flux to the measured average of the LPRM signals for each test. Also compared is the predicted neutron flux response to the average of the LPRM signals at each LPRM level (A, B, C, and D) in the core. A summary of the predicted and measured neutron flux peaks is given in Table 3.2.3.

The RETRAN predicted neutron flux response is in excellent agreement with the measured data. The magnitude and the timing of the core average neutron flux peak and the area under the flux peak are predicted accurately. Timing trends and relative peak magnitude are also predicted accurately in the individual LPRM levels. Table 3.2.4 presents a summary of peak core average neutron flux and area under the flux peak for each test. A Summary of the time of peak neutron flux is presented in Table 3.2.5.

The calculated net reactivity, scram reactivity, and net reactivity implied by the data are presented in Figures 3.2.28 through 3.2.30. The implied net reactivity was calculated using an inverse point kinetic algorithm and the average of the measured LPRM signals.

A summary of the calculated and implied net reactivities is presented in Table 3.2.6. The implied data indicates that the net reactivity turns (slope becomes negative) before scram occurs for each test. However, while the neutron flux turns before scram occurs for TT1 and TT2, the neutron flux for TT3 turns after the scram occurs. Thus, the peak neutron flux and area under the peak for TT3 are sensitive to the scram delay time. The peak net reactivity is slightly overpredicted for all three tests. This is due to the slight overprediction of the upper plenum pressure at the time of peak reactivity.

TABLE 3.2.3

PEACH BOTTOM TURBINE TRIP TESTS

SUMMARY OF NORMALIZED CORE AVERAGE AND

LPRM LEVEL NEUTRON FLUX PEAKS

		A	B	C	D	CORE AVG.
TT1	Calculation	3.72	4.98	5.99	6.15	5.41
	Data	3.48	4.46	5.23	5.59	4.83
	% Diff.	6.90	11.7	14.5	10.0	12.0
TT2	Calculation	3.49	4.68	5.09	4.82	4.68
	Data	3.52	4.50	4.91	5.02	4.54
	% Diff.	-0.9	4.0	3.7	-4.0	3.1
TT3	Calculation	3.84	5.42	6.06	5.74	5.39
	Data	3.68	4.83	5.45	5.47	4.90
	% Diff.	4.3	12.2	11.2	4.9	10.0

TABLE 3.2.4

PEACH BOTTOM TURBINE TRIP TESTS

SUMMARY OF CORE AVERAGE PEAK NEUTRON FLUX

	PEAK NEUTRON FLUX (NORM)			AREA UNDER PEAK		
	CALC.	DATA	% DIFF.	CALC.	DATA	% DIFF.
TT1	5.41	4.83	12.0	0.960	0.888	8.1
TT2	4.68	4.54	3.1	0.769	0.743	3.5
TT3	5.39	4.90	10.0	0.717	0.669	7.2

TABLE 3.2.5

PEACH BOTTOM TURBINE TRIP TESTS

TIME OF PEAK NEUTRON FLUX

	TIME (SEC)	
	CALC.	DATA
TT1	.774	.774
TT2	.720	.726
TT3	.702	.702

TABLE 3.2.6

PEACH BOTTOM TURBINE TRIP TESTS

SUMMARY OF NET REACTIVITIES

	PEAK REACTIVITY ($)			TIME OF PEAK (SEC)	
	CALC.	DATA	% DIFF.	CALC.	DATA
TT1	0.804	0.776	3.6%	0.738	0.744
TT2	0.780	0.767	1.7%	0.690	0.696
TT3	0.836	0.812	2.5%	0.678	0.660

FIGURE 3.2.13

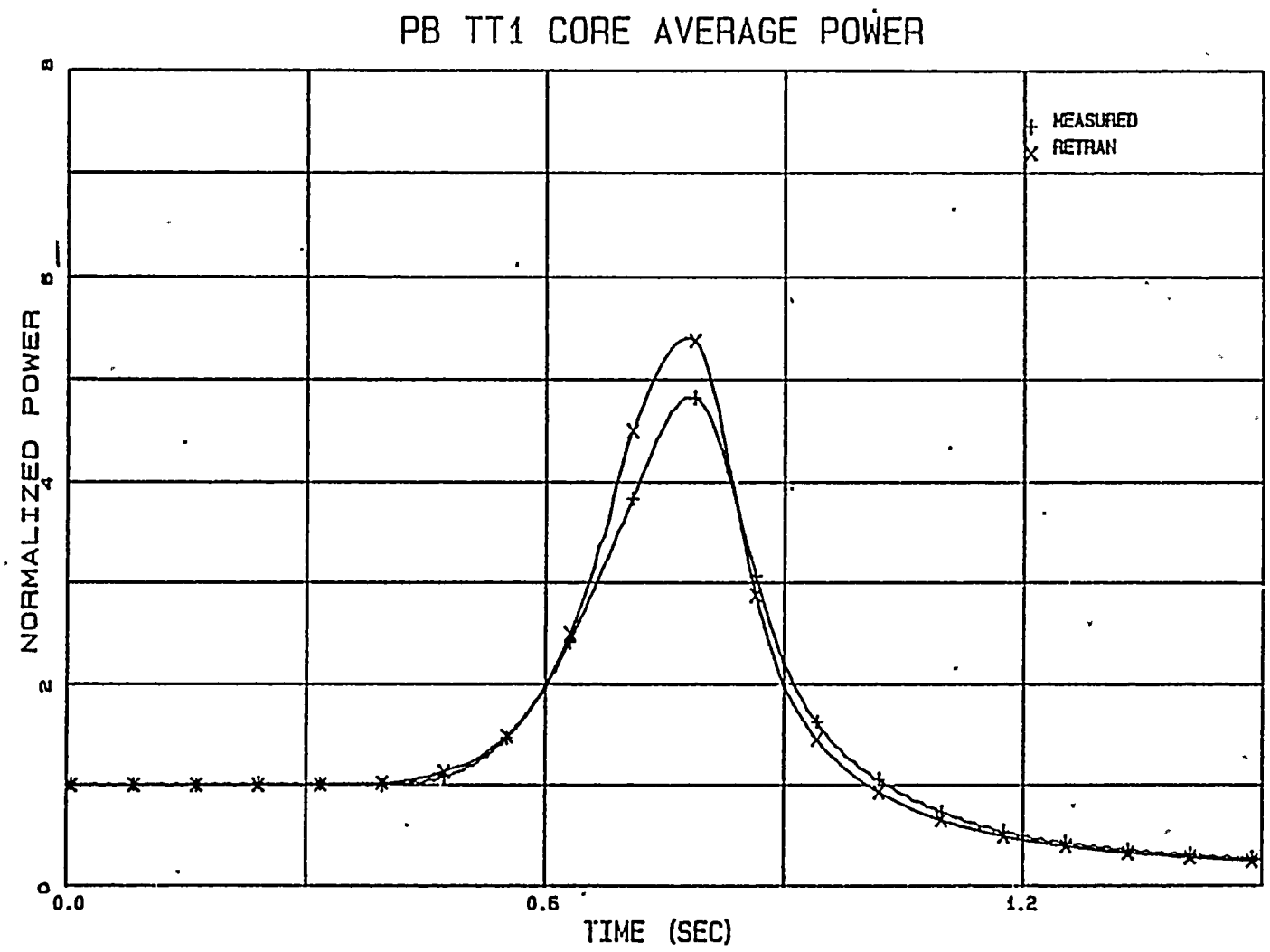
PB TT1 CORE AVERAGE POWER
MEASURED
RETRAN
NORMALIZED POWER
0
2
4
6
8
0.0
0.6
1.2
TIME (SEC)

FIGURE 3.2.14

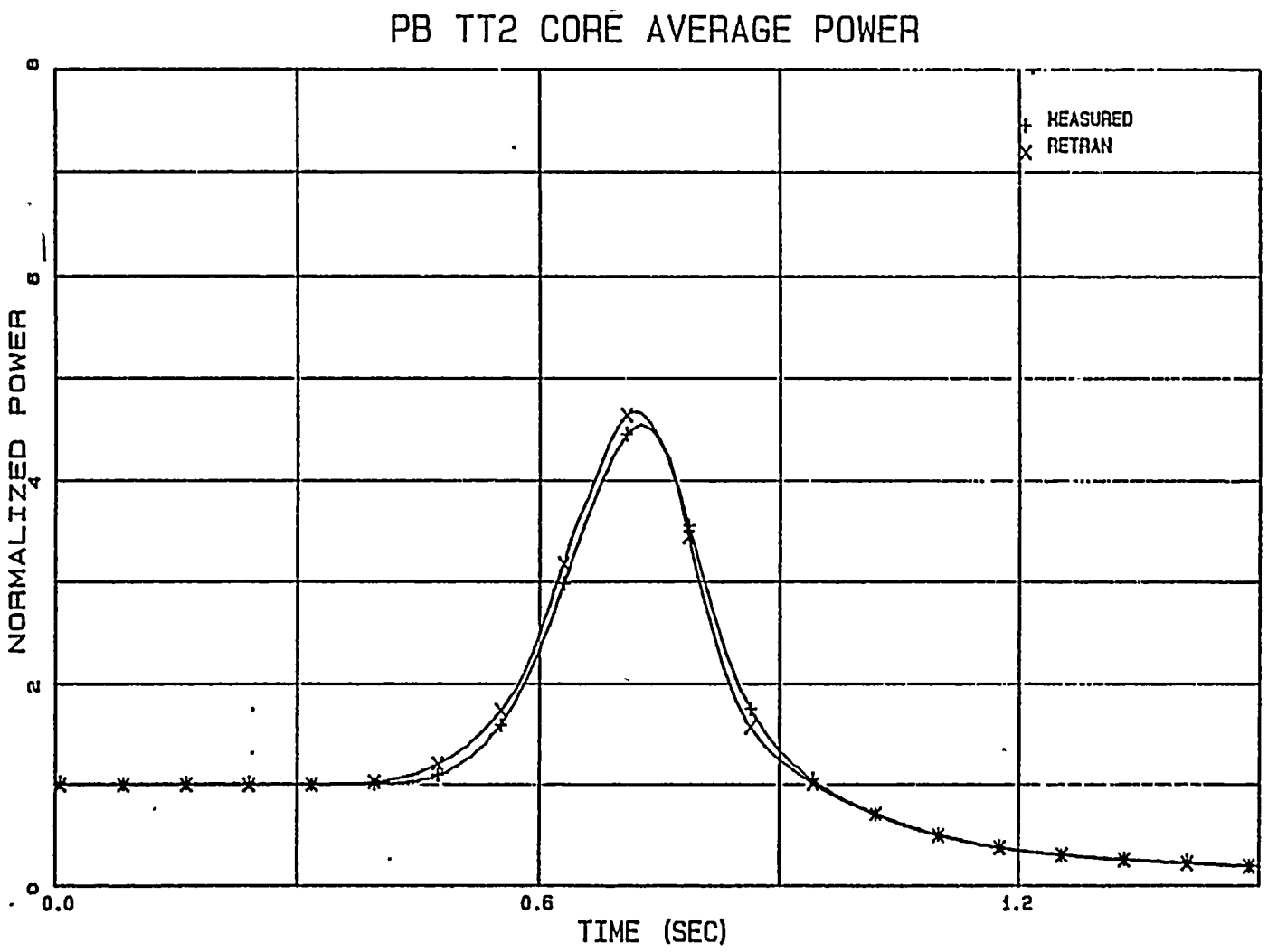
PB TT2 CORE AVERAGE POWER
MEASURED
RETRAN
NORMALIZED POWER
0
2
4
6
8
0.0
0.6
1.2
TIME (SEC)

FIGURE 3.2.15

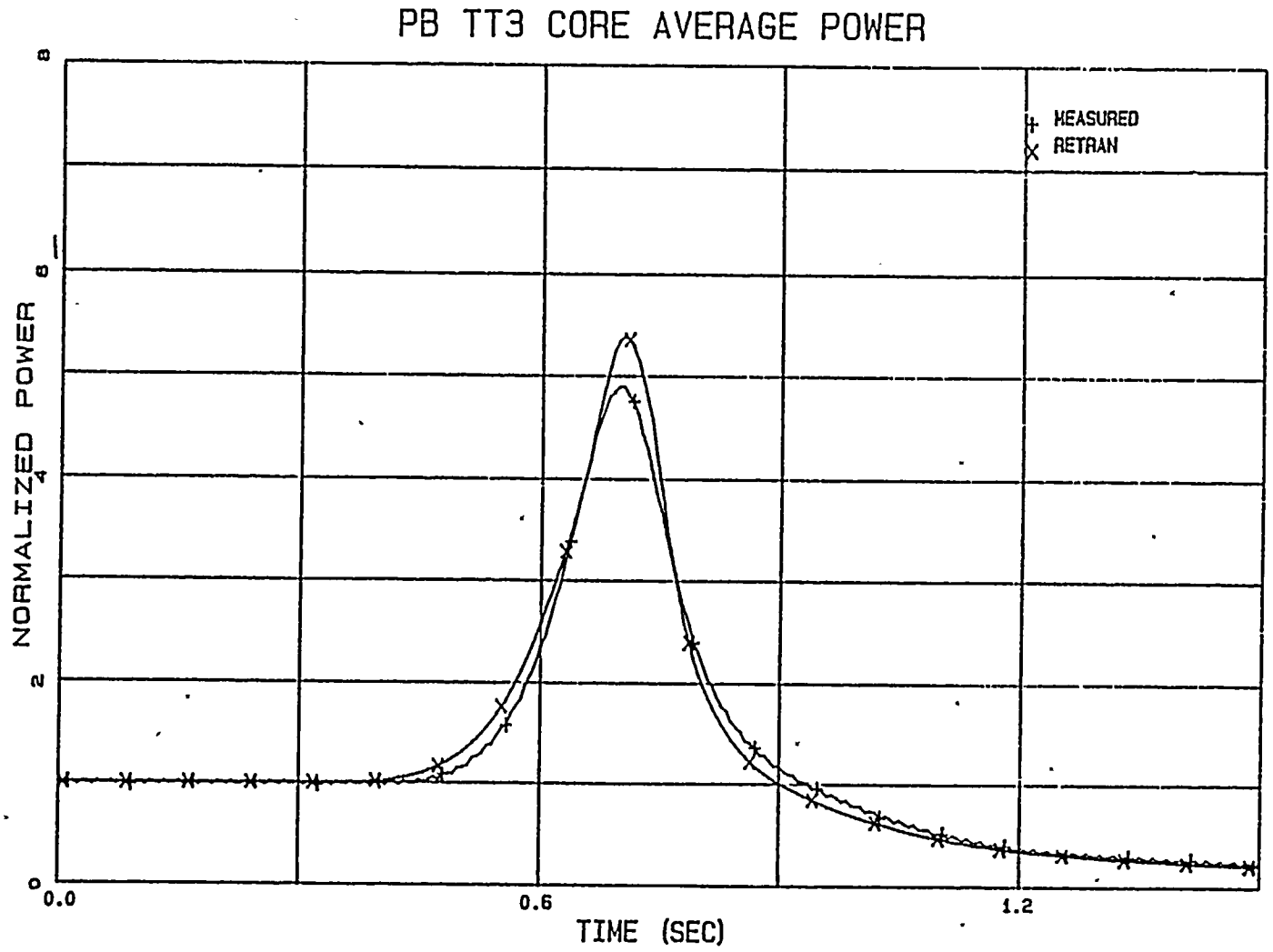
PB TT3 CORE AVERAGE POWER
MEASURED
RETRAN
NORMALIZED POWER
0
2
4
6
8
0.0
0.6
1.2
TIME (SEC)

FIGURE 3.2.16

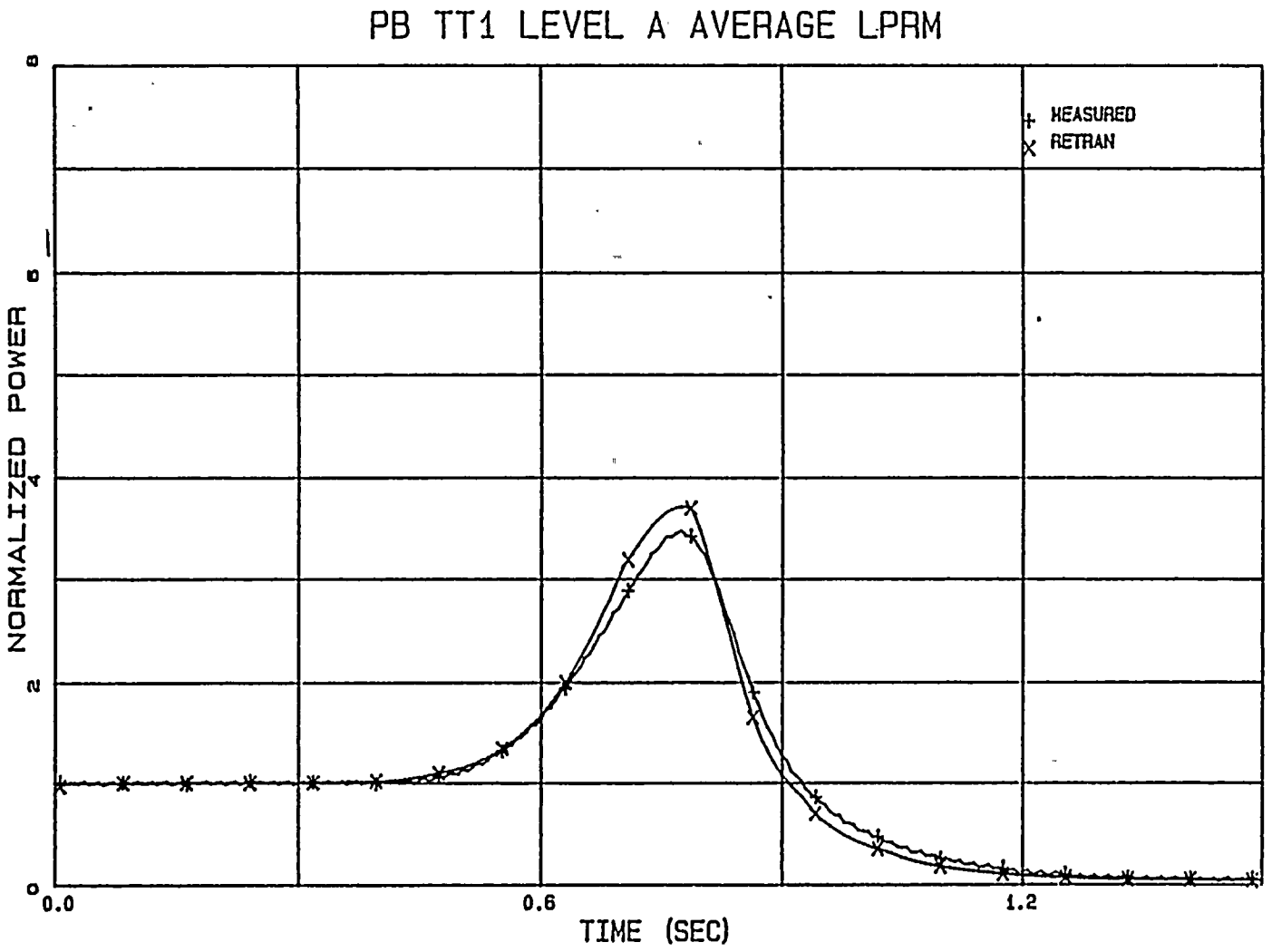
PB TT1 LEVEL A AVERAGE LPRM
MEASURED
RETRAN
NORMALIZED POWER
0
2
4
6
8
0.0
0.6
1.2
TIME (SEC)

FIGURE 3.2.17

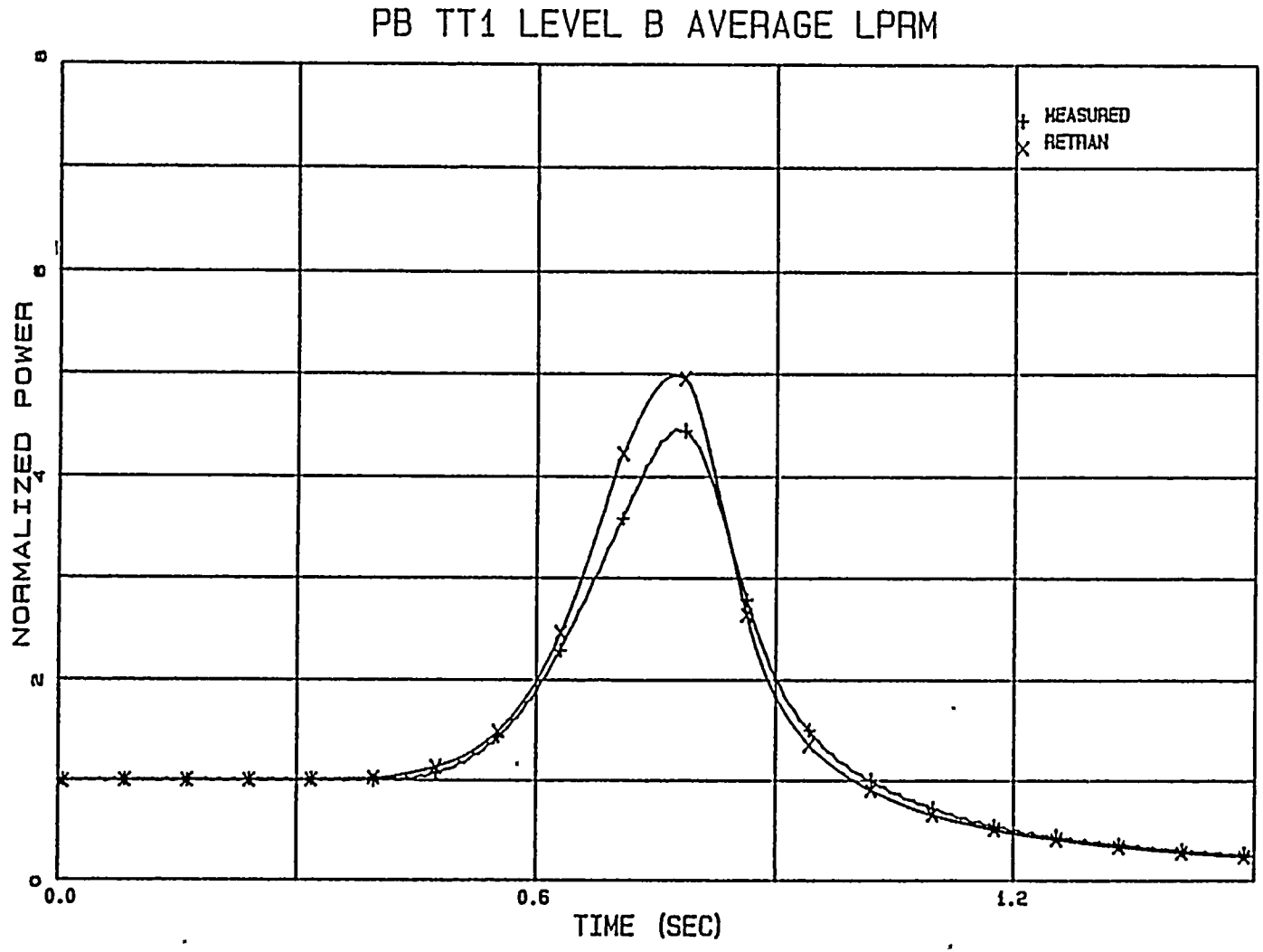
PB TT1 LEVEL B AVERAGE LPRM
MEASURED
RETRAN
NORMALIZED POWER
0
2
4
6
8
0.0
0.6
1.2
TIME (SEC)

FIGURE 3.2.18

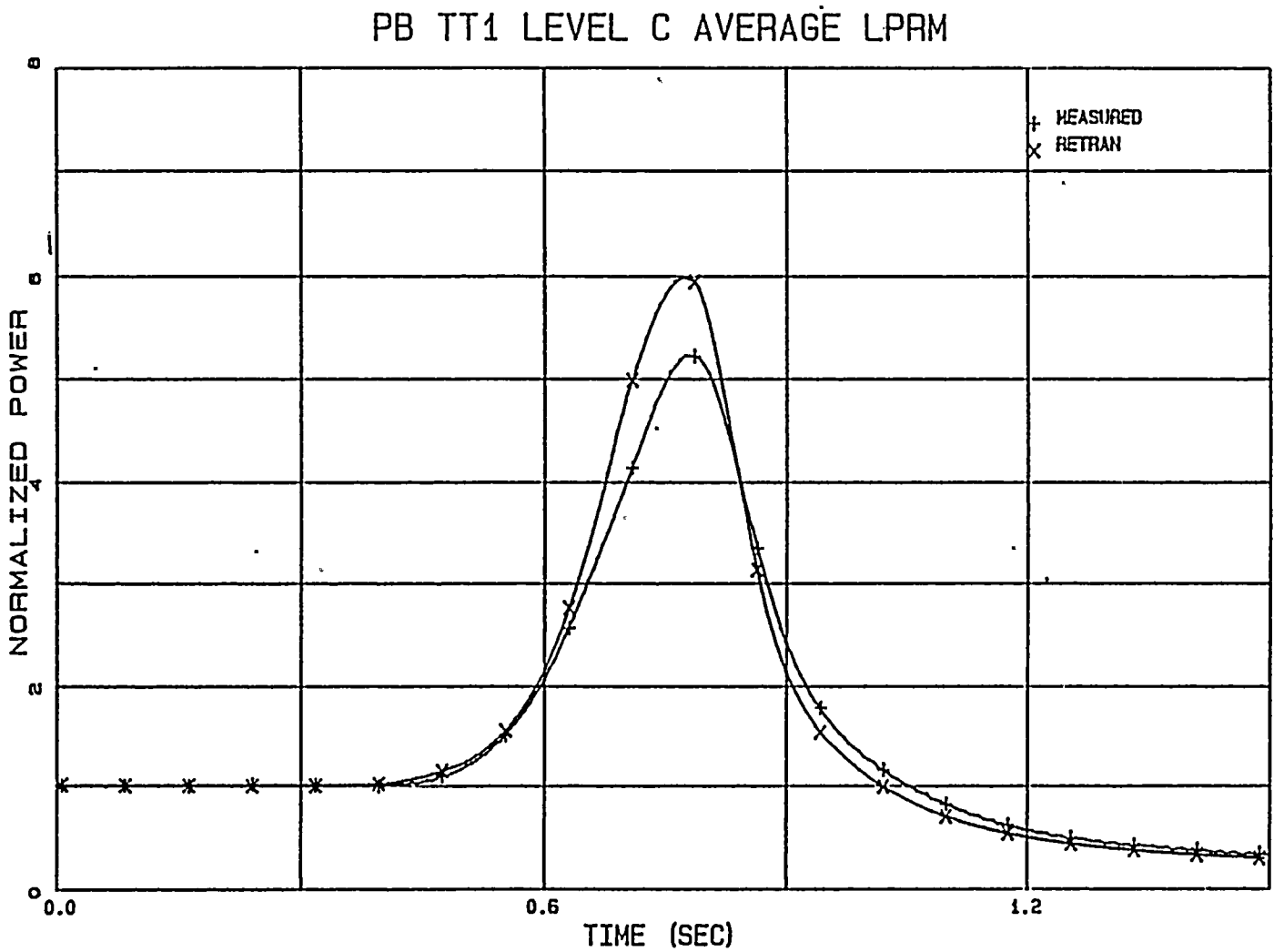
PB TT1 LEVEL C AVERAGE LPRM
MEASURED
RETRAN
NORMALIZED POWER
0
2
4
6
8
0.0
0.6
1.2
TIME (SEC)

FIGURE 3.2.19

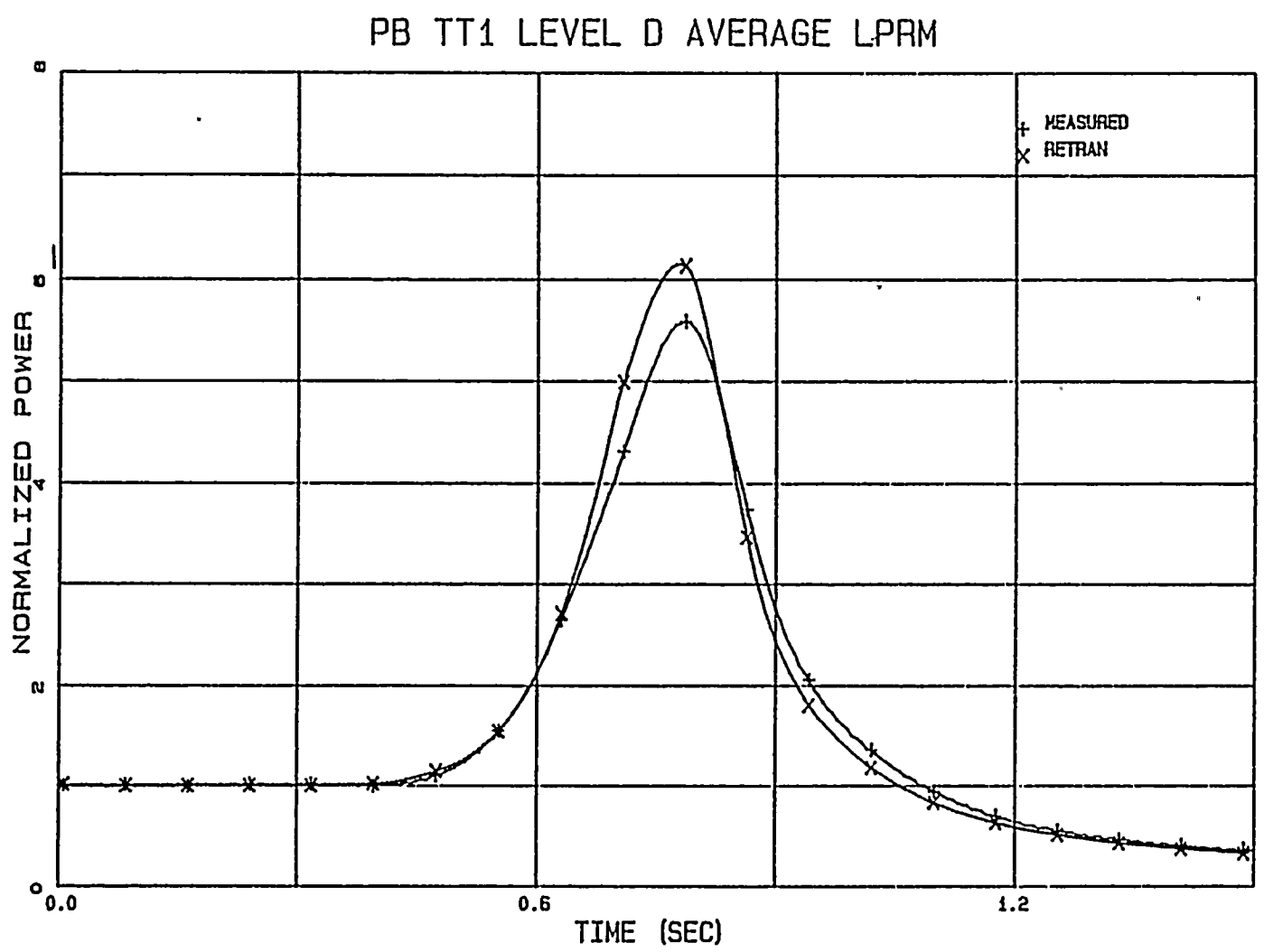
PB TT1 LEVEL D AVERAGE LPRM
MEASURED
RETRAN
NORMALIZED POWER
0
2
4
6
8
0.0
0.6
1.2
TIME (SEC)

FIGURE 3.2.20

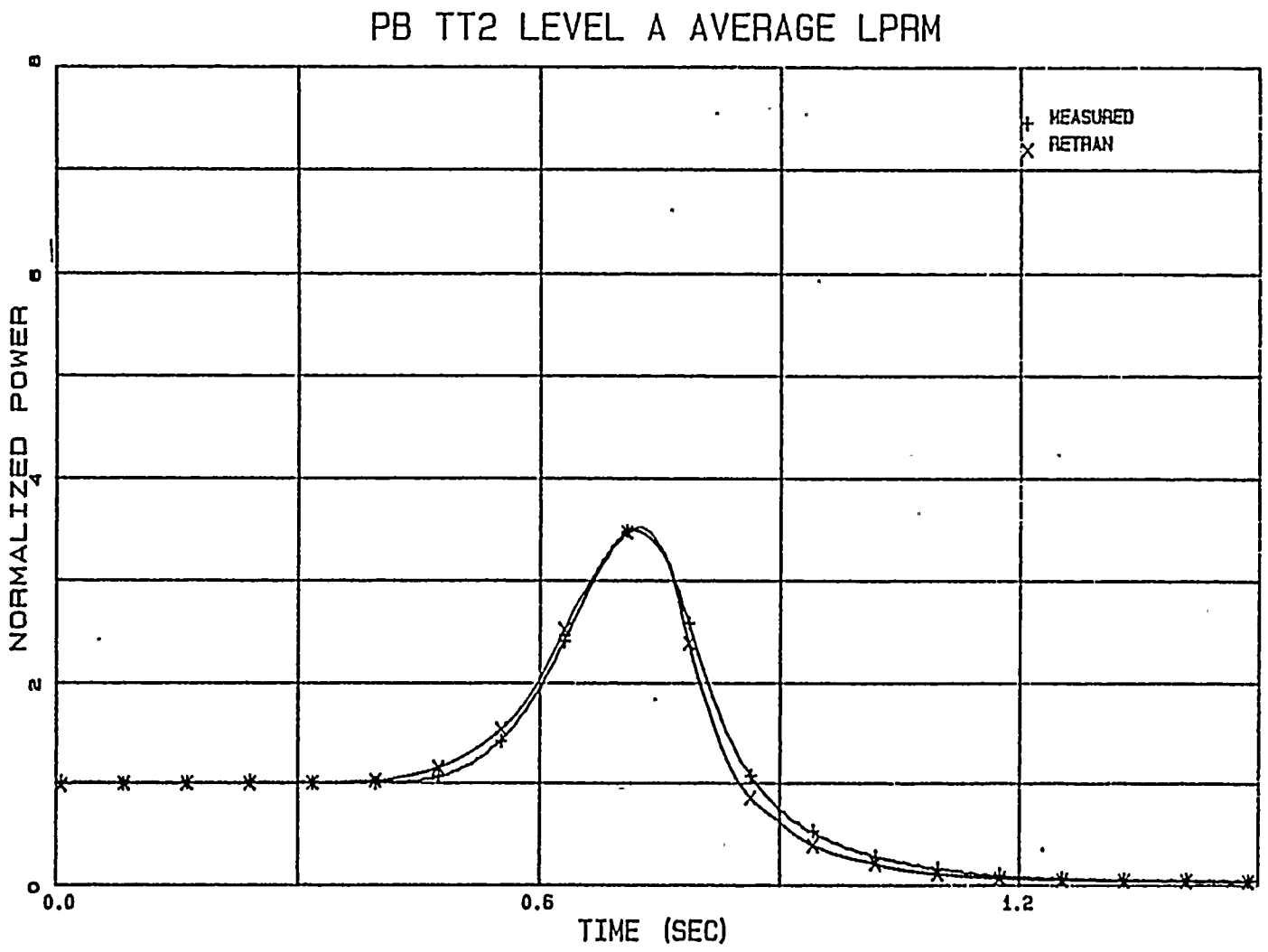
PB TT2 LEVEL A AVERAGE LPRM
MEASURED
RETRAN
NORMALIZED POWER
0
2
4
6
8
0.0
0.6
1.2
TIME (SEC)

FIGURE 3.2.21

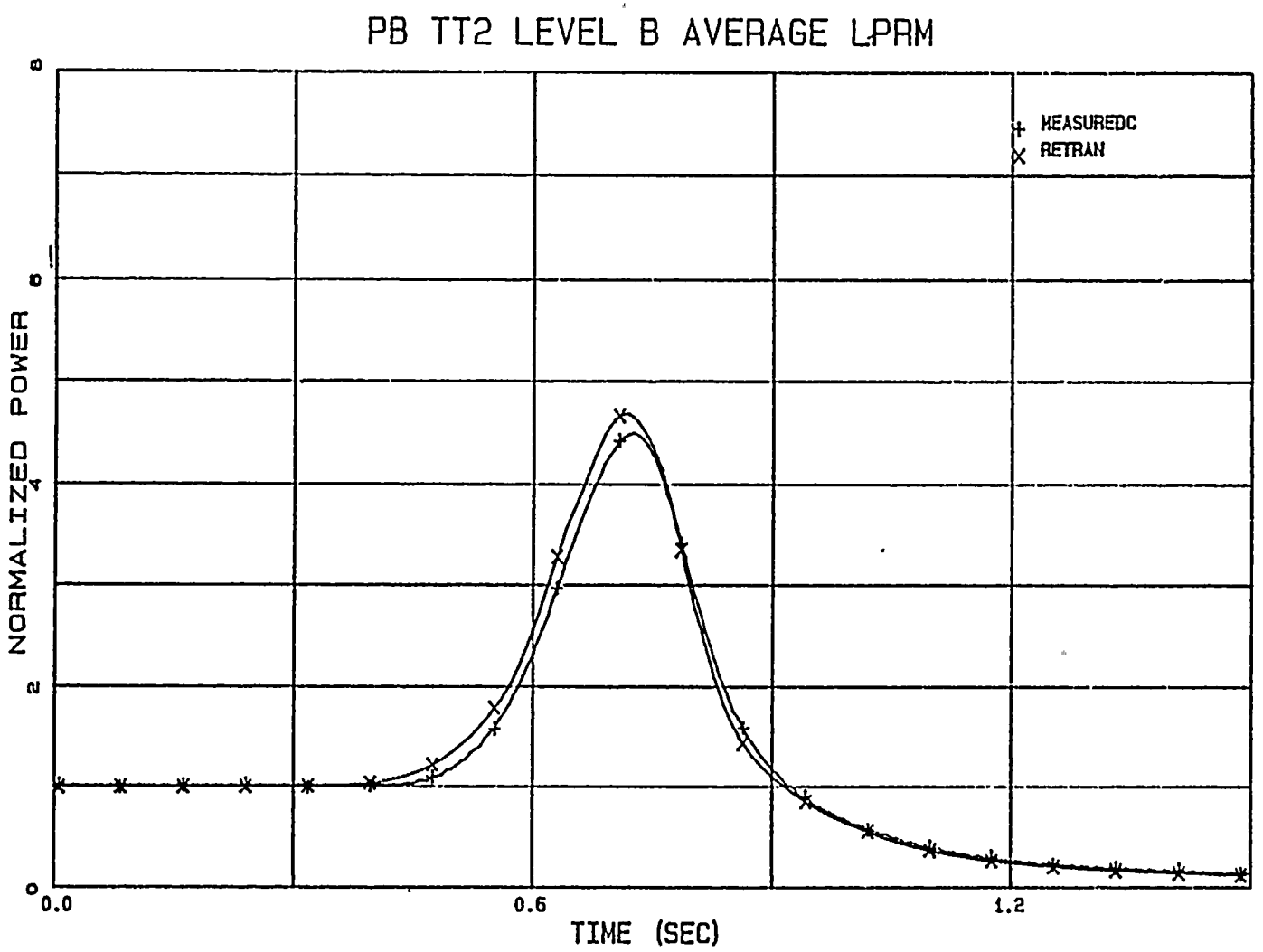
PB TT2 LEVEL B AVERAGE LPRM
MEASUREDC
RETRAN
NORMALIZED POWER
0
2
4
6
8
0.0
0.6
1.2
TIME (SEC)

FIGURE 3.2.22

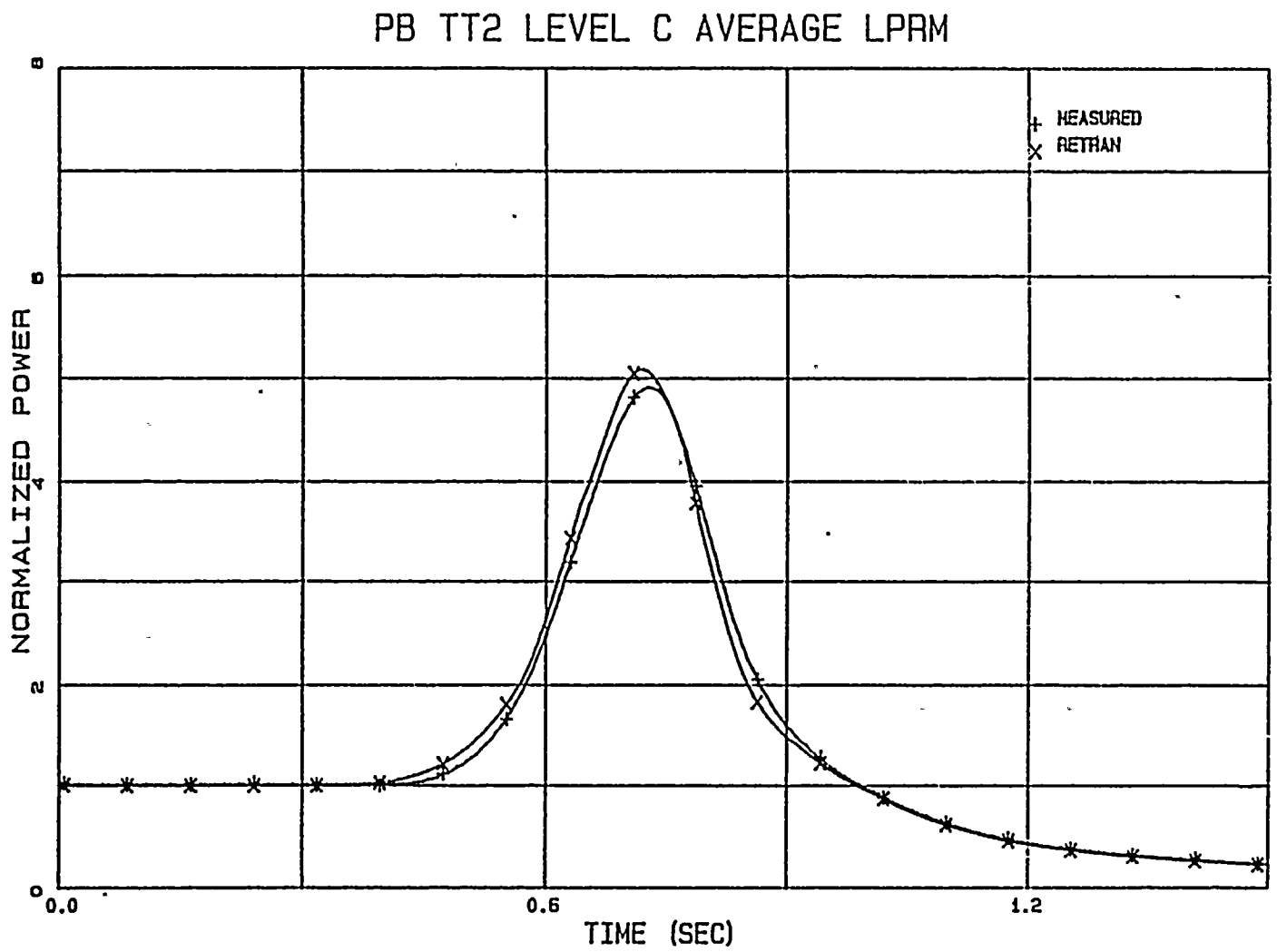
PB TT2 LEVEL C AVERAGE LPRM
MEASURED
RETRAN
NORMALIZED POWER
0
2
4
6
8
0.0
0.6
1.2
TIME (SEC)

FIGURE 3.2.23

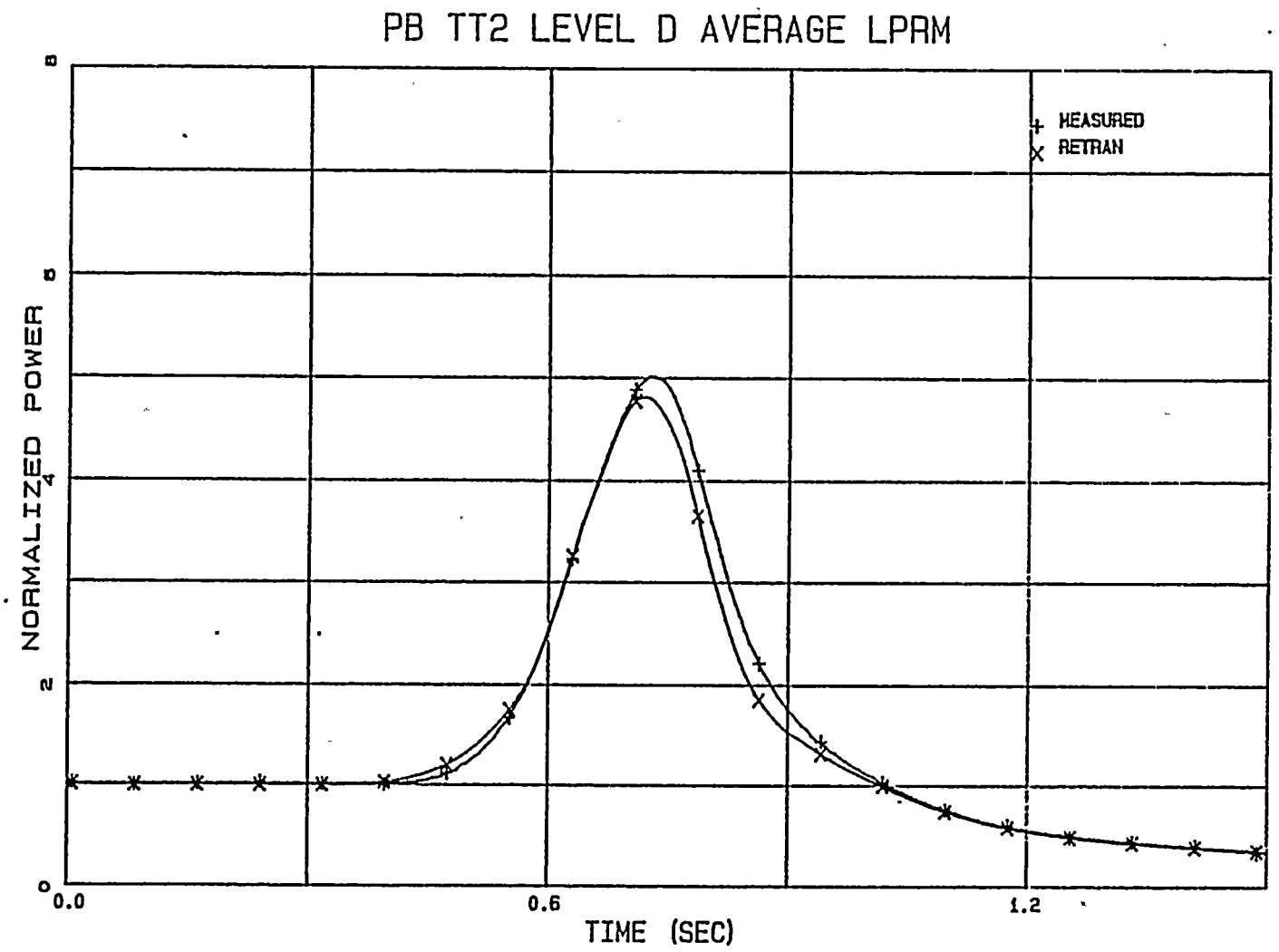
PB TT2 LEVEL D AVERAGE LPRM
MEASURED
RETRAN
NORMALIZED POWER
0
2
4
6
8
0.0
0.6
1.2
TIME (SEC)

FIGURE 3.2.24

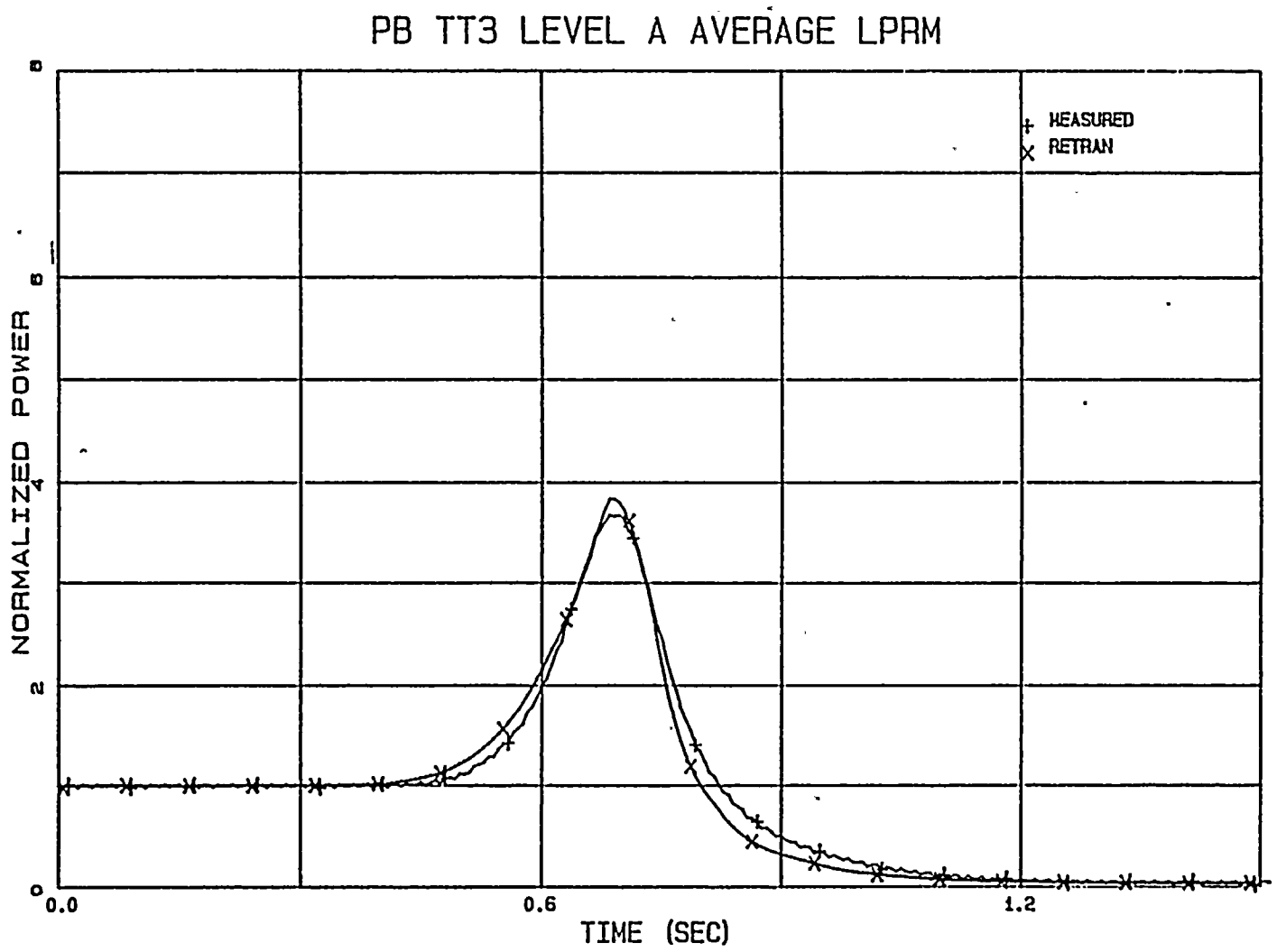
PB TT3 LEVEL A AVERAGE LPRM
MEASURED
RETRAN
NORMALIZED POWER
0
2
4
6
8
0.0
0.6
1.2
TIME (SEC)

FIGURE 3.2.25

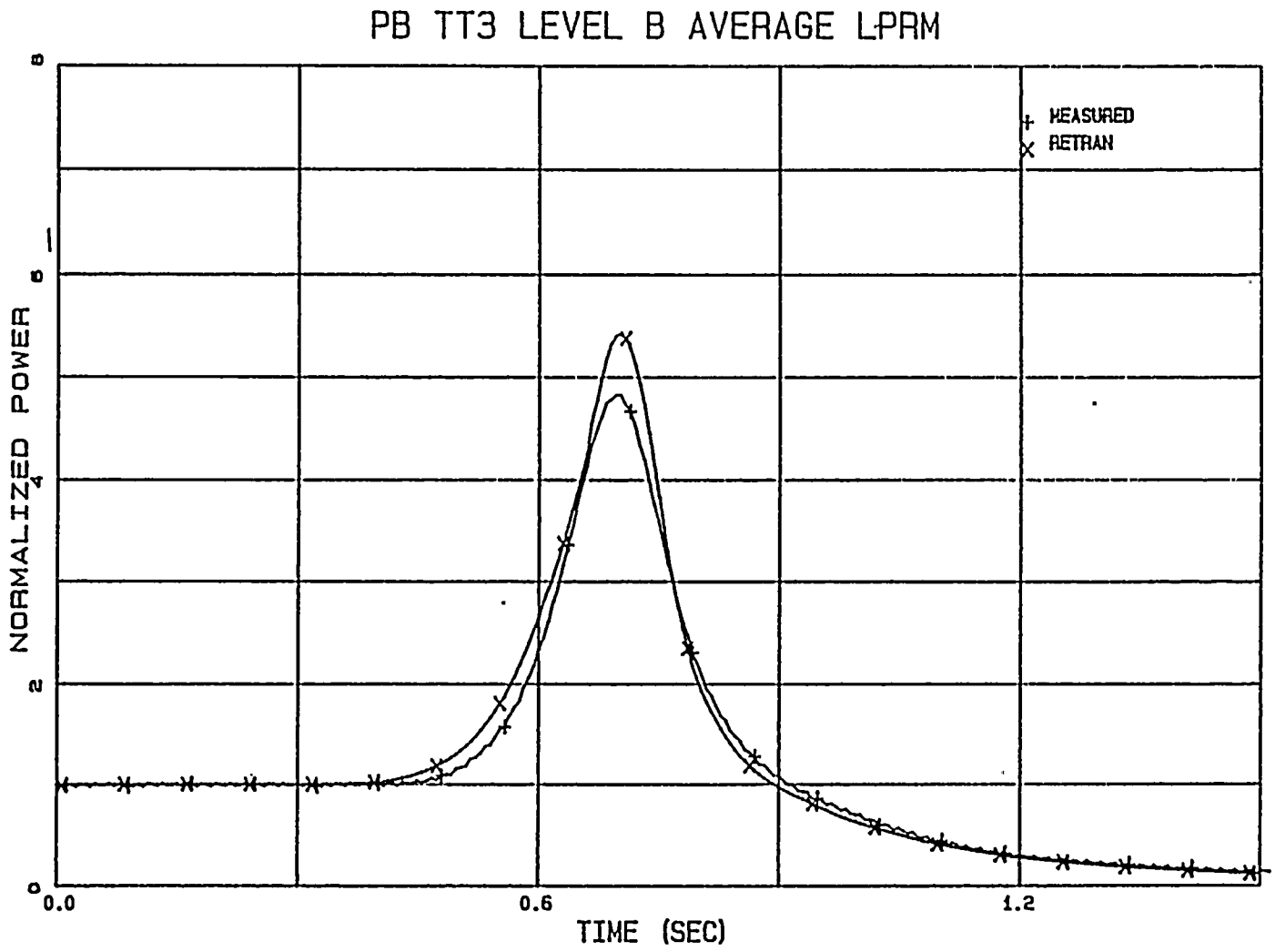
PB TT3 LEVEL B AVERAGE LPRM
MEASURED
RETRAN
NORMALIZED POWER
0
2
4
6
8
0.0
0.6
1.2
TIME (SEC)

FIGURE 3.2.26

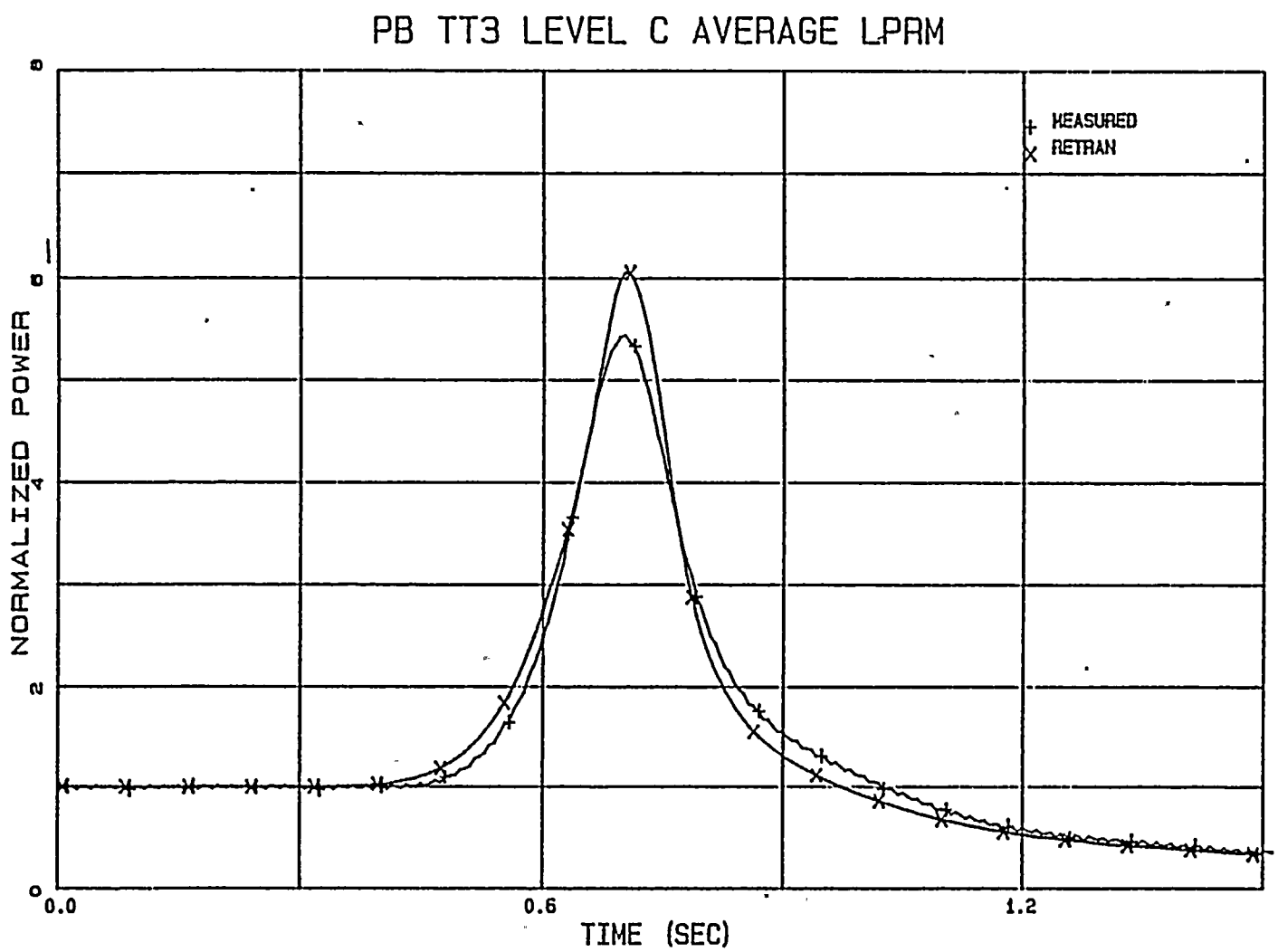
PB TT3 LEVEL C AVERAGE LPRM
MEASURED
RETRAN
NORMALIZED POWER
0
2
4
6
8
0.0
0.6
1.2
TIME (SEC)

FIGURE 3.2.27

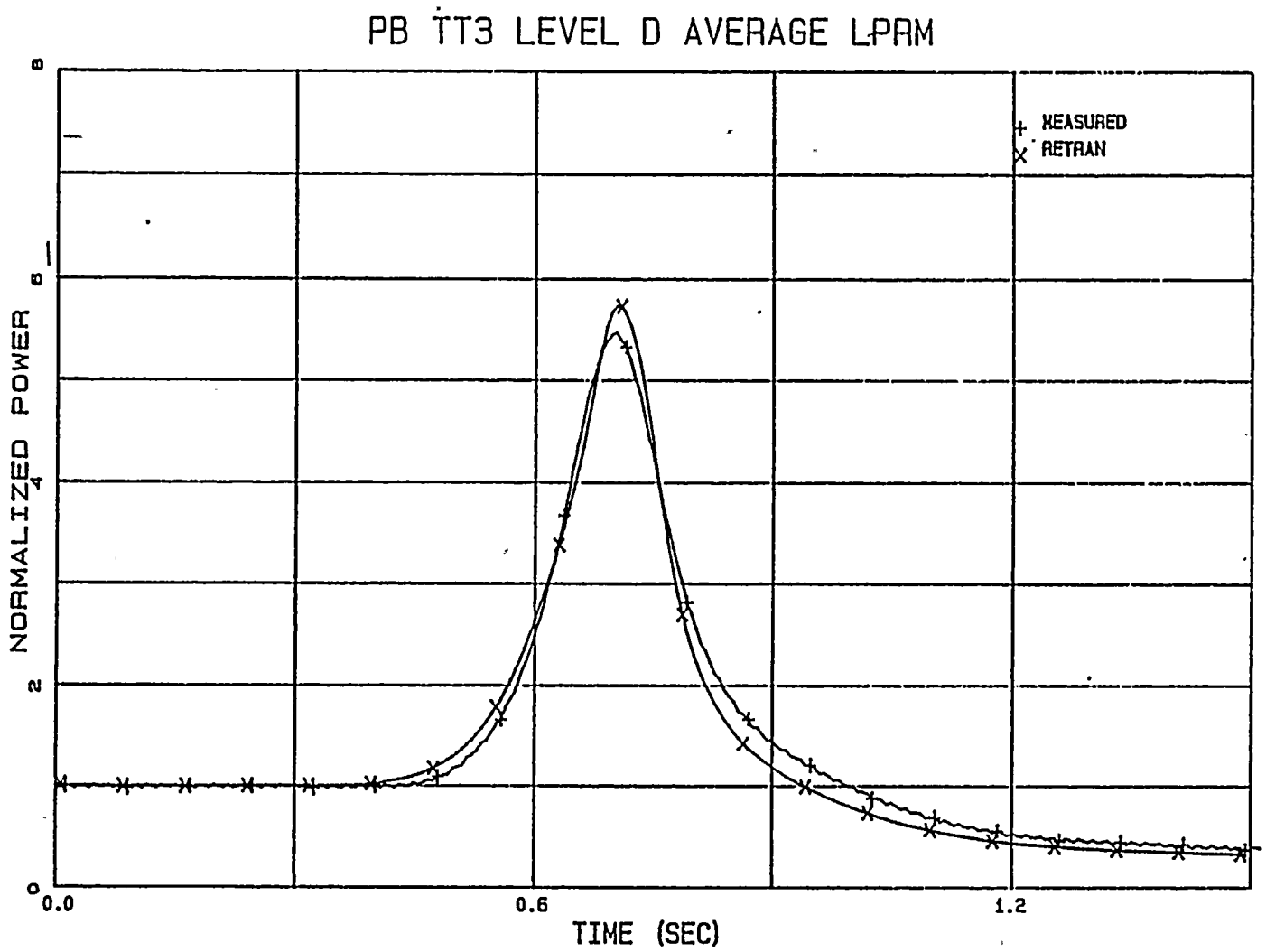
PB TT3 LEVEL D AVERAGE LPRM
MEASURED
RETRAN
NORMALIZED POWER
0
2
4
6
8
0.0
0.6
1.2
TIME (SEC)

FIGURE 3.2.28

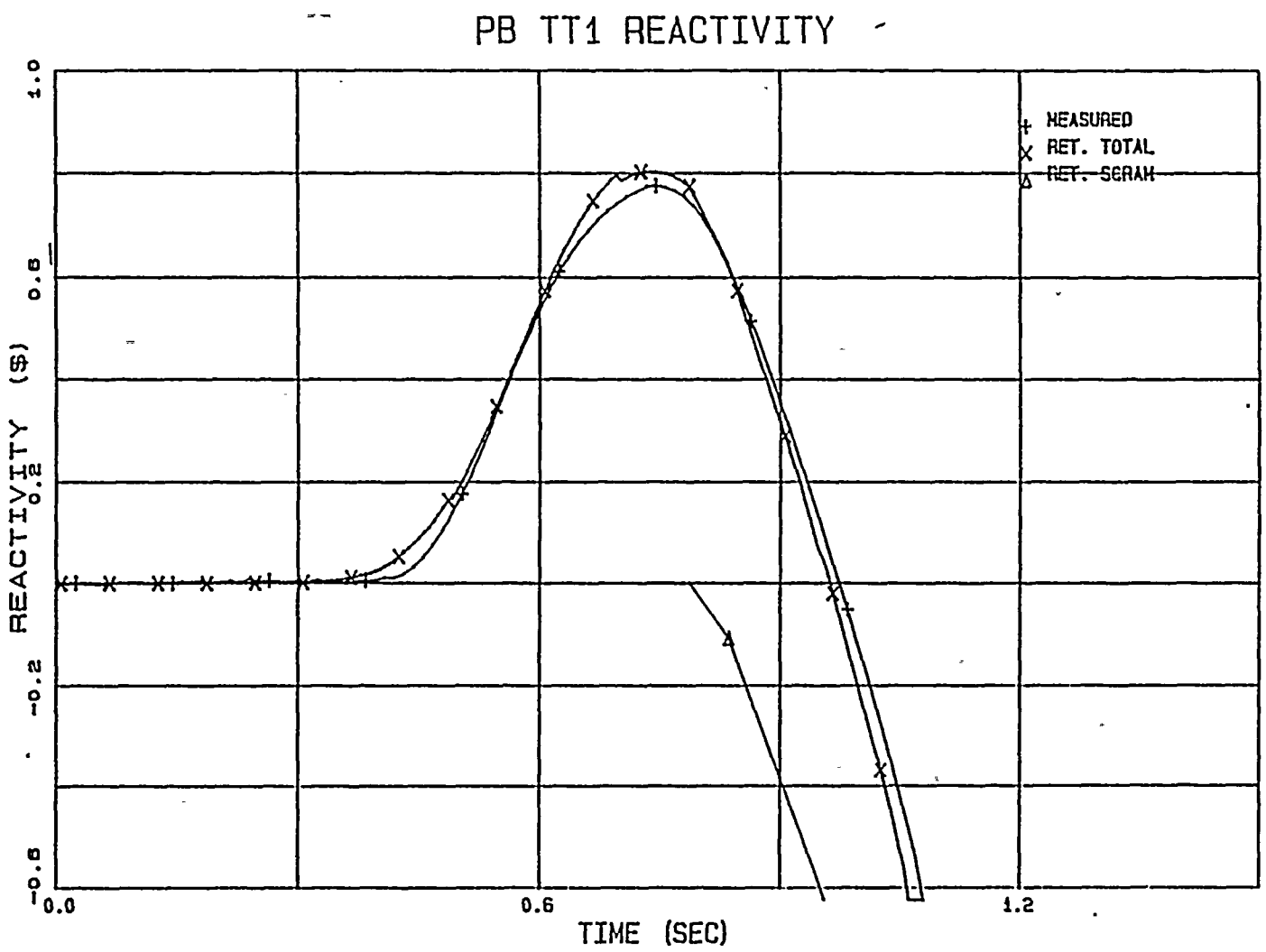
PB TT1 REACTIVITY
MEASURED
RET. TOTAL
RET. SCRAM
REACTIVITY ($)
1.0
0.6
0.2
-0.2
-0.6
0.0
0.6
1.2
TIME (SEC)

FIGURE 3.2.29

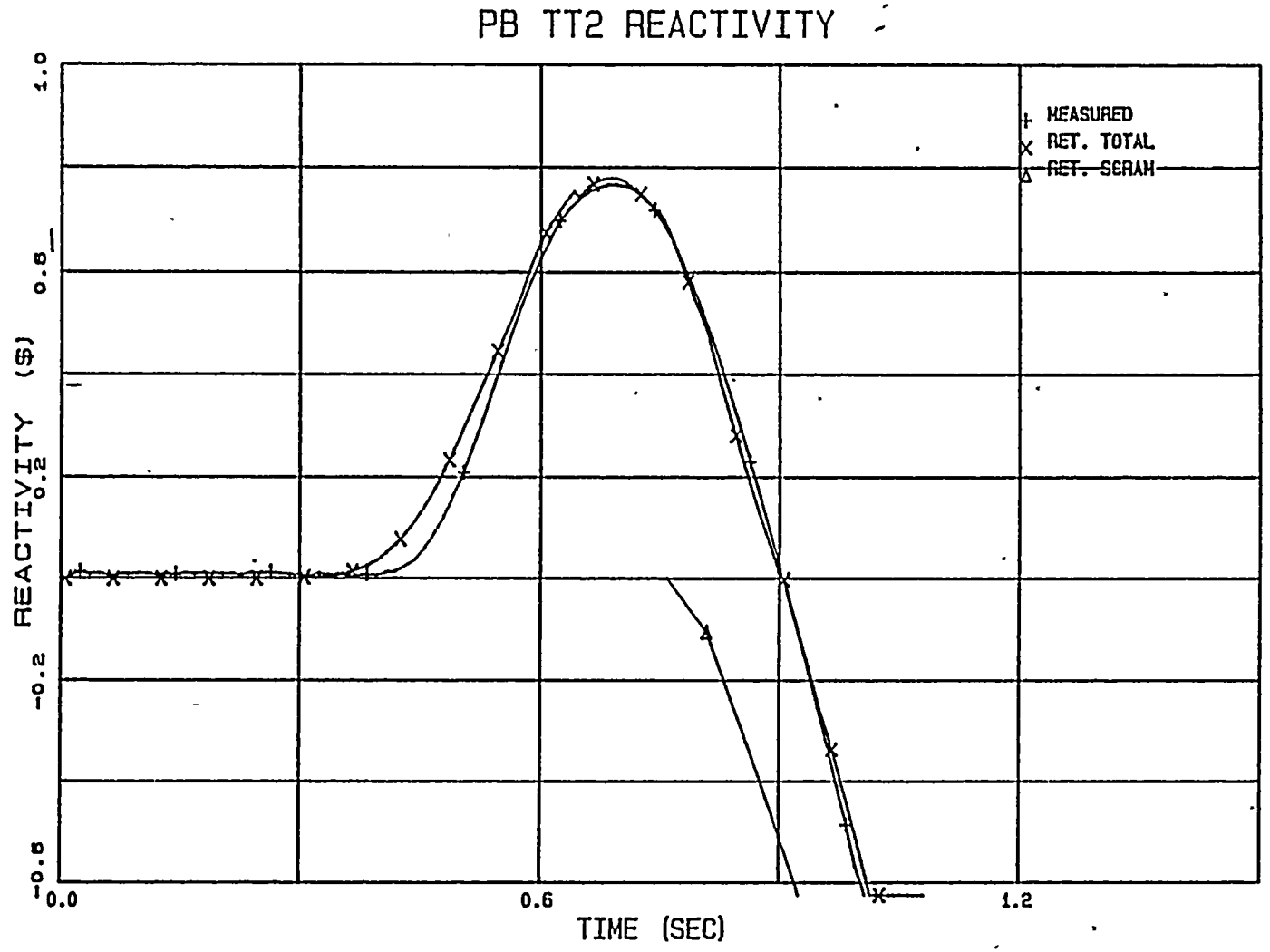
PB TT2 REACTIVITY
MEASURED
RET. TOTAL
RET. SCRAM
REACTIVITY ($)
1.0
0.6
0.2
-0.2
-0.6
0.0
0.6
1.2
TIME (SEC)

FIGURE 3.2.30

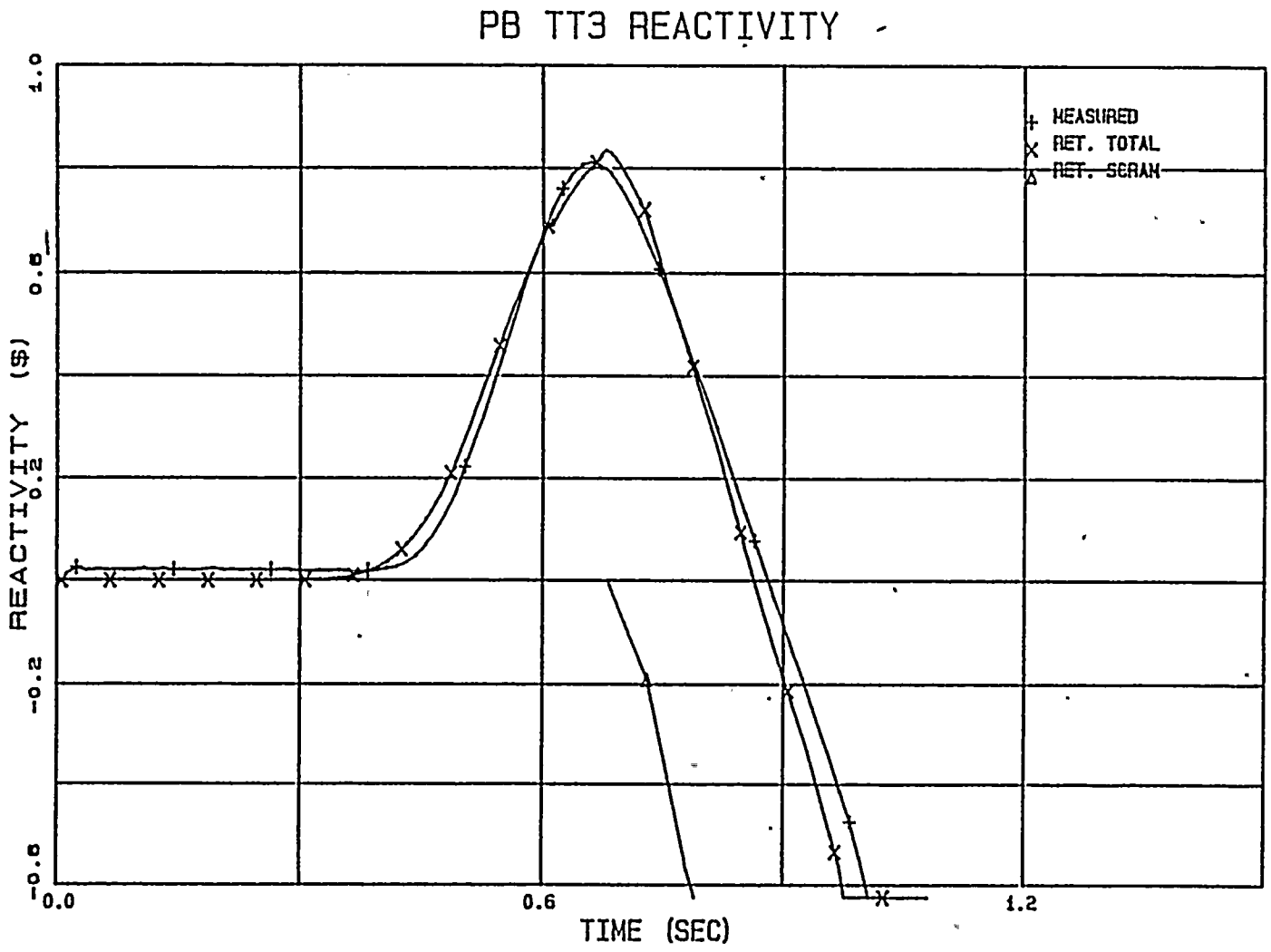
PB TT3 REACTIVITY
MEASURED
RET. TOTAL
RET. SCRAM
REACTIVITY ($)
1.0
0.6
0.2
-0.2
-0.6
0.0
0.6
1.2
TIME (SEC)

4.0 LICENSING BASIS ANALYSIS

A broad spectrum of transient events have been analyzed for WNP-2; the results are presented in the Final Safety Analysis Report. These events cover a wide range of scenarios and conditions contributing to Technical Specification Limits. Most of these transient events are not sensitive to changes in reload core configuration, or are within the conservative limits established by the original FSAR analysis. Changes in fuel design and core configuration are usually bounded by the analysis of selected limiting events. Based on previous analyses performed by vendors for WNP-2[20,21] and utilities on similar plants[22], the two most limiting events requiring a reanalysis with each reload core are:

1. Load Rejection Without Bypass (LRNB)
2. Feedwater Controller Failure to Maximum Demand (FWCF)

The results of these transients determine Technical Specification limits for minimum critical power ratio (MCPR). This chapter describes the system analysis for these transients. The sensitivity analysis and the hot channel analysis from which the operating limits are obtained are reported separately.

4.1 Licensing Basis Model

The licensing basis model described in this chapter is a generic model using the Cycle 4 core configuration. For future applications, specific reload configurations and plant parameters will be used. These calculations are typical of planned WNP-2 reload analyses.

The licensing basis RETRAN model is a modification of the WNP-2 best-estimate model. The modifications assure the conservatism of the calculated results by using the values of the key parameters which bound the expected operating range.

Table 4.1 compares licensing basis model inputs with the nominal values. The nominal values and conditions show conservatism in the licensing basis modeling.

4.1.1 Core Exposure

The licensing analysis performed in this report uses the end-of-cycle exposure for the calculation of the nuclear design data. As cycle exposure increases, control rods are withdrawn from the core to counteract the consumption of excess reactivity. The average control rod scram distance is greater with more rods withdrawn, so scram performance degrades near the end of cycle. Scram reactivity insertion rate is the dominant power reversal phenomenon for

pressurization transients; the most severe results occur at the maximum cycle exposure, when scram performance is least effective.

TABLE 4.1

INPUT PARAMETERS AND INITIAL TRANSIENT CONDITIONS
COMPARISON OF LICENSING BASIS AND NOMINAL PLANT CONDITIONS

Parameter	Nominal	Licensing Basis
Core Exposure	BOC - EOC	EOC
Thermal Power (MWt)	3323	3468
Steam Flow (lbs/sec)	3970.97	4161.11
Feedwater Flow Rate (lbs/sec)	3970.97	4161.11
Feedwater Temperature (°F)	420[a]	424[a]
Vessel Dome Pressure (psia)	1020	1035
Rod Insertion Speed	Measured	Tech. Spec.
Core Inlet Enthalpy (Btu/lb)	527.6	529.3
Fuel Rod Gap Conductance	Axially Non-uniform	Uniform
Fuel Radial Heat Generation	Non-uniform	Uniform
Jet Pump Ratio	2.33	2.41
Safety/Relief Valves Relief Function (psig)		
Group 1 Opening Setpoint	1076	1106
Group 1 Closing Setpoint	1026	1056
Group 2 Opening Setpoint	1086	1116
Group 2 Closing Setpoint	1036	1066
Group 3 Opening Setpoint	1096	1126
Group 3 Closing Setpoint	1046	1076
Group 4 Opening Setpoint	1106	1136
Group 4 Closing Setpoint	1056	1086
Group 5 Opening Setpoint	1116	1146
Group 5 Closing Setpoint	1066	1096
Opening Stroke Time (sec)	0.07	0.1
Closing Stroke Time (sec)	0.0	0.0
Opening Delay Time (sec)	0.3	0.4

a. RETRAN will adjust this value at initialization to complete the heat balance.

TABLE 4.1

INPUT PARAMETERS AND INITIAL TRANSIENT CONDITIONS
COMPARISON OF LICENSING BASIS AND NOMINAL PLANT CONDITIONS
(Continued)

Parameter	Nominal	Licensing Basis
Safety/Relief Valves Safety Function (psig)		
Group 1 Opening Setpoint	1150	1177
Group 1 Closing Setpoint	1126	1153
Group 2 Opening Setpoint	1175	1187
Group 2 Closing Setpoint	1151	1163
Group 3 Opening Setpoint	1185	1197
Group 3 Closing Setpoint	1161	1173
Group 4 Opening Setpoint	1195	1207
Group 4 Closing Setpoint	1171	1183
Group 5 Opening Setpoint	1205	1217
Group 5 Closing Setpoint	1181	1193
Opening Stroke Time (sec)	0.07	0.1
Closing Stroke Time (sec)	0.0	0.0
Opening Delay Time (sec)	0.3	0.4
Reactor Protection System		
High Flux Scram, % NBR	118	126.2
High Vessel Dome Pressure Scram (psig)	1037	1071
APRM Thermal Trip (% NBR at 100% Core Flow)	113.5	122.03
Low Water Level (L3), in above instrument zero	13	7.5
Turbine Stop Valve Closure Position Scram (% Closed)	5	10
MSIV Closure Position Scram (% Closed)	10	15

INPUT PARAMETERS AND INITIAL TRANSIENT CONDITIONS
COMPARISON OF LICENSING BASIS AND NOMINAL PLANT CONDITIONS
(Continued)

Parameter	Nominal	Licensing Basis
Containment Isolation and Pump Trip		
Low Water Level (L2), in below instrument zero	50	70
Low Pressure in Steamline (psig)	831	795
RPT High Vessel Pressure (psig)	1135	1170
RPT Delay Time (msec)	97	190
High Water Level - Turbine and Feedwaters Pump Trip (inches above instrument zero)	54.5	59.5
Recirculation Pump Moment of Inertia (10^4 lbm - ft^2)	2.27	2.47

4.1.2 Initial Conditions

The initial power in the licensing basis model is set consistent with the maximum steam flow capability at 105% NBR. A high value of initial steam flow conservatively results in a more rapid pressurization and higher maximum pressures. The initial reactor dome pressure is set at 1035 psia which is conservatively high relative to normal plant operation, allowing less analytical margin to the safety limit. A maximum value of feedwater temperature is input to RETRAN. However, during the steady-state initialization, the code will recalculate the feedwater temperature to allow a heat balance for the system under licensing basis conditions.

Unless the problem statepoint requires otherwise, the core flow is initialized at the maximum expected value. This is normally the rated capacity of 108.5 mlb/hr.

4.1.3 Scram Reactivity

The dominant conservatism in the licensing basis modeling is in the scram reactivity insertion rate. The initial control rod configuration is selected to minimize the rate of scram reactivity insertion (i.e., control rod configuration at EOC when the number of partially inserted control rods is at a minimum). The analysis conservatively assumes that all control rods move at the same speed following scram. In practice, the partially inserted rods reach

the axial zone of maximum worth sooner than the fully withdrawn rods and have a faster effective scram time. Use of a uniform speed for all control rods yields a slower effective initial scram reactivity insertion rate than a best-estimate distribution of control rod speeds with the same average motion.

The analyses in this report used the technical specification limits on control rod movement versus time. Table 4.2 shows the assumed rod motion following scram[23]. Actual plant performance data shows more rapid insertion.

TABLE 4.2
Technical Specification Limits
Maximum Control Rod Insertion Time to Position
After Deenergization of Pilot Valve Solenoids

Position Inserted from Fully Withdrawn (Notch Number)	Time (Sec)
6.25% (45)	0.430
18.75% (39)	0.868
47.92% (25)	1.936
89.58% (05)	3.497

4.1.4 Fuel Rod Gap Conductance

The licensing basis core model conservatively uses an axially uniform fuel rod gap conductance that remains constant during the transient. The actual gap conductance is generally higher in the central areas of the core. The axial power shape tends to shift upwards in the core during pressurization transients, increasing the importance of high gap conductance areas. The actual gap conductance increases during power increase transients due to fuel pellet expansion.

Higher gap conductance will lead to faster heat transfer from the fuel to the coolant, which generates more steam voids and lower gap temperature differentials, which results in lower stored heat in the higher power nodes. The faster conversion of fuel stored energy to steam voids in the core helps to mitigate the transient due to negative void reactivity feedback.

During limiting pressurization transients, the fuel gap conductance increases transiently above its initial steady-state value due to thermal expansion of the fuel pellet. Higher gap conductance leads to a less severe transient. Therefore, the use of a constant, core average gap conductance is conservative for the system analysis.

4.1.5 Equipment Specifications

The model inputs for equipment performance (e.g., valves, protective systems, etc.) are chosen from a combination of conservative equipment design specifications and plant technical specification limits. Conservative inputs are employed for relief valve opening response and for closure rates for stop, control, and main steam isolation valves. Reactor protection system setpoints and delays are also conservatively set.

4.1.6 Recirculation Pump Coastdown Time

A conservative moment of inertia for the recirculation pump is used in the licensing basis model. A larger value results in longer coastdown time after pump trip, delaying the effect of void formation in the core and increasing the process of void collapsing. Positive reactivity effects are magnified by this conservatism.

4.2 Load Rejection Without Bypass (LRNB)

Whenever external disturbances result in loss of electrical load on the generator, fast closure of the turbine control valves (TCV) is initiated. The turbine control valves are required to close as rapidly as possible to minimize overspeed of the turbine generator rotor. Closure of the main turbine control valves will cause a sudden reduction in steam flow which results in an increase in system pressure and reactor shutdown.

4.2.1 Sequence of Events

A loss of generator electrical load at high power with bypass failure produces the sequence of events listed in Table 4.3.

In the analysis, the turbine control valves operate in the full arc (FA) mode and have a full stroke closure time of 0.15 seconds. The most severe initial condition for this transient is the assumption of full arc operation at 105% NBR steam flow. The plant value of 0.07 seconds given in Table 4.3 represents actual expected closure time, since the turbine control valves are partially open during normal operation.

TABLE 4.3

Sequence of Events for LRNB Transient

Time-Sec	Event
0.0	Turbine generator power load unbalance (PLU) devices trip to initiate turbine control valve fast closure when loss of electrical load is detected.
0.0	Turbine bypass valves fail to operate
0.0	Fast turbine control valve closure initiates scram trip
0.0	Fast turbine control valve closure initiates a recirculation pump trip (RPT)
0.07	Turbine control valves closed
0.19	Recirculation pump motor/circuit breakers open, causing decrease in core flow
0.28	Control rod insertion starts (scram trip designed at 0 sec), RPS delay : 0.08 sec; solenoid deenergizing delay : 0.2 sec)
1.35	Group 1 relief valves actuated
1.40	Group 2 relief valves actuated
1.44	Group 3 relief valves actuated
1.50	Group 4 relief valves actuated
1.63	Group 5 relief valves actuated
4.43	Group 5 relief valves close
5.0	End of simulation

4.2.2 Results of LRNB RETRAN Analysis

The WNP-2 LRNB analysis at the end of cycle 4 conditions was performed with the licensing basis model. Since most of the fuel in the core at EOC4 was the Advanced Nuclear Fuels (ANF) design, the average fuel parameters in the best-estimate model were changed from the GE design to the ANF design. The fast closure of the turbine control valves (TCV) is simulated by linearly decreasing the flow at fill junction 380 (representing steam flow to the turbine) to zero at 0.07 seconds. Rapid closure of the TCV initiates a scram.

Several key results of this analysis were compared with analyses of record[24] performed by Advanced Nuclear Fuels (ANF). It should be noted that both sets of analyses were performed conservatively. This comparison is intended to show the similarity of results rather than to demonstrate analytical accuracy. The accuracy of the WNP-2 RETRAN model is demonstrated by the benchmarks of power ascension tests reported in Section 3.1.

The pressure in the steam line near the turbine increases rapidly as shown in Figure 4.2.1. The acronym "LRNB LBM" in the figure stands for Load Rejection without Bypass Licensing Basis Model. The pressure disturbance propagates upstream to the reactor vessel, causing the oscillations in vessel steam flow shown in Figure 4.2.2. The decreased steam flow at about 0.4 seconds causes the

rapid pressurization of the reactor dome and inside the core as shown in Figures 4.2.3, 4.2.4 and 4.2.5. The delay in the vessel pressure rise following control valve closure is approximately 0.30 seconds and is determined by the length of the steam lines. After 0.42 seconds, the net reactivity becomes positive because the positive void reactivity exceeds the negative scram reactivity. As shown in Figure 4.2.6 the net reactivity reaches a maximum of approximately 0.76$ at 0.78 seconds then begins to decrease as the scram reactivity increases.

The ANF prediction[24] of dome pressure during the transient is also shown in Figure 4.2.3. The WNP-2 RETRAN model predicts a pressure which is consistently higher than that predicted by ANF for WNP-2.

The transient variation in reactor power is shown in Figure 4.2.7. The reactor power rises rapidly to a peak value of 398% NBR at 0.89 seconds then rapidly decreases as Doppler feedback and scram reactivity terminate the power excursion. ANF's prediction of core power is also shown in Figure 4.2.7. The power history predicted by RETRAN peaks earlier in the transient than the ANF prediction at a lower maximum power level. The earlier power peak can be attributed in part to the higher pressure throughout the transient. The lower magnitude of the peak is attributed to differences in neutronics calculations leading to differences in kinetics data and cross sections.

The behavior of the core average clad surface heat flux during the LRNB is shown in Figure 4.2.8. The initial pressure rise in the core causes a reduction in clad-to-coolant heat transfer due to the rise in saturation temperature of the liquid phase. As the power rises, the heat flux quickly reverses and begins to rise, reaching a peak of 133.4% of the rated steady-state power value at 1.1 seconds. Following the peak, the heat flux decreases at a rate driven by the core power and the fuel rod time constant. ANF's calculation of core average heat flux is also shown in Figure 4.2.8. The two models predict consistent trends in heat flux and agree closely in the later part of the transient.

The feedwater flow and water level during LRNB are shown in Figures 4.2.9 and 4.2.10. When the TCV fast closure calls for scram, the feedwater controller reduces the water level setpoint by 18 inches. It then responds to this setpoint change by reducing feedwater flow. Pressure variations, steam flow oscillations, and void collapse contribute to the changing water level throughout the remainder of the transient.

Figures 4.2.11 and 4.2.12 give the void fractions at mid-core and core exit. Core voids collapse as the steamline pressure wave reaches the core. For the remainder of the transient, variations in steam flow and pressure drive oscillations in the void fraction. Figure 4.2.13 shows the recirculation flow. The recirculation pumps start to coast down after RPT initiation at 0.19 seconds, causing

flow reduction in the core as shown in Figure 4.2.14.

FIGURE 4.2.1

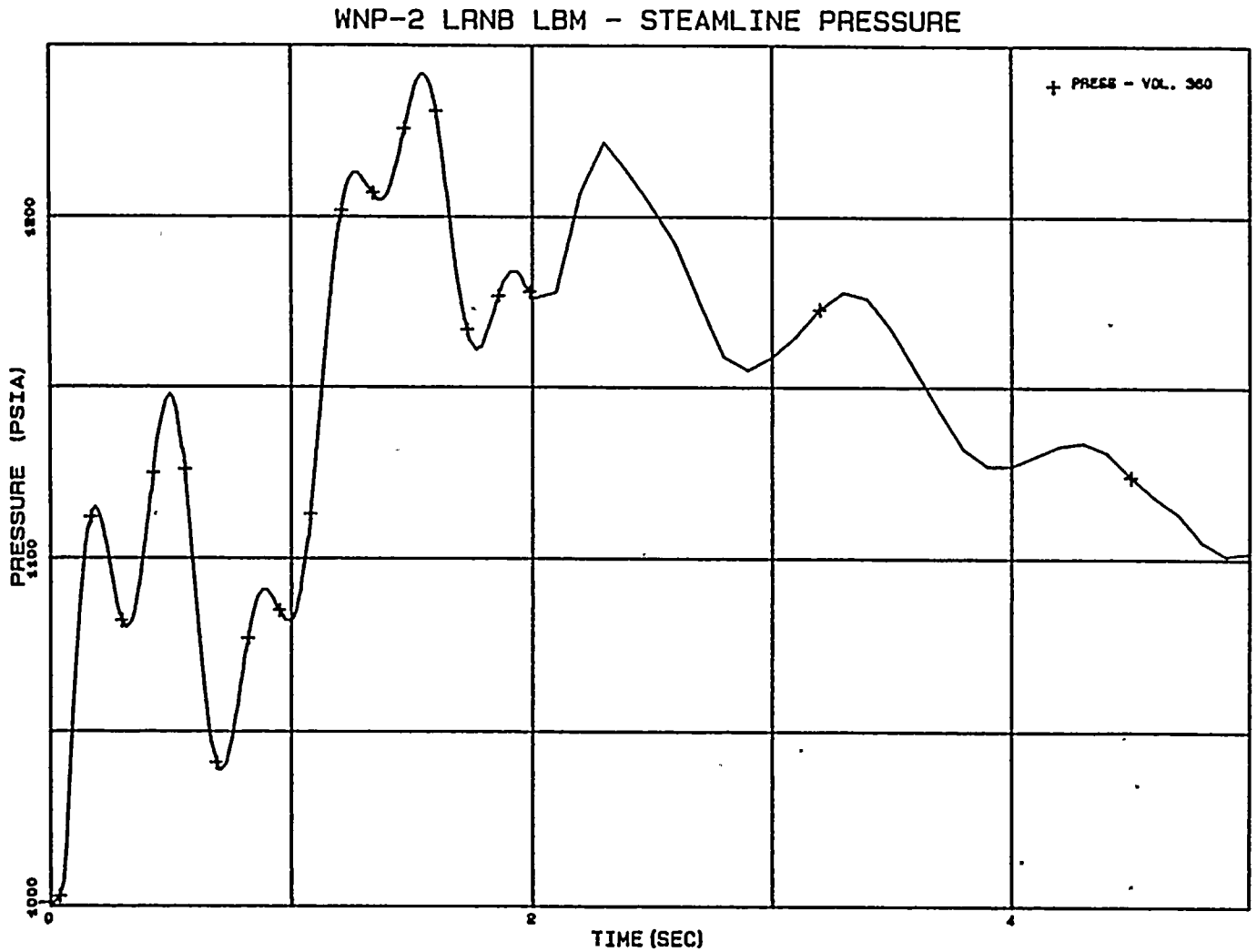
WNP-2 LRNB LBM - STEAMLINE PRESSURE
+ PRESS - VOL. 360
PRESSURE (PSIA)
1200
1100
1000
0
2
4
TIME (SEC)

FIGURE 4.2.2

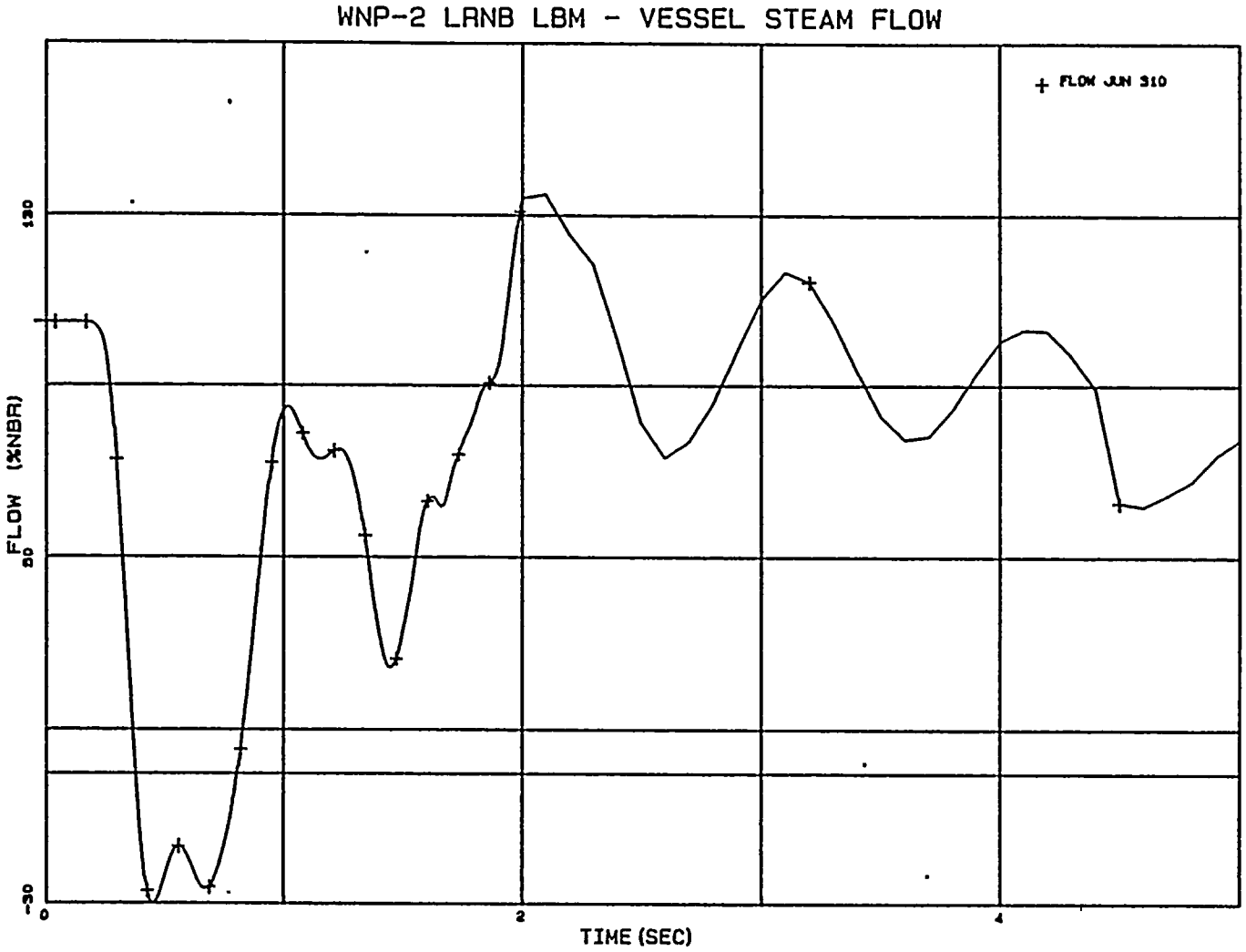
WNP-2 LRNB LBM - VESSEL STEAM FLOW
+ FLOW JUN 310
130
50
-30
FLOW (%NBR)
0
2
4
TIME (SEC)

FIGURE 4.2.3

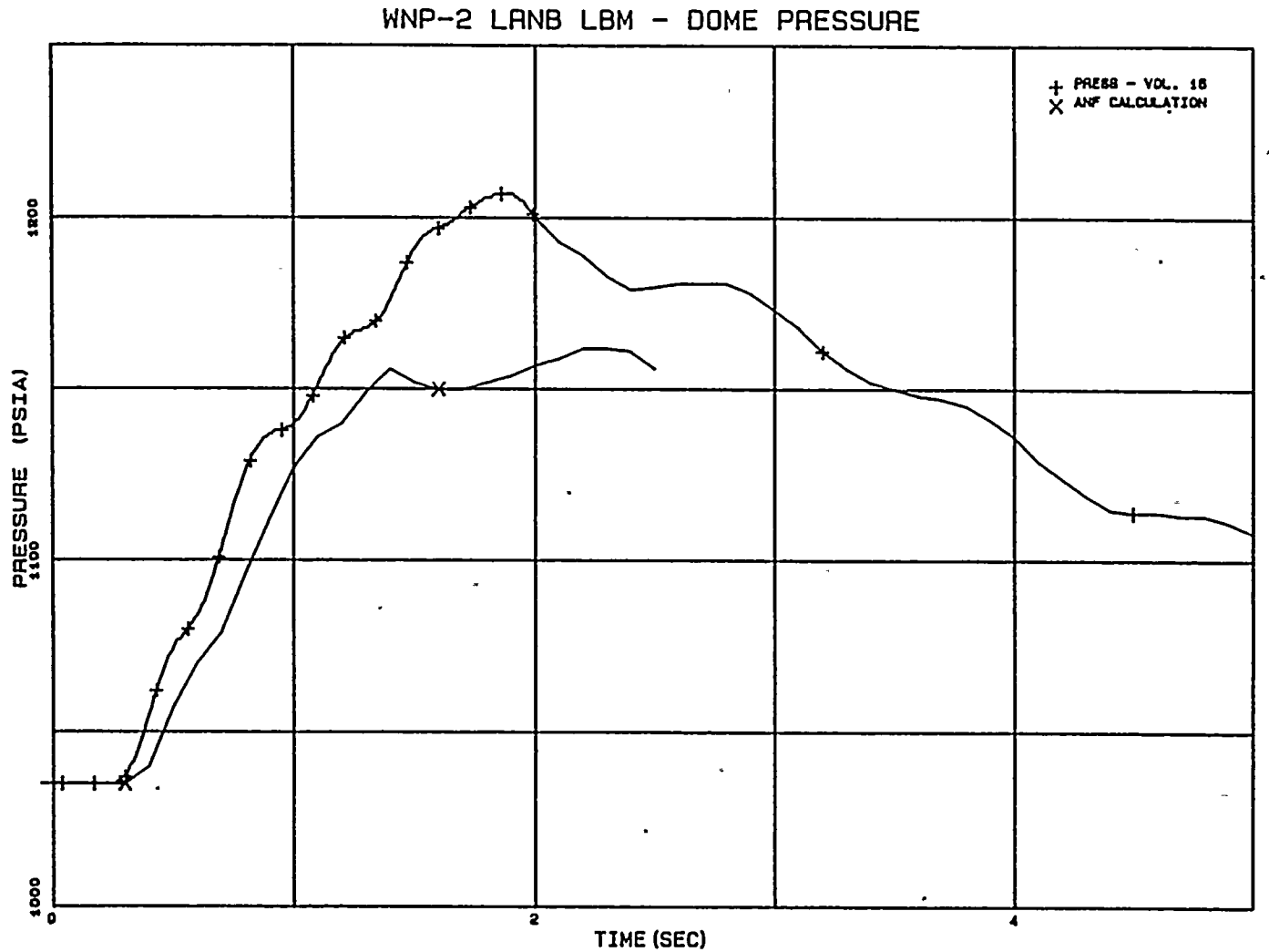
WNP-2 LANB LBM - DOME PRESSURE
+ PRESS - VOL. 16
X ANF CALCULATION
PRESSURE (PSIA)
1200
1100
1000
0
2
4
TIME (SEC)

FIGURE 4.2.4

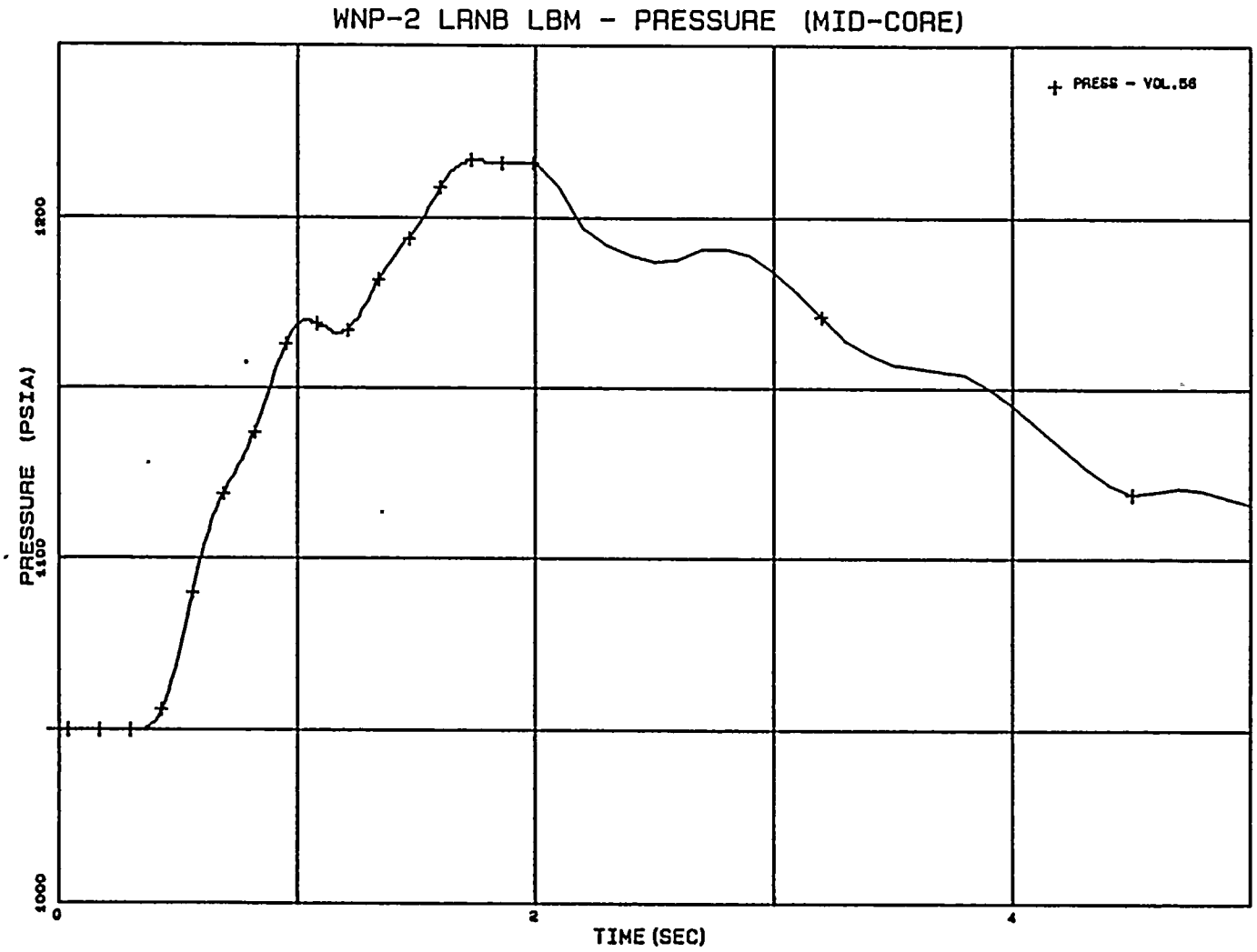
WNP-2 LANB LBM - PRESSURE (MID-CORE)
+ PRESS - VOL.56
PRESSURE (PSIA)
1200
1100
1000
0
2
4
TIME (SEC)

FIGURE 4.2.5

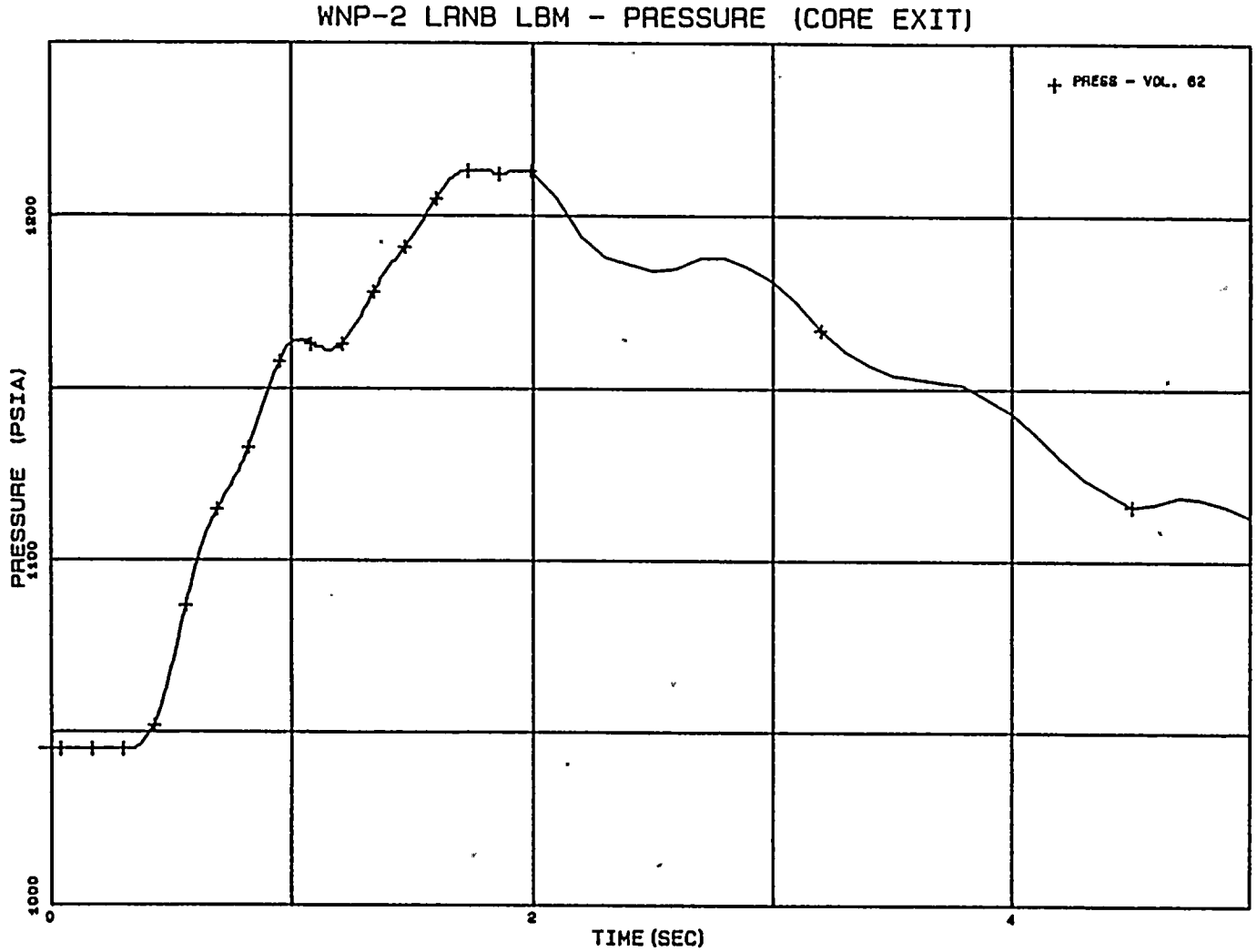
WNP-2 LANB LBM - PRESSURE (CORE EXIT)
+ PRESS - VOL. 62
PRESSURE (PSIA)
1200
1100
1000
0
2
4
TIME (SEC)

FIGURE 4.2.6

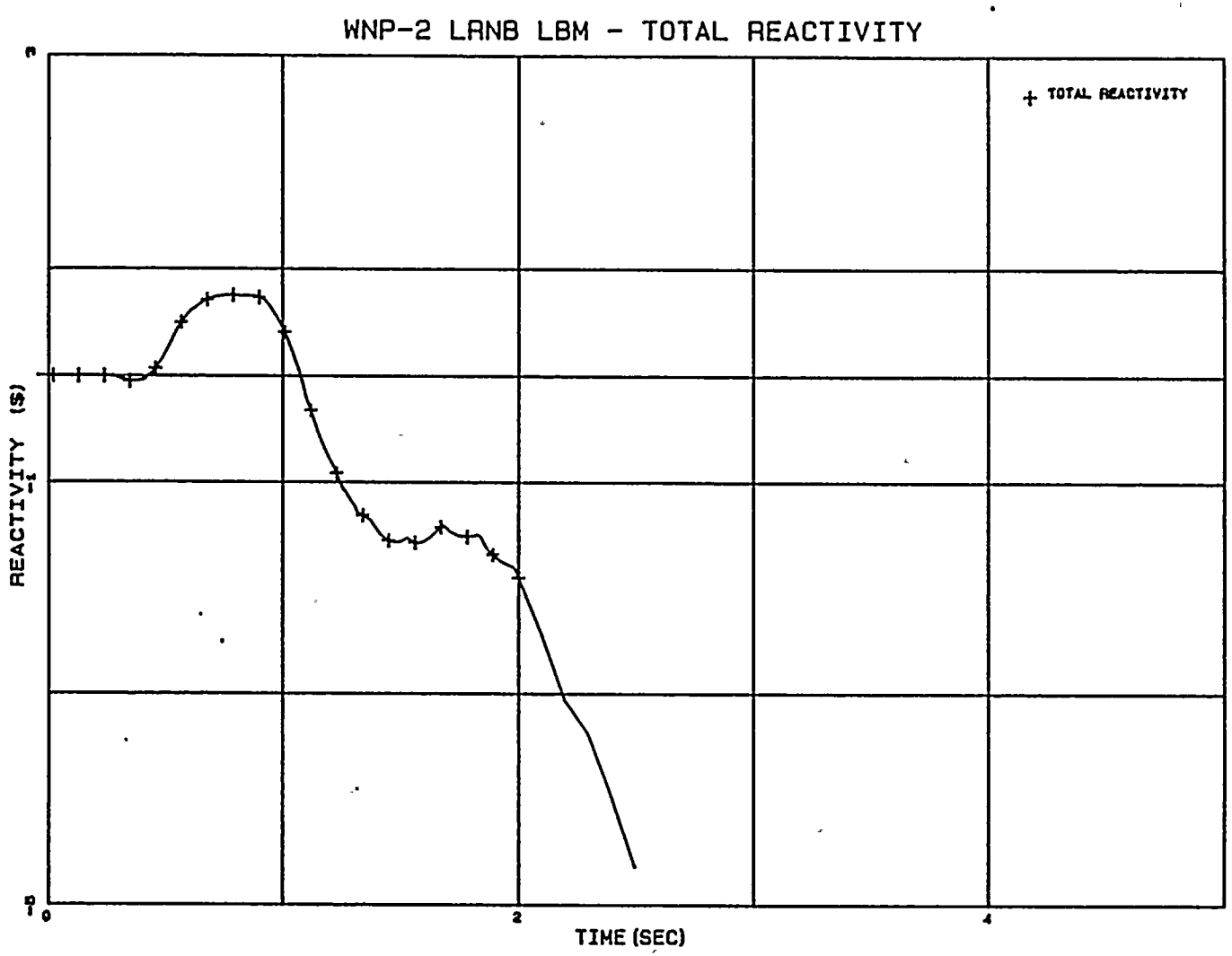
WNP-2 LANB LBM - TOTAL REACTIVITY
TOTAL REACTIVITY
REACTIVITY ($)
1
0
-1
0
2
4
TIME (SEC)

FIGURE 4.2.7

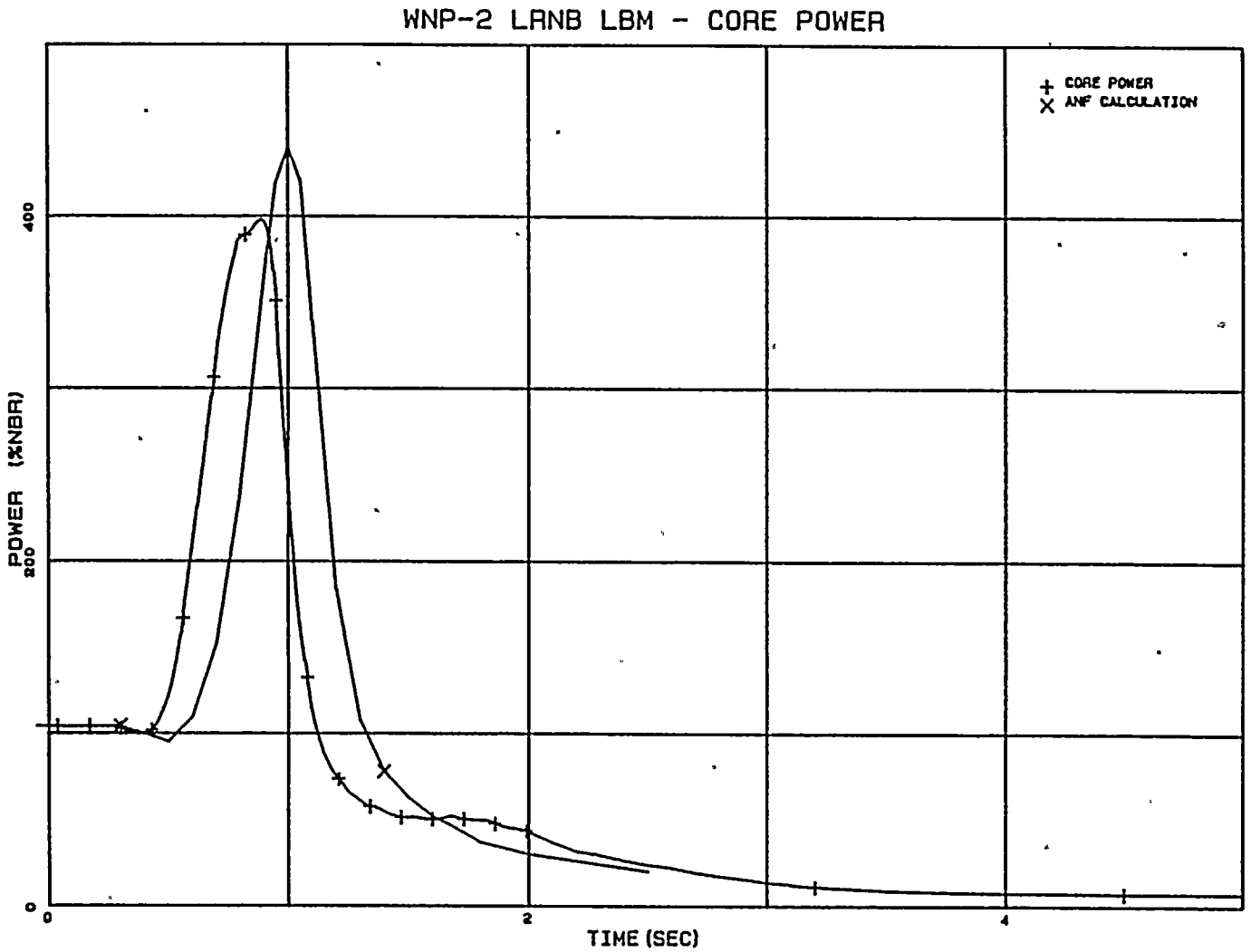
WNP-2 LANB LBM - CORE POWER
+ CORE POWER
X ANF CALCULATION
POWER (%NBR)
400
200
0
0
2
4
TIME (SEC)

FIGURE 4.2.8

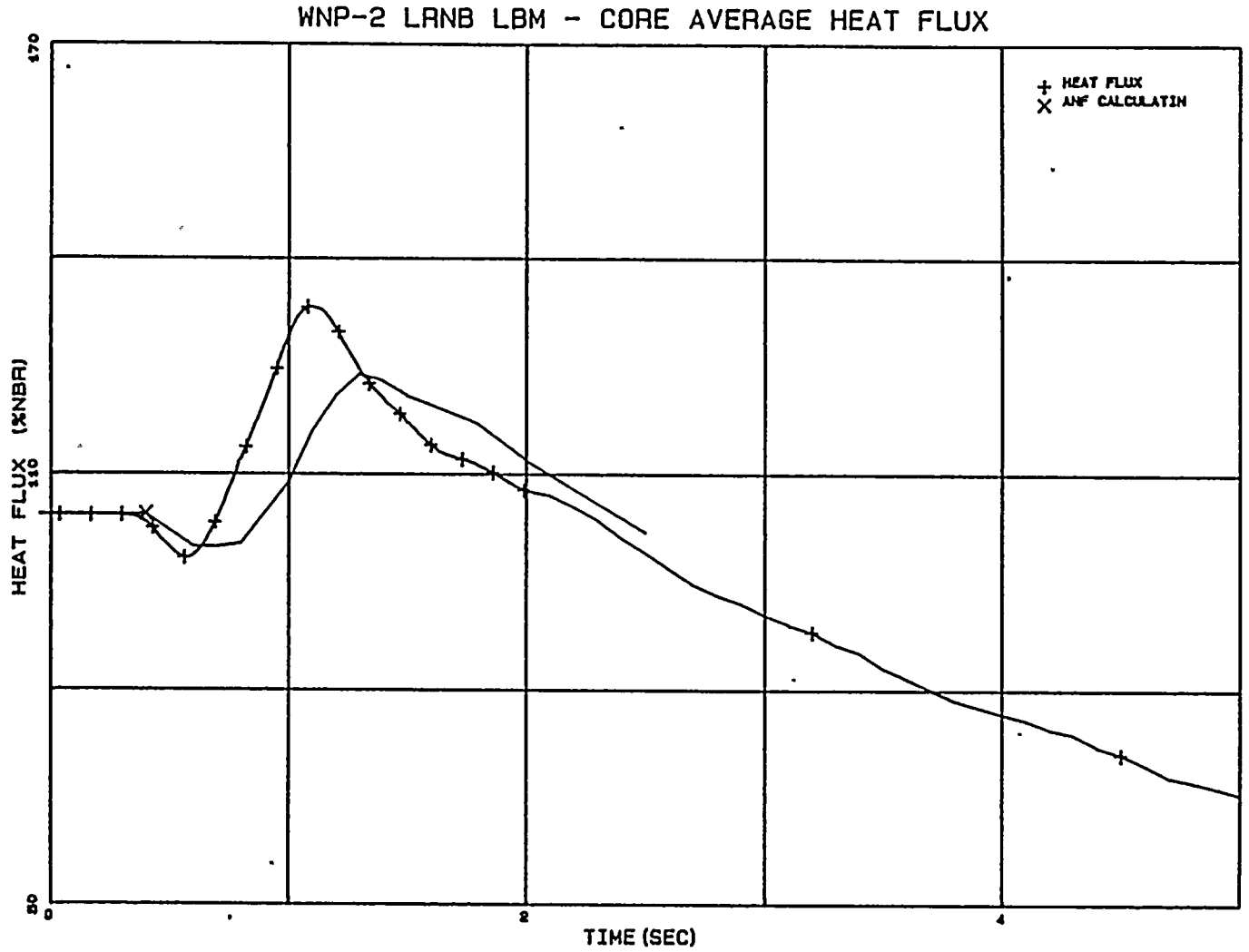
WNP-2 LRNB LBM - CORE AVERAGE HEAT FLUX
HEAT FLUX
ANF CALCULATIN
HEAT FLUX (%NBR)
170
110
50
0
2
4
TIME (SEC)

FIGURE 4.2.9

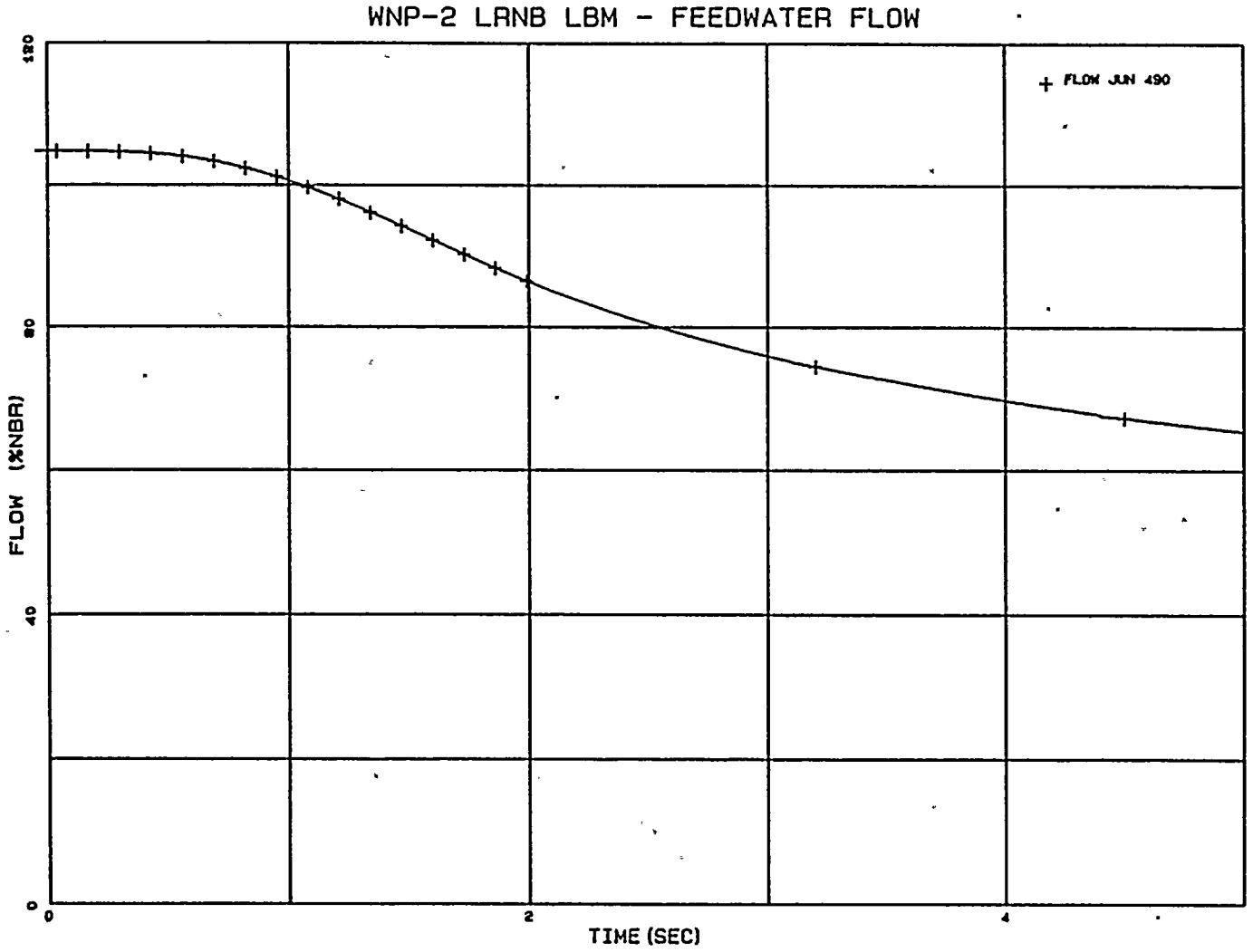
WNP-2 LRNB LBM - FEEDWATER FLOW
+ FLOW JUN 490
120
80
40
0
FLOW (%NBR)
0
2
4
TIME (SEC)

FIGURE 4.2.10

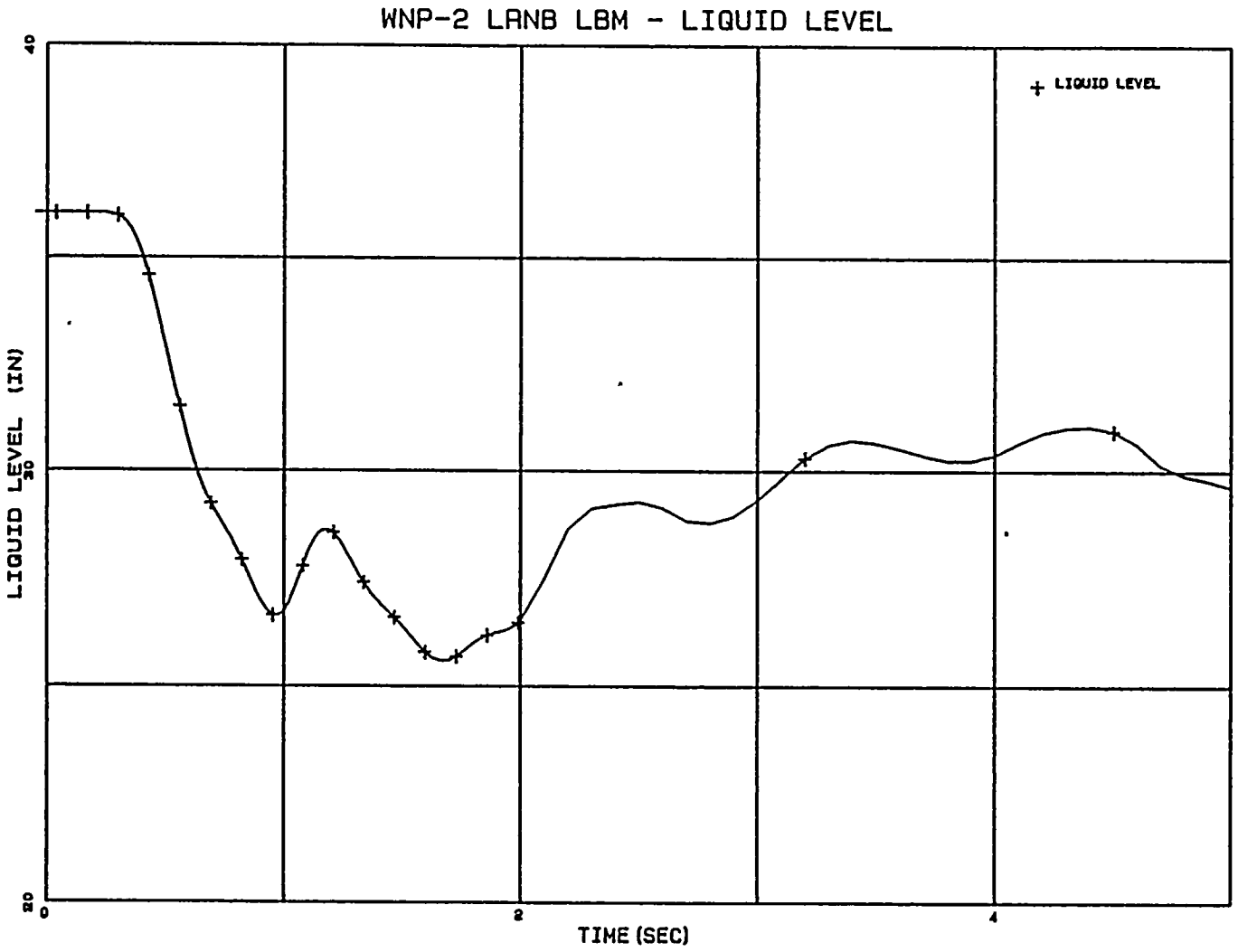
WNP-2 LANB LBM - LIQUID LEVEL
+ LIQUID LEVEL
LIQUID LEVEL (IN)
40
30
20
0
2
4
TIME (SEC)

FIGURE 4.2.11

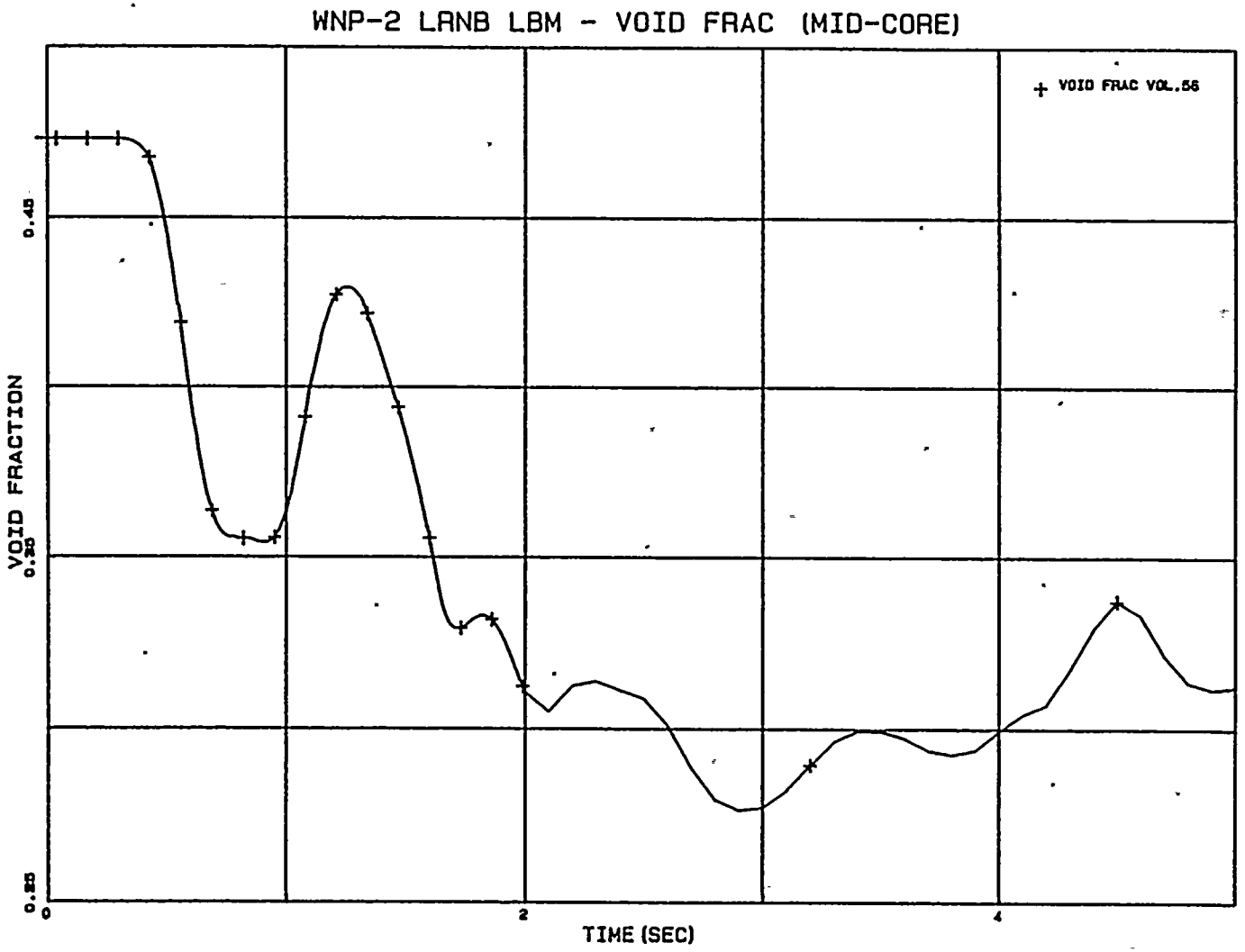
WNP-2 LRNB LBM - VOID FRAC (MID-CORE)
+ VOID FRAC VOL.56
VOID FRACTION
0.45
0.25
0.05
0
2
4
TIME (SEC)

FIGURE 4.2.12

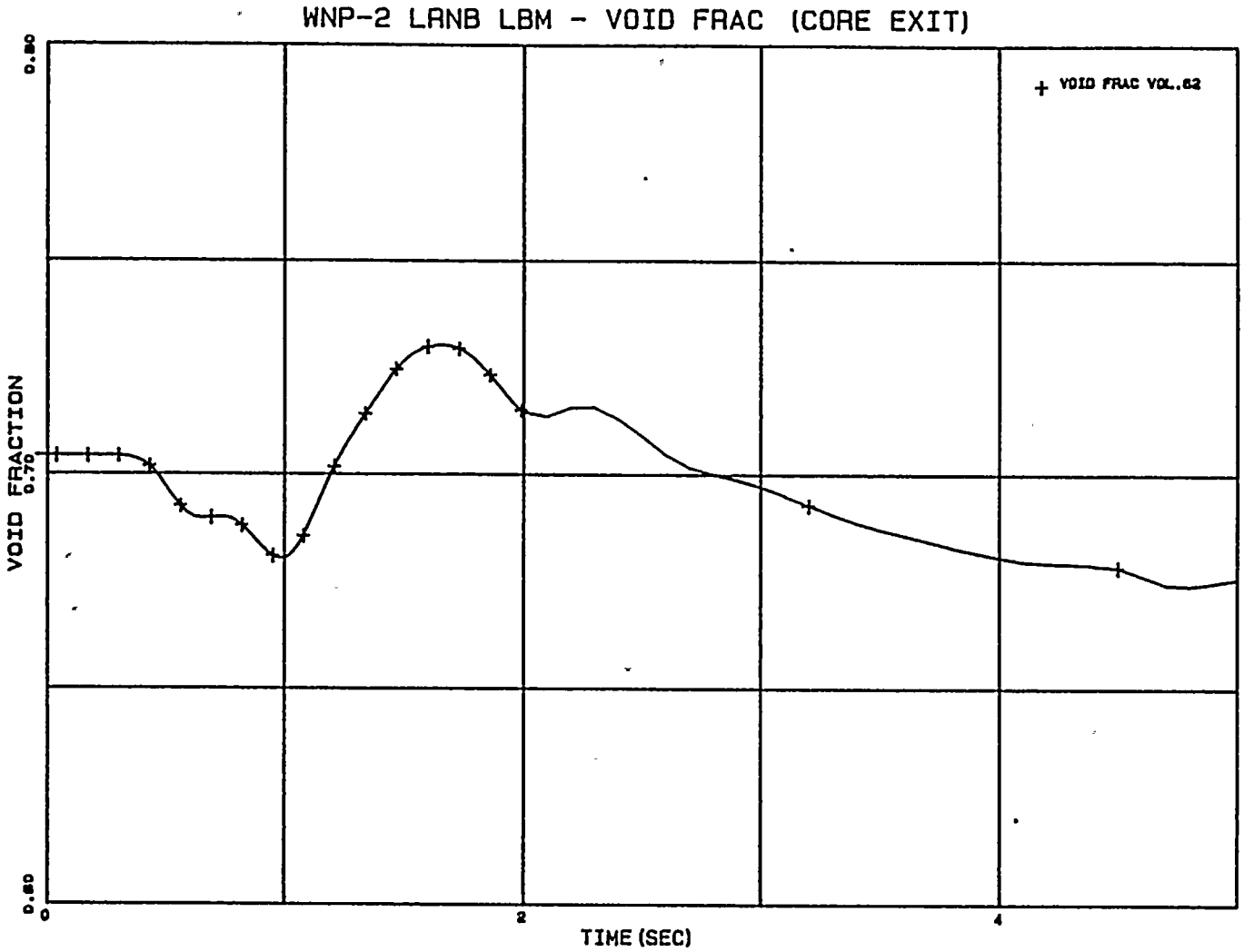
WNP-2 LANB LBM - VOID FRAC (CORE EXIT)
+ VOID FRAC VOL.62
VOID FRACTION
0.80
0.70
0.60
0
2
4
TIME (SEC)

FIGURE 4.2.13

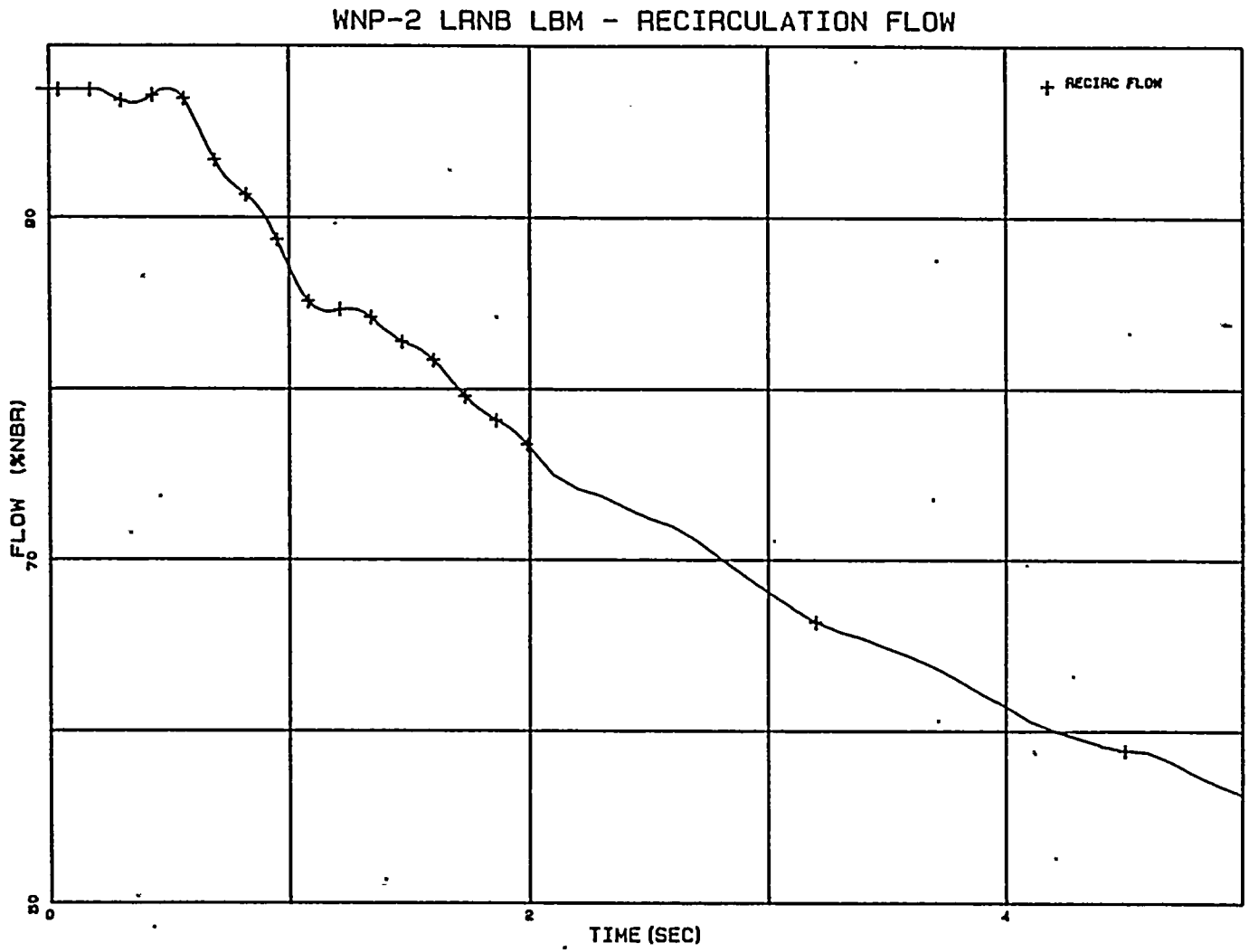
WNP-2 LRNB LBM - RECIRCULATION FLOW
+ RECIRC FLOW
FLOW (%NBR)
90
70
50
0
2
4
TIME (SEC)

FIGURE 4.2.14

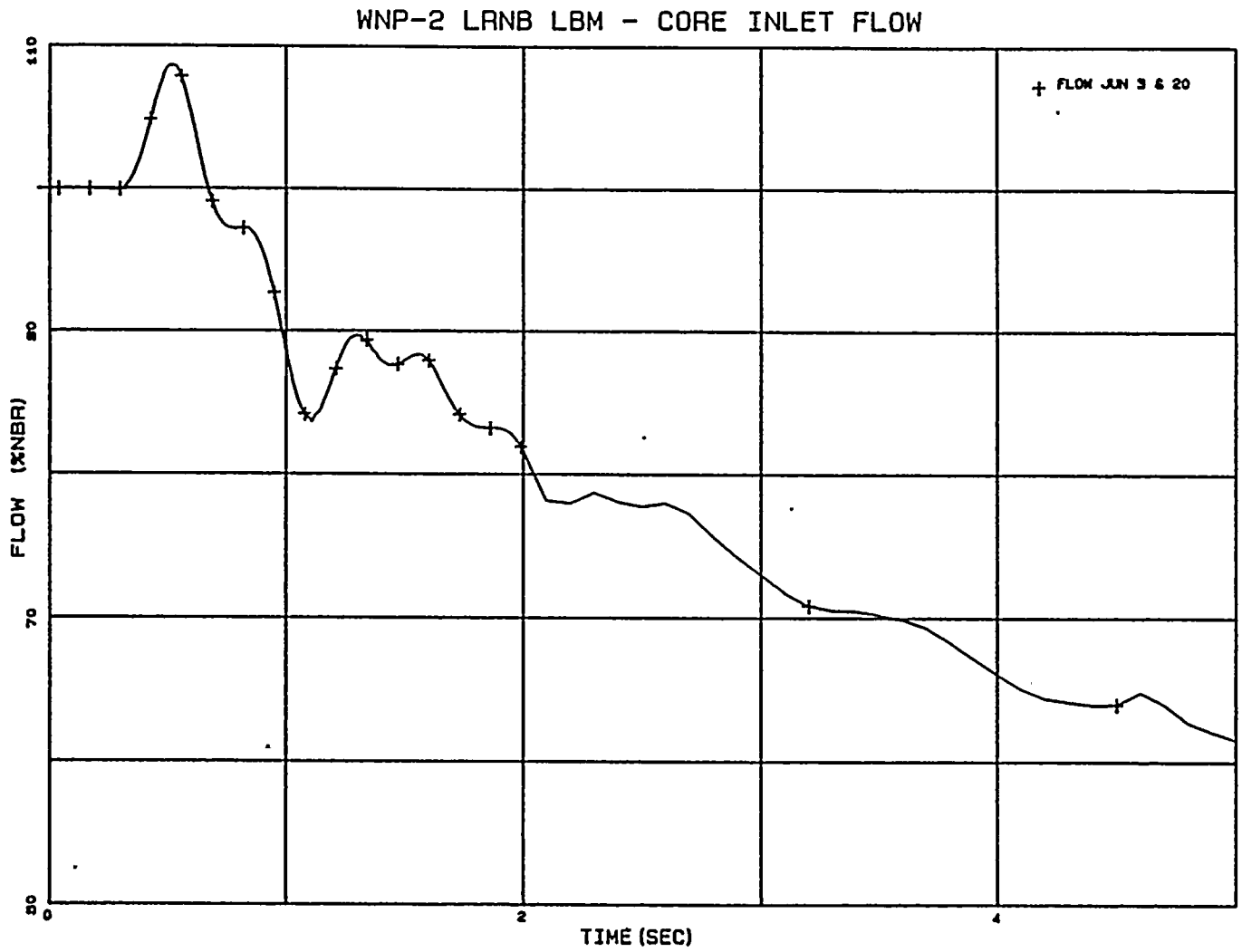
WNP-2 LRNB LBM - CORE INLET FLOW
+ FLOW JUN 3 & 20
110
90
70
50
FLOW (%NBR)
0
2
4
TIME (SEC)

FIGURE 4.3.1

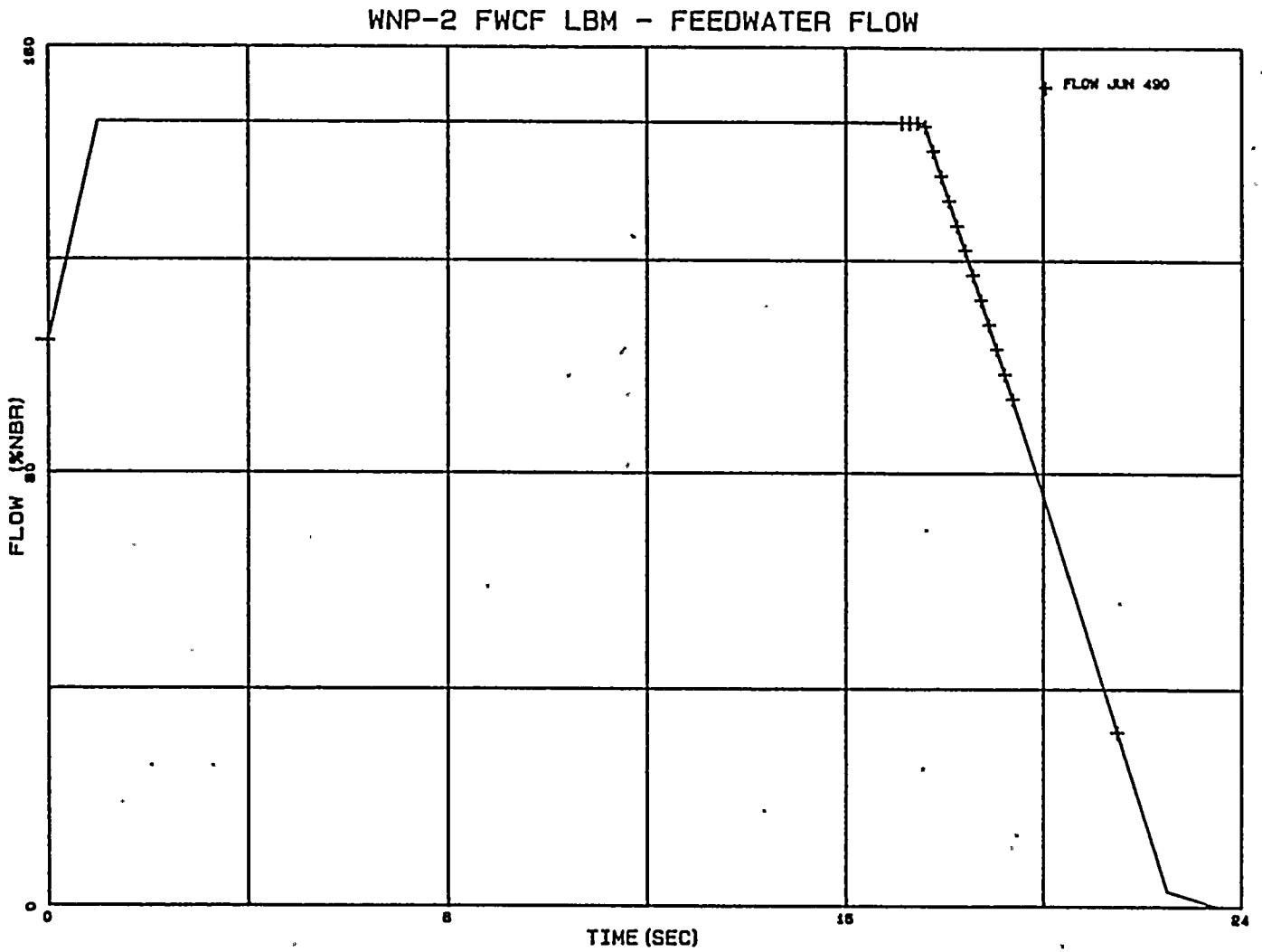
WNP-2 FWCF LBM - FEEDWATER FLOW
FLOW JUN 490
FLOW (%NBR)
160
80
0
0
8
16
24
TIME (SEC)

FIGURE 4.3.2

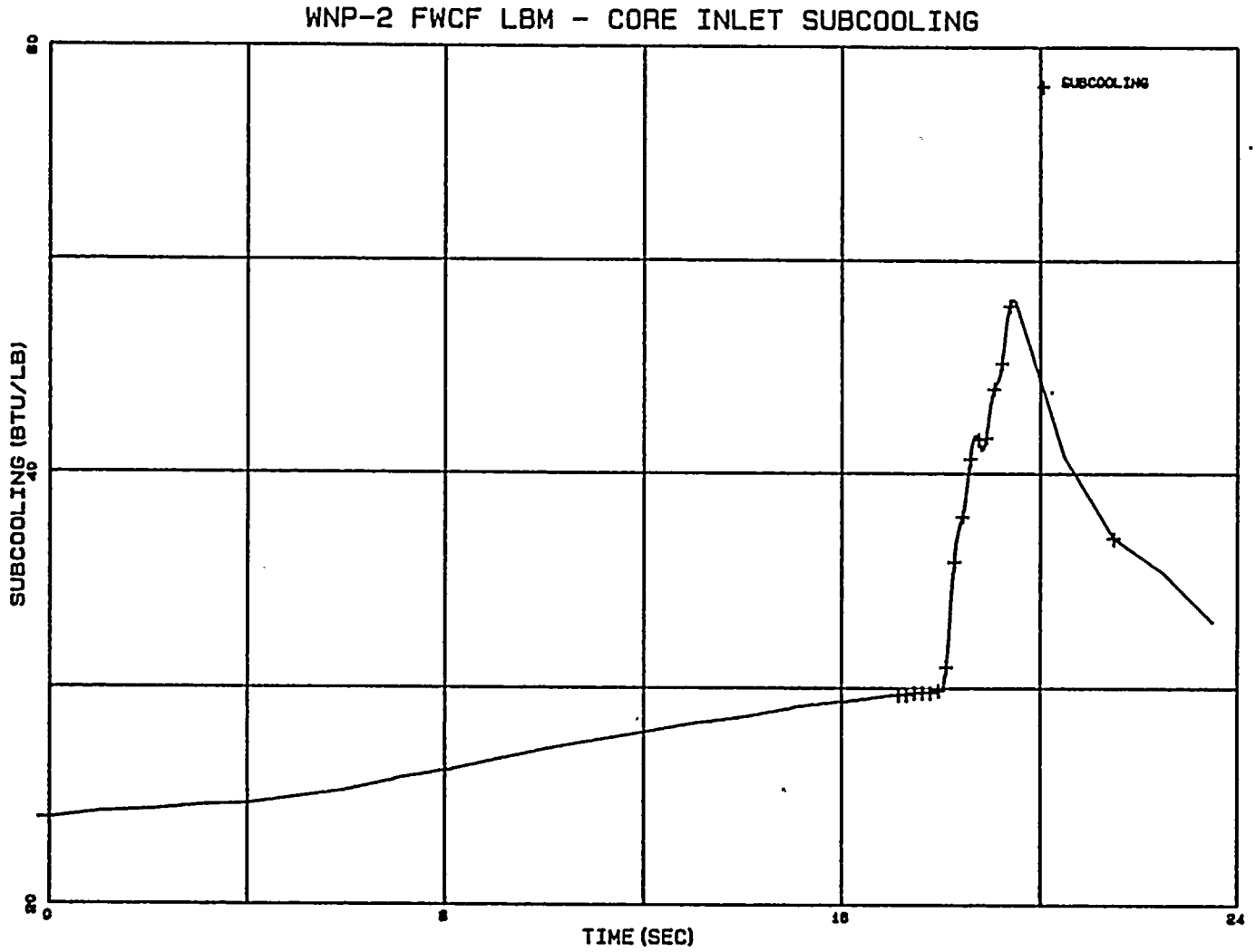
WNP-2 FWCF LBM - CORE INLET SUBCOOLING
SUBCOOLING
SUBCOOLING (BTU/LB)
60
40
20
0
8
16
24
TIME (SEC)

FIGURE 4.3.3

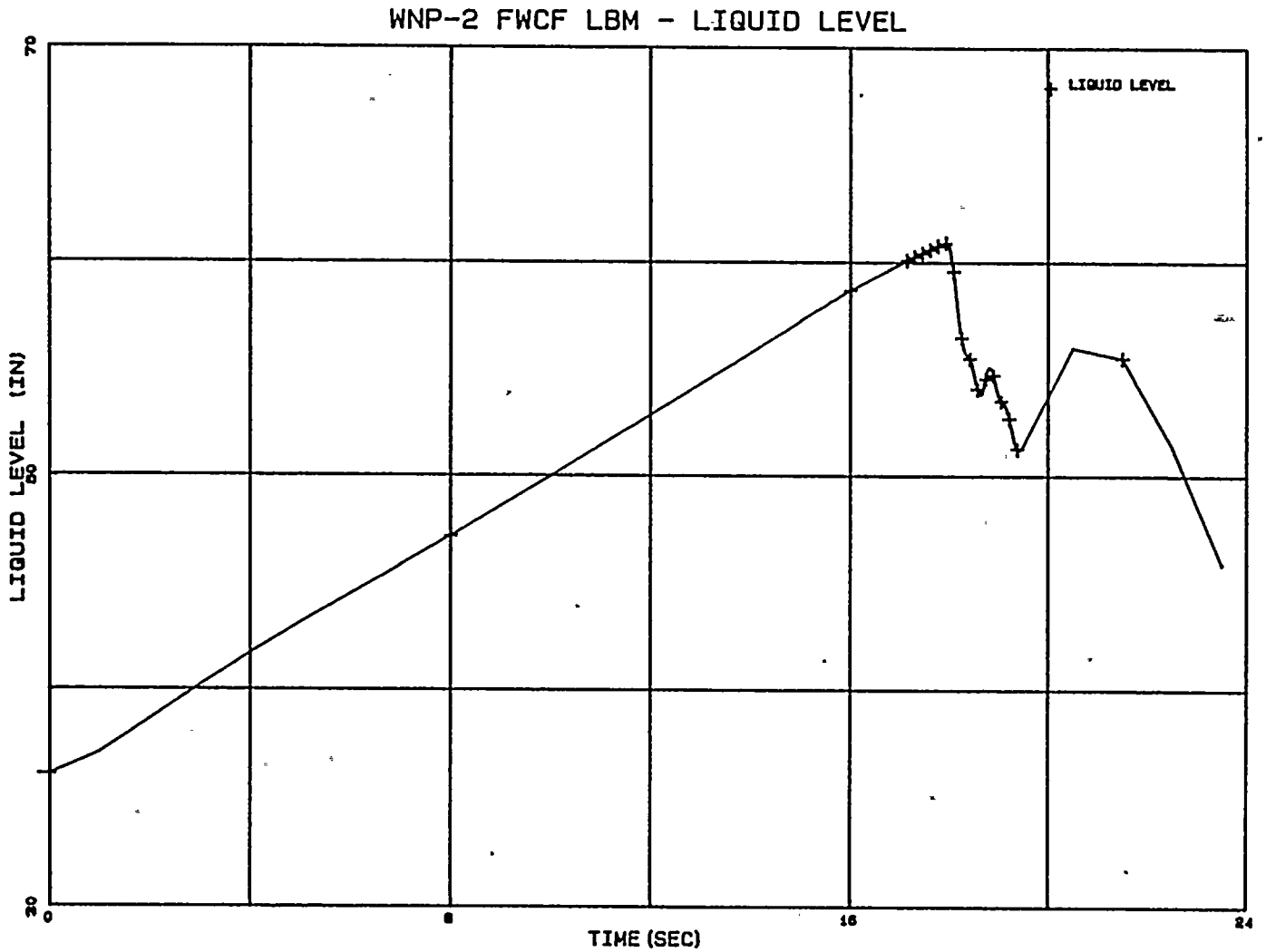
WNP-2 FWCF LBM - LIQUID LEVEL
LIQUID LEVEL
LIQUID LEVEL (IN)
70
50
30
0
8
16
24
TIME (SEC)

FIGURE 4.3.4

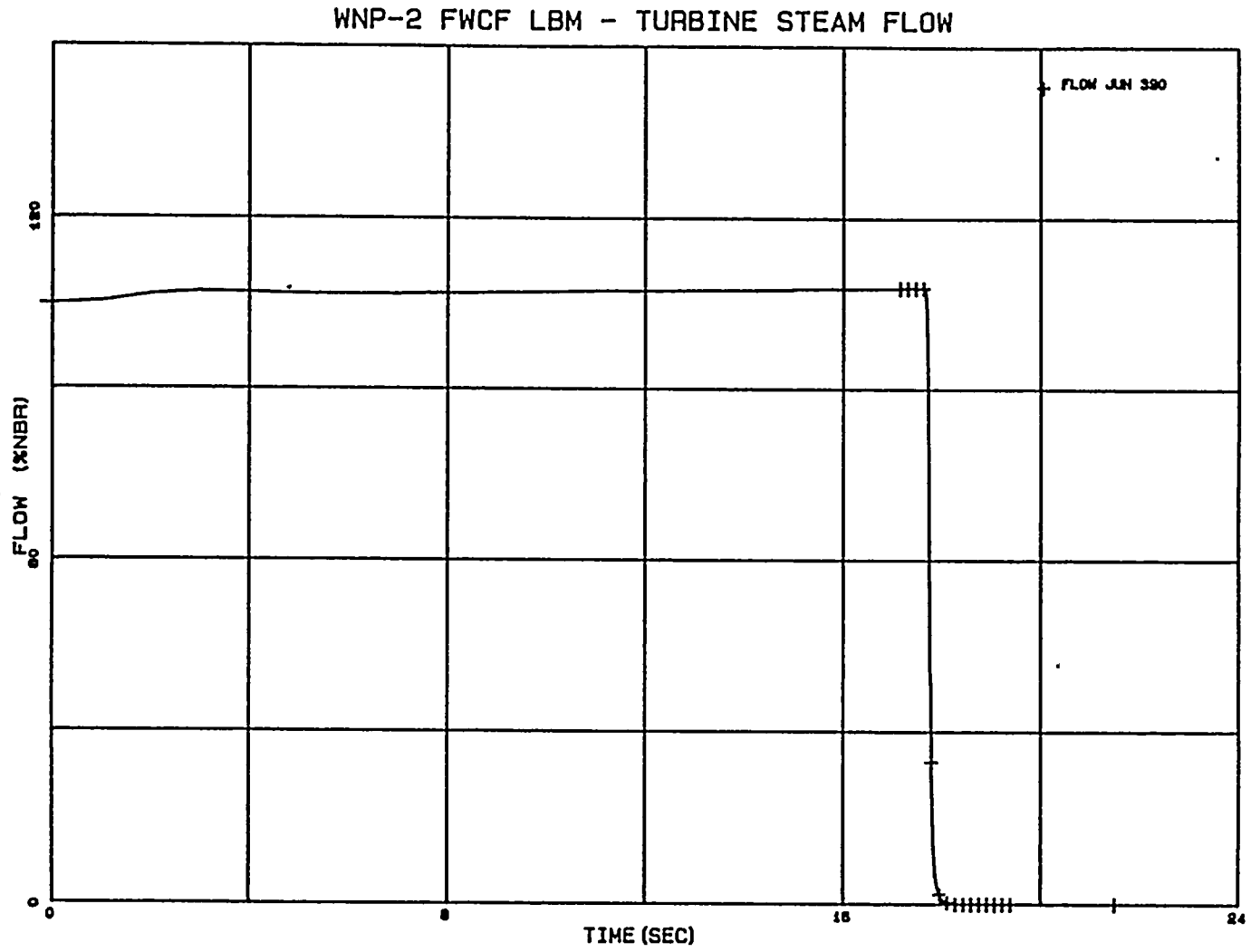
WNP-2 FWCF LBM - TURBINE STEAM FLOW
FLOW JUN 390
100
80
0
FLOW (%NBR)
0
8
16
24
TIME (SEC)

FIGURE 4.3.5

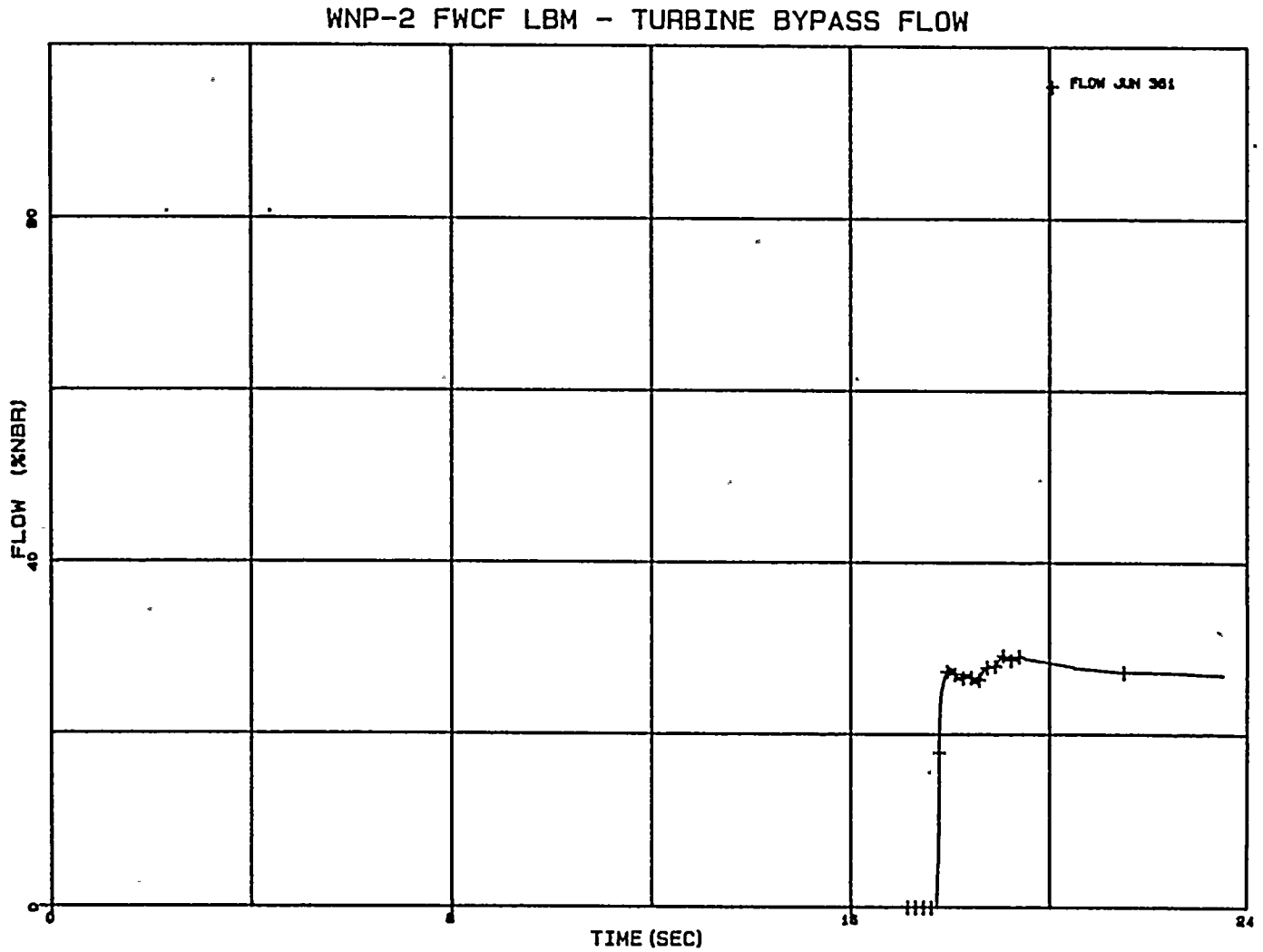
WNP-2 FWCF LBM - TURBINE BYPASS FLOW
FLOW JUN 361
80
40
0
FLOW (%NBR)
0
8
16
24
TIME (SEC)

FIGURE 4.3.6

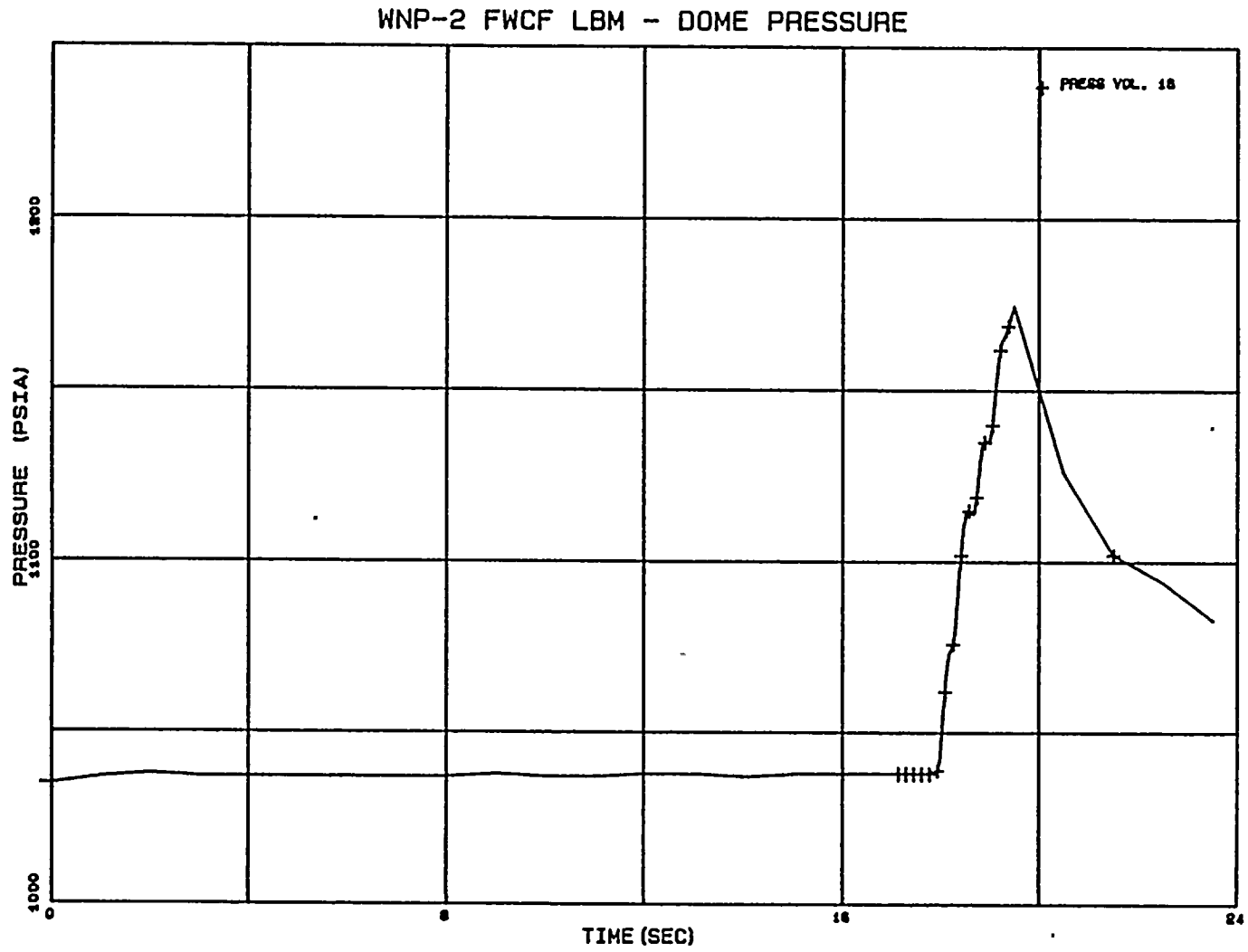
WNP-2 FWCF LBM - DOME PRESSURE
PRESS VOL. 18
PRESSURE (PSIA)
1200
1100
1000
0
8
16
24
TIME (SEC)

FIGURE 4.3.7

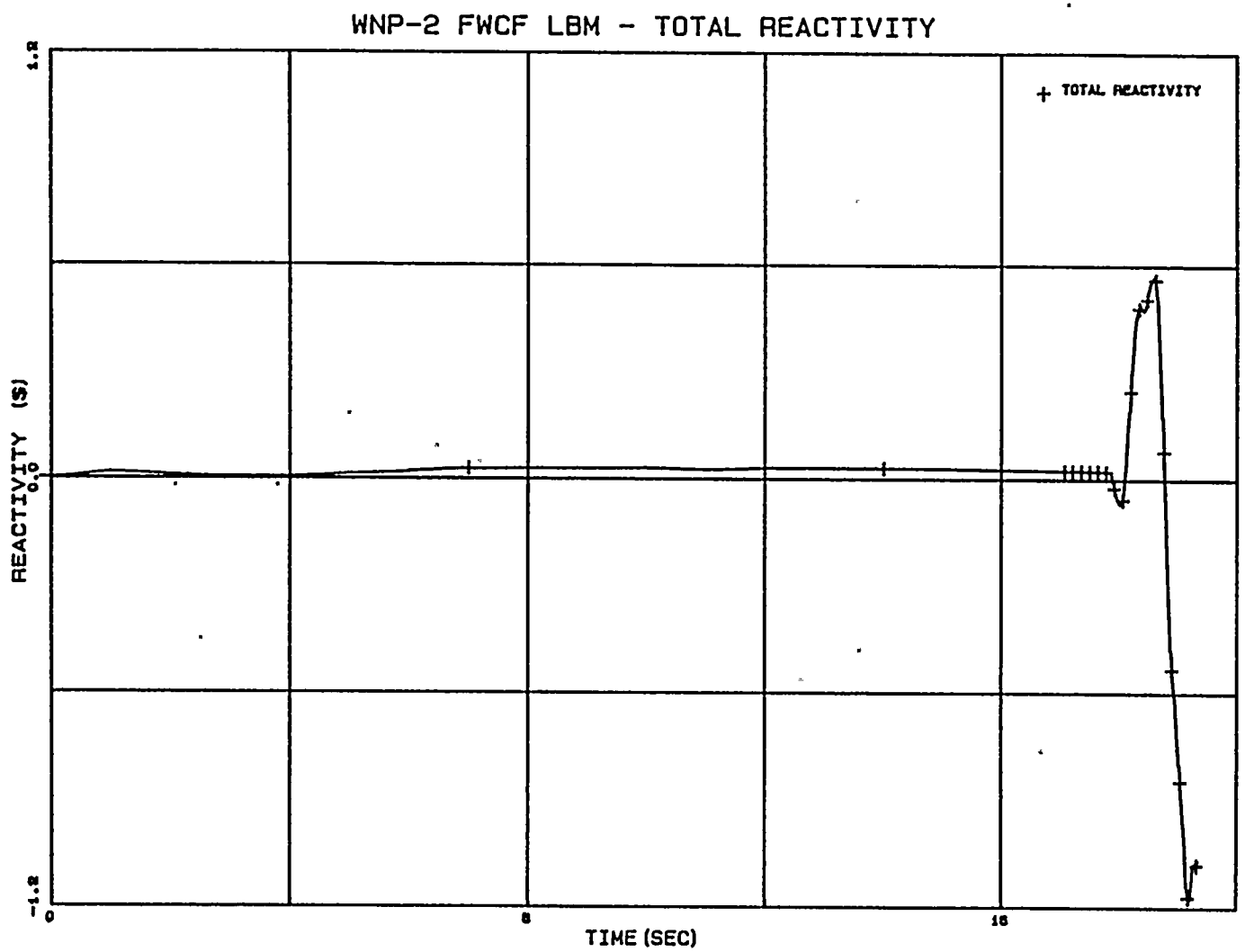
WNP-2 FWCF LBM - TOTAL REACTIVITY
+ TOTAL REACTIVITY
REACTIVITY ($)
1.0
0.0
-1.0
0
8
16
TIME (SEC)

FIGURE 4.3.8

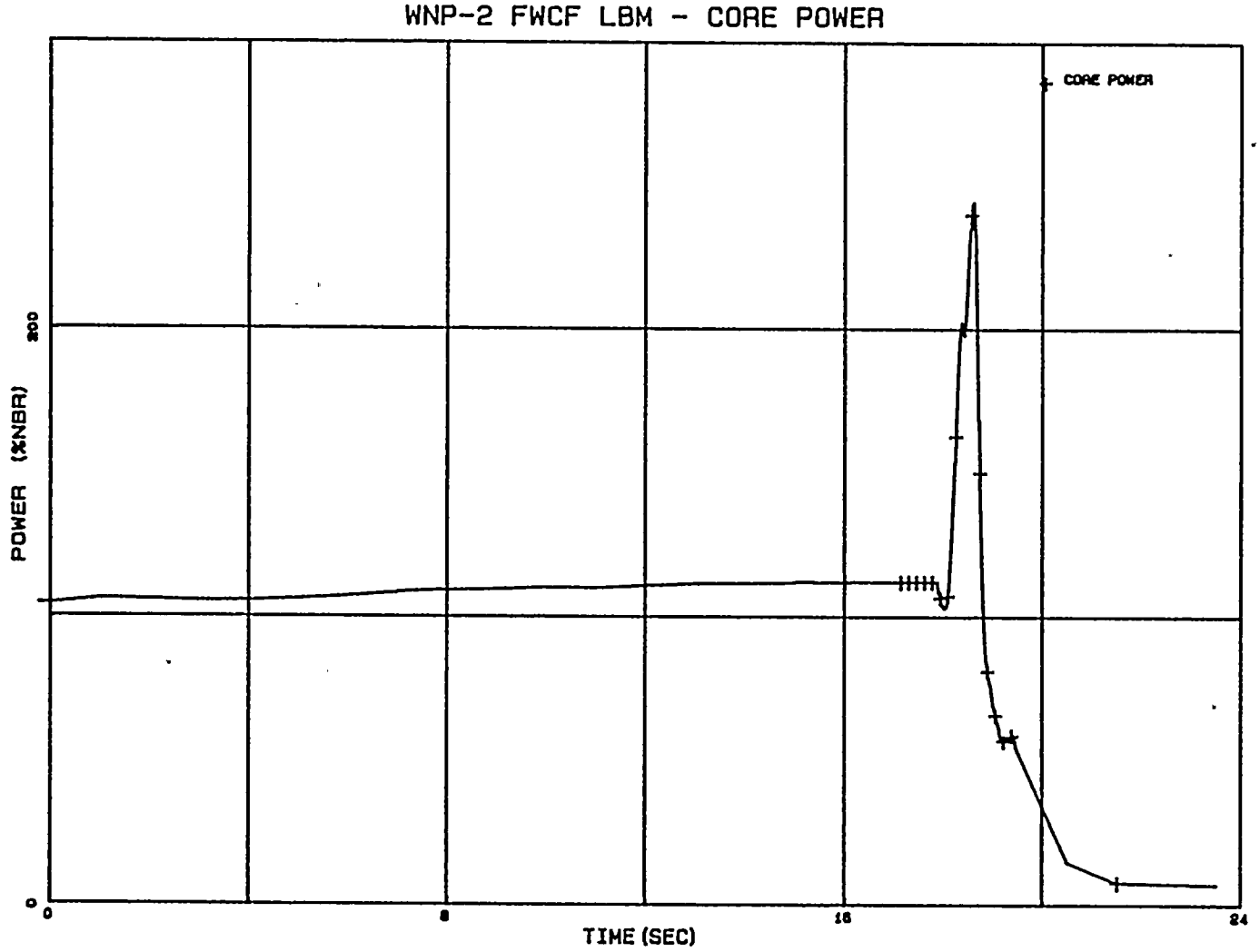
WNP-2 FWCF LBM - CORE POWER
CORE POWER
POWER (%NBR)
200
0
0
8
16
24
TIME (SEC)

FIGURE 4.3.9

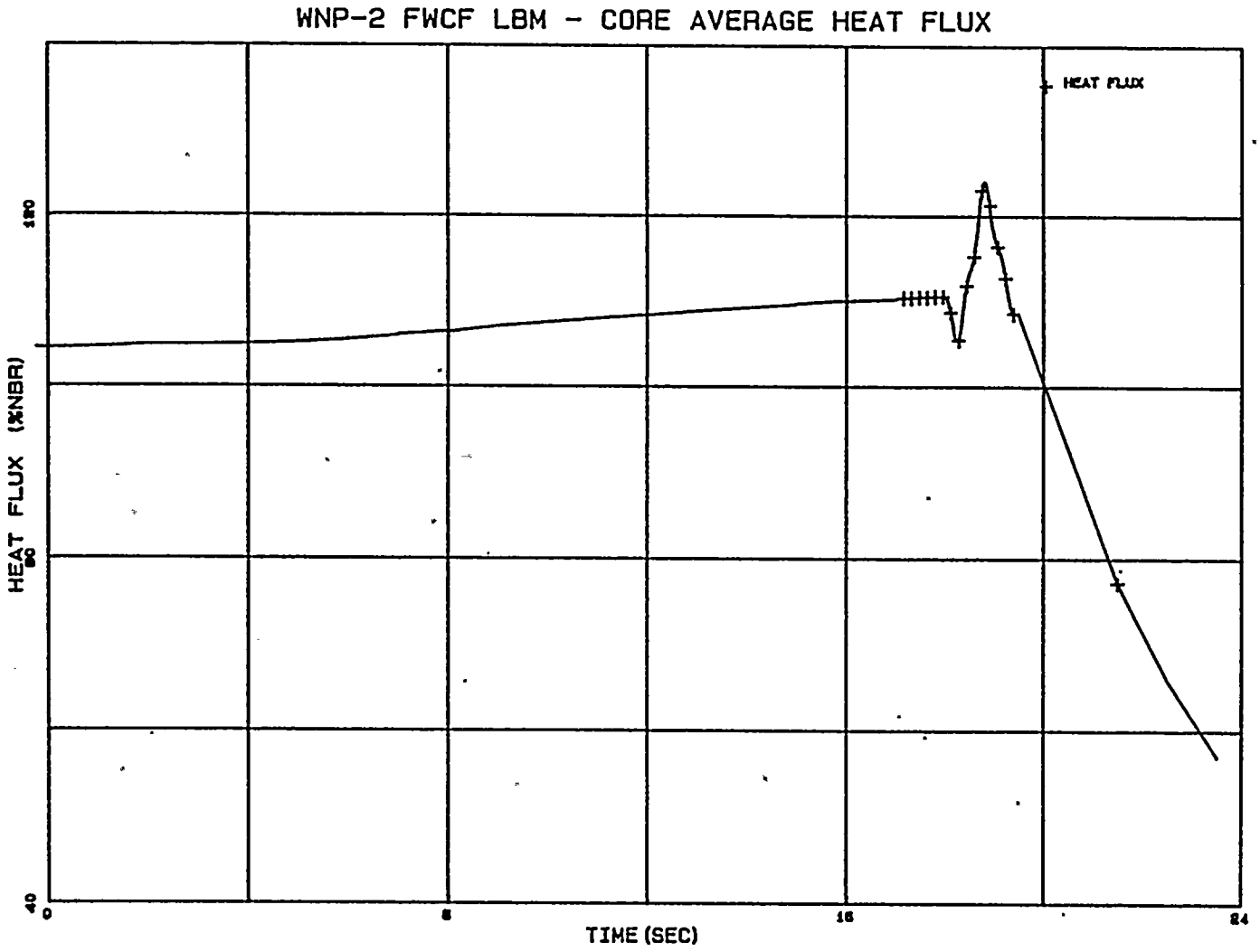
WNP-2 FWCF LBM - CORE AVERAGE HEAT FLUX
HEAT FLUX
HEAT FLUX (%NBR)
120
80
40
0
8
16
24
TIME (SEC)

FIGURE 4.3.10

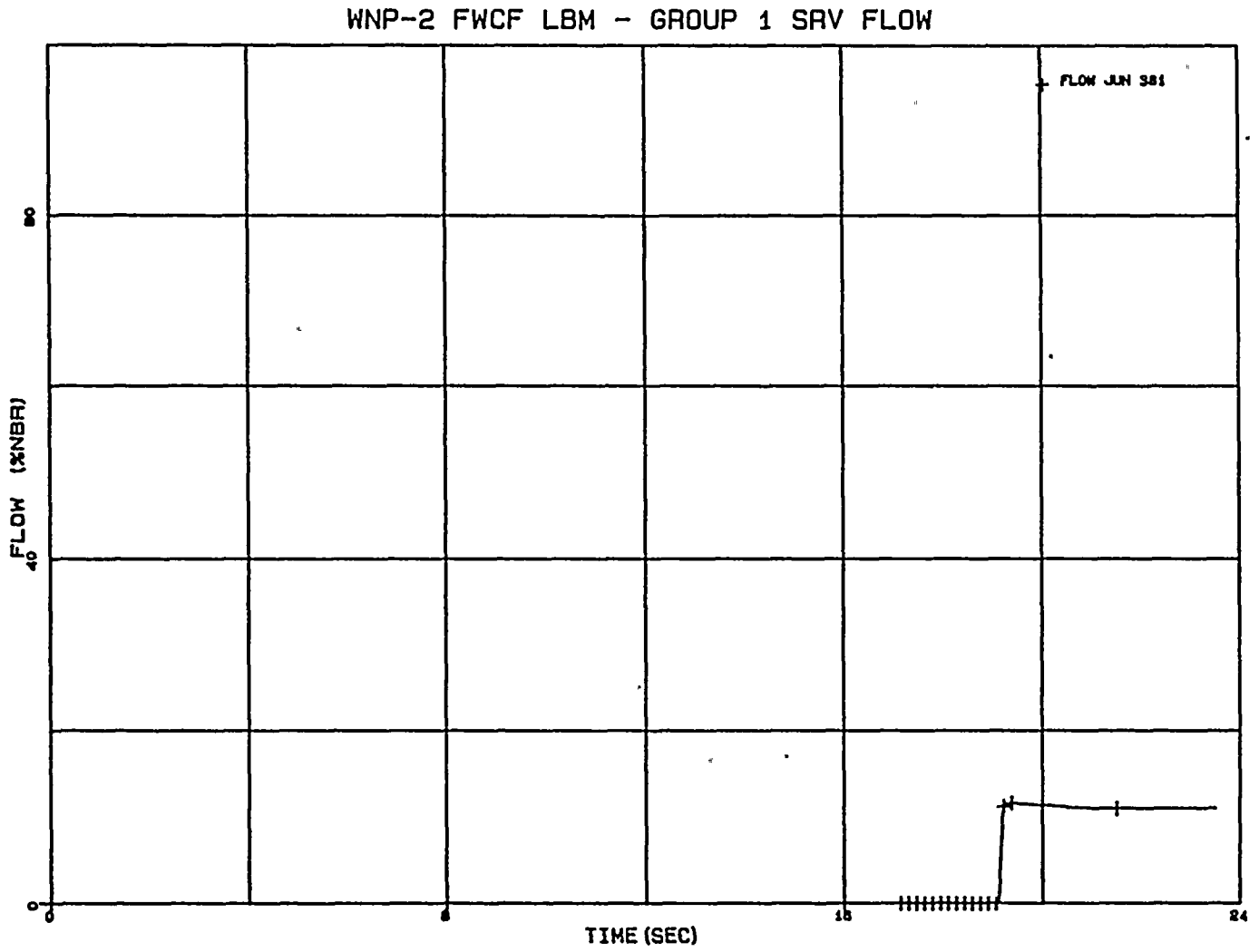
WNP-2 FWCF LBM - GROUP 1 SRV FLOW
FLOW JUN 381
80
40
0
FLOW (%NBR)
0
8
16
24
TIME (SEC)

FIGURE 4.3.11

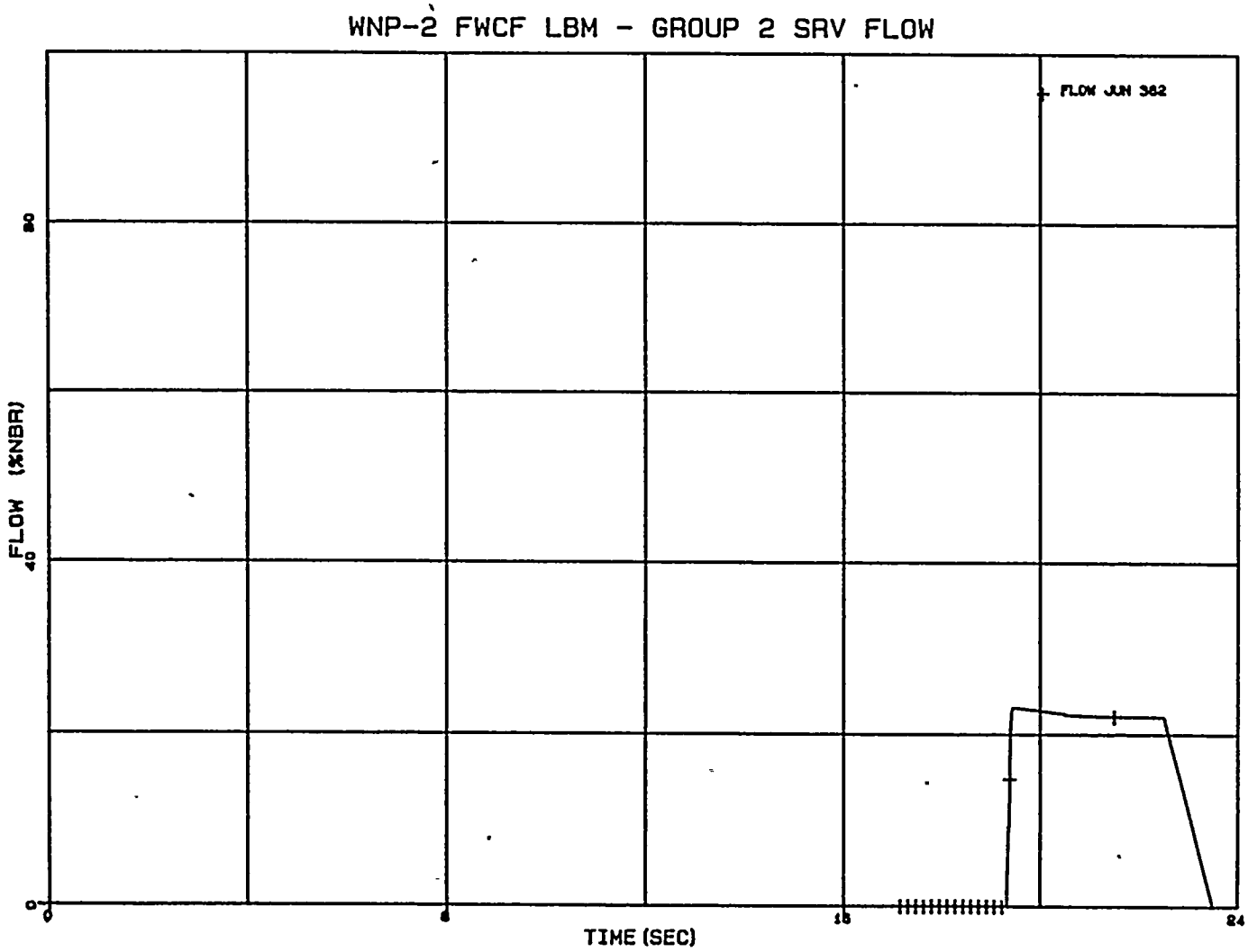
WNP-2 FWCF LBM - GROUP 2 SRV FLOW
FLOW JUN 382
80
40
0
FLOW (%NBR)
0
8
16
24
TIME (SEC)

FIGURE 4.3.12

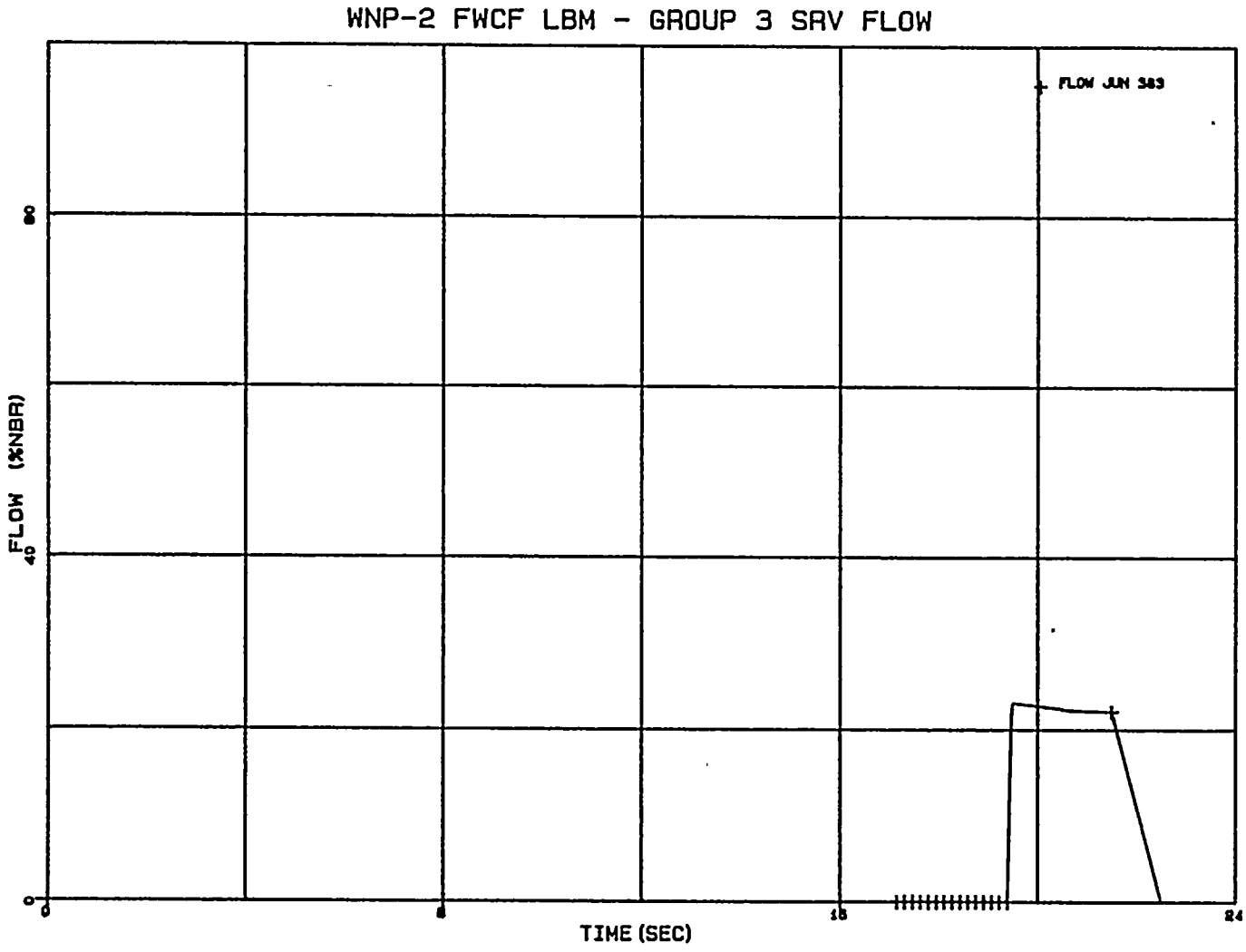
WNP-2 FWCF LBM - GROUP 3 SRV FLOW
FLOW JUN 383
80
40
0
FLOW (%NBR)
0
8
16
24
TIME (SEC)

FIGURE 4.3.13

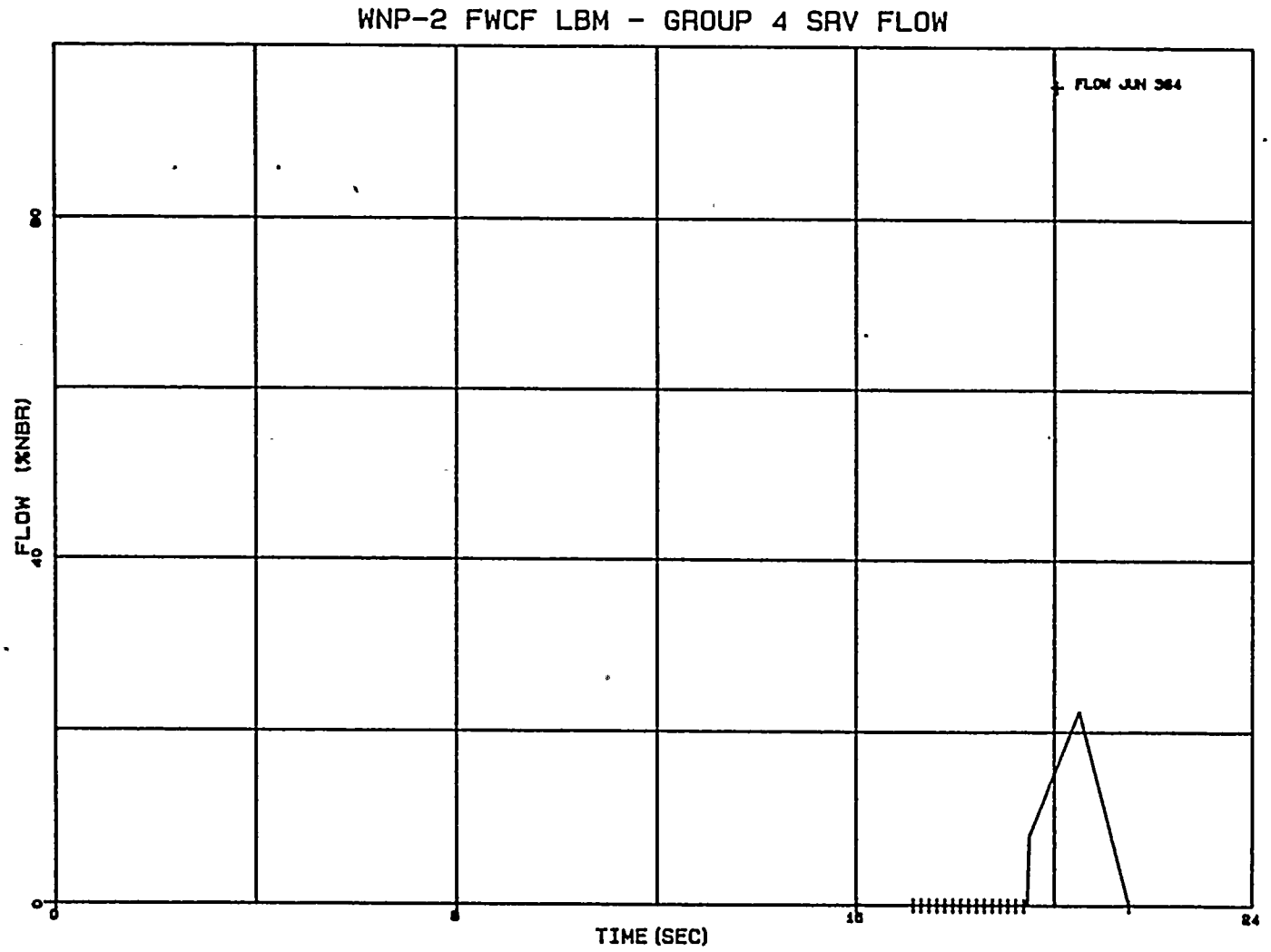
WNP-2 FWCF LBM - GROUP 4 SRV FLOW
FLOW JUN 384
80
40
0
FLOW (%NBR)
0
8
16
24
TIME (SEC)

FIGURE 4.3.14

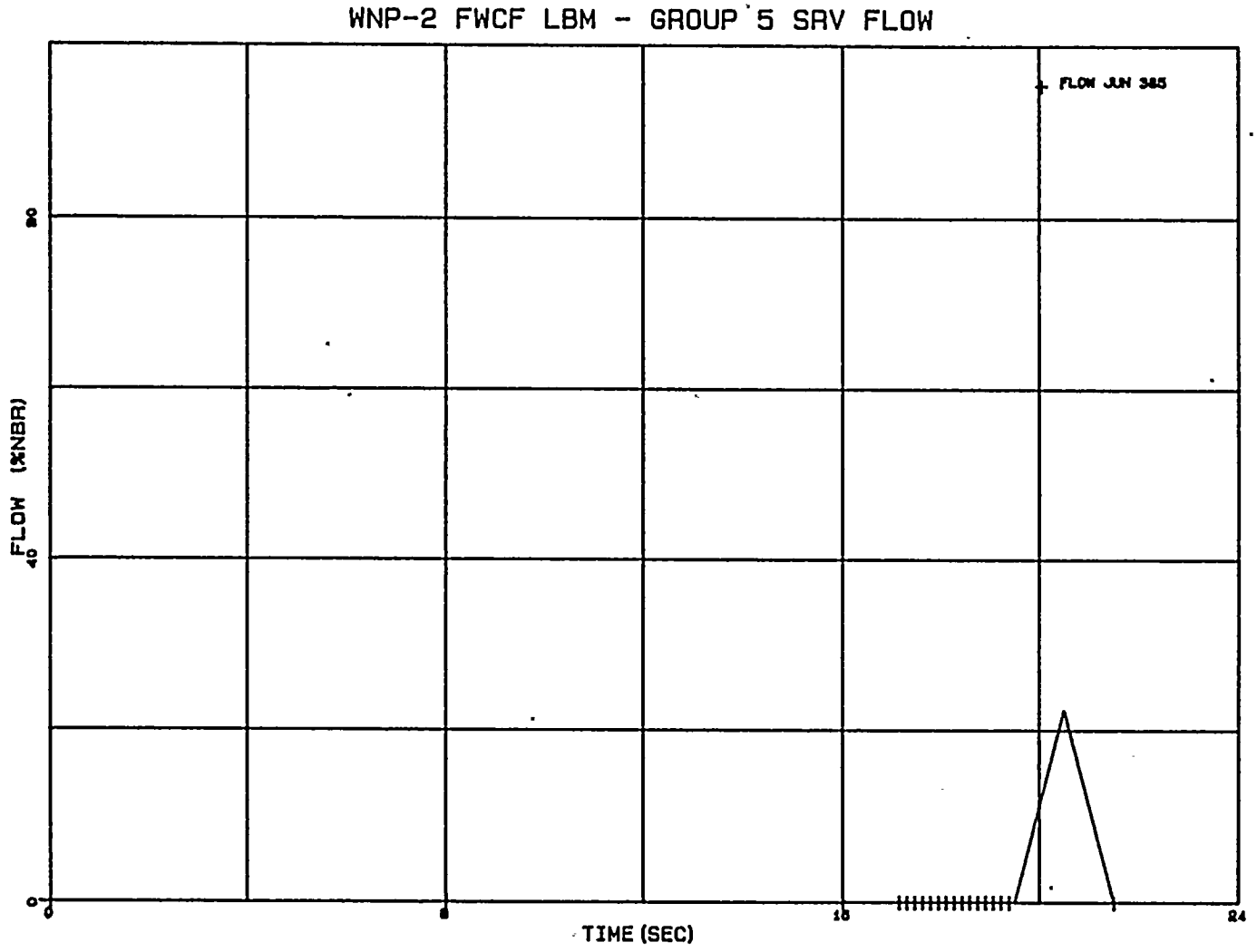
WNP-2 FWCF LBM - GROUP 5 SRV FLOW
FLOW JUN 385
FLOW (%NBR)
80
40
0
0
8
16
24
TIME (SEC)

FIGURE 4.3.15

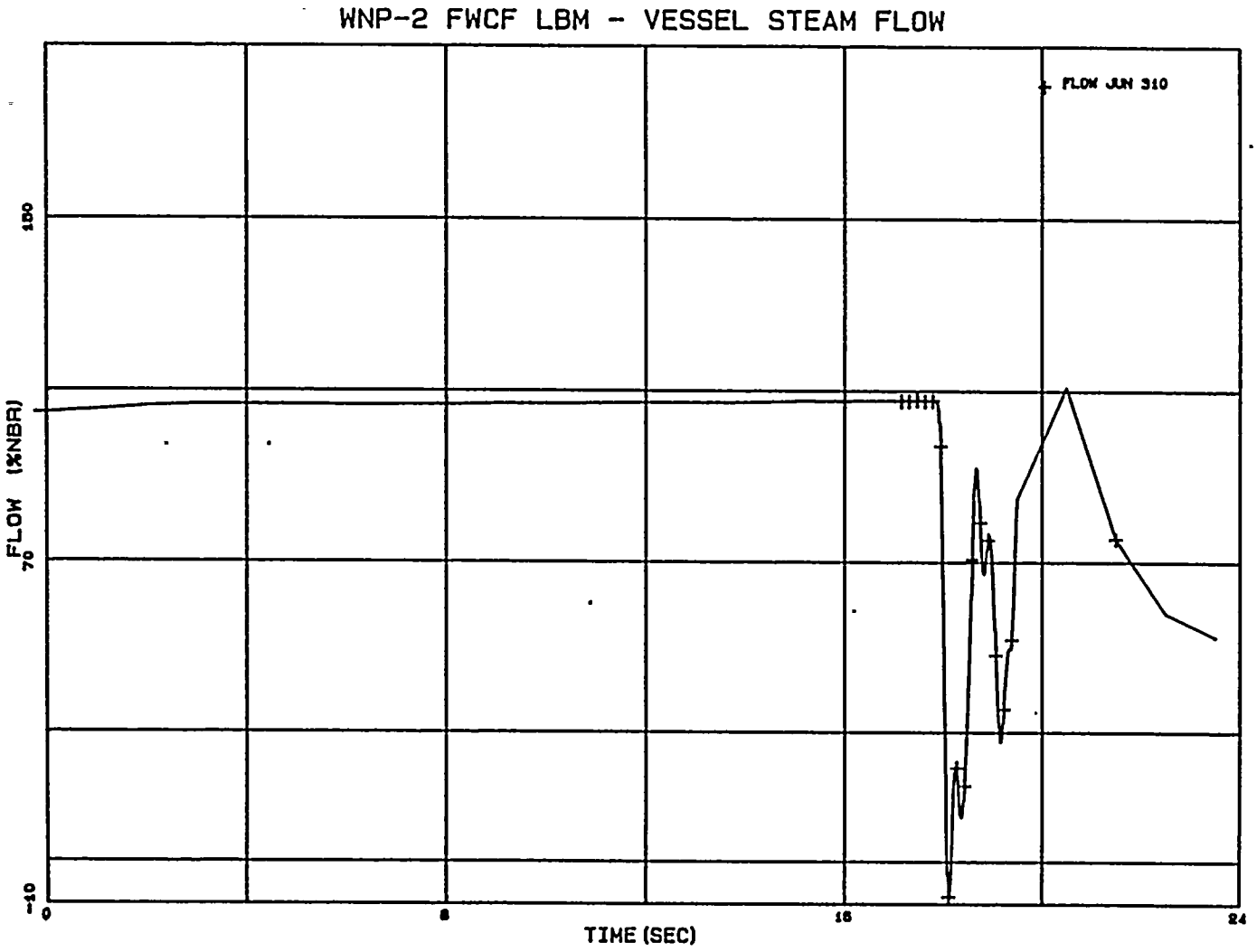
WNP-2 FWCF LBM - VESSEL STEAM FLOW
FLOW JUN 310
180
70
-10
FLOW (%NBR)
0
8
16
24
TIME (SEC)

FIGURE 4.3.16

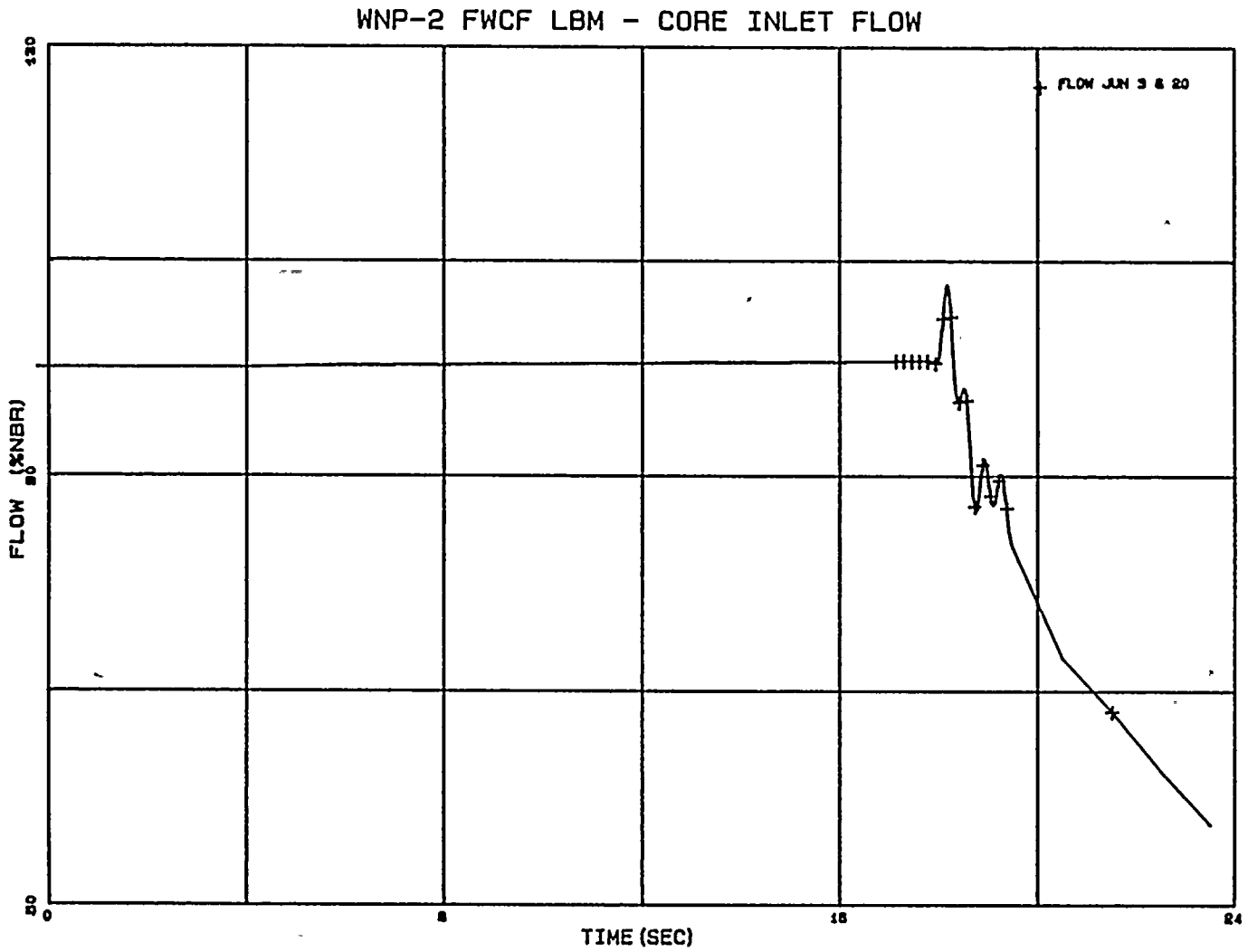
WNP-2 FWCF LBM - CORE INLET FLOW
FLOW JUN 3 & 20
FLOW (%NBR)
120
80
20
0
8
16
24
TIME (SEC)

FIGURE 4.3.17

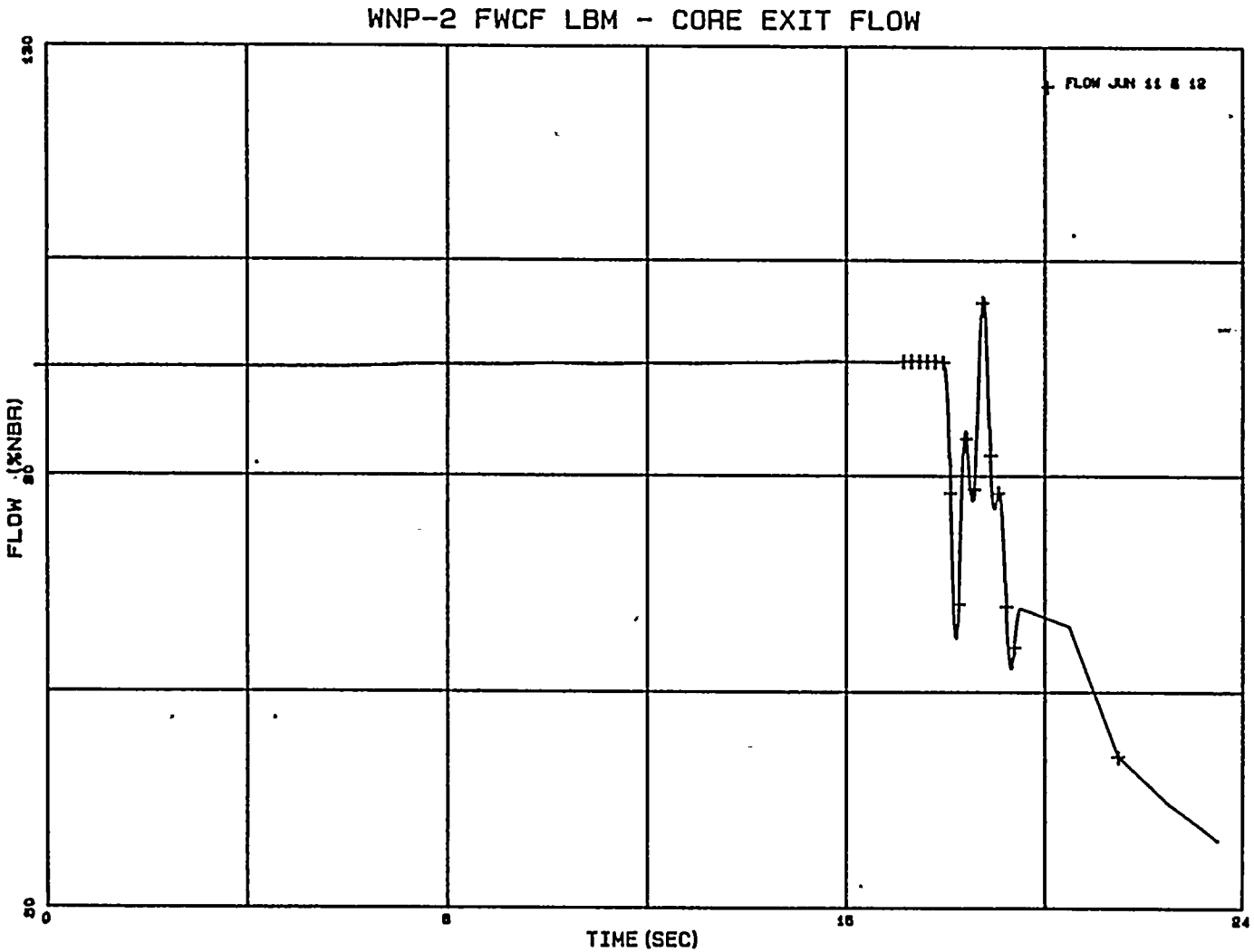
WNP-2 FWCF LBM - CORE EXIT FLOW
FLOW JUN 11 6 12
FLOW (%NBR)
100
80
50
0
8
16
24
TIME (SEC)

FIGURE 4.3.18

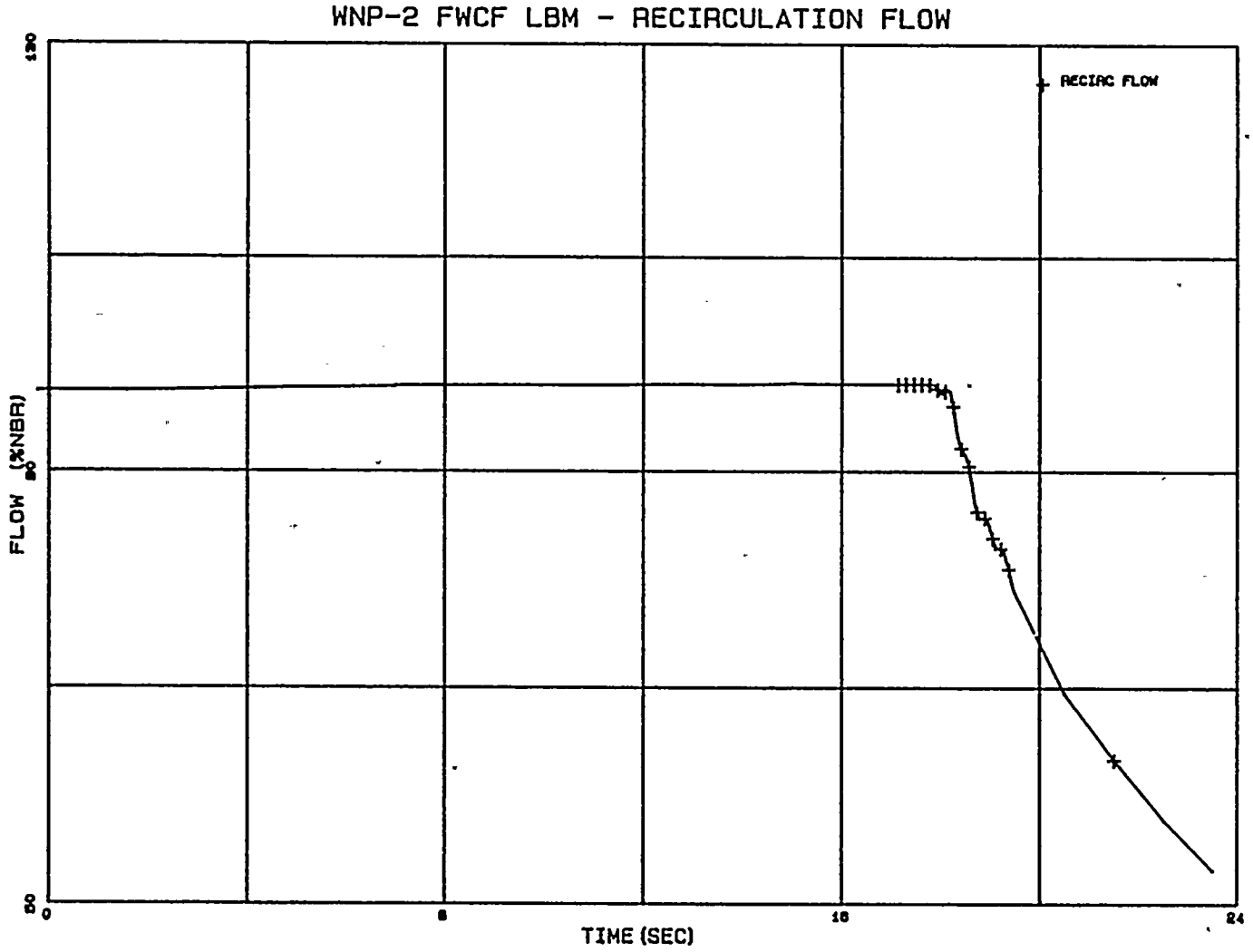
WNP-2 FWCF LBM - RECIRCULATION FLOW
RECIRC FLOW
FLOW (%NBR)
100
80
60
0
8
16
24
TIME (SEC)

FIGURE 4.3.19

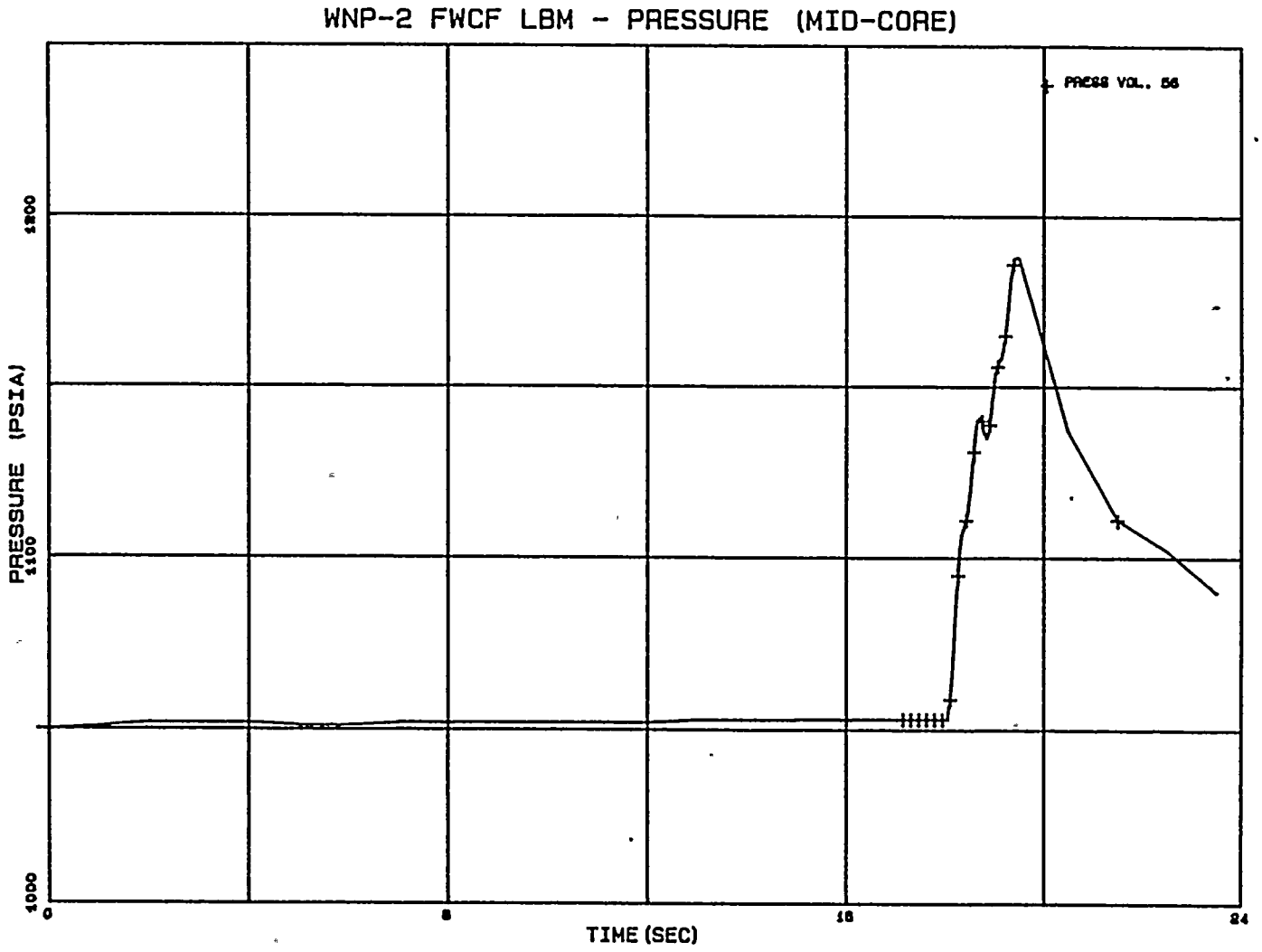
WNP-2 FWCF LBM - PRESSURE (MID-CORE)
PRESS VOL. 56
PRESSURE (PSIA)
1200
1100
1000
0
8
16
24
TIME (SEC)

FIGURE 4.3.20

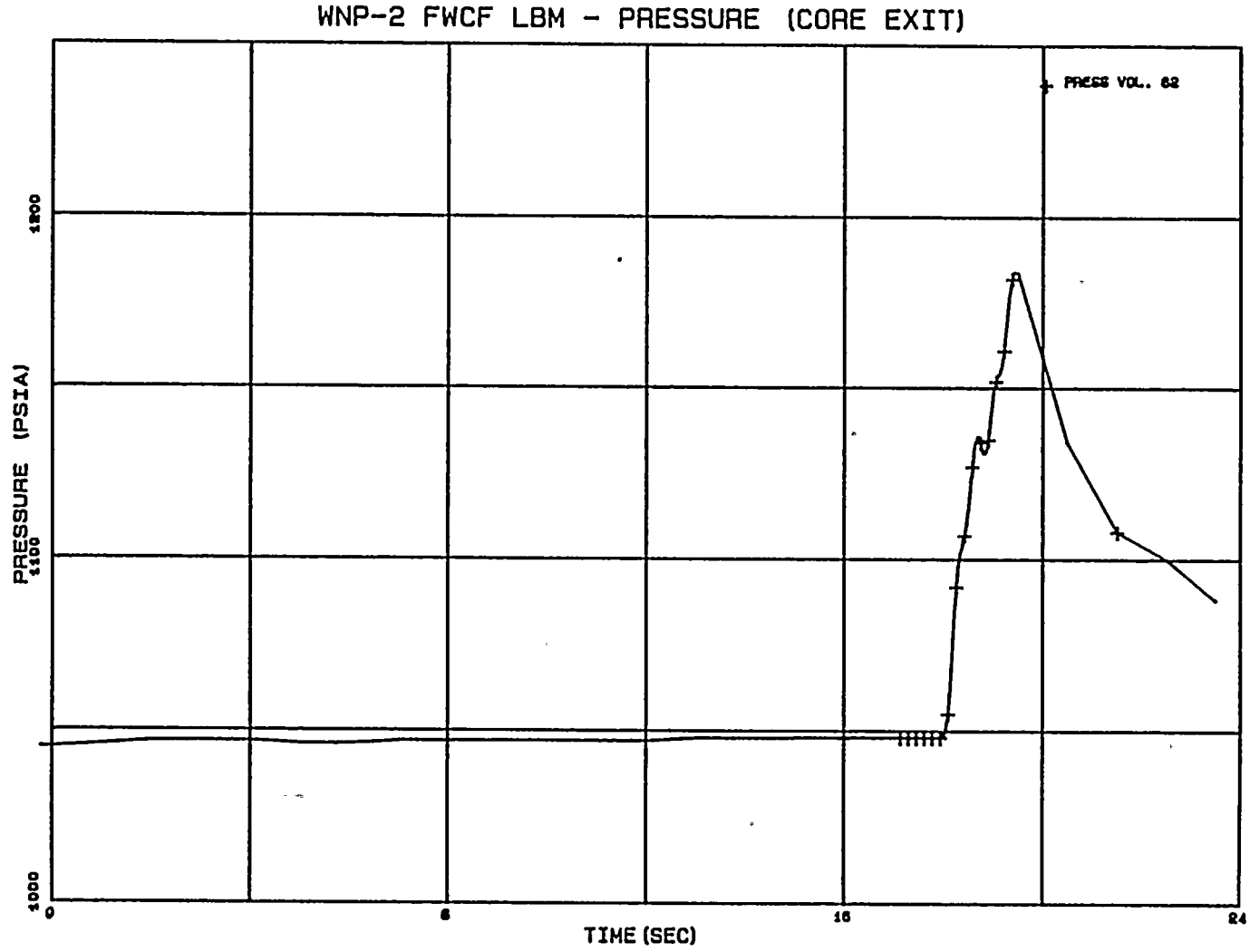
WNP-2 FWCF LBM - PRESSURE (CORE EXIT)
PRESS VOL. 62
PRESSURE (PSIA)
1200
1100
1000
0
8
16
24
TIME (SEC)

FIGURE 4.3.21

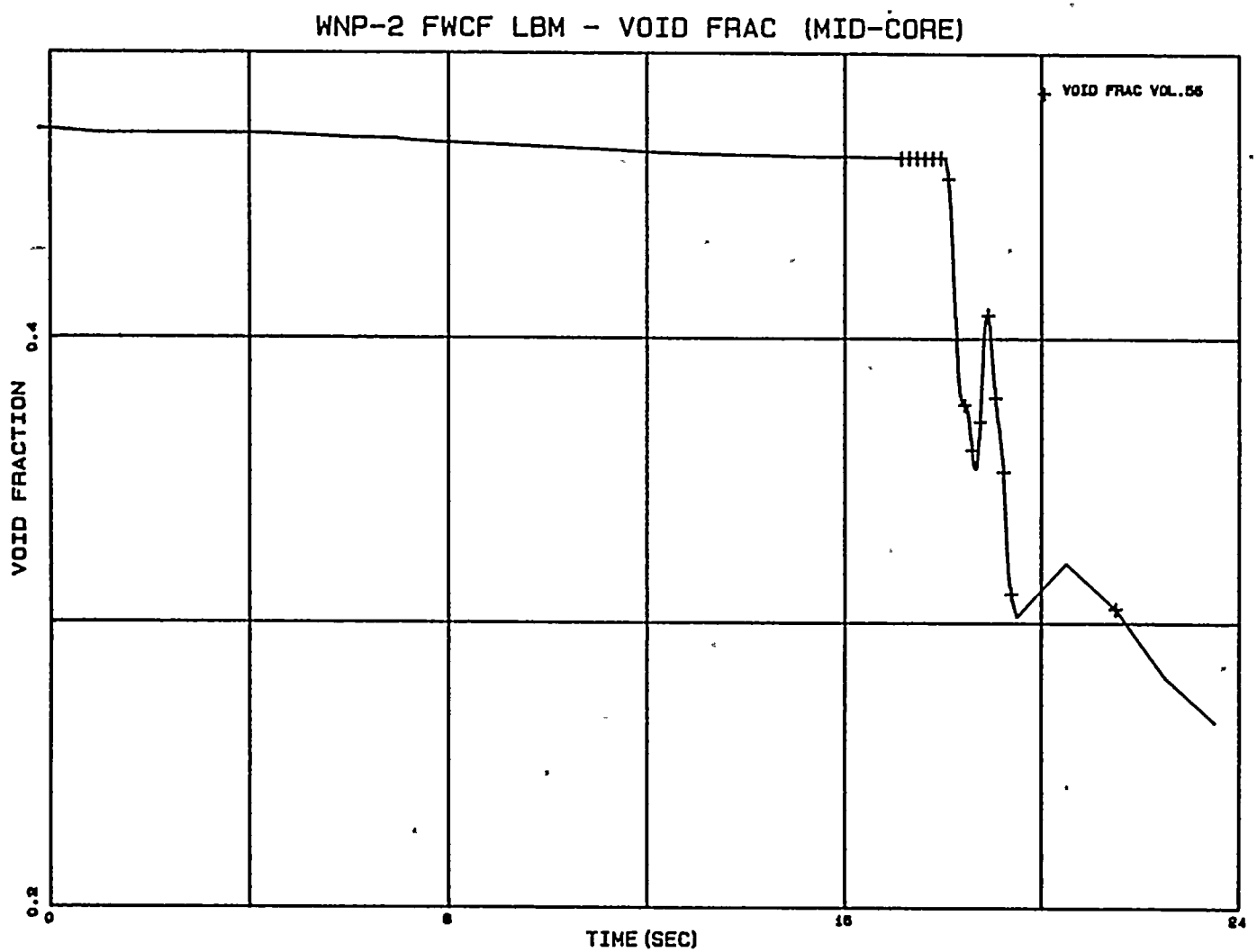
WNP-2 FWCF LBM - VOID FRAC (MID-CORE)
VOID FRAC VOL.56
VOID FRACTION
0.4
0.2
0
8
16
24
TIME (SEC)

FIGURE 4.3.22

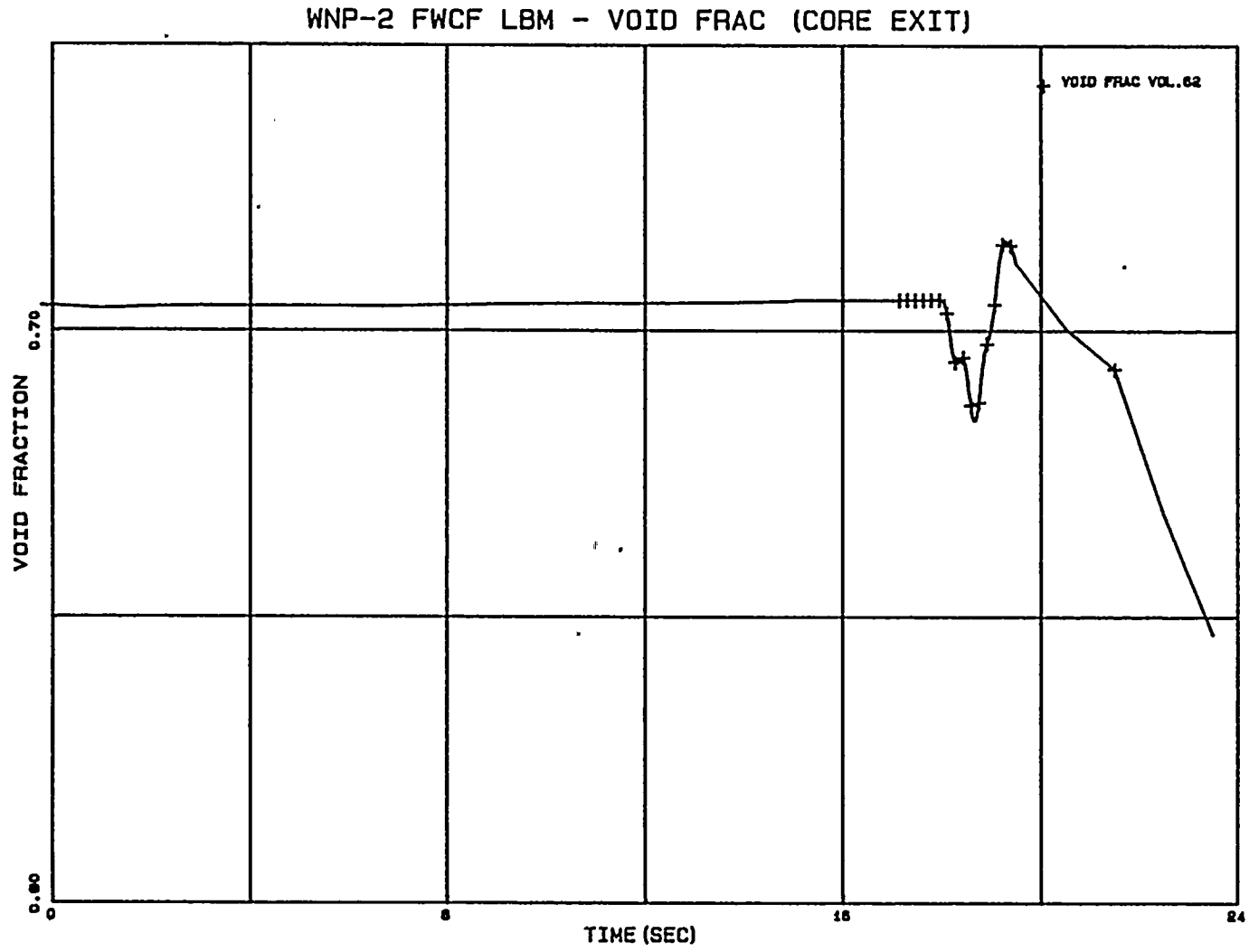
WNP-2 FWCF LBM - VOID FRAC (CORE EXIT)
VOID FRAC VOL.62
VOID FRACTION
0.70
0.60
0
8
16
24
TIME (SEC)

4.4 Summary of Transient Analysis

The key transient simulation results for the two MCPR limiting transients are summarized in Table 4.6.

TABLE 4.5

Summary of Thermal-Limiting Transient Results

	LRNB	FWCF
Max Power (%NBR)	398	245
Time at max power (seconds)	0.89	18.6
Max core avg heat flux (%NBR)	133	124
Time at max heat flux (seconds)	1.1	18.8
Max dome pressure (psia)	1207	1175
Time at max dome pressure (sec)	1.9	19.5

5.0 SUMMARY AND CONCLUSIONS

Benchmark analyses covering specific Power Ascension Tests as described in Section 3.1 demonstrate the capability of the WNP-2 RETRAN model to predict core and system behavior during normal operation and mild transients. These analyses validate the modeling of the feedwater and pressure regulator control systems and the performance of the recirculation pumps, jet pumps, and steam lines as modeled for WNP-2.

Benchmark analyses covering the turbine trip tests performed at Peach Bottom 2 at the end of Cycle 2 as described in Section 3.2 demonstrate RETRAN's ability to model conditions more challenging than the WNP-2 startup tests and the Supply System technical staff's competence to perform these analyses. These analyses validate the capabilities of the modeling beyond the normal operating envelope of the reactor.

Example calculations covering typical limiting transients as reported in Chapter 4 demonstrate the WNP-2 RETRAN model's ability to predict system performance under conditions which challenge operating limits. These analyses show consistence with existing analyses of record and validate the Supply System technical staff's ability to formulate and analyze limiting transient events.

The analyses performed in this report demonstrate the ability of the WNP-2 RETRAN model and the qualifications of the Supply System technical staff to predict the course of a wide variety of transient events. The model is applicable to the evaluation of normal and anticipated operation for plant operational support and core reload analysis.

6.0 REFERENCES

1. J.H. McFadden et al., "RETRAN-02 - A Program for Transient Thermal-Hydraulic Analysis of Complex Fluid Flow Systems," EPRI NP-1850-CCM-A, Revision 4, Volumes I-III, Electric Power Research Institute, November 1988.

2. B.M. Moore, A.G. Gibbs, J.D. Imel, J.D. Teachman, D.H. Thomsen, and W.C. Wolkenhauer, "Qualification of Core Physics Methods for BWR Design and Analysis," WPPSS-FTS-127, Washington Public Power Supply System, March 1990.

3. J.A. McClure et al., "SIMTRAN-E - A SIMULATE-E to RETRAN-02 Data Link," EPRI NP-5509-CCM, Electric Power Research Institute, December 1987.

4. C.W. Stewart et al.,"VIPRE-01 - A Thermal-Hydraulic Code for Reactor Cores," EPRI NP-254-CCM-A, Revision 3, Volumes I-III, Electric Power Research Institute, August 1989.

5. D.L. Hagerman, G.A. Reymann, and R.E. Manson, "MATPRO - Version 11 (Revision 2): A Handbook of Materials Properties for Use in the Analysis of Light Water Reactor Fuel Rod Behavior," NUREG/CR-0479, TREE-1280, Revision 2, Idaho National Engineering Laboratory, August 1981.

6. "WREM, Water Reactor Evaluation Model, Revision 1," NUREG-75/065, U.S. Nuclear Regulatory Commission, May 1975.

7. WPPSS Nuclear Plant 2 Updated Final Safety Analysis Report, Washington Public Power Supply System, 1989.

8. "Qualification of the One-Dimensional Core Transient Model for Boiling Water Reactors," NEDO-24154, Volume 1, General Electric Company, October 1978.

9. Letter, J. Armenta (GE) to W.C. Wolkenhauer (WPPSS), "Instruction for Use of 4-Quadrant Curve," dated March 26, 1985.

10. "Recirculation System Performance," Publication 457HA802, General Electric Company, September 1976.

11. B.J. Gitnick et al., "FIBWR - A Steady-State Core Flow Distribution Code for Boiling Water Reactors," EPRI NP-1924-CCM, Electric Power Research Institute, July 1981.

12. R.E. Polomik and S.T. Chow, "Hanford-2 Nuclear Power Station Control System Design Report," GEZ-6894, General Electric Company, February 1980.

13. "Turbine Dynamic Response Parameters," Publication CT-24659, Westinghouse Electric Corporation, August 1979.

14. "Power Ascension Test Program," WNP-2 Plant Procedure Manual, Section 8.2, Washington Public Power Supply System, 1984.

15. L.A. Carmichael and R.O. Niemi, "Transient and Stability Tests at Peach Bottom Atomic Power Station Unit 2 at End of Fuel Cycle 2," EPRI NP-564, Electric Power Research Institute, June 1978.

16. K. Hornyik and J.A. Naser, "RETRAN Analysis of the Turbine Trip Tests at Peach Bottom Atomic Power Station Unit 2 at End of Cycle 2," EPRI NP-1076-SR, Electric Power Research Institute, April 1979.

17. A.M. Olson, "Methods for Performing BWR System Transient Analysis," PECO-FMS-0004-A, Philadelphia Electric Company, November 1988.

18. N.H. Larsen, "Core Design and Operating Data for Cycles 1 and 2 of Peach Bottom Unit 2," EPRI NP-563, Electric Power Research Institute, June 1978.

19. D.M. Ver Planck, W.R. Cobb, R.S. Borland, B.L. Darnell, and P.L. Versteegen, "SIMULATE-E (Mod. 3) Computer Code Manual," EPRI NP-4574-CCM, Part II, Electric Power Research Institute, September 1987.

20. J. E. Krajicek, "WNP-2 Cycle 2 Plant Transient Analysis", XN-NF-85-143, Exxon Nuclear Co., Inc., Richland, WA, December 1985.

21. J. E. Krajicek, "WNP-2 Cycle 5 Plant Transient Analysis", ANF-89-01, Rev. 1, Advanced Nuclear Fuels Corp., Richland, WA, March 1989.

22. S. L. Forkner, et al., "BWR Transient Analysis Model Utilizing the RETRAN Program", TVA-TR81-01, Tennessee Valley Authority, December 1981.

23. WPPSS Nuclear Plant 2 Technical Specifications, Docket No. 50-397.

24. J. E. Krajicek and M. J. Hibbard, "WNP-2 Cycle 4 Plant Transient Analysis", ANF-88-01, Advanced Nuclear Fuels Corp., Richland, WA, January 1988.

APPENDIX A

GENERATION OF KINETICS DATA FOR RETRAN

1. Introduction

The Supply System develops one-dimensional kinetics data for RETRAN in two steps. The kinetics data input to RETRAN is a set of polynomials which correlate changes in water density and fuel temperature with calculated two-group cross sections, diffusion coefficients, neutron velocities, radial bucklings, and delayed neutron fractions.

The first step in the process uses the EPRI codes SIMULATE-E and SIMTRAN-E. SIMULATE-E predicts core power and burnup distributions during detailed depletion analyses of the reactor core. Qualification of the Supply System's SIMULATE-E methodology is provided elsewhere.

SIMTRAN-E was developed under EPRI sponsorship for linking SIMULATE-E and RETRAN. SIMTRAN-E reads restart files written by SIMULATE-E, extracts the appropriate information for determining the kinetics parameters required by RETRAN, and generates the direct RETRAN input for transient analysis. Verification and validation of the Supply System's version of SIMTRAN-E is discussed in Section 4, below.

The first step in the kinetics process produces data that can be used by RETRAN. Without the adjustments described below, however, SIMTRAN-E generated kinetics data produces very conservative results for severe pressurization events. For benchmark analysis of pressurization events, this conservatism can create artificially large uncertainty factors.

The kinetics conservatism results from a difference between the SIMULATE-E core average thermal hydraulics and the RETRAN average channel thermal hydraulics. SIMULATE-E and RETRAN calculate different changes in average moderator density for the same change in core pressure. SIMTRAN-E does not account for this difference. Instead, a manual adjustment is applied to the SIMTRAN-E output in the second step in the kinetics process. The end result of the kinetics process is a set of adjusted polynomials that can be used directly by RETRAN in the best estimate mode.

Except as noted in the text, all of the transient benchmark and example analyses in this report used the adjusted kinetics parameters as produced by the second step of the kinetics process. For transients which do not involve a substantial change in moderator density, the adjustment is unnecessary because the induced conservatism is small.

2. Calculation of Basic Kinetics Input Data

The first step in the kinetics process creates unadjusted one-dimensional kinetics data for RETRAN using CASMO-2/SIMULATE-E and SIMTRAN-E. SIMTRAN-E utilizes a set of SIMULATE-E cases to create RETRAN kinetics parameter polynomials in the relative change in water density and the change in the square root of the fuel temperature.

SIMULATE-E cases are run at a core configuration consistent with the initial conditions for the given transient. The nominal SIMULATE-E case uses power and void feedback to determine the three-dimensional core power and flux distributions and the critical eigenvalue. Although it may be a fully independent case, the nominal case is usually run from a SIMULATE-E restart file. If a transient does not require a scram, then only the nominal case is needed.

For transients requiring a scram, an additional SIMULATE-E case is generated. This case is based on the nominal case and is run with power feedback disabled. The only difference between the nominal case and the perturbed state case is the control rod position array, which has all rods fully inserted.

SIMTRAN-E reads the restart files generated by the SIMULATE-E cases. It then collapses the three-dimensional SIMULATE-E data to one-dimensional data for RETRAN and determines the kinetics parameter dependence on relative water density, square root of fuel temperature, and control state.

SIMTRAN-E collapses most of the kinetics parameters used in the diffusion equation solution by adjoint flux weighting. Since $k\delta_{f1}$ and $k\delta_{f2}$ do not appear in the diffusion equations, they are radially collapsed by volume weighting. Perturbation theory is used to determine the dependence of the kinetics parameters on water density and fuel temperature. All perturbations are done in three dimensions and then each perturbed state is radially collapsed. The base and perturbed state parameters are then correlated to produce polynomials that are dependent on the relative change in water density in the fuel bundles and the change in the square root of the average fuel temperature. This procedure is performed for the nominal case and for any additional states run during the analysis.

3. Adjustment of Kinetics Data

The second step in the kinetics process corrects for thermal hydraulic calculational differences between SIMULATE-E and RETRAN. This correction is needed for best estimate simulation of transients where substantial changes in the thermal hydraulic

state of the core are expected. Severe pressurization transients fall in this category.

Sensitivity studies determine the adjustments to be made in the final SIMTRAN-E calculation. Using the SIMTRAN-E output from the first step, parallel SIMULATE-E and RETRAN cases quantify the difference in axial moderator density distributions between the two models for identical variations in core pressure, which is the primary variable influencing the thermal hydraulic state. The differences between the axial arrays determine moderator density weighting factors for use in the final SIMTRAN-E calculation.

The first term in a kinetics parameter polynomial is a constant. The constant terms determine the initial steady state eigenvalue in the RETRAN unperturbed state. Since the weighting factors do not change the unperturbed state, the constant terms are not modified when the new polynomial fit is developed. The SIMULATE-E eigenvalue is preserved in the RETRAN unperturbed state because the constant terms are not altered.

The cross section libraries used in the core physics analysis are based on ENDF/B-III. ENDF/B-III includes delayed neutron fractions which are artificially low. Preliminary ENDF/B-V data shows an increase in delayed neutron fraction ranging upwards from 5.4% in all fissile isotopes. To bring the delayed neutron fraction closer to those specified in ENDF/B-V, a +5% manual

adjustment is applied to all delayed neutron fractions before final data is put into the RETRAN input file.

4. SIMTRAN-E Verification and Validation

The SIMTRAN-E code version in use at the Supply System was verified by comparison with hand calculations. In the SIMTRAN-E verification, a representative hand calculation for the major computational sequences was performed, and the results of the hand calculation were compared to the values calculated within SIMTRAN-E. The results of the verifications show exact agreement between the hand calculation and computer solution. This effort demonstrates that the equations as derived and presented in the SIMTRAN-E manual are those that appear in the computer coding.

Since the Supply System SIMTRAN-E version is not a formally released EPRI computer code, validation of the code was accomplished from the results of a separate validation study carried out by EI International under contract to the Supply System.

The ultimate validation of the SIMTRAN-E calculation is the accuracy with which RETRAN predicts system behavior in benchmark transient analyses. Figures A-1, A-2, and A-3 show the axial power shapes predicted by SIMULATE-E, RETRAN, and the Process Computer for the initial state for Peach Bottom turbine trip

tests TT1, TT2, and TT3. The close agreement between the RETRAN prediction and both the SIMULATE-E prediction and the Process Computer indicates the validity of the SIMTRAN-E calculation in the steady state mode. The transient mode is validated by the predictions of the Peach Bottom turbine trip tests, which also match the data closely.

5. References

1. D.M. Ver Planck, W.R. Cobb, R.S. Borland, B.L. Darnell, and P.L. Versteegen, "SIMULATE-E (Mod. 3) Computer Code Manual," EPRI NP-4574-CCM, Electric Power Research Institute, September 1987.

2. J.A. McClure et al., "SIMTRAN-E - A SIMULATE-E to RETRAN-02 Data Link," EPRI NP-5509-CCM, Electric Power Research Institute, December 1987.

3. B.M. Moore, A.G. Gibbs, J.D. Imel, J.D. Teachman, D.H. Thomsen, and W.C. Wolkenhauer, "Qualification of Core Physics Methods for BWR Design and Analysis," WPPSS-FTS-127, Washington Public Power Supply System, March 1990.

4. J.D. Atchison, "Final Report on Anticipated Transients Without Scram Analyses for the WNP-2 Nuclear Power Plant," EI International Inc., December 1989.

FIGURE A-1
Initial Axial Power Distribution
Peach Bottom Unit 2 TT1

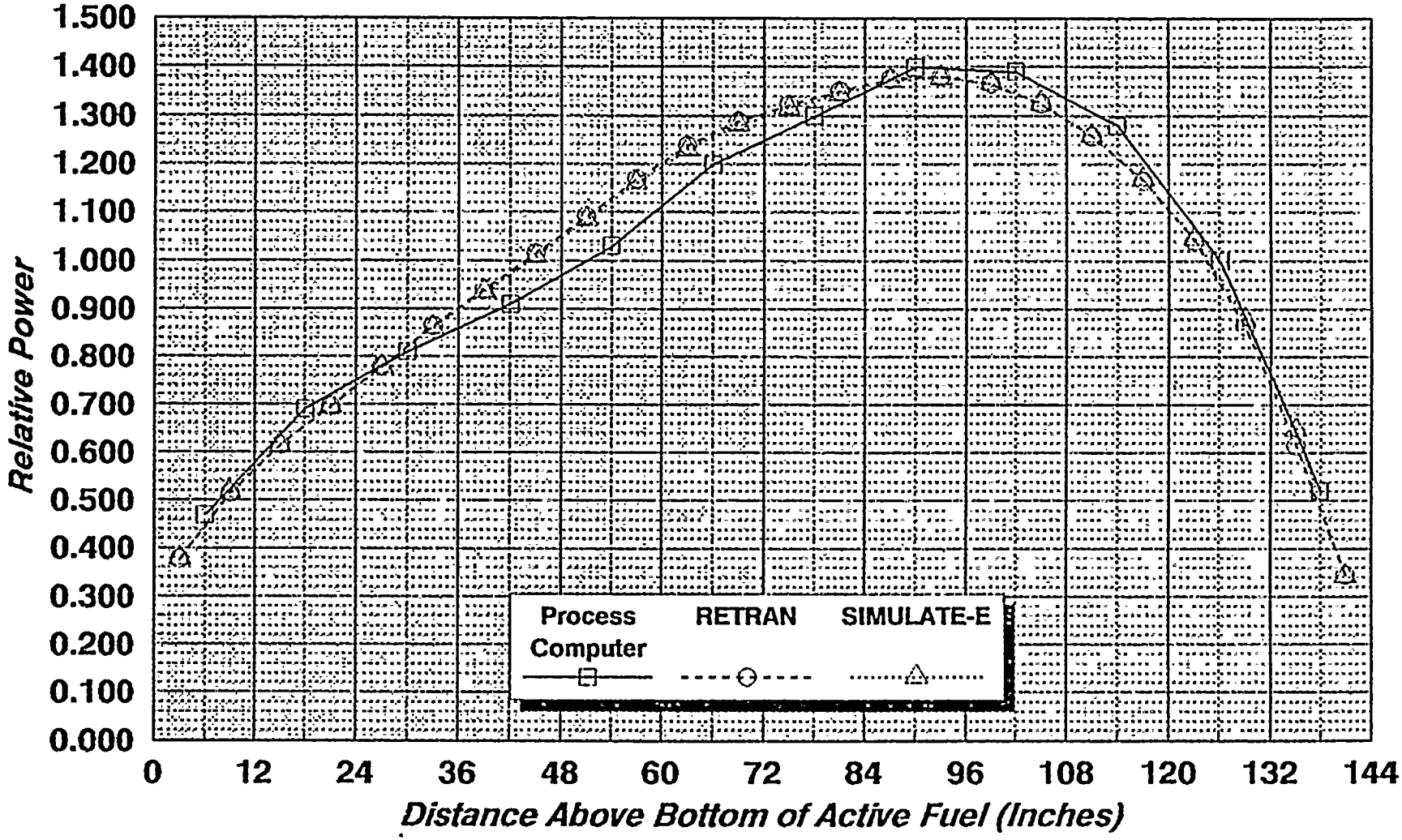

FIGURE A-2
Initial Axial Power Distribution
Peach Bottom Unit 2 TT2

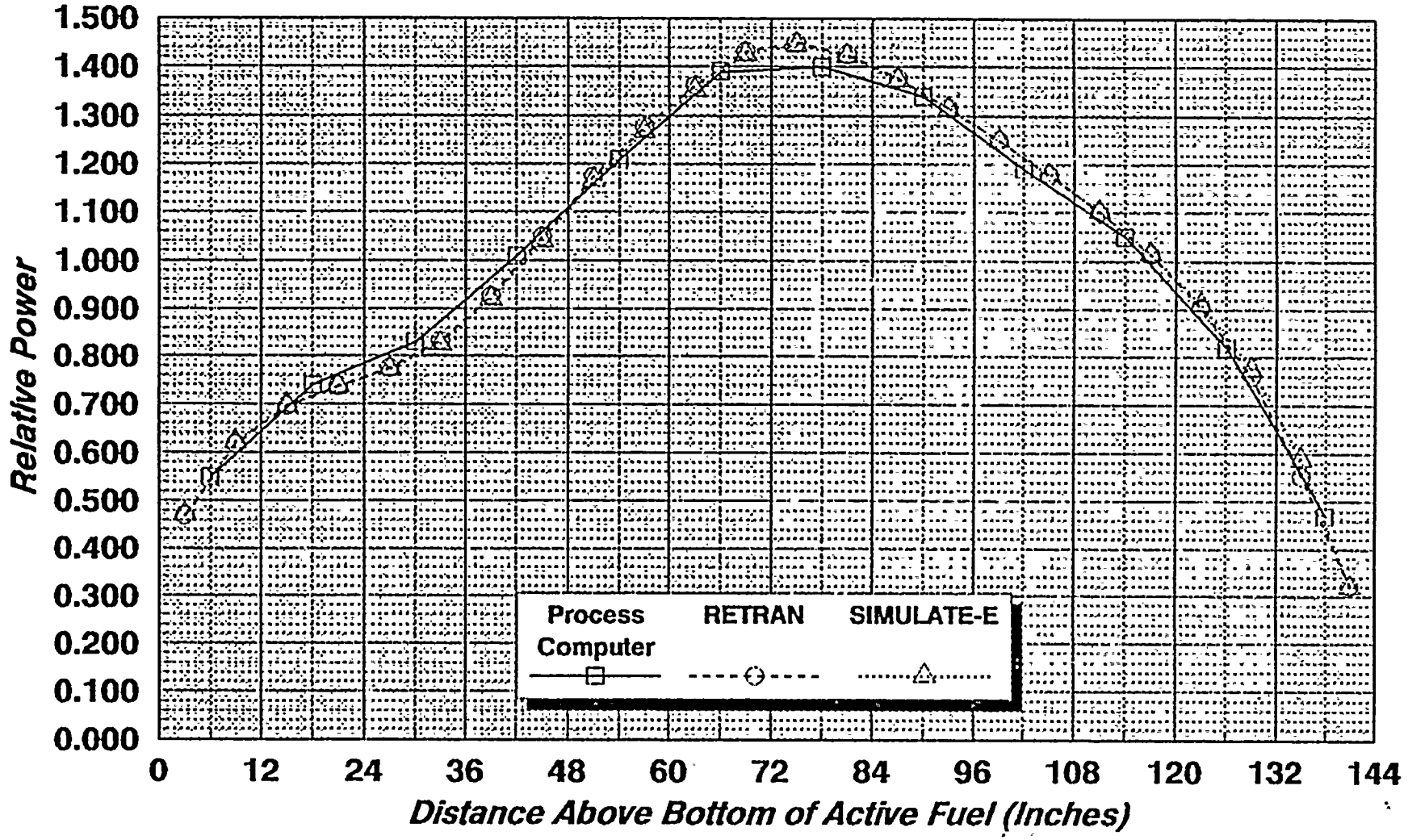

FIGURE A-3
Initial Axial Power Distribution
Peach Bottom Unit 2 TT3